MOLECULAR INVESTIGATIONS OF CELLULAR ROLES OF CALMODULIN AND CALCIUM/CALMODULIN-DEPENDENT KINASES IN STRESS RESPONSES, ASEXUAL AND SEXUAL DEVELOPMENTS IN *NEUROSPORA CRASSA*

A thesis

submitted in partial fulfillment of the requirements for the degree of

DOCTOR OF PHILOSOPHY

by

CHRISTY NOCHE K MARAK

Department of Biosciences and Bioengineering

Indian Institute of Technology Guwahati

Guwahati-781039, Assam, India

September 2022

भारतीय प्रौद्योगिकी संस्थान गुवाहाटी
INDIAN INSTITUTE OF TECHNOLOGY GUWAHATI
Department of Biosciences and Bioengineering
Guwahati-781039

DECLARATION

I do hereby declare that the content embodied in this thesis entitled "**Molecular investigations of cellular roles of calmodulin and calcium/calmodulin-dependent kinases in stress responses, asexual and sexual developments in *Neurospora crassa***" is the result of investigations carried out by me in the Department of Biosciences and Bioengineering, Indian Institute of Technology Guwahati, for the award of the degree of Doctor of Philosophy, under the supervision of **Prof, Ranjan Tamuli**. The research presented in this thesis is original and has not been submitted in part or full for any degree or diploma to any other institute or university to the best of my knowledge and belief.

Guwahati
September, 2022

Christy Noche k. Marak
(Roll No. 156106034)

भारतीय प्रौद्योगिकी संस्थान गुवाहाटी
INDIAN INSTITUTE OF TECHNOLOGY GUWAHATI
Department of Biosciences and Bioengineering
Guwahati-781039

CERTIFICATE

This is to certify that the research work in this thesis entitled "**Molecular investigations of cellular roles of calmodulin and calcium/calmodulin-dependent kinases in stress responses, asexual and sexual developments in *Neurospora crassa***" has been carried out at the Indian Institute of Technology Guwahati, by Christy Noche K. Marak (Roll No. 156106034), for the award of the degree of Doctor of Philosophy in Biosciences and Bioengineering under my supervision. The outcome of the research work presented in this thesis is original and has not been submitted in part or full for any degree or diploma to any other institute or university.

Guwahati
September, 2022

Thesis Supervisor: Prof. Ranjan Tamuli
Professor
Department of Biosciences & Bioengineering

Dedicated

to

my loving parents

Late Pr. Berun R. Sangma

and

Mrs. Gracifills K. Marak

ACKNOWLEDGEMENTS

I take this opportunity to convey my gratitude to all the people who have helped me throughout my Ph.D. journey with their advice, encouragement, valuable input, discussion, friendship, and inspiration.

First of all, I thank our Heavenly Father for all His blessings throughout my life and for helping me successfully complete this research work journey.

I would like to express my heartfelt gratitude and sincere thanks to my supervisor, Prof. Ranjan Tamuli, for his constant guidance, support, and sharing of his immense knowledge of *Neurospora crassa*. Without his continuous motivation and careful supervision, this thesis would not have materialized. He provided a relaxed research environment that made this Ph.D. journey a productive learning process.

I am sincerely grateful to my doctoral committee members, Prof. Pranab Goswami, Prof. Manish Kumar, and Dr. Lal Mohan Kundu, for their valuable suggestions and constructive criticisms on my work that have eventually helped me to complete my thesis work.

I thank the present and previous Directors of IITG and Heads of the Department of Biosciences and Bioengineering for providing all the necessary facilities and support. I especially acknowledge the financial support from MHRD for providing me with a fellowship to carry out my research work successfully. Also, I am grateful to Prof. Qun He from State Key Laboratory of Agrobiotechnology, College of Biological Sciences, China Agricultural University, Beijing, China, for providing me with the *pp-1*^{KO} heterokaryotic strain.

A special thanks to my lab members Darshana, Serena, Rahul, Surabhi, Sangeeta, Krishna, Megha, and Rebecca, who have been like a family helping me in countless ways and adding joy and fun to all the hard work in the lab. I am also grateful to my seniors, Dr.Vijya

Laxmi, Dr. Ananya Barman, Dr. Dibakar Gohain, Dr. Ajeet Kumar, Dr. Avishek Roy, and Dr. Anand Tiwari, for their valuable advice, and for helping me learn the skills and techniques for my research work.

I thank all my friends, Ching Thian Moi, Emily, Thangsei, Bhagyashree, Renu, Rachayeeta, Nayan, and Manas, who have always been a source of encouragement and added lots of fun moments to my life here on the IITG campus. A special mention would be my closest friend Serena who has been with me as a sister and an advisor in dealing with my challenging moments and celebrating the joyous occasions with me throughout my Ph. D. tenure.

Finally, my heartfelt thanks also go to my mother, my sister, my brother-in-law, my brother, and my sister-in-law for their love, motivation, and support in helping me complete journey. I also thank and acknowledge my late father and my mother, who brought me up with all the love, care, and discipline to become who I am today.

And to my dearest husband, Benuel, I thank you from the bottom of my heart for always being there for me. Thank you for sharing your life with me, adding happiness, always listening to my worries and frustrations, and giving me the strength and courage to go on. You have always been so patient and supportive. I look forward to continuing our journey and fulfilling our dreams together.

September, 2022 Christy Noche K. Marak

CONTENTS

List of Figures

List of Tables

Abbreviations

ANOVA	analysis of variance
bp	base pair
BLAST	basic local alignment search tool
BOD	biological oxygen demand
CDD	Conserved Domain Database
cDNA	complementary deoxyribonucleic acid
CHIP	chromatin immunoprecipitation
DNA	deoxyribonucleic acid
ExPASy	Expert Protein Analysis System
FGS	fructose glucose sorbose
FGSC	Fungal Genetics Stock centre
g	relative centrifugal force
GFP	green fluorescent protein
hph	hygromycin B resistance gene
Jm^{-2}	joule per square metre
KV	kilovolt
kb	kilo base pair
kDa	kilo Dalton
LG	linkage group
M	molar

mA	milliampere
µg	microgram
µl	microlitre
µm	micrometre
µM	micromolar
ml	millilitre
mm	millimetre
mM	millimolar
N	normal
NCBI	National Center for Biotechnology Information
NCU	*Neurospora crassa* unit
NEB	New England Biolab
ng	nanogram
nM	nanomolar
Ω	ohm
OD	optical density
ORF	open reading frame
PCR	polymerase chain reaction
pm	picometre
psi	pound-force per square inch
qRT-PCR	quantitative real time polymerase chain reaction
RIP	repeat induced point mutation
RNA	ribonucleic acid
rpm	revolution per minute
RT-PCR	reverse transcription polymerase chain reaction

SCM	synthetic crossing media
SOC	super optimal broth with Catabolite repression
UCR	University of California Riverside
UV	ultra violet
VM	Vogel's minimal media
V	volt

Synopsis

In this thesis work, I studied the cellular roles of calmodulin (CaM) and calcium/calmodulin-dependent kinases (Ca^{2+}/CaMKs) in stress conditions, circadian clock, and sexual development. The *cmd*^{RIP}, Δ*camk-1*, and Δ*camk-2* mutants showed growth defects and reduced survival rates under temperature, pH, oxidative, and ER stress conditions. The *cmd*^{RIP} mutant was female sterile as it could not form the protoperithecium. In addition, the *cmd*^{RIP} mutant strain was unable to support the wild type perithecia graft, showed defects during cell fusion, and a drastic decline in life span. Furthermore, the Δ*camk-1*, Δ*camk-2*, Δ*camk-3*, and Δ*camk-4* mutants showed increased circadian period length without affecting the temperature compensation. Moreover, I found that the *cmd*, *camk-1*, and *camk-2* genes were upregulated under heat stress and during nitrogen-starved conditions, suggesting their involvement in regulating the heat shock response and the pheromone response pathways.

Thesis title: "**Molecular investigations of cellular roles of calmodulin and calcium/calmodulin-dependent kinases in stress responses, asexual and sexual developments in *Neurospora crassa*"**

Objectives:

1. To investigate the cellular roles and mechanism of CaM and Ca^{2+}/CaMKs in coping with stress conditions in *N. crassa*,
2. To determine the functions of the CaM and Ca^{2+}/CaMKs during sexual development in *N. crassa*, and
3. Understanding the molecular details of calmodulin and the transcriptional regulation of the heat shock and the pheromone response pathways in *N. crassa*.

.

Chapters:

Chapter 1: Introduction to *Neurospora crassa* and calcium signaling

Chapter 2: Materials and Methods

Chapter 3: Understanding the cellular roles and mechanism of calmodulin and calcium/calmodulin-dependent kinases in coping with stress conditions in *N. crassa*

Chapter 4: Role of calmodulin and calcium/calmodulin-dependent kinases in sexual development and circadian clock in *N. crassa*

Chapter 5: Molecular analysis of calmodulin, transcriptional regulation of the heat shock and the pheromone response pathways in *N. crassa*

Chapter 1: Introduction to *Neurospora crassa* and calcium signaling

Chapter 1 briefly describes the history and biology of *Neurospora crassa* and the importance of calcium (Ca^{2+}) signaling in various eukaryotes. *N. crassa* is a heterothallic fungus belonging to the family of ascomycetes. *N. crassa*, found mainly in humid tropical and subtropical regions, grows commonly on burned vegetation (Turner et al. 2001). *N. crassa* has been established as a major model filamentous fungus and contributed immensely to the development and understanding of genetics, biochemistry, molecular biology, cell biology, and signaling, including the Ca^{2+} signaling machinery (Galagan et al. 2003; Roche et al. 2014; Carillo et al. 2020). In eukaryotes, Ca^{2+} plays a versatile role in modulating all aspects of cellular functions (Cai et al. 2015; Luan and Wang 2021). *N. crassa* has a complex Ca^{2+} signaling machinery consisting of 48 Ca^{2+}-signaling proteins, with three Ca^{2+} channel proteins, two Ca^{2+}/Na^{+} exchangers, six Ca^{2+}/H^{+} exchangers, nine Ca^{2+}/cation- ATPases, four phospholipase C-δ subtype (PLC- δ) proteins, one calmodulin (CaM), and 23 Ca^{2+} and/or CaM binding proteins (Galagan et al. 2003; Borkovich et al. 2004; Zelter et al. 2004). The transient increase in the cytosolic free Ca^{2+} concentration ($[Ca^{2+}]_c$) from the resting level of ~100 nM to 1 μM or more activates Ca^{2+} sensing proteins, inducing an intracellular signal in response to various extracellular stimuli (Chin and Means 2000; Bootman et al. 2001).

Ca^{2+} binds and activates the primary Ca^{2+} sensing protein calmodulin (CaM), which then undergoes a conformational change enabling the further activation of over 300 target proteins (Means and Dedman 1980; Hoeflich and Ikura 2002; Halling et al. 2016). CaM is a small ~17 kDa protein that binds to four Ca^{2+} with the help of structural motifs known as EF-hand, which is comprised of two α-helices flanking a loop characterized by 12 residues rich in glutamate and aspartate to chelate the Ca^{2+} ion (Gifford et al. 2007). CaM is essential for viability in *N. crassa*, therefore, the cellular roles of CaM were studied using CaM antagonists and repeat-induced point mutation (RIP; Cambareri et al. 1989; Selker 1990). These studies

showed that CaM is important for the growth, hyphal development, circadian rhythm, activation of chitin synthase required for cell wall formation, carotenoid accumulation, ultraviolet survival, and sexual development (Sadakane and Nakashima 1996; Suzuki et al. 1996; Suresh and Subramanyam 1997; Laxmi and Tamuli 2015, 2017).

Chapter 1 also describes the Ca^{2+}/calmodulin-dependent kinases (Ca^{2+}/CaMKs), which are Ser/Thr kinases and downstream target proteins of CaM. Their domain organization comprises an N-terminal catalytic domain and a C-terminal regulatory domain consisting of the overlapping autoinhibitory and Ca^{2+} /CaM-binding regions (Swulius and Waxham 2008). In *N. crassa*, four Ca^{2+}/CaMKs (CaMK-1, 2, 3, and 4) have been identified; CaMK-1and CaMK-2 are essential for full fertility, stress adaptation, and light-induced shifting of the circadian clock (Tamuli et al. 2011; Kumar and Tamuli 2014).

The cellular roles of CaM and Ca^{2+}/CaMKs in stress tolerance and sexual development were reported previously. However, the detailed cellular roles and mechanisms in mediating various stress conditions and sexual development remained unknown in *N. crassa*. Therefore, I studied the cellular roles and the possible mechanistic pathways of CaM and Ca^{2+}/CaMKs in response to different abiotic stress conditions, sexual development, and regulating the circadian clock. Furthermore, I investigated the probable transcriptional regulator of CaM during sexual development.

Chapter 2: Materials and Methods

Chapter 2 describes the media, chemicals, and experimental procedures used in this research work. The chemicals and reagents were purchased from the standard suppliers and used after being autoclaved or filter sterilized as per requirement. Molecular experiments such as cloning, polymerase chain reaction (PCR), reverse Transcriptase PCR, and quantitative real-time PCR were performed using either standard protocols (Russell and Sambrook 2001) or as stated by the manufacturer's instructions. All the statistical analyses of the experimental data and the graphs were plotted using Microsoft Excel and SigmaPlot®.

Routine growth, maintenance, and crosses of *N. crassa* strains were performed essentially as described previously (Westergaard and Mitchell, 1947; Davis and de Serres, 1970). The *N. crassa* wild type and various knockout mutant strains used in this study were obtained from the Fungal Genetics Stock Center (FGSC, Manhattan, KS). The other *N. crassa* strains were either generated in the laboratory of Prof. Katherine A. Borkovich (University of California Riverside, USA) or in our laboratory. The *pp-1* mutant strain was a kind gift from Prof. Qun He (State Key Laboratory of Agrobiotechnology, College of Biological Sciences, China Agricultural University, Beijing, China).

<u>Chapter 3</u>: Understanding the cellular roles and mechanism of calmodulin and calcium/ calmodulin-dependent kinases in coping with stress conditions in *N. crassa*

Chapter 3 describes the role of CaM and its downstream target protein CaMKs in coping with different abiotic stress conditions in *N. crassa*. The *cmd*^{RIP}, Δ*camk-1*, and Δ*camk-2* mutants were sensitive to temperature variations and showed reduced growth rates at lower (20 °C) and elevated (40 °C) temperatures in comparison to their growth rates at normal ambient (30 °C) temperature. In alkaline pH and dithiothreitol (DTT) induced endoplasmic reticulum (ER) stress conditions, the *cmd*^{RIP}, Δ*camk-1*, and Δ*camk-2* mutants showed reduced aerial hyphae growth. However, the mutants showed no defect under osmotic stress conditions of high NaCl and sorbitol concentrations. In addition, the *cmd*^{RIP}, Δ*camk-1*, and Δ*camk-2* mutants also showed reduced growth rate and survival rates under hydrogen peroxide (H_2O_2) induced oxidative stress. Furthermore, the *cmd*^{RIP}, Δ*camk-1*, and Δ*camk-2* mutants showed reduced survival rates on exposure to an induced thermotolerance condition. The Δ*camk-3* and Δ*camk-4* mutants showed no significant defect in their growth and survival rates under all the stress conditions tested. The parental strain of the *cmd*^{RIP}, and the Δ*camk-1* and Δ*camk-2* mutant strains carrying the *camk-1* and *camk-2* transgenes, respectively, complemented the temperature sensitivity, pH stress, oxidative stress, ER stress, and thermotolerance phenotypes of the respective mutants. Therefore, the *cmd*, *camk-1*, and *camk-2* genes are necessary for survival under various stress conditions.

Chapter 4: Role of calmodulin and calcium/calmodulin-dependent kinases in sexual development and circadian clock in *N. crassa*

Chapter 4 describes the role and mechanism of CaM during sexual development. The *cmd*^{RIP} mutant was unable to form the female sexual structure the protoperithecium and was sterile as a female parent but fertile as a male parent. In addition, the *cmd*^{RIP} mutant formed an incompetent mycelium, which was unable to support the freshly fertilized wild type perithecia graft. Also, the *cmd*^{RIP} mutant was unable to form mycelial network when grown in VG liquid, suggesting a defect in cell fusion. Because aging is accompanied with decline in fertility and increased mortality (Kirkwood 2000), I examined the conidial aging rate and found that the *cmd*^{RIP} mutant showed a drastic decline in the survival rate of conidia when maintained under starved condition.

I also investigated the role of CaM and CaMKs in regulating the circadian clock at three different temperatures in *N. crassa*. The knockout mutants of *camk-1*, *camk-2*, *camk-3* and *camk-4* exhibited increased period lengths at 20, 25 and 30 °C compared to the *ras-1*^{bd} strain. Since the *cmd*^{RIP} mutant showed severe growth defects, the period length in this mutant could not be determined. Temperature compensation is a phenomenon where the period length of the circadian clock shows insensitivity to a range of temperature differences (Gardner and Feldman 1981). The Q_{10} values for the mutants were in the range of ~1 like the *ras-1*^{bd} strain, suggesting that the temperature compensation was not affected in the *camk* mutants.

Therefore, this study revealed that 1) the *cmd* gene is important for proper mycelium development, which is essential for sexual development, and critical for normal aging process, 2) the *camk-1, camk-2, camk-3,* and *camk-4* genes are required for normal period length, but do not affect the temperature compensation of the circadian clock in *N. crassa*.

Chapter 5: Molecular analysis of calmodulin, transcriptional regulation of the heat shock and the pheromone response pathways in *N. crassa*

Chapter 5 describes the molecular basics of the CaM protein and the pathways regulated by CaM and CaMKs in stress conditions and sexual development phase. The *cmd*^{RIP} mutant showed severely reduced Ca^{2+} distribution across the hyphae, which indicated a disruption of the Ca^{2+} homeostasis. In addition, the *cmd*^{RIP} mutant showed abnormal and increased septation with decreased hyphal width. Furthermore, the comparison of the wild type CaM and the CaM^{RIP} structure built using homology-modelling revealed that the EF-hand 2 of CaM^{RIP} could not to bind to Ca^{2+}. Therefore, the loss of one of the four bound Ca^{2+} might affect the Ca^{2+} gradient in the hyphal tip and the formation of normal septations, which are essential for the normal growth and development of *N. crassa*.

To determine the expressions of CaM and CaMKs under different cellular conditions, I performed real time expression analysis of the *cmd* and *camks* genes. The expression levels of the *cmd, camk-1*, and *camk-2* genes under heat stress and nitrogen starved conditions were increased, suggesting that these genes were upregulated in response to heat and nitrogen starvation. In addition, the expression analysis of genes encoding the heat shock proteins *hsp70* and *hsp80* and the pheromone response pathway genes *pre-1*, *pre-2*, *ccg-4*, *mfa-1*, and *fmf-1* were reduced in the *cmd*^{RIP}, Δ*camk-1*, and Δ*camk-2* mutant strains, suggesting that CaM and CaMKs are involved in the heat shock response and pheromone response pathways.

To understand how Ca^{2+}/CaMKs regulate the circadian clock, I studied relative expressions of *frequency* (*frq*) and *white collar-1* (*wc-1*) genes that encode two distinct clock regulators. The expression level of *frq* and *wc-1* in the *camk* mutants were similar to that in the wild type, indicating that the CaMKs may not play a major role in regulating the circadian clock regulators.

I also investigated the probable transcriptional regulators of the *cmd* gene during sexual development. Promoter analysis for the *cmd* gene was performed by analyzing ~2 kb upstream of the 5' flanking region of *cmd* using MatInspector (Quandt et al. 1995). The promoter analysis revealed putative sequences for several transcription factors, including the binding site for STE12, a transcriptional activator involved in pheromone response in yeast, which is encoded by *protoperithecium-1* (*pp-1*) gene in *N. crassa*. The phenotypic analysis of the Δ*pp-1* mutant showed defects in growth morphology, with reduced aerial hyphae and female sterility, a similar phenotype to the cmd^{RIP} mutant strain. I also found decreased expression of *cmd* gene in the Δ*pp-1* mutant under nitrogen starved condition, suggesting that PP-1 is involved in regulating the *cmd* gene during sexual development. In *N. crassa*, *pp-1* is activated by MAK-2 MAP kinase signaling pathway (Li et al. 2005; Herzog et al. 2015). The MAK-2 pathway of *N. crassa* shows homology to the pheromone response pathway of *S. cerevisiae* (Fischer et al. 2018). Taken together, these results suggested a crosstalk between the Ca^{2+}signaling and the MAPK signaling pathways in *N. crassa*.

Conclusions and future perspectives

This chapter describes the conclusions and future prospects of my thesis work. In this study I have shown that CaM, CaMK-1 and CaMK-2 are required for adaptation to various stress conditions mediated by temperature, pH, oxidative, and ER targeting compounds. During sexual development, CaM is necessary to form the female sexual structure called protoperithecium. CaM is also critical for normal vegetative hyphae development, cell fusion, and normal aging, which determines full fertility during the sexual developmental phase. In addition, I found that the CaMKs are required for the normal circadian period length but do not affect temperature compensation.

Mutations in the EF-hand result in the inability of CaM to bind to one of the 4 Ca^{2+} ions, which might cause defects in the intracellular Ca^{2+} gradient. The possible disruption of the Ca^{2+} gradient might be responsible for the abnormal septation, decreased hyphal width, and defects in the morphology, growth, and development in the CaM^{RIP} mutant. This study also showed that the *cmd*, *camk-1*, and *camk-2* genes are upregulated during heat stress and nitrogen-starved condition, suggesting their involvement in regulating the heat shock and pheromone response pathways. Finally, under nitrogen starved condition, which initiates sexual development, the *cmd* gene was regulated by PP-1, a transcription factor involved in pheromone response. Therefore, this work also established a crosstalk between the Ca^{2+} signaling pathway and the MAPK kinase pathway in *N. crassa*.

Future perspectives of this research work

Future directions of this thesis work will be (i) to study the interaction of the transcriptional factor PP-1 in the promoter region of *cmd* gene by using chromatin immunoprecipitation (ChIP), followed by electrophoretic mobility shift assay (EMSA) to determine the specific binding sequence of PP-1 in the promoter of *cmd* gene, (ii) to determine how CaM and CaMKs interact with the MAPK signaling pathway, (iii) to investigate the mechanism of CaM and CaMKs in the activation of heat shock transcription factor (HSF-1), and (iv) to understand the role and mechanism of CaM and CaMKs in the regulation of reactive oxygen species (ROS) homeostasis.

CHAPTER 1

Introduction to *Neurospora crassa* and calcium signaling

1.1 Brief history of the establishment of *Neurospora crassa* as a model organism

The filamentous fungus *Neurospora* also called the 'organism behind the molecular revolution', has been at the forefront as a model system due to the ease in correlating its genetics with its biochemical and molecular traits (Perkins 1992; Weist et al. 2013). Over the years, *Neurospora* research has provided valuable insights in the areas of cell biology, genetics, biochemistry, and molecular biology, which have shown to be applicable to other fungi and other kingdoms of life as well (Borkovich et al. 2004; Roche et al. 2014).

The genus name *Neurospora*, meaning 'nerve spore', comes from the longitudinal striations on the fungal spores, resembling animal axons belonging to the nervous system (Goncalves and Videira 2014). *Neurospora crassa*, a member of the phylum Ascomycota, was first discovered in 1843 as orange bread mold infestations in French bakeries and described independently as *Oidium aurantiacum* (Payen 1843) and *Penicillium sitophilum* (Montagne 1843). In 1927, Dodge and Shear assigned the fungus to the genus *Neurospora* based on the grooved ascospores and identified the fungi as a heterothallic organism consisting of two mating types *A* and *a* with eight ordered asci (Shear and Dodge 1927; Perkins 1992). Later in 1939, Dodge and Lindegren developed the organism's genetics by demonstrating the Mendelian inheritance in individual asci and quoted "The fungi in their reproduction and inheritance follow exactly the same laws that govern these activities in higher plants and animals." (Dodge 1939; Perkins 1992). In 1941, Beadle and Tatum obtained the first *N. crassa* biochemical mutants and found that a typical gene controlled the synthesis of a particular enzyme and proposed the famous "one gene-one enzyme" hypothesis (Beadle and Tatum 1941), which won the Nobel prize in "Physiology in medicine" in 1958. Thereafter, *N. crassa* gained intensive investigations and emerged as an excellent eukaryotic model organism for understanding various biological processes such as cellular differentiation and development, photobiology, circadian rhythm, population biology, DNA methylation and repair, genome

defense mechanisms, mitochondrial transport, and post-transcriptional gene silencing (Davis 2000; Davis and Perkins 2002; Galagan et al. 2003; Borkovich et al. 2004). The founding of the Fungal Genetic Stock Center (FGSC) in 1960 was a significant milestone, as it ensured the availability of strains from earlier studies for the following generations of researchers (McCluskey 2003). In 2003, sequencing of *N. crassa* was completed, which revealed a genome size of 43 Mb, consisting of 10,082 protein-coding genes spanning within seven chromosomal linkage groups (I-VII) (Galagan et al. 2003). The availability of the whole genome sequence led to a high-throughput knockout project to generate gene replacement mutants for all genes (Colot et al. 2006; Collopy et al. 2010; Park et al. 2011). This enabled the elucidation of the functions of many genes and the identification of transcription factors regulating various biochemical pathways and cellular responses (Roche et al. 2014; Seibert et al. 2016).

1.2 Life cycle of *N. crassa*

N. crassa, ubiquitous in tropical and subtropical regions, is one of the first colonists on burned vegetation after forest fires (Turner 2001; Gladieux et al. 2020). *N. crassa* is a haploid heterothallic multicellular organism consisting of both asexual and sexual mode of reproduction depending on the environment and growth conditions (Figure 1.1; Seale 1973; Springer 1993). In the vegetative phase, which occurs in a nutrient-rich environment, *N. crassa* grows as filamentous multinucleated hyphae that intertwine and fuse to form a hyphal network called mycelium (Springer and Yanofsky 1989; Springer 1993). The internal cross walls or ‘septa’ are incomplete, having a central pore that allows the free movement of cytoplasm, nuclei, and other cellular organelles from the older region of hyphae towards the growing tip (Schmit and Brody 1976). In response to nutrient-deprived condition or exposure to an air-water interface, the fungus gives rise to specialized aerial hyphae to form conidiophores, which

subsequently produce uninucleate asexual spores called microconidia or multinucleate macroconidia (Springer 1993).

N. crassa consists of two non-switching mating types, *mat A* and *mat a*, that are determined by alternate DNA sequences called idiomorphs present at Linkage Group 1L (Shear and Dodge 1927; Perkins et al. 1982; Glass et al. 1990; Staben and Yanofsky 1990). The sexual phase is activated under nitrogen starvation and low-temperature conditions resulting in the formation of nascent fruiting bodies called protoperithecia (Raju 1992). The female sexual structure protoperithecium is composed of coiled multicellular hyphae (ascogonium) enclosed within the enveloping hyphae (Nelson and Metzenberg 1992; Bistis 2003). Specialized hyphae called trichogyne extend from the protoperithecium and grow chemotropically towards the male cell of opposite mating type, which can be a microconidium, macroconidium, or hyphal fragment (Bistis 1981; Kim et al. 2012). After the fusion (plasmogamy) between the trichogyne and conidium, the male nucleus travels through the trichogyne into the protoperithecium and coexists with the female nuclei as a dikaryon in a specialized structure called ascogenous hypha (Bistis 1981; Springer 1993; Kim et al. 2012). The fertilization transforms the protoperithecium into a young perithecium (Aramayo and Selker 2013). The dikaryotic tissue undergoes synchronous nuclear division to form a three-cell hook-shaped structure called crozier (Raju 2009; Aramayo and Selker 2013). The middle cell in the crozier is known as the ‘ascus mother cell’ that undergoes karyogamy, meiosis, and postmeiotic mitosis to give eight sexual spores termed as ascopores, packed in a linear order in a narrow ascus (Bistis 2003; Aramayo and Selker 2013). The mature ascospores are then ejected through the ‘ostiole’, a pore at the tip of the perithecium (Harris et al. 1975; Springer 1993). The ascospores germinate and produce multinucleate mycelium upon heat activation (Raju 1992).

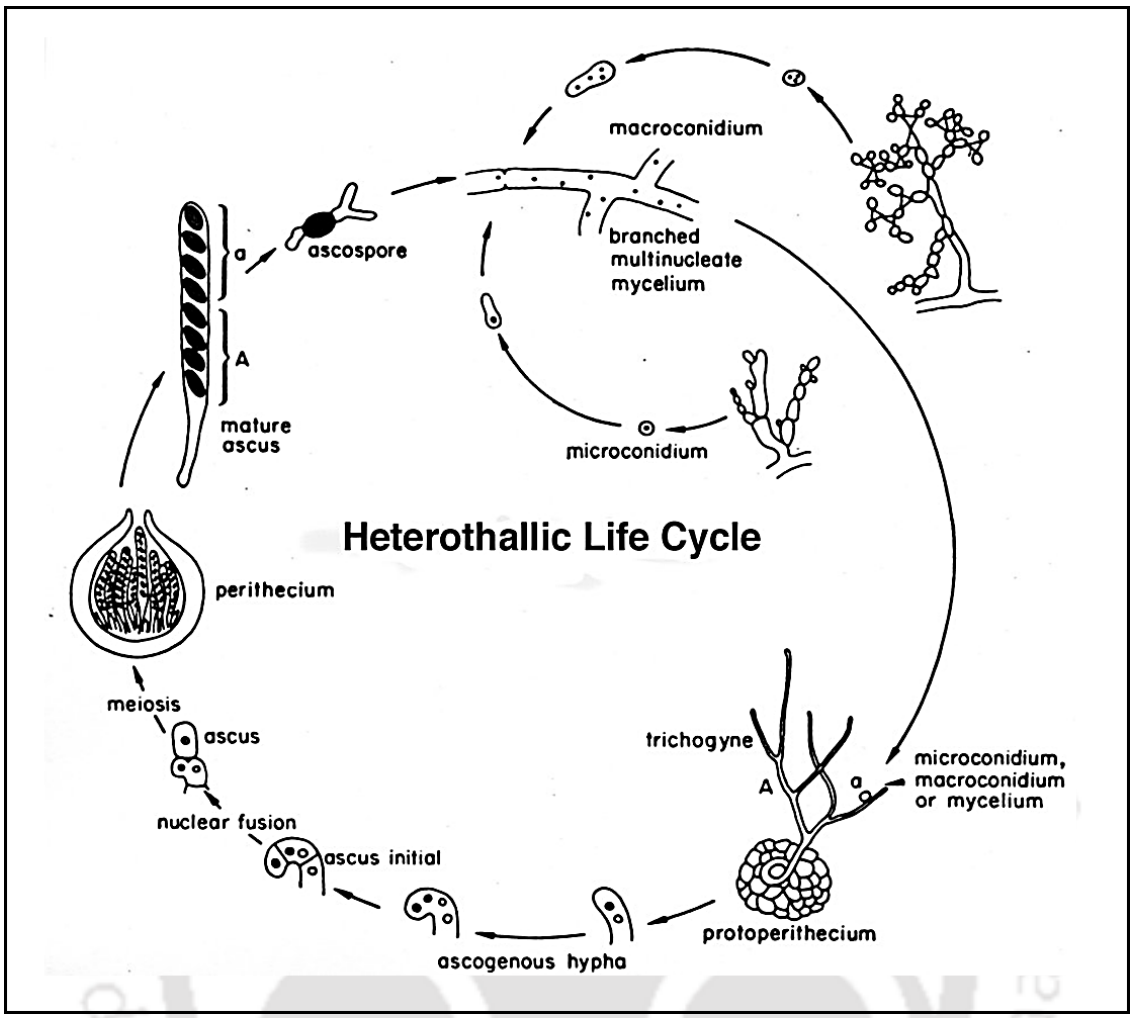

Figure 1.1 The life cycle of *N. crassa*. During the asexual phase of this cycle, the haploid asexual spore (conidium) germinates and grows as branched threads (vegetative hyphae) to form a colony of hyphal network. The colony buds off from the aerial hyphae and produces millions of multinucleate macroconidia and uninucleate microconidia, which disperse and repeats the asexual cycle if landed on a suitable substrate. The sexual cycle initiates with nitrogen starvation and low temperature. Colonies of either *mat A* or *mat a* mating types form the female sexual structure known as protoperithicium, which is fertilized by the conidia of the opposite mating type and develops into a mature perithecium, where the dikaryon undergoes a series of mitosis and meiosis forming eight linearly ordered ascospores within an ascus. Adapted from FGSC (http://www.fgsc.net/Neurospora/sectionB2.htm).

1.3 Genome defense mechanisms in *N. crassa*

Mobile DNA or transposable elements (TE) are present in the genomes of nearly all species, generating intra- and inter-specific variability (Castanera et al. 2016). Any sequence of ~1 kb or larger, when present in more than a single copy, is likely to be a retrotransposon capable of damaging the integrity of the genome (Shiu and Metzenberg 2002). In *N. crassa*, only 9 % of the genome consists of repetitive DNA, most of which are inactivated transposable elements (Aramayo and Selker 2013). *N. crassa* possesses active genome defense mechanisms functioning at both asexual and sexual phases of its life cycle to protect from the invasion of viruses, retrotransposons, and insertion sequences which could be lethal to the organism if left unchecked (Pratt et al. 2004; Tamuli 2013). In *N. crassa*, three gene silencing mechanisms have been found operating; (1) quelling, (2) repeat-induced point mutation (RIP), and (3) meiotic silencing.

1.3.1 Quelling

Quelling is an RNAi-based post-transcriptional gene silencing (PTGS) phenomenon that detects and inactivates repeated sequences during the haploid, vegetative growth phase in *N. crassa* (Figure 1.2 A; Romano and Macino 1992; Cogoni and Macino 1997, 1999). This gene silencing phenomenon is related to the co-suppression in plants and RNA interference (RNAi) in animals (Fulci and Macino 2006). Quelling functions by producing small interfering RNAs (siRNAs), which interferes with the propagation of repeated elements within the nuclei (Catalanotto et al. 2002). In *N. crassa*, three classes of quelling defective genes, *qde-1* encoding for an RNA-dependent RNA polymerase (RdRP), *qde-2* encoding a protein belonging to the Argonaut family, and *qde-3* encoding a RecQ helicase, are found to mediate quelling (Cogoni and Macino 1997, 1999a, 1999b; Catalanotto et al. 2000, 2002). Large repeated sequences potentially form cruciform-like secondary structures, which are recognized by QDE-3 and

attract QDE-1 to the transgenic locus (Cogoni and Macino 1999a, 199b). QDE-1 then converts the single-stranded RNA into a dsRNA molecule, which is subsequently chopped into siRNAs of 21–25 nucleotides by one of the two redundant DICER-like ribonuclease proteins, DCL-1 and DCL-2 (Catalanotto et al. 2004). The siRNAs are then incorporated into QDE-2 containing RNA-inducing silencing complex (RISC), which degrades the complementary mRNA targets (Catalanotto et al. 2002, 2006).

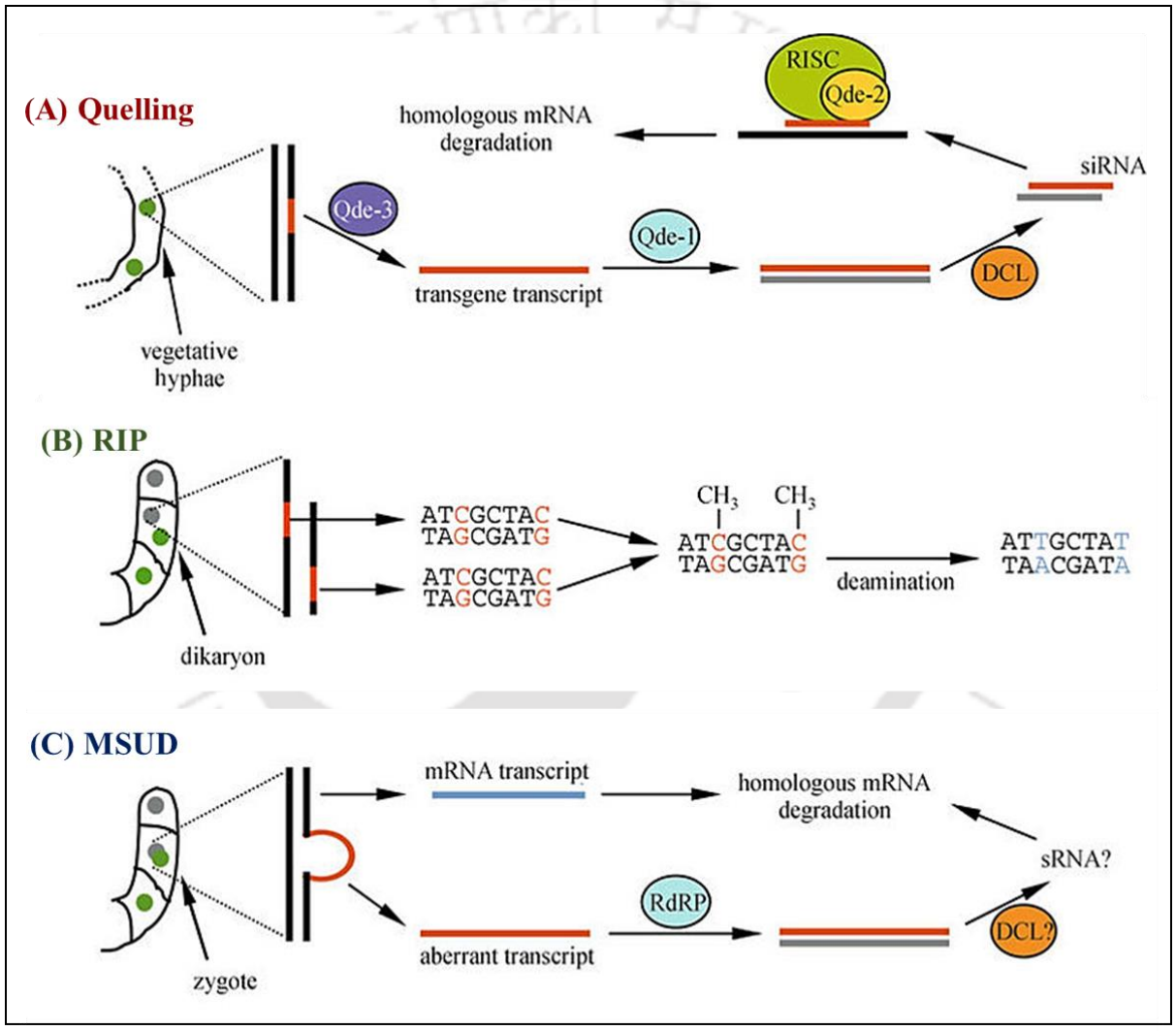

Figure 1.2 Gene Silencing Mechanism in *N. crassa*. (A) Quelling occurs in the haploid mycelium during the vegetative phase, which is induced by the introduction of transgenes. **(B)** Repeat-induced point (RIP) mutation occurs on duplicated DNA sequences present in the haploid nuclei, which are confined to the hook-shaped crozier. The red C:G pair represent the

targets of methylation by a putative DNA methyltransferase, RID (RIP defective, Freitag et al. 2002). Putative deamination of these bases leads to A:T conversion (blue). **(C)** In the zygote, the unpaired DNA sequences are detected and silenced by meiotic silencing by the unpaired DNA pathway (Adapted and modified from Schumann et al. 2010).

1.3.2 Repeat-induced point mutation

Repeat-induced point mutation (RIP) is a homology-based genome defense mechanism that detects and hypermutates repeated DNA sequences in the sexual phase of the life cycle (Figure 1.2 B; Cambareri et al. 1991; Galagan and Selker 2004; Tamuli 2013). This process occurs before the fusion (karyogamy) of the parental nuclei in the fertilized premeiotic cells (Cambareri et al. 1991). RIP identifies duplicate DNA sequences that are greater than 400 base pairs in length, sharing 80% or above sequence identity, and causes C:G to T:A mutations in both the original and duplicated sequences (Cambareri et al. 1989; Watters et al. 1999). The mutations induced by RIP occur preferentially in the CpA dinucleotides and in most cases they become the targets for DNA methylation leading to epigenetic silencing of repetitive DNA (Cambereri et al. 1989; Grayburn and Selker 1989; Galagan and Selker 2004). In addition to the duplicated sequences, RIP mutations can also occur in the single copy sequences adjacent to the duplicated sequences (Irelan and Selker 1997; Vyas and Kasbekar 2005). Mutation from RIP occurs by enzymatic deamination of 5-methylcytosines (5mC) or by the deamination of Cytosine residues followed by DNA replication (Selker 1990). In *N. crassa*, RIP is proposed to function by two largely independent pathways (Carlier et al. 2021). The first pathway involves a putative C5-cytosine methyl transferase (CMT) called RID (RIP-defective) which is primarily limited to duplicated sequences (Frietag et al. 2002; Carlier et al. 2021). The second pathway relies on DIM-2 (defective in methylation, a canonical CMT), which along with DIM-5 (a histone H3 lysine-9 [H3K9] methyltransferase) and HP1 (Heterochromatin Protein 1),

tends to mutate the adjacent non-repetitive regions (Kouzminova and Selker 2001; Aramayo and Selker 2013; Gladyshev 2017; Carlier et al. 2021).

1.3.3 Meiotic silencing

During prophase I of meiosis, unpaired DNA sequences are detected and silenced by a post-transcriptional silencing process known as 'Meiotic silencing by unpaired DNA' (MSUD) (Figure 1.2 C; Shiu et al. 2001; Shiu and Metzenberg 2002). Meiotic silencing is thought of as a silencing mechanism of a non-two-copy sequence that silences unpaired segments and genes present in any odd number or homologous genes present as single-copy in each parent occupying nonhomologous positions (Shiu et al. 2001). Broadly, the MSUD mechanism occurs in two steps. First, the pairing of the homologous chromosomes in the diploid zygote reveals the location of the unpaired DNA by a process called trans-sensing, which gives rise to an aberrant RNA (aRNA). Second, the aRNA is processed by the perinuclear RNA silencing machinery and converted to dsRNA, which is then cut into fragments of 21-23 base pairs in length, producing the small interfering RNA (siRNA) that acts as guide RNAs for an ATP-dependent cleavage of homologous mRNA through a process known as RNA interference (RNAi) (Zamore et al. 2000; Aramayo and Selker 2013). In the perinuclear region, the aRNA encounters six known MSUD proteins (Figure 1.3), which include Suppressor of ascus dominance-1 (SAD-1), an RNA-dependent RNA polymerase that turns aRNA to dsRNA (Shiu et al. 2001); SAD-3, a helicase that aids SAD-1 to form dsRNA (Hammond et al. 2011); Dicer like -1 (DCL-1), a dicer protein that cleaves the dsRNA into siRNAs (Alexander et al. 2008); quelling defective-2 interacting protein (QIP), an exonuclease that processes the siRNAs into single strands (Lee et al. 2010; Xiao et al. 2010); Suppressor of meiotic silencing-2 (SMS-2), an Argonaute protein that helps siRNAs to target complementary mRNAs (Lee et al. 2003); and SAD-2 protein, necessary for perinuclear localization of SAD-1 and also serves as a

scaffold protein for other MSUD proteins (Shiu et al. 2006; Hammond et al. 2013; Decker et al. 2015).

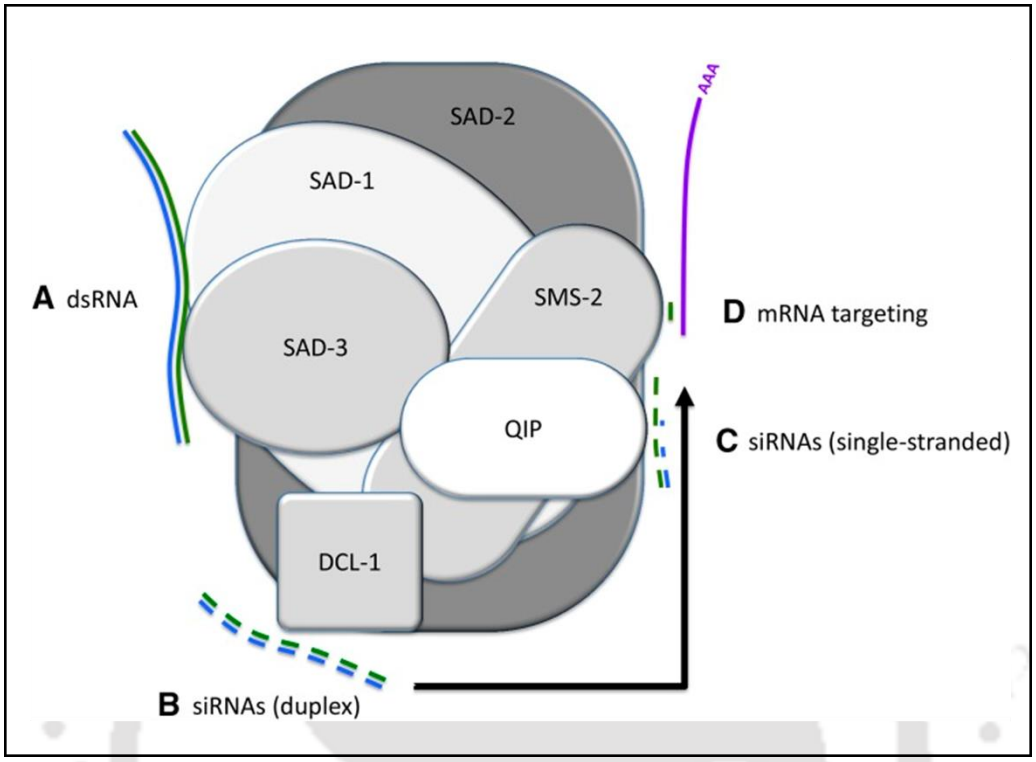

Figure 1.3 Model for the meiotic silencing complex in the perinuclear region. (**A**) The aberrant RNA (blue) is converted into double-strand by SAD-1RdRP and SAD-3 helicase. (**B**) DCL-1 Dicer processes the dsRNA into siRNAs. (**C**) siRNA duplex is further processed by QIP exonuclease into single-stranded siRNA (green). (**D**) Finally, single-stranded siRNAs are used by SMS-2 Argonaute to the target homologous mRNAs (purple). SAD-2 serves as a scaffold and holds other silencing factors (Adapted from Decker et al. 2015).

1.4 Calcium: a versatile signaling molecule

Calcium (Ca^{2+}) is a universal second messenger involved in the regulation of almost all cellular processes in prokaryotes and eukaryotes (Domiguez 2004; Petersen et al. 2005; Clapham 2007; Permyakov and Kretsinger 2009). The first landmark discovery about the biological role of Ca^{2+} was made in 1883, when Sidney Ringer, a London physiologist, reported the requirement

of Ca^{2+} to maintain heart contraction, which was later known as the "Ringer solution" (Ringer 1883; Fedrizzi et al. 2008). It was not until 1940 that Ca^{2+} was accepted as a regulator of cellular processes (Fedrizzi et al. 2008).

The function of a protein is governed by its shape and charge (Clapham 2007). The binding of Ca^{2+} changes the conformation and charge of a protein, which are the two universal tools for signal transduction (Clapham 2007). The versatility of Ca^{2+} as a second messenger comes from its chemistry, which includes the molecular structure, valence state, binding strength, ionization potential, and kinetic parameters in biological reactions (Jaiswal 2001). Ca^{2+} has a high affinity for carboxylate oxygen and therefore binds to amino acids like aspartic acid and glutamic acid that contain carboxylate oxygen, which occurs more frequently in proteins (Ochiai 1991). The Ca^{2+} ion is accommodated by 6 to 7 oxygen atoms at ~2.5 Å in a pentagonal bipyramid geometry (Strynadka and James 1989; Clapham 2007). Most known proteins that bind to Ca^{2+} consist of a EF-hand domain (named after the E and F regions of parvalbumin), which are classical motifs for chelating Ca^{2+} ion (Nakayama and Kretsinger 1994; Clapham 2007; Gifford et al. 2007). The EF-hand motif consists of two roughly orthogonal helices flanking 12 amino acid loop where Ca^{2+} is coordinated to side chains and carbonyl oxygens of five or six invariant residues (Carafoli 2005; Gifford et al. 2007). The proteins with the EF-hand (also known as Ca^{2+} sensors) bind to Ca^{2+} and pass the decoded information to cellular (enzyme) targets (Carafoli 2005).

1.5 Calcium signaling in *N. crassa*

In *N. crassa*, 90% of cellular Ca^{2+} is distributed in different concentrations to the Golgi, endoplasmic reticulum, plasma membrane vesicles, microsomes, and mitochondria (Bowman et al. 2011). Ca^{2+} homeostasis in the cell is maintained by active Ca^{2+}-pumps, Ca^{2+}-transporter proteins, and the Ca^{2+}-buffering capacity of the cytoplasm at a resting concentration or

cytosolic free Ca^{2+} concentration ($[Ca^{2+}]_c$) of ~100 nM (Chin and Means 2000; Bowman et al. 2011; Tamuli et al. 2013). Transient increase in the Ca^{2+} concentration level (500-1000 nM) activates various Ca^{2+} sensing proteins inducing an intracellular signal (Berridge et al. 2000; Bootman et al. 2001).

Genome sequence analysis of *N. crassa* has identified 48 Ca^{2+}-signalling proteins comprised of three Ca^{2+} channel proteins, nine Ca^{2+} cation-ATPases, six recognizable Ca^{2+}/H^+ exchangers, two novel putative Ca^{2+}/Na^+ exchangers, four novel phospholipase C-δ subtype (PLC- δ) proteins, 23 Ca^{2+}/calmodulin regulated proteins, and one calmodulin (Figure 1.4; Table 1.1; Borkovich et al. 2004; Tamuli et al. 2013). The signaling machinery in *N. crassa* significantly differs from plants and animal cells as they lack (a) receptors for second messengers such as inositol-1,4,5-trisphosphate (InsP3), ryanodine and cyclic ADP ribose (cADPR), which are responsible for Ca^{2+} release from internal stores in other plants and animals, and (b) extracellular Ca^{2+}-sensing receptor proteins for sensing changes in the extracellular concentration of Ca^{2+} (Brown et al. 1993; Berridge et al. 2000; Sanders et al. 2002; Bootman et al. 2001; Borkovich et al. 2004). Moreover, both Ca^{2+}/Na^+ exchangers and Ca^{2+}/H^+ exchangers are identified in *N. crassa*, whereas animals possess only Ca^{2+}/Na^+ exchangers and plants possess only $Ca^{2+/}H^+$ exchangers (Borkovich et al. 2004). These differences make the Ca^{2+} signaling system in *N. crassa* unique, with the possibility of novel intracellular Ca^{2+} release mechanisms which are yet to be explored completely.

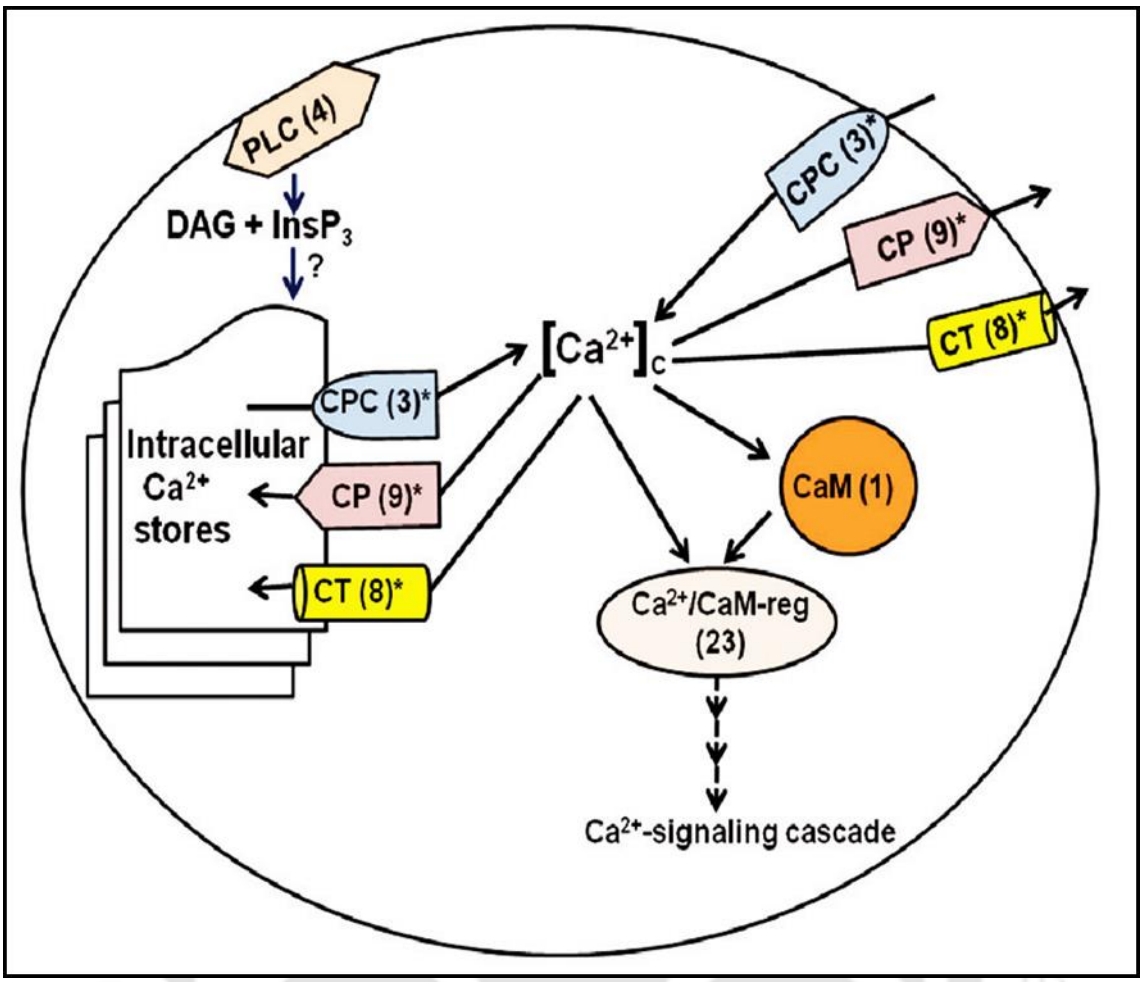

Figure 1.4 Overview of the calcium signaling system in *N. crassa*. CPC, Ca^{2+}-permeable channel; CA, Ca^{2+}-and cation-ATPases; CT, Ca^{2+}/H^{+} and Ca^{2+}/Na^{+} exchanger; CaM, Calmodulin; Ca^{2+}/ CaM-reg, calcium- and calmodulin regulated; PLC, phospholipase C; DAG, diacylglycerol; InsP3, inositol -1,4,5-trisphosphate (Adapted from Tamuli et al. Calcium signaling In: Kasbekar DP, Mc Cluskey (eds). Neurospora: Genomics and Molecular Biology. HP, UK. 2013).

[a] **Table 1.1: Ca^{2+} signaling proteins in *N. crassa***

Sl. No.	NCU No.	Gene name	Protein name	Protein type	Best overall[b] (e-value; organism; protein name; accession number)
1	02762	*cch-1*	Cch-1	Ca^{2+} permeable channel	0; *Verticillium dahlia* (cch1); EGY18507.1
2	06703	*mid-1*	MID-1	Ca^{2+} permeable channel	2e-97; *Paracoccidioides brasiliensis* (MID1); EEH23338.1
3	11680[c]			Ca^{2+} permeable channel	0; *Ajellomyces dermatitidis* (Yvc1); EGE78766.1
4	03305	*nca-1*	NCA-1	Ca^{2+}-ATPase	0; *Trichophyton tonsurans* (SCA-1); EGD96734.1
5	04736	*nca-2*	NCA-2	Ca^{2+}-ATPase	0; *Magnaporthe oryzae* (Plasma membrane calcium transporting ATPase 3); EHA56671.1
6	05154	*nca-3*	NCA-3	Ca^{2+}-ATPase	0; *Glomerella graminicola* (Calcium translocating P-type ATPase); EFQ29373.1
7	03292	*pmr-1*	PMR-1	Ca^{2+}-ATPase	0; *Uncinocarpus reesii* (PMR1); XP_002541437.1
8	08147	*ph-7*	PH-7	Ca^{2+}-ATPase	0; *G. graminicola* (Potassium/sodium efflux Ptype ATPase); EFQ36596.1

9	04898	*trm-9*	TRM-9	Ca^{2+}-ATPase	0; *Cordyceps militaris* (Cation transporting ATPase 4); EGX91104.1
10	03818	*trm-10*	TRM-10	Ca^{2+}-ATPase	0; *V. dahlia* (Neo1p); EGY18069.1
11	07966	*trm-1*	TRM-1	Cation-ATPase	0; *T. tonsurans* (Cta3p); EGD97988.1
12	10143[d]	*atp-11*	ATP-11	Cation-ATPase	0; *C. militaris* (ATPase type 13A2); EGX92563.1
13	07075	*cax*	CAX	Ca^{2+}/H^{+} exchanger	0; *G. graminicola* (Calcium/proton exchanger); EFQ30300.1
14	00916	*trm-15*	TRM-15	Ca^{2+}/H^{+} exchanger	2e-176; *Aspergillus fumigatus* (membrane-bound cation transporter, XP_001481534.1)
15	00795	*trm-14*	TRM-14	Ca^{2+}/H^{+} exchanger	1e-149; *A. niger* (membrane-bound cation transporter, XP_001400827.2)
16	06366	*trm-18*	TRM-18	Ca^{2+}/H^{+} exchanger	0; *Sclerotinia sclerotiorum* (Ca^{2+}/H^{+} antiporter, XP_001589752.1)
17	07711	*trm-19*	TRM-19	Ca^{2+}/H^{+} exchanger	4e-160; *T. tonsurans* (vacuolar calcium ion transporter/H^{+} exchanger, EGD98067.1)
18	05360	*trm-17*	TRM-17	Ca^{2+}/H^{+} exchanger	0; *Metarhizium anisopliae* (calcium permease, EFY95914.1)

19	02826	*trm-16*	TRM-16	Ca^{2+}/Na^{+} exchanger	0; *Verticillium albo-atrum* (sodium/calcium exchanger protein, XP_003004985.1)
20	08490	*trm-20*	TRM-20	Ca^{2+}/Na^{+} exchanger	1e-83; *A. niger* (sodium/calcium transporter, XP_001397155.1)
21	01266	*plc-2*	PLC-2	Phospholipase C	0; *Sordaria macrospora* (phosphoinositide-specific phospholipase C, XP_003348116.1)
22	06245	*plc-1*	PLC-1	Phospholipase C	0; *G. graminicola* (phosphatidylinositol-specific phospholipase C, EFQ28596.1)
23	11415[e]	*inl-7*	INL-7	Phospholipase C	0; *G. graminicola* (Phosphatidylinositol-specific phospholipase C); EFQ31595.1
24	02175	*inl-15*	INL-15	Phospholipase C	3e-125; *Botryotinia fuckeliana* (BcPLC2); CCD34776.1
25	04120	*cmd*	CaM	Calmodulin	1e-103; *Gibberella zeae* (CaM); XP_382067.1
26	03804	*cna-1*	CNA-1	Ca^{2+} and/or CaM binding protein	0; *Sordaria macrospora* (Serine/threonine-protein phosphatase 2B catalytic subunit protein, XP_003352213.1)

27	03833	*cnb-1*	CNB-1	Ca^{2+} and/or CaM binding protein	2e-119; *Trichoderma reesei* (calcineurin, beta subunit, EGR44907.1)
28	09265	*cnx-1*	CNX-1	Ca^{2+} and/or CaM binding protein	0; *S. macrospora* (cnx1, XP_003347545.1)
29	05225[f]	*nde1*	NDE-1	Ca^{2+} and/or CaM binding protein	0; *M. oryzae* (mitochondrial NADH dehydrogenase, EHA47323.1)
30	02115			Ca^{2+} and/or CaM binding protein	0; *M. oryzae* (EF hand domain-containing protein, EHA48778.1)
31	01564	*mic-4*	MIC-4	Ca^{2+} and/or CaM binding protein	0; *M. oryzae* (calcium dependent mitochondrial carrier protein, EHA48778.1)
32	06948			Ca^{2+} and/or CaM binding protein	2e-54; *Mycosphaerella graminicola* (calcium ion binding, calmodulin, EGP88834.1)
33	04379	*ncs-1*	NCS-1	Ca^{2+} and/or CaM binding protein	4e-126; *Grosmannia clavigera* (neuronal calcium sensor 1, EFX03580.1)
34	02738	*pef-1*	PEF-1	Ca^{2+} and/or CaM binding protein	2e-130; *V. dahliae* (Peflin, EGY21808.1)
35	09871	*nup-34*	NUP-34	Ca^{2+} and/or CaM binding protein	4e-33; *V. dahliae* (Centrin-3,EGY16271.1)

36	01241	*mic-2*	MIC-2	Ca^{2+} and/or CaM binding protein	0; *T. reesei* (mitochondrial carrier protein, EGR44893.1)
37	06347	*ask-2*	ASK-2	Ca^{2+} and/or CaM binding protein	0; *S. macrospora* (actin cytoskeleton–regulatory complex protein, XP_003350109.1)
38	06617	*cdc4-2*	CDC4-2	Ca^{2+} and/or CaM binding protein	7e-93; *V. albo-atrum* (myosin regulatory light chain cdc4, XP_003009631.1)
39	03750	*cmd-2*	CMD-2	Ca^{2+} and/or CaM binding protein	8e-74; *B. fuckeliana* (calmodulin, XP_001560827.1)
40	08980	*nde-2*	NDE-2	Ca^{2+} and/or CaM binding protein	0; *G. clavigera* (alternative NADH-dehydrogenase, EFX03867.1)
41	02283	*camk-2*	CaMK-2	Ca^{2+} and/or CaM binding protein	0; *S. macrospora* (calcium/calmodulin-dependent protein kinase type I, XP_003344498.1)
42	09123	*camk-1*	CaMK-1	Ca^{2+} and/or CaM binding protein	0; *Sporothrix schenckii* (calcium/calmodulin-dependent kinase, AAV80434.1
43	09212	*camk-4*	CaMK-4	Ca^{2+} and/or CaM binding protein	0; *G. clavigera* (serine/threonine-protein kinase chk2, EFX01629.1)
44	02814	*prd-4*	PRD-4	Ca^{2+} and/or CaM binding protein	0; *V. dahliae* (serine/threonine-protein kinase srk1, EGY15110.1)

45	06650	*spp-3*	SPP-3	Ca^{2+} and/or CaM binding protein	3e-61; *Nectria haematococca* (phospholipase A2, XP_003042542.1)
46	02411			Ca^{2+} and/or CaM binding protein	0; *G. graminicola* (microtubule-associated protein, EFQ31793.1)
47	06177	*camk-3*	CaMK-3	Ca^{2+} and/or CaM binding protein	0; *M. grisea* (CMKK2, ACM41720.1)
48	04265	*inv*	INV	Ca^{2+} and/or CaM binding protein	7e-85; *Bacillus megaterium* (betafructosidase FruA, AEN90524.1)

[a]Adapted from Tamuli *et al*, 2013.

[b]BLASTp search was performed at NCBI (http://blast.ncbi.nlm.nih.gov/Blast.cgi ; Altschul et al. 1990, 1997, 2005) with default parameters for each of the 48 Ca^{2+} signaling proteins against the non-redundant protein sequence databases and the respective best overall match in other organisms with *e*-value has been indicated.

[c]Split from NCU07605.1

[d]Split from NCU01437.1

[e]Split from NCU0955.1

[f]NCU05225.5 (was indicated as NCU08980.1 in Borkovich et al. 2004)

1.6 Calmodulin

Calmodulin (CaM) is a ubiquitous and the primary Ca^{2+} binding protein expressed in all eukaryotes and regulates various cell processes (Stevens 1983, Walsh 1983; Stigler and Rief 2012). It was discovered as an activator of cyclic nucleotide phosphodiesterase in brain and heart (Cheung 1970; Kakiuchi and Yamazaki 1970). CaM is a small ~17 kDa acidic protein consisting of two homologous EF-hand domains which can bind to four Ca^{2+} ions with binding affinities K_i (Inhibition constant) ranging from 10^{-4} to 10^{-6} M (Babu et al. 1988; Meador et al. 1993; Lewit-Bentley and Réty 2000; Liu et al. 2019). CaM domain structure consists of an N-terminal and a C-terminal lobes arranged in a trans configuration, each lobe is composed of a pair of EF-hands, helix-loop-helix motifs connected by a highly flexible central α helix (Hoeflick et al. 2002). The loop in each EF-hand motif is characterized by a sequence of 12 residues, where the 1(+X), 3(+Y), 5(+Z), 7(−Y), 9(−X), 12(−Z) residues provide the oxygen ligands for Ca^{2+} co-ordination (Figure 1.5 A; Lewit-Bentley and Rety 2000; Gifford et al. 2007). In the absence of Ca^{2+}, CaM is referred to as apocalmodulin (ApoCaM), with the two domains adopting ‘closed’ (N-terminal) and ‘semiopen’ (C-terminal) conformations (Jurado et al. 1999; Chin and Means 2000). The binding of Ca^{2+} to CaM (Holo CaM) causes changes in the conformations of both the EF-hand domain from the closed to open configuration (Figure 1.5 B) and results in the exposure of hydrophobic groups for Ca^{2+}-dependent interactions with a myriad of target proteins (Chin and means 2000; Zhang et al. 2012).

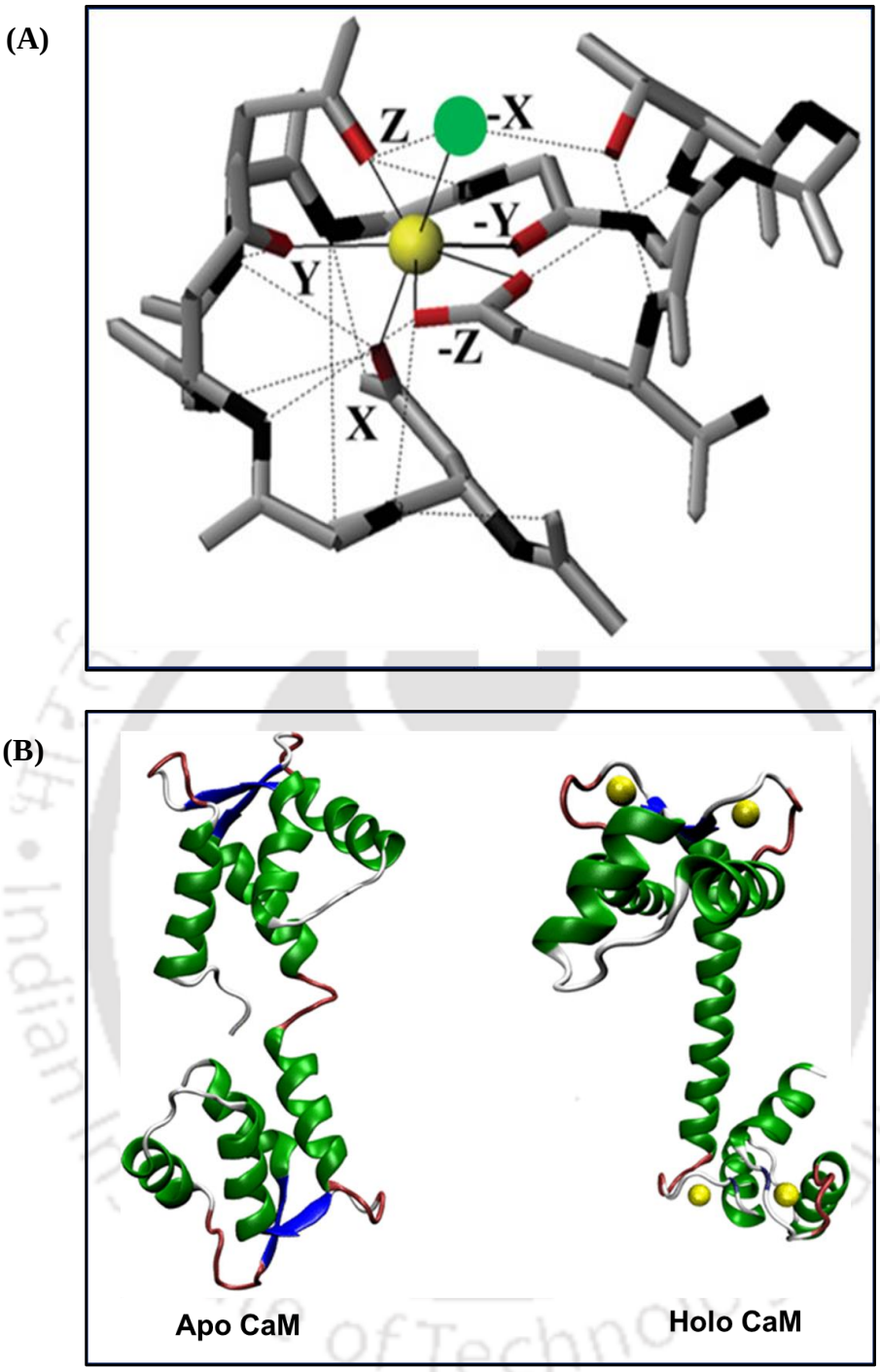

Figure 1.5 Ca^{2+} co-ordination and schematic structure of calmodulin. (A) Ca^{2+} co-ordination by the canonical EF-hand (EF1 of CaM). The continuous lines illustrate the pentagonal bipyramidal co-ordination of the Ca^{2+} ion (yellow) and the broken lines depict the extensive hydrogen bonding pattern found in the loop (Adapted from Gifford et al. 2007). **(B)** Calmodulin in the Ca^{2+}-free or apo state and the Ca^{2+}-bound or holo state. Two lobes are

connected by a linker, and each lobe has two Ca^{2+} (yellow) binding sites (Adapted from Basit et al. 2022).

The mechanisms by which CaM interacts and regulates its target proteins are diverse (Tidow and Nissen 2013). Based on the mode of regulation, CaM-binding proteins can be categorized into at least six classes; (A) proteins that binds irreversibly to CaM irrespective of Ca^{2+} (e. g. phosphorylase kinase) , (B) proteins that bind to CaM in the absence of Ca^{2+} (i. e. to the apo-CaM form), but dissociate reversibly in the presence of Ca^{2+}(e. g. neuromodulin and neurogranin), (C) effectors that form low-affinity, inactive complexes with CaM at low concentrations of Ca^{2+}, when CaM is unoccupied or partially occupied by Ca^{2+} (e. g. smooth-muscle myosin-light-chain kinase (MLCK) and calcineurin), (D) effectors that binds to CaM in the presence of Ca^{2+}, but, in this case, CaM inhibits their function (e. g. G-protein-receptor kinases and inositol (1,4,5)-trisphosphate receptor type 1), (E) effectors that exhibit more conventional behaviour and are activated by Ca^{2+}-CaM (e. g. CaM-dependent protein kinases I, II, and IV), (F) one CaM-dependent protein (class E) is directly regulated by another CaM-dependent protein demonstrating the convergence of different CaM-regulated pathways (Chin and Means 2000). The Ca^{2+}-CaM binding domain sequences in different target proteins show less similarity (Jurado et al. 1999). The CaM binding sites known as CaM recruitment signaling (CRS) motifs are typically hydrophobic and basic in nature consisting of 15-30 amino acid residues that form an α-helix (Yap et al. 2000). Based on the CRS motif found in 180 protein sequences, CaM binding proteins are divided into four different subclasses: 3 predominantly Ca^{2+}-dependent motifs (1-10, 1-14, 1-16) and IQ motif, which is typically independent of calcium concentration; each subclass representing a distinct structural mode of molecular recognition of CaM (Yap et al. 2000; Minhas and Ben-Hur 2012). Thus, by activating over 300 proteins, CaM plays a fundamental role in regulating various cellular functions from fungi to

mammals (Jurado et al. 1999; Tidow and Nissen 2013; Halling et al. 2016). The roles of calmodulin in different fungi (Table 1.2) and higher eukaryotes (Table 1.3) are enlisted below.

Table 1.2 Cellular roles of CaM in different fungi

Sl. No.	Organism	Functions	Reference
1	*Saccharomyces cerevisiae*	Essential for growth, mitotic spindle formation, induced thermotolerance, cell cycle progression, stress responses, and antifungal drug resistance	Davis et al. 1986; Anraku et al. 1991; Sun et al. 1992; Geiser et al. 1993; Stirling et al. 1994; Iida et al. 1995; Cyert 2001; Edlind et al. 2002; Kahl and Means 2003; Kim et al. 2016
2	*Schizosaccharomyces pombe*	Essential for cell growth, nuclear division, and sporulation	Takeda and Yamamoto 1987; Takeda et al. 1989; Moser et al. 1997; Flory et al. 2002; Itadani et al. 2010
3	*Aspergillus nidulans*	Essential for growth, germination, apical organization, conidiation, nuclear division, and cell cycle progression	Rasmussen et al. 1990,1992; Lu et al. 1992,1995; Wang et al. 2006; Chen et al. 2010
4	*Candida albicans*	Morphogenesis, phospholipid biosynthesis, yeast to mycelial	Roy and Datta 1987; Sabie and Gadd 1989; Krajewska-Kułak and Niczyporuk 1993; Sharma

		transition, cell cycle progression, stress response, virulence, and drug resistance	et al. 2001; Dhillon et al. 2003; Kraus and Heitman 2003; Sato et al. 2004; Davis et al. 2013; Park et al. 2019
5	*Cryptococcus neoformans*	Essential for growth, virulence, morphogenesis, and stress response	Kraus et al. 2005; Brown et al. 2007; Kuzubowski et al. 2009; Park et al. 2019
6	*Ceratocystis ulmi*	Mycelial growth and yeast to mycelium dimorphism	Muthukumar and Nickerson 1984, 1985; Muthukumar et al. 1986
7	*Magnaporthe grisea*	Essential for growth and appressorium formation	Lee and Lee 1998; Liu and Kolattukudy 1999; Ma et al. 2009
8	*Colletotrichum trifolii*	Spore germination and appressorium formation	Warwar and Dickman 1996
9	*Fusarium sp.*	Hyphal extension and branching, germ-tube formation, and cell fusion	Robson et al. 1991; Kurian et al. 2022
10	*Beauveria bassiana*	Stress response and secondary metabolite production	Kim et al. 2016, 2017; Kim et al. 2019

Table 1.3 Cellular roles of CaM in higher eukaryotes

Sl. No.	Organisms	Functions	References
1	*Arabidopsis thaliana*	Gravitropic sensing and transduction, pollen germination, ROS homeostasis, stress response, and senescence	Sinclair et al. 1996; Golovkin and Reddy 2003; Magnan et al. 2008; Takahashi et al. 2011; Dai et al. 2018
2	*Caenorhabditis elegans*	Essential for embryonic growth and development and fertility	Karabinos et al. 2003
3	*Homo sapiens*	Cell proliferation, cell motility, synaptic strength, maintaining cardiac functions, and apoptosis	Kikuchi et al. 1984; Pan et al. 1999; Wu et al. 2005; Pang et al. 2010; Sorensen et al. 2013; Berchtold et al. 2014; Jensen et al. 2018

1.7 CaM in *N. crassa*

In *N. crassa*, only a single CaM protein was isolated using affinity chromatography, and it was identified based on the characteristics of Ca^{2+} dependent shift in electrophoretic migration, activation of bovine heart CAMP phosphodiesterase (PDE), and distinct peaks (located at 276, 268, 264, 258 and 252 nm) in an absorption spectrum (Perez et al. 1981). The *N. crassa* CaM shows 59% homology to yeast, 85% homology to the human CaM protein, and differs from *Aspergillus nidulans* CaM by a single amino acid (Rasmussen et al. 1990, Melnick et al. 1993). The *N. crassa* CaM is encoded by a single copy gene NCU04120, which contains five introns and six exons that translate to form a 149 amino acid residues protein of 16.95 kDa (Figure 1.6; Capelli et al. 1993; Melnick et al. 1993; Galagan et al. 2003; Tamuli et al. 2013). *N. crassa* CaM resembles plant CaM consisting of typical amino acid composition as that of plant CaMs, with the exception that trimethyllysine is absent and the serine content is unusually high (Cox et al. 1982). Compared to vertebrate calmodulin, *N. crassa* CaM is less acidic but shows similar Ca^{2+}-binding properties and can fully activate heart phosphodiesterase and smooth myosin light chain kinase of vertebrates (Perez et al. 1981; Cox et al. 1982). In *N. crassa*, CaM is essential for viability (Tamuli et al. 2013). Earlier reports showed that CaM is important for the activation of soluble adenylate cyclase, protein kinase, cyclic CAMP phosphodiesterase, and protein phosphatase (Reig et al. 1984; Van Tuinen et al. 1984; Tellez-Inon et al. 1985; Higuchi et al. 1991). In addition, the inhibition of CaM using trifluoperazine (TFP), chlorpromazine (CPZ), and W7 affected light-induced phase shifting, activation of chitin synthase enzyme, vegetative growth, hyphal development, and sexual development in *N. crassa* (Suzuki et al. 1996; Sadakane and Nakashima 1996; Suresh and Subramanyan 1997; Laxmi and Tamuli 2015). Moreover, the repeat-induced point mutation (RIP) strain of *cmd,* Δ*pan-2*::*bar*::$P_{tcu\text{-}1}$::cmd^{RIP}::*V5*::*gfp* (#26) showed that *cmd* is important for normal vegetative growth, carotenoid

accumulation, ultraviolet (UV) survival, and sexual development in *N. crassa* (Laxmi and Tamuli 2017).

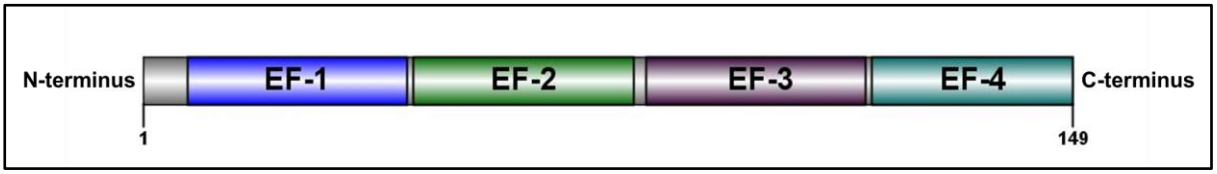

Figure 1.6 Domain organization of *N. crassa* CaM. The domain organization of CaM (149 amino acids) consists of four EF-hands that bind to four Ca^{2+}. The domain organization of CaM (Accession No. P61859) is represented using the IBS 1.0 illustrator (Liu et al. 2015).

1.8 Calcium/calmodulin-dependent kinases

In response to Ca^{2+} stimulus, CaM interacts with numerous proteins and enzymes involved in all aspects of cellular functions (James et al. 1995). The kinases belonging to the multifunctional enzyme family called Ca^{2+}/CaM-dependent kinases (Ca^{2+}/CaMKs) are one of the main effector proteins of CaM, which are ubiquitous to all eukaryotic cells (Braun and Schulman 1995; Bredow and Monaghan 2022). Ca^{2+}/CaMKs are serine /threonine protein kinases that catalyze the transfer of phosphate from the gamma position of ATP to the hydroxyl group of Ser/Thr within protein substrates (Swulius and Waxham 2008). Based on their substrate specificity, Ca^{2+}/CaMKs are classified into two groups; the broad substrate specificity group are multifunctional Ca^{2+}/CaMKs that can phosphorylate several substrates and include kinases such as CaMKK, CaMKI, CaMKII, and CaMKIV. The narrow substrate specificity group consists of dedicated Ca^{2+}/CaMKs with a single substrate, such as CaMKIII and MLCK (Hook and Means 2001). Both groups have a similar domain organization (Swulius and Waxham 2008). The general domain architecture of Ca^{2+}/CaMKs includes a highly conserved N-terminal kinase domain followed by a C-terminal regulatory region that consists of an

autoinhibitory domain overlapped by the Ca^{2+}-CaM binding domain (Figure 1.7; Braun and Schulman 1995; Hook and Means 2001; Swulius and Waxham 2008; Tamuli et al. 2011).

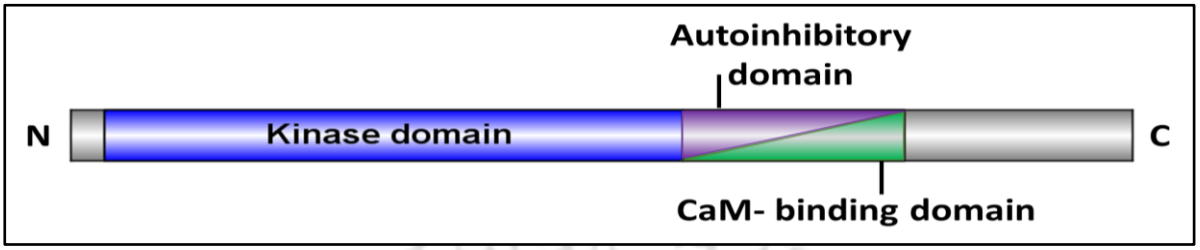

Figure 1.7 Domain organization of calcium/calmodulin-dependent kinases (Ca^{2+}/CaMKs). Ca^{2+}/CaMKs contain an N-terminal kinase domain (blue), followed by an autoinhibitory (purple) and overlapping CaM-binding domain (green), (Adapted from Tamuli et al. 2011).

Ca^{2+}/CaMKs are activated upon binding of the Ca^{2+}-CaM complex to the CaM binding domain, which disrupts the interaction of specific residues releasing the autoinhibition (Griffith 2004). In addition to activation by binding of Ca^{2+}-CaM, Ca^{2+}/CaMKs can be further regulated by phosphorylation and autophosphorylation by some other kinases (Hook and Means 2001). CaMKK activates CaMKI and CaMKIV by phosphorylating their "activation loop" consisting of serine/threonine residues, resulting in increased activity of the kinases (Tokomitsu et al. 1995). The role of Ca^{2+}/CaMKs in different fungi (Table 1.4) and higher eukaryotes are listed below (Table 1.5).

Table 1.4 Cellular roles of Ca^{2+}/CaMKs in different fungi

Sl. No.	Organisms	Functions	Reference
1	*S.cerevisiae*	Spore germination, induced thermotolerance, survival of pheromone induced growth arrest, calcium homeostasis, stress response, drug resistance, and antideath activity	Pausch et al. 1991; Iida et al. 1995; Moser et al. 1996; Holyoak et al. 2000; Dudgeon et al. 2008; Coleman et al. 2022
2	*S. pombe*	Cell cycle progression	Rasmussen and Rasmussen 1994; Rasmussen 2000
3	*A. nidulans*	Hyphal growth and nuclear division	Dayton and Means 1996; Joseph and Means 2000
4	*Colletotrichum gloeosporioides*	Conidial germination and appressorium formation	Kim et al. 1998
5	*Sporothrix schenckii*	Thermotolerance and dimorphism	Valle-Aviles et al. 2007; Rodriguez-Caban et al. 2011
6	*Arthrobotrys oligospora*	Growth, conidiation, environmental stress tolerance, trap formation, and virulence	Zhen et al. 2019
7	*Penicillium italicum*	Vegetative growth, conidiation, virulence, and environmental stress tolerance	Li et al. 2022

Table 1.5 Cellular roles of Ca^{2+}/CaMKs in higher eukaryotes

Sl. No.	Organism	Functions	Reference
1	*Zea mays*	Light-regulated gravitropism, growth and development, antioxidant defense, and drought tolerance	Lu et al.1996; Wang et al. 2001; Zhu et al. 2016; Liu et al. 2021
2	*Caenorhabditis elegans*	Locomotion, behavioural clock, neurotransmitter release and synaptic strength, learning, and habituation	Reiner et al. 1999; Robatzek and Thomans 2000; Liu et al. 2007; Ardiel et al. 2018
3	*Homo sapiens*	Learning and memory, sperm motility, modulate skeletal muscle during exercise, maintaining normal cardiac functions, immune response, cell growth and proliferation, and apoptosis	Kirchhefer et al. 1999; Hudmon and Schulman 2002; Marín-Briggiler et al. 2005; Rose et al. 2006; Maier and Bers 2007; Timmins et al. 2009; Fischer et al. 2013; Koga and Kawakami 2018; Naz et al. 2019

1.9 Ca^{2+}/CaMKs in *N. crassa*

In *N. crassa*, there are four Ca^{2+}/CaMKs, namely *camk-1*, *camk-2*, *camk-3*, and *camk-4* (Tamuli et al. 2011). All four Ca^{2+}/CaMKs belong to the broad substrate specificity group, having a CaM binding domain and 11 conserved kinase domains (Kumar and Tamuli 2014). Earlier studies revealed that *camk-1* plays a role in growth, circadian clock, and fertility (Yang et al. 2001; Deka et al. 2011; Tamuli et al. 2011). Another Ca^{2+}/CaMK, *camk- 2*, was found to be involved in fertility (Deka et al. 2011; Tamuli et al. 2011, 2013). In addition, Ca^{2+}/CaMKs also play a role in stress responses in *N. crassa* (Kumar and Tamuli 2014). Furthermore, CaMK-1 was shown to phosphorylate the circadian clock protein FREQUENCY (FRQ) and the deletion of *camk-1* affected the light-induced phase shifting of the circadian conidiation rhythm in *N. crassa* (Yang et al. 2001).

1.10 Objective of this study

In higher eukaryotes, CaM and Ca^{2+}/CaMKs are important for regulating various cellular processes such as growth, cell proliferation, circadian rhythm, fertility, immune responses, apoptosis, and many other functions. In fungi, CaM and Ca^{2+}/CaMKs are necessary for various cell functions, including nuclear division, germination, growth development, and stress responses. Notably, common and divergent functions of homologous proteins in different species suggest that in many cases, the physiological role of a protein in one species is not conserved in other species (Lange and Peiter 2020). Preliminary studies of CaM and Ca^{2+}/CaMKs in *N. crassa* demonstrated their involvement in stress response, sexual development, and in regulating the circadian system (Yang et al. 2001; Kumar and Tamuli 2014; Laxmi and Tamuli 2015, 2017). However, the role and mechanism or the pathway by which CaM and Ca^{2+}/CaMKs regulate the cell during the different phases of life cycle and under different conditions are not clearly understood in *N. crassa*. Therefore, investigating the

detailed cellular roles and mechanism of CaM and Ca^{2+}/CaMKs during different stress conditions, sexual development, circadian clock, and identifying their downstream targets under specific conditions will help to understand how they regulate stress responses, asexual and sexual developments in *N. crassa.*

To understand the role and molecular mechanism of CaM and Ca^{2+}/CaMKs in *N. crassa*, the thesis work was divided into following three broad objectives.

The broad objectives of this thesis are:

1. To investigate the cellular roles and mechanism of CaM and Ca^{2+}/CaMKs in coping with stress conditions in *N. crassa*,
2. To determine the functions of the CaM and Ca^{2+}/CaMKs during sexual development in *N. crassa*, and
3. Understanding the molecular details of calmodulin, the transcriptional regulation of the heat shock and the pheromone response pathways in *N. crassa*.

CHAPTER 2

Materials and Methods

2.1 Materials

2.1.1 Chemicals and other materials

All laboratory chemicals and reagents such as ammonium iron (II) sulfate hexahydrate [$Fe(NH_4)_2(SO_4)_2.6H_2O$], ammonium nitrate (NH_4NO_3), L-arginine ($C_6H_{14}O_2$), bathocuproinedisulfonic acid disodium salt ($C_{26}H_{18}N_2Na_2O_6S_2$), D-biotin ($C_{10}H_{16}N_2O_3S$), boric acid ($H_3BO_3$), calcofluor white stain, calcium chloride ($CaCl_2.H_2O$), calcium D-pantothenate ($C_{18}H_{32}CaN_2O_{10}$), cetyltrimethyl ammonium bromide (CTAB, $C19H_{42}NBr$), chloroform ($CHCl_3$), chlortetracycline hydrochloride ($C_{22}H_{24}Cl_2N_2O_8.HCl$), citric acid monohydrate ($C_6H_8O_7.H_2O$), copper sulphate pentahydrate ($CuSO_4.5H_2O$), diethyl pyrocarbonate (DEPC, $C_6H_{10}O_5$), dimethyl sulphoxide (DMSO, C_2H_6OS), dithiothreitol (DTT, $C_4H_{10}O_2S_2$), absolute ethanol (C_2H_5OH)), ethidium bromide (EtBr, $C_{21}H_{20}BrN_3$), ethylenediaminetetra acetic acid disodium salt dihydrate (EDTA, $C_{10}H_{14}N_2Na_2O_8.2H_2O$), ferrous sulphate heptahydrate ($FeSO_4.7H_2O$), formaldehyde (CH_2O), fructose ($C_6H_{12}O_6$), glacial acetic acid (CH_3COOH), D-glucose ($C_6H_{12}O_6$), glufosinate ammonium (Basta, $C_5H_{15}N_2O_4P$), glycerol ($C_3H_8O_3$), hydrochloric acid (HCl), isopropanol (C_3H_7OH), lithium chloride (LiCl), magnesium chloride ($MgCl_2$) magnesium sulphate heptahydrate ($MgSO_4.7H_2O$), manganous chloride tetrahydrate ($MnCl_2.4H_2O$), manganous sulphate ($MnSO_4.H_2O$), β-mercaptoethanol (C_2H_6OS), 3-(N-Morpholino) propanesulfonic acid (MOPS, $C_7H_{15}NO_4S$), NP-40, 1,4-Piperazinediethanesulfonic acid (PIPES, $C_8H_{18}N_2O_6S_2$), Phenol: Chloroform: Isoamyl mixture (25:24:1), N-Phenyl-1-napthylamine ($C_{10}H_7NHC_6H_5$), potassium acetate (CH_3COOK), potassium hydroxide (KOH), potassium nitrate (KNO_3), potassium phosphate dibasic (K_2HPO_4), potassium phosphate monobasic (KH_2PO_4), silica gel (6-12 mesh), sodium bicarbonate ($NaHCO_3$), sodium chloride (NaCl), sodium citrate dihydrate ($Na_3C_6H_5O_7.2H_2O$), sodium dodecyl sulphate (SDS, $NaC_{12}H_{25}SO_4$), sodium hydroxide (NaOH), sodium molybdate ($Na_2MoO_4.2H_2O$), sodium nitrate ($NaNO_3$), D-sorbitol ($C_6H_{14}O_6$),

sorbose ($C_6H_{12}O_6$), sucrose ($C_{12}H_{22}O_{11}$), Tris base ($C_4H_{11}NO_3$), Triton X-100, and zinc sulphate heptahydrate ($ZnSO_4.7H_2O$) were procured from various manufacturers such as Fischer scientific (USA), Himedia (Mumbai, India), Loba Chemie (Mumbai, India), Merck (Mumbai, India), Sigma Aldrich (USA), SRL (Mumbai, India) and RANKEM (Haryana, India).

Media for bacterial growth such as Luria-Bertani (LB) agar and broth and Super Optimal broth with Catabolite repression (SOC); skimmed milk powder; antibiotics like ampicillin and hygromycin B solution; bacto-agar were obtained from Himedia (Mumbai, India). Agarose, TRIzol™ reagent, SYBR Green Real-Time PCR Master Mix and nuclease-free water were purchased from Life Technologies (USA). All restriction enzymes, DNA size markers, Blue Gel Loading Dye (6X), Quick Ligation™ Kit, routine Taq DNA polymerase, Phusion® High-Fidelity DNA Polymerase and Dynazyme II DNA polymerase for PCRs were purchased from New England Biolabs (USA) and Themo scientific (USA). Kits for Plasmid DNA isolation, Gel purification and PCR Clean-up were obtained from Qiagen (USA) and from GCC Biotech (Kolkata, India). Verso cDNA synthesis kit was purchased from Thermo Fisher Scientific (USA). Glasswares were purchased from Borosil (Mumbai, India), and Jain scientific glassworks (Ambala, India). Plasticwares were procured from Tarsons (Kolkata, India) and Genaxy (New Delhi, India).

2.1.2 Organisms and strains used in this study

2.1.2.1 *N. crassa* strains

N. crassa strains used in this study were either obtained from the Fungal Genetics Stock Centre or generated in our laboratory (Table 2.1). The *pp-1*^{KO} heterokaryotic strain (FGSC 21335) was a gift from Prof. Qun He of State Key Laboratory of Agrobiotechnology, College of Biological Sciences, China Agricultural University, Beijing, China.

Table 2.1 List of strains used in the study

Sl. No.	Strains	Strain type or NCU no.	Genotype	Reference
1	74-OR23-IVA	Wild type	Wild type; *mat A*	FGSC 2489
2	ORS-SL6a	Wild type	Wild type; *mat a*	FGSC 4200
3	Δ*camk-1*	09123	Δ*camk-1*::*hph*; *mat A*	FGSC 12547
4	Δ*camk-1*	09123	Δ*camk-1*::*hph*; *mat a*	FGSC12548
5	Δ*camk-2*	02283	Δ*camk-2*::*hph*; *mat a*	FGSC 12448
6	Δ*camk-2*	02283	Δ*camk-2*::*hph*; *mat A*	FGSC 12449
7	Δ*camk-3*	06177	Δ*camk-3*::*hph*; *mat A*	FGSC 11536
8	Δ*camk-3*	06177	Δ*camk-3*::*hph*; *mat a*	FGSC 11537
9	Δ*camk-4*	09212	Δ*camk-4*::*hph*; *mat a*	FGSC 11545
10	Δ*camk-4*	Homokaryotic	Δ*camk-4*::*hph*; *mat A*	Our Laboratory
11	*850 a*	Homokaryotic	Δ*rid-1*::*nat*; Δ*pan-2*::P_{tcu-1}::*cmd*::*V5*::*gfp*; *mat a*	Our laboratory (Laxmi et al. 2017)
12	*26*	Homokaryotic	Δ*pan-2*::*bar*::P_{tcu-1}::cmd^{RIP}::*V5*::*gfp*; *mat A*	Our laboratory (Laxmi et al. 2017)
13	P-4	Homokaryotic	Δ*camk-1*::*hph*; Δ*mus-53*::*hph*; *mat A*	Our Laboratory

14	P-13	Homokaryotic	Δ*mus-53*::*hph*; Δ*camk-2*::*hph*; *mat A*	Our Laboratory
15	19	Homokaryotic	Δ*camk-1*; Δ*pan-2*::P_{nit-6}::*camk-1*::*V5*::*gfp*; *mat A*	Our Laboratory
16	8	Homokaryotic	Δ*camk-2*; Δ*pan-2*::P_{nit-6}:: *camk-2*::*V5*::*gfp*; *mat A*	Our Laboratory
17	1858	Homokaryotic	*ras-1*^{bd}; *mat a*	FGSC 1858
18	1859	Homokaryotic	*ras-1*^{bd}; *mat A*	FGSC 1859
19	Δ*camk-1; ras-1*^{bd} (11)	Homokaryotic	Δ*camk-1*; *ras-1*^{bd} ; *mat A*	Our Laboratory
20	*ras-1*^{bd} ; Δ*camk-2* (15)	Homokaryotic	*ras-1*^{bd} ; Δ*camk-2*; *mat A*	Our Laboratory
21	Δ*camk-3; ras-1*^{bd} (22)	Homokaryotic	Δ*camk-3*; *ras-1*^{bd} ; *mat A*	Our Laboratory
22	Δ*camk-4; ras-1*^{bd} (31)	Homokaryotic	Δ*camk-4*; *ras-1*^{bd} ; *mat A*	Our Laboratory
23	*ras-1*^{bd}; *cmd*^{RIP} (19)	Homokaryotic	*ras-1*^{bd}; *cmd*^{RIP} (19) ; *mat A*	Our Laboratory
25	21335	Heterokaryotic	Δ*pp-1*::*hph*; *mat a*	Prof. Qun He Lab
26	Δ*pp-1*(3)	Homokaryotic	Δ*pp-1*::*hph*; *mat A*	Our Laboratory
27	Δ*pp-1*(11)	Homokaryotic	Δ*pp-1*::*hph*; *mat a*	Our Laboratory

2.1.2.2 Bacterial strains

For routine bacterial cloning, transformations, plasmid growth and isolation, the *Escherichia coli* DH5α strain with genotype *SupE*44 Δ*lac*U169 (φ80*lacZ* ΔM15) *hsdR*17 *recA*1 *end A*1 *gyrA*96 *thi*-1 *relA*1 was used (Sambrook and Russel 2001).

2.1.2.3 Plasmid Vector

1. **pRS426PVG/pnit-6_1.5 kb:** This vector consists of the backbone from the yeast/*E. coli* shuttle vector pRS426PVG (Ouyang et al. 2015). The pRS426PVG/pnit-6_1.5 kb vector (Figure 2.1) confer uracil prototrophy to *ura-3* yeast mutant (URA3) and ampicillin resistance (Ap^R) in *E. coli*. The pRS426PVG/pnit-6_1.5 kb vector contains the *N. crassa* nitrogen-controlled *nit-6* (NCU04720) promoter (P_{nit-6}), 5' and 3' flanking regions of the *N. crassa pan-2* (NCU10048) ORF surrounding P_{nit-6}, a multiple cloning site (MCS), a 5xGly linker, a V5 peptide tag and the *gfp* gene. It also contains *bar* gene as the selection marker, which confer resistance to glufosinate ammonium commonly known as Basta® or Ignite®. P_{nit-6} is repressed by glutamine and induced by the addition of $NaNO_3$ in the medium as a nitrogen source (Exley et al. 1993; Ouyang et al. 2015).

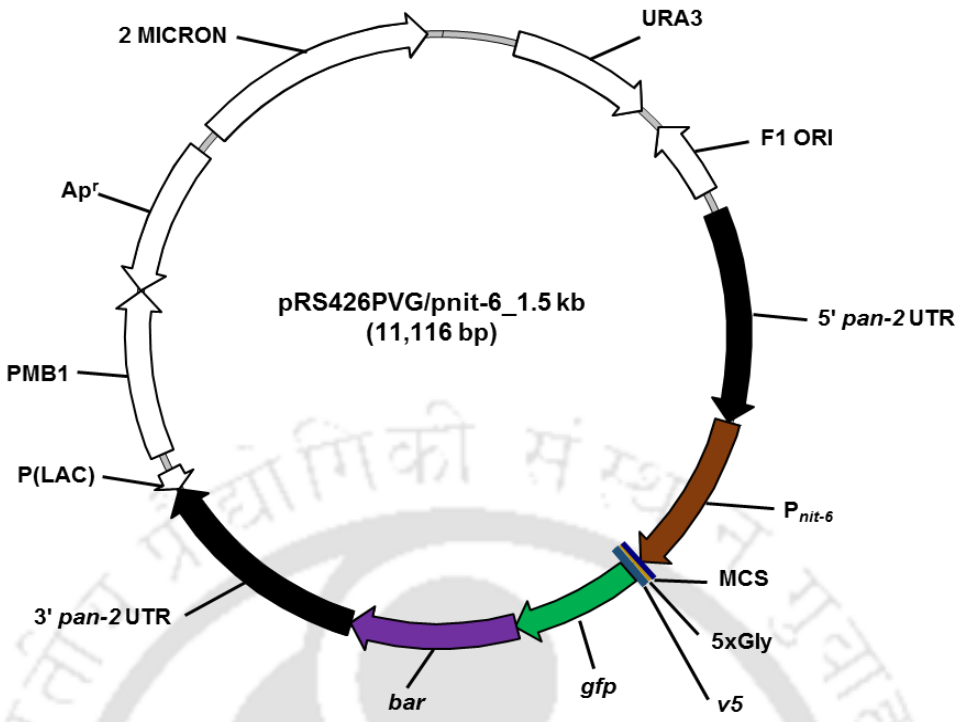

Figure 2.1 Schematic of the pRS426PVG/pnit-6_1.5 kb. The vector size is 11,116 bp and described previously by Ouyang et al. (2015).

2.1.3 Media for bacterial growth

LB broth and agar, Terrific broth, and SOC media were purchased from Himedia (Mumbai, India) and were prepared in distilled water as per the manufacturer's protocol. All the bacterial media were sterilized by autoclaving.

2.1.4 Antibiotics and other commonly used solutions

The solutions described below were prepared as described by Sambrook and Russell 2001.

1. **Ampicillin:** A stock solution of 100 mg/ml was prepared by dissolving 100 mg of ampicillin powder in 1 ml sterile double-distilled water and stored at -20 °C.
2. **Hygromycin B:** A ready-to-use solution of 50 mg/ml Hygromycin B from Himedia (Mumbai, India) was used.

3. **Glufosinate ammonium (Basta):** A stock solution of 100 mg/ml was prepared by dissolving 100 mg of glufosinate ammonium in 1 ml sterile distilled water and stored at -20 °C.
4. **Calium-D-Pantothenate solution:** A stock solution of 1 mg/ml, was prepared by dissolving 100 mg of calcium D-pantothenate was dissolved in 100 ml of distilled water, sterilized by autoclaving and stored at 4 °C.
5. **Bathocuproinedisulfonic acid disodium salt (BCS) solution:** A stock solution of 0.2 M was prepared by dissolving 113 mg BCS in 1 ml sterile distilled water.
6. **1 M sorbitol:** 1 M sorbitol was prepared by dissolving 18.21 g of sorbitol in 70 ml distilled water and the final volume adjusted to 100 ml by adding distilled water and was sterilized by autoclaving.
7. **1 M glucose:** 1 M glucose was prepared by dissolving 16.02 g of D-glucose in 70 ml distilled water and volume was adjusted to 100 ml. The stock was sterilized by filtering through a 0.45-µm syringe filter and stored at room temperature.
8. **Diethylpyrocarbonate (DEPC):** 0.1% DEPC solution was prepared in sterile distilled water and sterilized by autoclaving.
9. **8 M LiCl:** 8 M LiCl was prepared by dissolving 33.9 g of LiCl in a final volume of 100 ml of DEPC-treated sterile distilled water and sterilized by autoclaving.
10. **5 M NaCl**: 5 M NaCl was prepared by dissolving 29.22 g of NaCl in 80 ml of distilled water, and adjusted the volume to 100 ml. The stock was then sterilized by autoclaving and stored at room temperature.
11. **3 M Na-acetate (pH 5.2):** 24.61 g Na-acetate was dissolved in 70 ml DEPC-treated water and pH was adjusted to 5.2 with glacial acetic acid. Volume was adjusted to 100 ml by adding DEPC-treated water and sterilized by autoclaving.

12. **2 N NaOH:** 8 g of NaOH pellet was dissolved in 80 ml of DEPC-treated water, the volume was adjusted to 100 ml and sterilized by autoclaving.
13. **10 N NaOH:** 40 g of NaOH pellet were slowly in 80 ml of distilled water, stirring continuously in a plastic beaker placed on ice, adjusted the volume to 100 ml and stored at room temperature.
14. **10% SDS:** 1 g of SDS was dissolved in 5 ml sterile double-distilled water and heated at 65 °C. The volume was adjusted to 10 ml and stored at room temperature.
15. **1 M Tris-HCl (pH 7.5):** 12.11 g of Tris base was dissolved in 70 ml distilled water. The pH was adjusted to 7.5 by adding concentrated HCl, and the volume was adjusted to 100 ml with distilled water and sterilized by autoclaving.
16. **1 M Tris-HCl (pH 8.0):** 12.11 g of Tris base was dissolved in 70 ml of DEPC-treated water. The pH was adjusted to 8.0 by adding concentrated HCl, the volume was adjusted to 100 ml with DEPC-treated water and sterilized by autoclaving.
17. **0.5 M EDTA (pH 8.0):** 18.61 g of EDTA was dissolved in 70 ml DEPC-treated water. The pH was adjusted to 8.0 by adding NaOH pellets, and volume was adjusted to 100 ml and sterilized by autoclaving.
18. **Ethidium bromide (EtBr):** A stock solution of EtBr (10 mg/ml) was prepared by dissolving 10 mg EtBr in 1 ml distilled water and stored at 4 °C.
19. **6X Gel-loading Buffer (Type III):** A solution of 0.25% (w/v) bromophenol blue, 0.25% (w/v) xylene cyanol FF, and 30% glycerol (v/v) was made in sterile water and stored at 4°C.
20. **50X TAE:** 1 L of the 50X TAE stock solution was prepared by adding 242 g Tris base, 57.1 ml of glacial acetic acid and 100 ml of 0.5 M EDTA (pH 8.0) and the volume was adjusted to 1 L by adding distilled water. The solution was stored at 4 °C.
21. **1X TE:** The solution was prepared by adding 10 mM Tris-HCl (pH 8.0) and 1 mM EDTA (pH 8.0) from their respective stocks and stored at 4 °C.

22. **10X MOPS electrophoresis buffer:** The 10X MOPS stock solution of 1000 ml was prepared by dissolving 41.8 g of MOPS (0.2 M) in 400 ml of DEPC-treated water. After dissolving the pH was adjusted to 7.0 with 2 N NaOH, and 16 ml of 1 M sodium acetate solution (20 mM), and 20 ml of 0.5 M EDTA pH 8.0 (10 mM) was added. The volume was adjusted to 1000 ml with DEPC-treated water. The solution was filter sterilized using 0.45-µm Millipore filter and stored at room temperature protected from light.
23. **0.5 M PIPES buffer (pH 6.7):** 1.5 g PIPES was dissolved in 6 ml distilled water and pH was adjusted to 6.7 by adding 10 N NaOH solution and adjusted the volume to 10 ml. The solution was sterilized by filtering through a 0.45 µm syringe filter and stored at minus 20 °C.
24. **Alkaline lysis Solution I:** Alkaline lysis Solution I is composed of 50 mM glucose, 25 mM Tris-Cl (pH 8.0), and 10 mM EDTA (pH 8.0).
25. **Alkaline lysis Solution II:** Alkaline lysis Solution II is prepared freshly prior to use and is composed of 0.2 N NaOH and 1% SDS.
26. **Alkaline lysis Solution III:** Alkaline lysis Solution III is prepared by mixing 60 ml of 5 M potassium acetate, 11.5 ml of glacial acetic acid, and making up the volume to 100 ml by adding distilled water. The solution was sterilized by autoclaving and stored at 4 ºC.
27. **Inoue transformation buffer:** The Inoue transformation buffer (Inoue et al. 1990) is composed of 55 mM $MnCl_2$, 15 mM $CaCl_2$, 250 mM KCl and 10 mM PIPES buffer (pH 6.7).
28. **Lysis buffer for *N. crassa* genomic DNA isolation:** The lysis buffer is composed of 10 mM Tris HCl (pH 7.5), 0.5 M NaCl, 10 mM EDTA, 1% SDS, and 1% CTAB.
29. **Lysis buffer for *N. crassa* RNA isolation:** The lysis buffer is composed of 100 mM Tris HCl (pH 8.0), 0.6 M NaCl, 10 mM EDTA (pH 8.0), 4.5 % SDS, and 2 % *β*-mercaptoethanol.

2.1.5 Solutions for growth, maintenance and crossing of *N. crassa* strains

(i) Biotin solution: 5 mg biotin was dissolved in 100 ml 50% (v/v) ethanol, stored at 4 °C.

(ii) Trace element solution: Trace element solution was prepared by dissolving the following chemicals sequentially in 90 ml of distilled water with constant stirring.

$C_6H_8O_7.H_2O$	5.00 g
$ZnSO_4.7H_2O$	5.00 g
$Fe(NH_4)_2(SO_4)_2.6H_2O$	1.00 g
$CuSO_4.5H_2O$	0.25 g
$MnSO_4.1H_2O$	0.05 g
H_3BO_3	0.05 g
$Na_2MoO_4.2H_20$	0.05 g

The final volume was adjusted to 100 ml; 1 ml of chloroform was added as a preservative and stored at room temperature.

(iii) Vogel's Medium N (VGN): A 50X stock of Vogel's Medium N (Vogel, 1956; Vogel, 1964) was prepared by adding following chemicals sequentially in 75 ml distilled water with constant stirring.

$Na_3C_6H_5O_7.2H_2O$	12.5 g
KH_2PO_4	25 g
NH_4NO_3	10 g
$MgSO_4.7H_2O$	1 g
$CaCl_2.2H_2O$	0.5 g
(Pre-dissolved in 2 ml H_2O)	
Biotin solution	500 µl
Trace element solution	500 µl
Chloroform	300 µl

The volume of the solution was adjusted to 100 ml and the chloroform was added as a preservative.

(iv) Vogel's glucose minimal media (VGM):

Vogel's Medium N	1X
Glucose	2% (w/v)

(v) Vogel's glucose minimal media (VGM) agar:

Vogel's Medium N	1X
Glucose	2% (w/v)
Agar	2% (w/v)

(vi) 4X Synthetic crossing medium (SCM): 4X strength synthetic crossing medium (SCM) was prepared by dissolving the following chemicals sequentially in 80 ml distilled water with constant stirring.

KNO_3	0.4 g
K_2HPO_4	0.28 g
KH_2PO_4	0.2 g
$MgSO_4.7H_2O$	0.2 g
$CaCl_2.2H_2O$	40 mg
NaCl	40 mg
Biotin solution	20 µl
Trace element solution	20 µl

The volume of the solution was adjusted to 100 ml and sterilized by autoclaving.

(vii) SCM agar:

SCM	1X
Glucose	1.5% (w/v)
Agar	2% (w/v)

(viii) 10X FGS (Fructose, glucose, and sorbose) stock: 10X FGS stock was prepared by dissolving the following chemicals in 80 ml distilled water.

Fructose	5% (w/v)
Glucose	5% (w/v)
Sorbose	20% (w/v)

The volume of the solution was adjusted to 100 ml and sterilized by autoclaving.

(ix) FGS agar:

FGS	1X
Vogel's Medium N	1X
Agar	2% (w/v)

(x) Top agar:

FGS	1X
Vogel's Medium N	1X
Agar	2.8% (w/v)

(xi) Media for circadian clock study:

Vogel's Medium N	1X
Glucose	0.1% (w/v)
Arginine	0.17% (w/v)
Biotin	50 ng/ml
Agar	1.5% (w/v)

2.1.6 Primers used in the study

Custom oligonucleotide primers were purchased from Bioserve (Hyderabad, India) and from Integrated DNA Technologies (USA). List of primers used in this studies are enlisted in Table 3.7, 4.4, 5.5 and 5.7.

2.2 Methods

2.2.1 Growth conditions

The *N. crassa* strains were grown and maintained as described previously (Davis and De Serres 1970). For routine culture, 1X Vogel's glucose minimal medium N (VGM) was used for vegetative growth (Vogel 1956; Vogel 1964). For sexual development, strains of opposite mating type were crossed on 1X synthetic crossing medium (SCM; Westergaard and Mitchell 1947). Ascospores were germinated on FGS agar medium (Davis and De Serres 1970). For *cmd*^{RIP} strain, Calcium-D pantothenic acid (0.01 mg/ml) and bathocuproinedisulfonic acid (BCS) (250 µM) were supplemented in the mediums. *N. crassa* knockout mutants were selected by screening for growth on FGS agar medium supplemented with hygromycin at a concentration of 220 µg/ml (Colot et al. 2006). The *N. crassa* transformants were screened on FGS agar media supplemented with Basta® (Pall 1993) at a concentration of 400 µg/ml.

2.2.2 Setting up crosses and harvesting ascospores

Crosses between the opposite mating type of *N. crassa* strains were performed as described previously (Westergaard and Mitchell 1947; Davis and De Serres 1970). The agar plugs of opposite mating type were inoculated on SCM agar in 55 mm diameter Petri dishes allowing the confrontation of the mycelium of two mating types. The crosses were incubated at 22 °C in a BOD incubator for 21 to 30 days. The plates are flipped after 14 days and the ascospores begin to shoot within 16-18 days. The ascospores are then harvested by washing the lid with 1 ml of sterile water. Ascospores thus harvested are germinated by heat activation at 55-65 °C for 30-60 min and plating on FGS agar plates which are incubated at 30 °C for growth.

2.2.3 Maintenance of Stock

For long term preservation of *N. crassa* strains, silica and glycerol stocks were prepared for all the strains used in this study. The strains were grown in VGM agar slants for 3 days under constant darkness at 30 °C, and then transferred to room-temperature under constant light for 4 days. For silica stock, cryo tubes (4.5 ml) were filled with silica (6-12 Mesh, Grade 40; sterilized by autoclaving and dried at 60 °C) and chilled on ice for 30 minutes. Approximately 1 ml of 5% autoclaved skimmed milk was added to the culture tube and vortexed vigorously. The conidial suspension was drawn using a Pasteur pipette, dispensed on the pre-chilled silica, and vigorously vortexed for 5 minutes to break up any clumps. The cryo tubes were regularly vortexed for 8-10 days and then stored at -20 °C until further use. For glycerol stock, the conidia are suspended in 1 ml of sterile water and transferred to 2 ml cryo tube; then an equal amount of 40% sterile glycerol was added and mixed properly, and then stored at -80 °C till further use.

2.2.4 Conidial cell count

For quantification of conidia for various assays, conidia were harvested from freshly grown 5–6 days old strains in 1 ml sterile distilled water. Appropriate cell dilutions were done from the conidial suspension, and conidia counting was performed using a haemocytometer under a Trinocular Microscope (Nikon ECLIPSE E200, Japan).

2.2.5 Temperature sensitivity assay

For temperature sensitivity assay, freshly harvested conidial cell suspension of ~2×10^7 conidia/ml (~7 µl) was inoculated in the center of 90-mm-Petri dishes containing Vogel's glucose agar medium and incubated at three different temperatures of 20, 30, and 40 °C. The

colony diameter was measured at every 3 h interval starting at 12 h till 24 h. The radial growth rate was calculated as cm/h. The plates were photographed at 24 h.

2.2.6 pH stress assay

For pH stress assay, freshly harvested conidia from 5-day-old cultures were suspended in sterile distilled water. Approximately 1×10^6 conidia/ml were inoculated in tubes containing Vogel's glucose liquid medium and adjusted to three different pH conditions, acidic (pH 3.8), normal (pH 5.8), and alkaline (pH 7.8). The tubes were then incubated at 30 °C for 3 days and the aerial hyphae height was measured and photographed.

2.2.7 Osmotic stress assay

For osmotic stress assay, ~7 µl of ~2×10^7 freshly harvested conidial suspension of *N. crassa* strains were inoculated in 90-mm-Petri dishes containing Vogel's glucose agar medium supplemented with hyperosmotic agents, NaCl and sorbitol at different concentrations of 0 (control), 0.5, 1, and 1.5 M and incubated at 30 °C. The colony diameter was measured at every 3 h interval starting from 12 to 24 h and the growth rate was calculated. The relative colony growth rate percentage was calculated by dividing the growth rate at different concentrations of NaCl and sorbitol by the growth rate in the control plate and multiplied by 100.

2.2.8 Oxidative stress plate assay

To study H_2O_2-induced oxidative stress assay, colony growth rate and survival rate of conidia were estimated. For colony growth rate, ~7 µl of ~2×10^7 conidia/ml cell suspension was inoculated at the center of 90-mm-Petri dishes containing Vogel's glucose agar medium supplemented with (test) or without (control) 10 mM H_2O_2 and incubated at 30 °C. Colony diameter was measured at every 3 h interval from 12 to 24 h and the growth rate was calculated.

The average colony growth rate percentage was calculated by dividing the growth rate in the test plate by the growth rate in the control plate and multiplied by 100.

For conidial survival assay under H_2O_2 induced oxidative stress assay, ~1×10^6 conidia/ml were inoculated in Vogel's glucose liquid medium and incubated in the dark at 30 °C, shaking at 200 rpm for 2 h. The cultures were supplemented with (test) or without (control) 10 mM H_2O_2 and further germinated for 1 h at 30 °C. Germlings were then plated on the FGS agar medium and incubated at 30 °C for 16 to 24 h depending on the germling growth rate. Percent survival was scored by dividing the number of viable colonies in the test plates (exposed to H_2O_2) by the number of colonies in the control plates (not exposed to H_2O_2) and multiplied by 100 (Yang and Borkovich 1999).

2.2.9 Reactive oxygen species (ROS) estimation Assay

For qualitative ROS estimation, 5-day old freshly harvested conidial suspension of ~1×10^6 conidia were inoculated in Vogel's glucose liquid medium containing 10 µM of 2', 7'-dichlorofluorescein-diacetate (DCFH-DA) for 30 min and further treated with 10 mM H_2O_2 for 90 min. An aliquot of conidia was observed under Trinocular inverted microscope (AxioVert A1 FL, Carl Zeiss) with a 450-490 nm excitation filter and a 515 nm emission filter and the images were captured.

2.2.10 Endoplasmic Reticulum (ER) stress assay

For dithiothreitol (DTT) induced ER stress assay, ~1×10^6 conidia/ml were inoculated in tubes containing Vogel's glucose liquid medium supplemented with different concentrations of DTT, including 0 mM (control), 0.1 mM, 0.5 mM, 1 mM, and 2 mM, and incubated in dark at 30 °C for 3 days and then photographed. The height of the aerial hyphae was measured, and the

percent growth rate was calculated by dividing the growth rate in the tubes with different concentrations of DTT to that of growth in control tube and multiplied by 100.

2.2.11 Thermotolerance assay

For thermotolerance assay, fresh conidial suspension of ~1×10^6 conidia/ml were inoculated in Vogel's glucose liquid medium and incubated for 2 h in the dark at 30 °C with shaking at 180 rpm. The germlings were then divided equally into 3 tubes, which were held at 30 °C (control), 30 °C (uninduced), and 44 °C (induced). Both the 30 °C (uninduced) and 44 °C (induced) cultures were then given a lethal heat shock at 52 °C for 20 minutes. An aliquot of ~1000 cells or the germlings was plated on FGS agar medium followed by incubation at 30 °C for 24 h (Yang and Borkovich 1999). The germlings were then observed under a stereomicroscope, and viable colonies were counted for each condition. Percent survival rate was determined by dividing the number of viable colonies in the uninduced and induced treated plates by the number of viable colonies in the control plate and then multiplied with 100.

2.2.12 Fertility assay

For fertility assay, strains of two opposite mating type were crossed on a 55-mm-Petri dishes containing SCM media supplemented with calcium D-pantothenic acid and BCS. The Agar plug of one strain (female) is first cultured and incubated at 22 °C for one week. After 7 days, fresh conidia of the opposite mating type (male parent) were harvested, and the conidial suspension were inoculated and further incubated at 22 °C. Perithecia formation were observed after seven days post-fertilization. Further, after fourteen days post-fertilization, the ascospores shot onto the lid were observed under a microscope (Leica S9i Stereomiroscope, Leica Microsystems, Wetzlar, Germany) and images were captured. The ascospores were harvested by washing the lids with ~1 ml of sterile H_2O.

2.2.13 Perithecia Grafting Assay

Perithecia grafting assay was performed as previously described (Chinnici et al. 2014). The wild type strains of *mat A* and *mat a* were cultured on 90-mm-Petri dishes containing SCM with 0.5% sucrose, overlaid with a cellophane filter for 10 days. Fresh conidial suspension of the opposite mating type of wild type was inoculated and incubated for 24 h for fertilization. In addition, the wild type *mat A* and *mat a*, #850, and #26 host strains were cultured in SCM plates containing 0.5% sucrose for 10 days. From the fertilized plate, small pieces (0.5 cm approx.) of cellophane (grafts) were cut and transferred to the host plates, and incubated for another 7 to 14 days. After eight days, the perithecia was dissected to observe the maturation of the ascospores and after 14 days post-fertilization, the number of ascospores released on the lid were observed under a dissection microscope (Leica S9i Stereomiroscope, Leica Microsystems, Wetzlar, Germany).

2.2.14 Cell Fusion Assay

For cell fusion assay, the strains were first grown in VGM agar for 3 days in the dark at 30 °C and then under light for 2 days. Fresh conidia were harvested in sterile distilled water. Then, conidia were inoculated at a concentration of ~1×10^6 conidia/ml in 50 ml of liquid VGM and incubated in shaking condition at 180 rpm at 30 °C. The cells were observed under an inverted microscope (AxioVert A1 FL, Carl Zeiss, Göttingen, Germany) at 40X magnification at 3 h, 5 h, 7 h, and 48 h.

2.2.15 Chronological aging assay

For chronological aging assay, the strains were grown on Vogel's glucose agar medium at 30 °C for 3 days under dark condition and then kept at room temperature for 2 days under constant light for proper conidiation. On day 5, conidia were harvested using 1 ml sterile water and

counted. A concentration of ~1 x 10^7 cell/ml were maintained for 30 days at 25 °C (room temperature) to starve them (Case et al. 2014). Approximately 1000 cells (10 µl from 10^{-4} dilution) were plated on the FGS agar medium at an interval of 5 days starting from the days 5 to 30. The plates were incubated at 30 °C for 24 h and the number of colonies formed were counted. The total number of colonies formed on days 5 was taken as 100%. The rate of aging was determined by dividing the total number of colonies formed on the successive days (days 10 to 30) by the number of colonies formed on days 5 and multiplying with 100.

2.2.16 Circadian regulated conidiation assay

The inverted race tube assay was performed to study the circadian regulated conidiation. Freshly grown (24 h old) strains were inoculated at one end of a race tube containing ~13 ml circadian agar media and incubated at 25 °C under constant light for 24 h. At 24 h, the growth front was marked and the tubes were then inverted and incubated under constant darkness at 25 °C for a period of 6-7 days. The growth fronts were marked every 24 h interval under a safe red light. The period lengths were calculated by multiplying the distance between conidial bands by the inverse of the slope (http://www.fgsc.net/teaching/circad.htm). The experiments were also carried out at 20 °C and 30 °C to see the effect at different temperature conditions.

2.2.17 Assay for the visualization of intracellular Ca^{2+} distribution

For visualization of the intracellular Ca^{2+} distribution, strains were grown on a thin layer of Vogel's glucose agar medium overlaid on glass slides and incubated for 12-14 h at 30 °C. The growing hyphal tips were then supplemented with 200 M chlortetracycline hydrochloride (CTC) or 20 µM 1-N-Phenylnaphthylamine (NPN) dissolved in 0.1 % dimethyl sulphoxide (DMSO). Fluorescence emissions from CTC and NPN were observed using a Trinocular

inverted fluorescence microscope (Axio Vert A1 FL, Carl Zeiss) using DAPI filters with an exposure of 300-400 ms.

2.2.18 Assay for the visualization of internal hyphal septation

For visualization of internal septation in the growing hyphae, the strains were grown on a thin layer of Vogel's glucose agar medium overlaid on glass slides and incubated for 12-14 h at 30 °C. The growing hyphae were stained with calcofluor white (CFW; 0.1% in 0.05 M PBS) for 20 minutes in the dark. The samples were then observed under a Trinocular inverted fluorescence microscope (Axio Vert.A1 FL-LED, Carl Zeiss) using DAPI filters with exposure time of 300-400 ms.

2.2.19 Preparation of ultracompetent cells

Ultracompetent cells were prepared essentially as described previously (Inoue et al. 1990). A single colony of *E. coli* DH5α was picked from a fresh streaked LB agar plate and inoculated into 5 ml of LB broth, and incubated at 37 °C at 200 rpm for 16 h. Then,1 ml of the overnight culture was inoculated in 100 ml of LB broth and incubated at 37 °C at 200 rpm till the OD_{600} reached 0.450–0.55. The culture was chilled on ice and centrifuged at 3,900 rpm for 10 min at 4 °C to pellet the cells. The cells were then resuspended in 32 ml of ice cold transformation buffer (TB:10 mM PIPES pH 6.7, 15 mM $CaCl_2$, 250 mM KCl, 55 mM $MnCl_2$) and incubated on ice for 10 min. The centrifugation process was repeated and the cells were resuspended in 8 ml of TB containing 7% DMSO. Cell suspension was distributed into 100 µl aliquots, frozen in liquid nitrogen and stored at -80 °C. Ultracompetent cells were used for cloning experiments involving ligation of DNA fragments.

2.2.20 Small-scale isolation of plasmid DNA from bacterial culture (Mini preparation)

Small-scale or mini preparation of plasmid isolation was performed by alkaline lysis method (Sambrook and Russell 2001). Briefly, 5 ml of overnight bacterial culture was centrifuged in microfuge tube for 1 min at 12,000 rpm at 4 °C. The supernatant was discarded and pellets were suspended in 100 µl alkaline lysis solution I with vigorous vortexing. To this homogenous mixture, 200 µl of freshly prepared alkaline lysis solution II was added and mixed by rapidly inverting the tube 4-5 times. Then, 150 ml alkaline lysis solution III was added and mixed by inverting the tube 5–8 times and incubated on ice for 3–5 min. The bacterial lysate was centrifuged at 12,000 rpm for 10 min at 4 °C. The supernatant was transferred to fresh microfuge tubes and an equal volume of phenol: chloroform: isoamyl alcohol mixture (25:24:1) was added, and centrifuged at 12,000 rpm for 10 min at 4 °C. The aqueous phase was carefully transferred to a fresh 1.5 ml microfuge tube and 1 ml of absolute ethanol was added to precipitate plasmid DNA. The tube was gently inverted for few times and kept at room temperature for 10 min. The plasmid DNA was pelleted by centrifugation at 12,000 rpm for 10 min at 4 °C. The supernatant was discarded and the pellet was washed with 70% ethanol by centrifuging at 12,000 rpm for 10 min at 4 °C. The pellet was air dried for 20–30 min at room temperature. Finally, the pellet was dissolved in 30 µl of 1X TE buffer (pH 8.0) and stored at 4 °C.

2.2.21 Restriction digestion of plasmids

Restriction digestion of plasmid DNA for analytical and preparative was performed according to the manufacturer's instructions for the specific restriction endonucleases used (New England Biolabs, USA). An aliquot of ~1 µg plasmid DNA was digested with 1 µl (10 units) of restriction endonuclease in a final volume of 50 µl and the reaction was carried out in the

conditions as per the manufacturer's instruction. The digested DNA fragments were analysed by agarose gel electrophoresis.

2.2.22 Ligation of digested vectors and inserts

Ligation reactions were performed by using Quick Ligation™ Kit (Cat. no. M2200S, New England Biolabs, USA). A 20 µl ligation reaction mixture was made by adding ~50 ng of linearized DNA vector, a 3-fold molar excess of insert DNA, 10 µl of 2X ligation buffer, 1 µl quick T4 DNA ligase enzyme, and nuclease-free water to make up the remaining volume. The ligation reaction was performed for 15–20 min at 25 °C in a circulating water bath (MRC Scientific Instruments, Israel).

2.2.23 Transformation of ultracompetent *E. coli* DH5α cells by heat shock

The competent cells from the -80 °C freezer were taken out and thawed on ice. An aliquot of ~100 ng of ligated DNA sample was added to the competent, mixed gently and incubated on ice for 30 min. The cells were subjected to heat shock for 90 s at 42 °C in a water bath and kept on ice for 10–15 min, then recovered by the addition of pre-warmed 600 µl of SOC media, and incubated for 1 h at 37 °C and 200 rpm. Then, 200 µl each of cell cultures was plated on four LB agar plate (90-mm) supplemented with 100 µg/ml of ampicillin and incubated overnight at 37 °C.

2.2.24 Transformation of *N. crassa* by electroporation

The transformation procedure was performed as described previously (Margolin et al. 1997; Bhat et al. 2004). The recipient strain was inoculated on 50 ml of Vogel's glucose agar medium in a 250 ml flask and incubated in constant darkness for 3 days at 30 °C and then under constant light for 4 days at room temperature for proper conidiation. The conidia were harvested in 30

ml sterile water and separated from the mycelium by passing the suspension through sterile cheesecloth attached to a 50 ml falcon. The cheesecloth was removed and the falcon tube was capped, and centrifuged at 3,000 rpm for 10 min at 4 °C. The conidial pellet was washed twice in 30 ml sterile water and resuspended in 1M sorbitol at a concentration of 3 x 10^9 per ml. About 40 µl of the conidial suspension was mixed with the DNA construct to be transformed and placed in pre-chilled 2 mm electroporation cuvettes (Biorad Laboratories, Hercules, CA). Electroporation was done in BioRad gene pulsar apparatus (Biorad Laboratories, Hercules, CA). The parameters for electroporation were 1.5 kV (voltage gradient), 25 µF (capacitance) and 600 Ω (resistance). The time constant varied from 13 to 15 ms. Immediately after the pulse, 1 ml of chilled 1 M sorbitol was added to the cuvette and incubated on ice for 5 min. The transformant conidial suspension was mixed with warm top agar and plated on FGS agar plate supplemented with the Basta (400µg/ml) and calcium pantothenate (0.01 mg/ml), and incubated at 30 °C for 48 h.

2.2.25 Genomic DNA isolation from *N. crassa*

N. crassa strains of interest were grown in liquid VGM at 30 °C with shaking at 200 rpm for 3 days. The mycelia mass was harvested by filtration through sterile cheese cloth, cut into pieces and was lyophilized. The dried mycelia were ground into fine powder using a glass rod in a 2 ml microfuge tube. To this, 800 µl of DNA lysis buffer (10 mM Tris-HCl at pH 7.5, 0.5 M NaCl, 10 mM EDTA, 1% SDS, and 1% CTAB) was added and mixed thoroughly using a pipette tip or a toothpick. The microfuge tubes were incubated at 65 ˚C for 45 min, followed by centrifugation at 12,000 rpm for 10 min. The supernatant was transferred to a fresh 2 ml microfuge tube and 600 µl of phenol: chloroform: isoamyl alcohol mixture (25:24:1) was added. The tubes were kept in a cell mixer for 20 minutes and centrifuge at 12,000 rpm for 10 min. The aqueous phase was carefully pipetted to a fresh tube and washed with 600 µl of

chloroform to remove the last traces of phenol and then centrifuged at 12,000 rpm for 10 min. The aqueous phase was carefully pipetted to fresh 1.5-ml microfuge tube and the genomic DNA was precipitated by adding 1 ml of pre-chilled absolute alcohol. The tubes were gently inverted for few times and allowed to stand for 30 minutes for proper precipitation, which was then centrifuged at 12,000 rpm for 10 min to pellet down the DNA. The supernatant was discarded and pellet was washed with 70% ethanol by centrifuging at 12,000 rpm for 10 min. The tubes were air dried to at room temperature for 20–30 min to remove the traces of ethanol. In the final step, the pellet was dissolved in 30 µl of 1 X TE buffer (pH 8.0) and stored at 4 °C. All the centrifugation was carried out at 25 °C.

2.2.26 RNA isolation from *N. crassa* strains

RNA isolation from *N. crassa* strains was essentially performed as described previously (Sokolovsky et al. 1990; http://www.fgsc.net/fgn37/sokol.html). To isolate RNA from strains exposed to heat stress conditions, ~1 x 10^7 conidia/ml were inoculated in liquid VGM medium and incubated for 14 h at 28 °C 180 rpm under constant darkness, and then treated with heat shock for 1 h at 48 °C as describes previously (Kapoor and Lewis 1987; Roy and Tamuli 2021). For isolating RNA from nitrogen starved condition, ~1 x 10^7 conidia/ml were inoculated in liquid SCM medium and incubated for 18 h at 22 °C with shaking at 180 rpm under constant light (Barman and Tamuli 2017). For RNA isolation from circadian regulated condition, ~1 x 10^7 conidia/ml were inoculated in liquid circadian medium and incubated under light for 2 h at 20 or 25 °C and shaking at 125 rpm, and then transferred to dark condition for 16 h (Aronson et al.1994). The mycelia mass obtained from these cultures were harvested by filtration and frozen using liquid nitrogen. Immediately after freezing, the mycelia mass was crushed into fine powder in a 2 ml microfuge tube with a glass rod and mixed with 400 µl of TRIzol™ reagent (Cat. no. 15596026, Life Technologies, USA). Further, 750 µl of RNA lysis buffer and

750 µl of phenol: chloroform: isoamyl alcohol (PCI; 25:24:1) were added to the tubes, kept on rotary mixer for 20 min, and centrifuged for 10 min at 10,000 rpm. The upper aqueous phase was taken in a 2 ml microfuge tube and 750 µl of PCI was added, vortexed briefly and centrifuged for 10 min at 10,000 rpm. The aqueous phase was transferred to a new 2 ml microfuge tube and 750 µl of 8 M LiCl was added. The mixture was stored at 4 °C for 24 h. Then, on the next day, the tube was vortexed briefly and centrifuged for 10 min at 10,000 rpm. The supernatant was discarded and the isolated pellet was suspended in 300 µl double distilled DEPC treated water, to which 30 µl of 3 M Na-acetate (pH 5.2) and 750 µl of absolute ethanol was added and mixed by gently inverting the tubes. The mixture was stored at -80 °C for 2 h or -80 °C for 1 h and centrifuged for 10 min at 10,000 rpm. The RNA pellet was washed with 70% ethanol by centrifuging for 10 min at 10,000 rpm. The pellets were dried for 20–30 min at room temperature and finally dissolved in 30 µl DEPC treated water. The RNA was stored at -80 °C. All centrifugation steps were carried out at room temperature.

2.2.27 Quantification of nucleic acids

The concentration of nucleic acids (DNA or RNA) was estimated by measuring the OD at 260 nm using a NanoPhotometer® (IMPLEN, Germany). The following empirical relationships were used to calculate the concentrations. An OD_{260} of 1 corresponds to ~50 µg/ml of double stranded DNA, 40 µg/ml of single-stranded DNA and RNA, ~20 µg/ml of single-stranded oligonucleotides. The purity of nucleic acids was estimated by calculating the OD_{260}/OD_{280} ratio. Pure preparations of DNA and RNA have OD_{260}/OD_{280} values of 1.8 and 2.0, respectively.

2.2.28 Polymerase chain reaction (PCR)

The routine polymerase chain reaction (PCR) reaction was performed by using Taq DNA polymerase (Cat no. M0273S, New England Biolabs, USA), which is isolated from *Thermus aquaticus* or Dynazyme II DNA polymerase (Cat no. F-501 250U, Thermo Scientific). which was isolated from *Thermus brockianus*. For cloning, Phusion® High-Fidelity DNA polymerase (Cat. no. M0530S, New England Biolabs, USA) was used because it possesses 5'-3' polymerase activity and 3'-5' exonuclease proofreading activity. The Novel *Pyrococcus*-like enzyme is fused with a processivity-enhancing domain, which increases fidelity and speed with an error rate of > 50-fold lower than Taq DNA polymerase. The PCR conditions varied according to the size of the product and the annealing temperature of the primers. All PCRs were performed as per the manufacturer's protocol with a thermal cycler (Arktik Thermal Cycler, Thermo Fisher Scientific, USA).

2.2.29 Reverse transcription PCR for cDNA synthesis

For reverse transcription PCR (RT-PCR), RNA isolated from the mycelial mass (described in the section 2.2.26 above) was used for cDNA synthesis. The cDNA synthesis was performed by using Verso cDNA synthesis Kit (Cat. no. AB-1453/A, Thermo Fisher Scientific, USA). For 20 µl reaction, 2 µg of total RNA was used as a template. The cycling condition for cDNA synthesis was as follows; 42 °C for 30 min and then 95 °C for 2 min for one cycle. The synthesized cDNA templates were subjected to quantitative real time PCR cycling with gene-specific primers to analyze the expression of the target gene.

2.2.30 Quantitative real time PCR

Quantitative Real-Time PCR (qRT PCR) analysis was performed using the cDNA synthesized from the total RNA (described in the section 2.2.29 above), specific primer pairs for the gene

of interest, the SYBR Select Master Mix (Life, City, State, USA), and the 7500 Real-Time PCR System (Applied Biosystems, City, State, USA). In general, 10 µl reaction mixture contained 4.5 µl of cDNA (100 ng), 0.25 µl of forward, 0.25 µl reverse primer, and 5 µl SYBR green. For the negative control, instead of the cDNA template, sterile DEPC-treated distilled water was used. The PCR parameter used was as follows: 95°C for 10 min followed by 40 cycles of 95°C for 15 s and 60°C for 1 min. The fold change in the relative expression of the target genes was calculated by $2^{-\Delta\Delta C_T}$ method (Livak and Schmittgen 2001) with *β-tubulin* gene expression level as the reference control (Cusick et al. 2014) and the expression in the wild type as the calibrator.

2.2.31 Agarose gel electrophoresis

The gel was prepared by dissolving agarose in 1X TAE buffer by microwaving and adding 0.5 µg/ml ethidium bromide and poured into the cast with combs. The gels were prepared based on the size of the samples to be resolved ranging from 0.8% to 1.5%. The DNA sample was mixed with 1 µl of 6X DNA loading dye (0.25% bromophenol blue, 0.25% xylene cyanol, and 30% glycerol) and loaded into the wells. Electrophoresis was performed in 1X TAE at 80–100 V. To estimate the size of the DNA fragments, standard 1Kb DNA ladder (cat No. NEB #B7025, NEB; Ipswich, MA, USA) were run alongside the sample. The ethidium bromide-stained DNA samples were visualized using a gel doc (Image 4.1, Bio-Rad, USA; or Mega Bio print, Vilbert Lormat, France). RNA samples were resolved in 1.5% agarose gel containing 2.2 M formaldehyde and 1X MOPS buffer and 0.5 µg/ml ethidium bromide.

2.2.32 DNA fragments purification from agarose gels

PCR amplified DNA samples for cloning and transformation were purified from agarose gels by using Gel Extraction Kit (Qiagen, USA or GCC Biotech, India). The specific DNA bands

resolved in the gels was excised by visualizing in a UV trans illuminator and transferred to a 1.5 ml microfuge tube and weighed. The DNA samples were then purified from the agarose gel according to the manufacturer's protocol.

2.2.33 Statistical analysis

Statistical analysis was performed using one-way ANOVA from the data obtained from three independent experiments in Microsoft Excel. The data are represented as mean ± Standard Deviations. One-way ANOVA was used to test the significance where the P values of <0.05 (*), <0.01 (**), and <0.001 (***) were considered significant.

2.3 Databases and software programs used

1. **Basic Local Alignment Search Tool (BLAST):** BLAST (Altschul et al. 1990, 1997, 2005) was used to compare nucleotide or protein sequences to the reference sequence databases. This is available at http://blast.ncbi.nlm.nih.gov/Blast.cgi.
2. **Clustal X:** Clustal X (Thompson et al. 1997) software was used for multiple sequence alignment of DNA and protein sequences. Clustal X is available online at http://www.clustal.org/clustal2/#Webservers .
3. **ExPasy Translate tool:** The ExPasy Translate tool was used for translating DNA sequences to protein sequences. It is available at http://web.expasy.org/tools/DNA.
4. **Conserved Domain Database (CDD):** CDD (Marchler-Bauer et al. 2008) was used to identify conserved domains in the proteins. This is available at http://www.ncbi.nlm.nih.gov/Structure/cdd/wrpsb.cgi .
5. **GeneDoc:** GeneDoc software (Nicholas 1997) was used for finding conserved domains among aligned sequences of DNA or protein. It is available at http://www.nrbsc.org/gfx/genedoc/.

6. **Restriction Mapper:** This was used for restriction mapping of DNA sequences. It is available at http://www.restrictionmapper.org/.
7. ***Neurospora crassa* genome databases:** Genome resource for *Neurospora* is available at http://fungidb.org . The web site for Fungal Genetics Stock Center is http://www.fgsc.net.
8. **NCBI:** NCBI at http://www.ncbi.nlm.nih.gov/ was used to retrieve the proteins or nucleic acid sequences.
9. **EMBL:** EMBL at http://embl.org/ was used to retrieve the primary sequence of proteins or nucleic acid.
10. **UniProt:** UniProt at https://www.uniprot.org was used to retrieve the primary sequence of proteins.
11. **Site for reverse-complement:** The sequence manipulation suite (SMS) software package was used to convert a DNA sequence into reverse-complement sequence. It is available at http://www.bioinformatics.org/sms/index.html.
12. **MatInspector**: It is a software tool that utilizes a large library of matrix description for transcription factor binding site in a DNA sequence. It is available at https://www.genomatix.de/matinspector/.
13. **SWISS-MODEL:** SWISS-MODEL (Schwede et al. 2003) is a fully automated protein structure homology-modelling web server. It is available at https://swissmodel.expasy.org/.
14. **Structural Analysis and Verification Server (SAVES):** SAVES is an interactive web server used for protein structure analysis and validation. The PROCHECK, ERRAT, and VERIFY 3D programs from this server were used for protein structure validation. It is available at https://www.doe-mbi.ucla.edu/saves/.
15. **UCSF CHIMERA:** UCSF Chimera (Meng et al. 2006) was used for visualization of the protein structures. It is available at https://www.cgl.ucsf.edu/chimera/.

16. ImageJ/Fiji: ImageJ/Fiji is a software (Schindelin et al. 2012) for image processing. It is available at https://imagej.net/software/fiji/.

CHAPTER 3

Understanding the cellular roles and mechanism of calmodulin and calcium/calmodulin-dependent kinases in coping with stress conditions in *N. crassa*

3.1 Introduction

Fungi grow in a wide range of niches with constantly changing environmental conditions, which can affect their survival, growth, and reproduction (Belozerskaya and Gessler 2006; Ahmad et al. 2020). In response to the environmental changes, fungi activate certain signaling pathways for adaptation (Fuchs and Mylonakis 2009; Freitas et al. 2016). Ca^{2+} signaling is one of the main intracellular signaling pathways in *N. crassa* that responds to various external stimuli and regulates a vast range of cellular processes (Borkovich et al. 2004; Galagan et al. 2003; Zelter et al. 2004).

Calmodulin (CaM) is the principal intracellular Ca^{2+} receptor highly conserved in all eukaryotic cells that mediate diverse biological processes from cell proliferation to apoptosis (Means and Dedman 1980; Hoeflick and Ikura 2002; Berchtold and Villalobo 2015). The structure analysis showed that CaM is a dumbbell-shaped molecule consisting of two similar domains arranged in a trans-configuration. Each domain consists of 2 helix-loop-helix Ca^{2+} binding motifs known as EF-hand, enabling CaM to bind to 4 Ca^{2+} ions (Babu et al. 1988; Meador et al. 1992,1993; James et al. 1995). When the cytosolic Ca^{2+} concentration rises from the resting state (100 nM), reaching 1 µM or more due to various external stimuli, Ca^{2+} signaling is initiated by binding to CaM (Chin and Means 2000, Bootman et al. 2001). The binding of Ca^{2+} brings about a conformational change in CaM, enabling it to bind and activate over 300 target proteins (Means and Dedman 1980; Hoeflich and Ikura 2002; Halling et al. 2016).

The Ca^{2+}/CaM dependent kinases (Ca^{2+}/CaMKs) are Ser/Thr kinases that are activated by the Ca^{2+}-CaM complex (Hook and Means 2001). Their domain organization consists of an N-terminal catalytic domain and a C-terminal regulatory domain, which is autoinhibited in the absence of Ca^{2+}/CaM complex and regulated by either autophosphorylation or phosphorylation by other kinases (Sorderling and Stull 2001; Swulius and Waxham 2008).

In *N. crassa*, one CaM gene has been identified, showing 85% and 59% homology to human and yeast calmodulin, respectively, and only one amino acid difference to *A. nidulans* CaM (Ortega Perez 1981; Melnick et al. 1993; Tamuli et al. 2013). The amino acid composition of *N. crassa* CaM is similar to that of plant CaM except for an unusually high amount of serine and the absence of trimethyllysine, and slightly less acidic in comparison to the vertebrate CaM (Cox et al. 1982).

The *cmd* gene is essential in *N. crassa*; therefore, the generation of *cmd* knockout or site-directed mutagenesis of key residues is not possible due to its lethal effect (Tamuli et al. 2013). Previously, CaM functions were studied by using (i) CaM antagonists and (ii) generating *cmd* mutants through Repeat-induced point mutation (RIP; Cambareri et al. 1989; Selker 1990) (Sadakane and Nakashima 1996; Laxmi and Tamuli 2015, 2017). CaM is necessary for the growth, hyphal development, circadian rhythm, activation of chitin synthase required for cell wall formation, carotenoid accumulation, ultraviolet survival, and sexual development (Sadakane and Nakashima 1996; Suzuki et al. 1996; Suresh and Subramanyam 1997; Laxmi and Tamuli 2015, 2017). *N. crassa* also possesses four Ca^{2+}/CaMKs, of which CaMK-1and CaMK-2 are required for full fertility (Tamuli et al. 2011; Kumar et al. 2014). The functions of CaM and CaMKs during stress were not understood in *N. crassa*. In this chapter, I describe detailed cellular roles and the mechanistic pathway of CaM and its downstream target protein CaMKs under different abiotic stress conditions.

3.2 Results

3.2.1 Temperature sensitivity analysis for *cmd*^{RIP} (#26), Δ*camk-1*, Δ*camk-2*, Δ*camk-3*, and Δ*camk-4* mutant strains

Temperature is one of the significant environmental factors that directly affect fungal growth, development, and protein dynamics (Xu 1996; Bakar et al. 2020). Temperature affects the circadian clock, perithecia development, and carotenoid production in *N. crassa* (McNelly-Ingle and Frost 1964; Harding 1974; Brunner and Diernfellner 2006). The *N. crassa* vegetative or asexual developmental phase requires normal ambient temperature (~30 °C) and produces conidia; the sexual phase requires lower temperatures and produces ascospores that can resist heat stress (McNelly-Ingle and Frost 1964; Kronholm et al. 2016; Kronholm and Ketola 2018). To understand the role of CaM and CaMKs in response to different temperatures necessary for both asexual and sexual developmental phases, I analyzed the temperature sensitivity of the wild type, #26, Δ*camk-1*, Δ*camk-2*, Δ*camk-3*, and Δ*camk-4* mutant strains by growing the strains at normal ambient (30 °C), lower (20 °C), and elevated (40 °C) temperatures. The temperature sensitivity assay was performed by inoculating ~ 2×10^7 conidia/ml at the center of 90-mm-Petri dishes containing Vogel's glucose agar medium and incubating at 20 °C, 30 °C, and 40 °C for 24 h. The hyphal growth front was marked regularly from 12 to 24 h at 3 h intervals, and the growth rate per hour was calculated. The #26 strain showed severely reduced growth rate at all three temperatures (Figure 3.1). The growth rate of Δ*camk-1* and Δ*camk-2* mutants were significantly reduced at 20 °C and 40 °C compared to the growth rate of the wild type, while Δ*camk-3* and Δ*camk-4* mutants did not show much difference in the growth rate from the wild type (Figure 3.1).

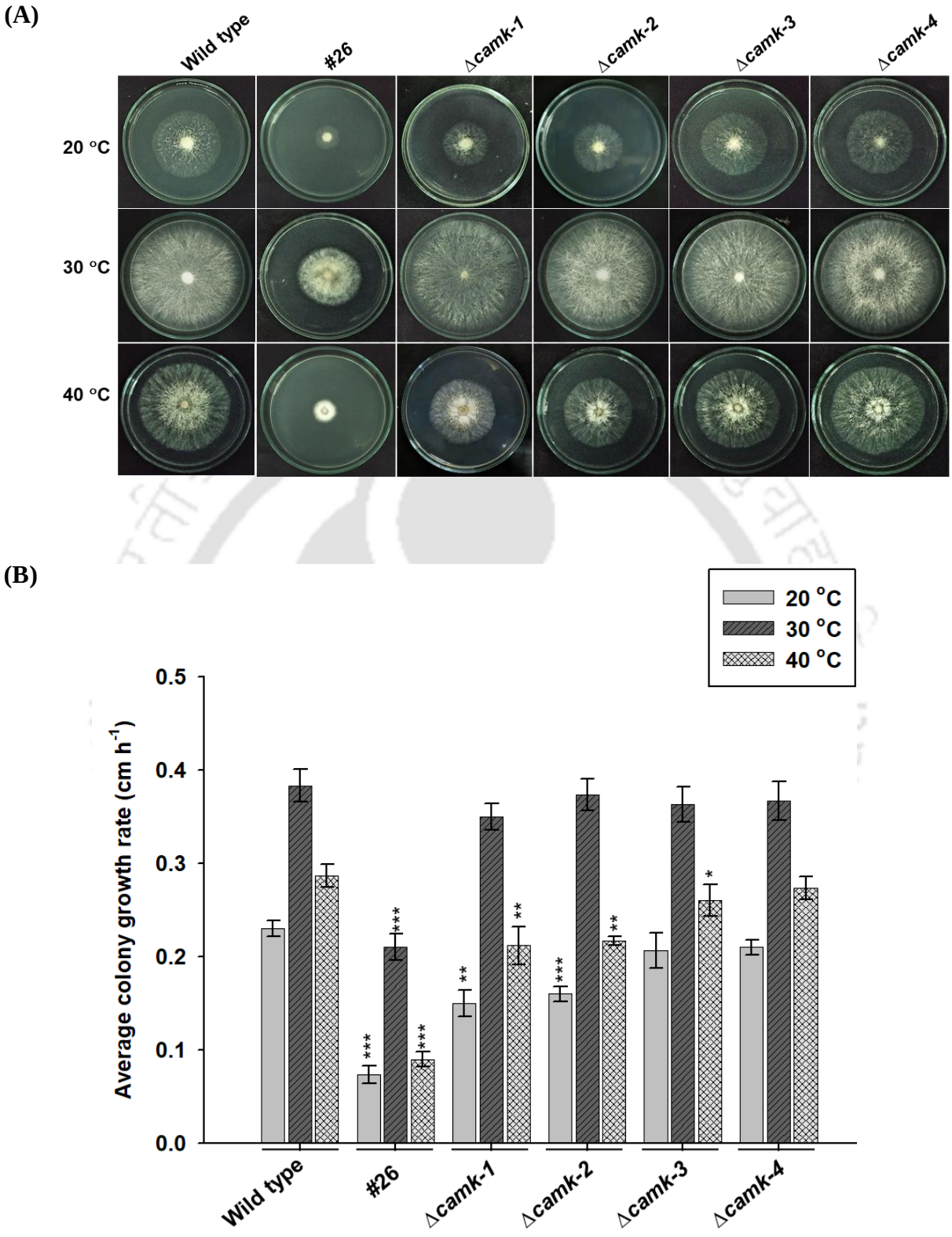

Figure 3.1 Temperature sensitivity assay. The wild type, #26, Δ*camk-1*, Δ*camk-3*, and Δ*camk-4* mutant strains were grown on Vogel's glucose agar medium and incubated at 20, 30, and 40 °C for 24 h. **(A)** Colony growth on Petri-dishes, and **(B)** Average colony growth rate

(cm h^{-1}). Standard deviations are indicated by error bars calculated from three independent experiments (n = 3), and the significance given by *P* values <0.05 (*), <0.01 (**), and <0.001 (***) compared to the wild type strain as measured by one-way ANOVA test.

3.2.2 The *cmd*^{RIP} (#26), Δ*camk-1* and Δ*camk-2* knockout mutants showed increased sensitivity to alkaline pH

The ability to sense changes in the environmental conditions, such as temperature, pH, and nutrient level, lead to the activation of intracellular pathways mediated by transcription factors that enable the organism to adapt to the changing environmental conditions (Martins et al. 2020). To determine the role of CaM and CaMKs under pH stress, I studied the growth of the wild type, #26, Δ*camk-1*, Δ*camk-2*, Δ*camk-3*, and Δ*camk-4* mutant strains at three different pH conditions, acidic (pH 3.8), normal (pH 5.8) and alkaline (pH 7.8). The aerial hyphae height of all the strains was like the wild type at acidic pH (Figure 3.2). However, in alkaline pH, the #26, Δ*camk-1*, and Δ*camk-2* mutants showed reduced aerial hyphae height (Figure 3.2). The aerial height of Δ*camk-3* and Δ*camk-4* was similar to the wild type (Figure 3.2). These results suggested that CaM, CaMK-1, and CaMK-2 are required for tolerance to alkaline pH in *N. crassa*.

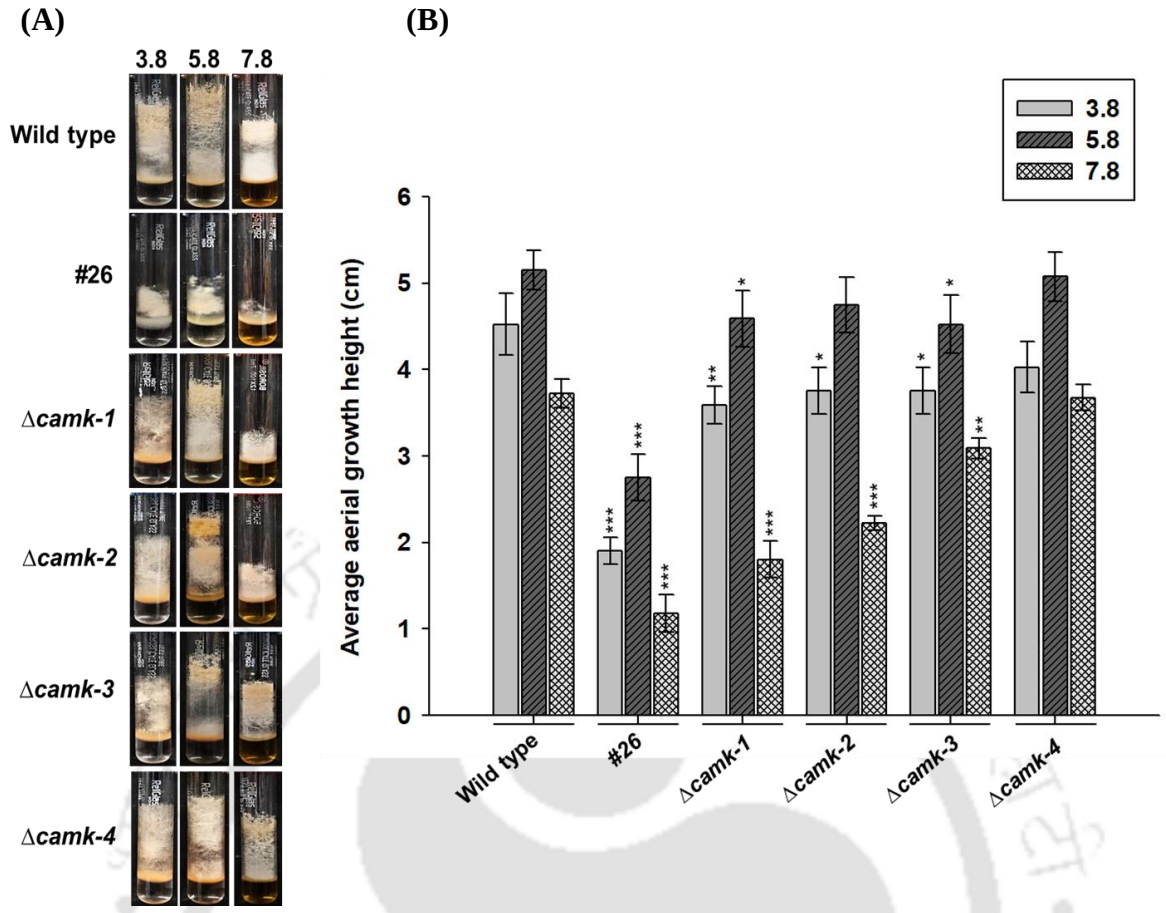

Figure 3.2 pH stress assay. Sensitivity to pH of the wild type, #26, Δ*camk-1*, Δ*camk-2*, Δ*camk-3*, and Δ*camk-4* mutant strains was evaluated by growing the strains in VGM liquid medium adjusted to three pH conditions, acidic (pH 3.8), normal (pH 5.8) and alkaline (pH 7.8) for 3 days at 30 °C. **(A)** Aerial hyphae at three different pH conditions **(B)** Average aerial hyphae height (cm). Error bars indicate the standard deviations calculated from three independent experiments (n = 3), and the significance given by *P* values <0.05 (*), <0.01 (**), and <0.001 (***) compared to the wild type strain as measured by one-way ANOVA test.

3.2.3 The *cmd*^{RIP} (#26) and *camk* knockout mutants were not sensitive to osmotic stress

Osmotic stress due to high salinity causes dehydration in the cell and affects physical development and metabolism (Seifikalhor et al. 2019). Transient increase in the $[Ca^{2+}]_c$ occurs as a result of hypo-osmotic and hyper-osmotic stresses (Kader and Lindberg 2010). Intracellular Ca^{2+} signaling is one of the earliest responses when exposed to osmotic stress

(Zhou et al. 2016). I, therefore, tested the sensitivity to osmotic stress for the wild type, #26, Δ*camk-1*, Δ*camk-2*, Δ*camk-3,* and Δ*camk-4* mutant strains. The strains were grown in Vogel's glucose agar medium supplemented with 0.5 M and 1 M of NaCl (Figure 3.3 A) and 1 M and 1.5 M of sorbitol (Figure 3.3 B). The growth front was measured starting from 12 h and at every 3 h interval till 24 h, and the average growth rate was measured by dividing the growth rate under stress to that of the growth rate under normal (0 M) condition. The #26, Δ*camk-1*, Δ*camk-2*, Δ*camk-3*, and Δ*camk-4* mutant strains showed growth rates similar to that of the wild type under NaCl and sorbitol stress conditions, suggesting that the #26, Δ*camk-1*, Δ*camk-2*, Δ*camk-3*, and Δ*camk-4* mutant strains were not sensitive to osmotic stress.

(A)

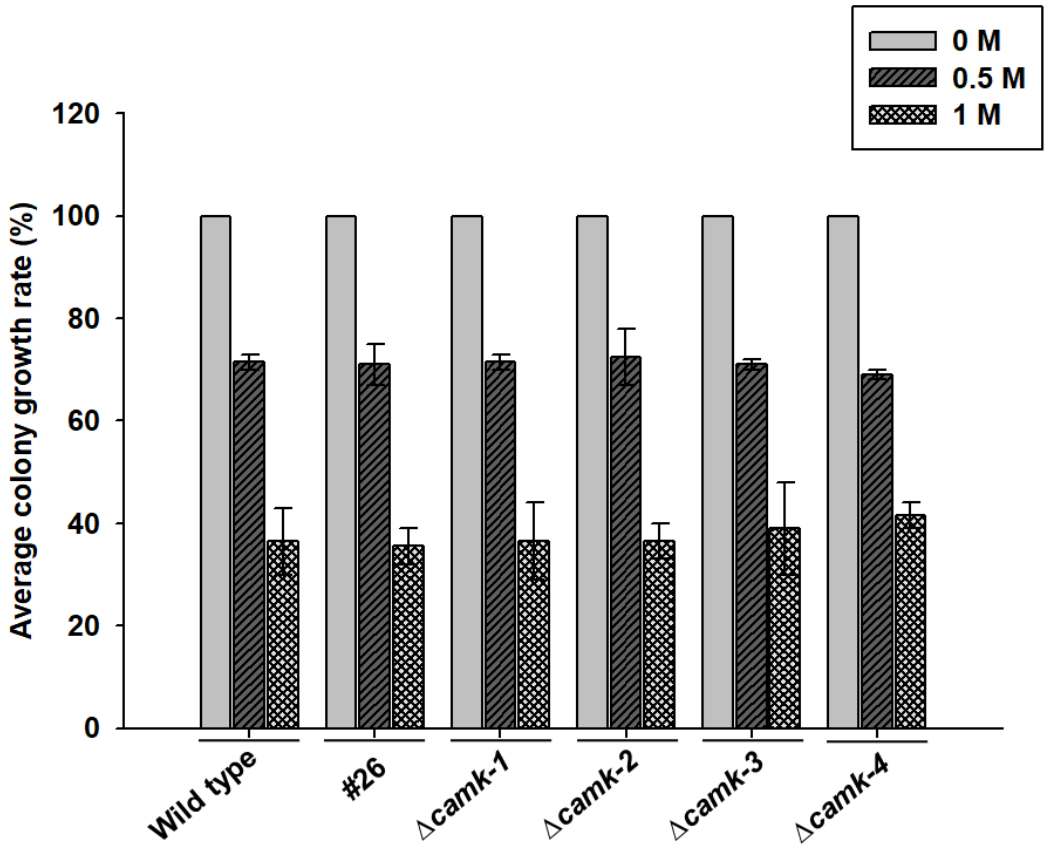

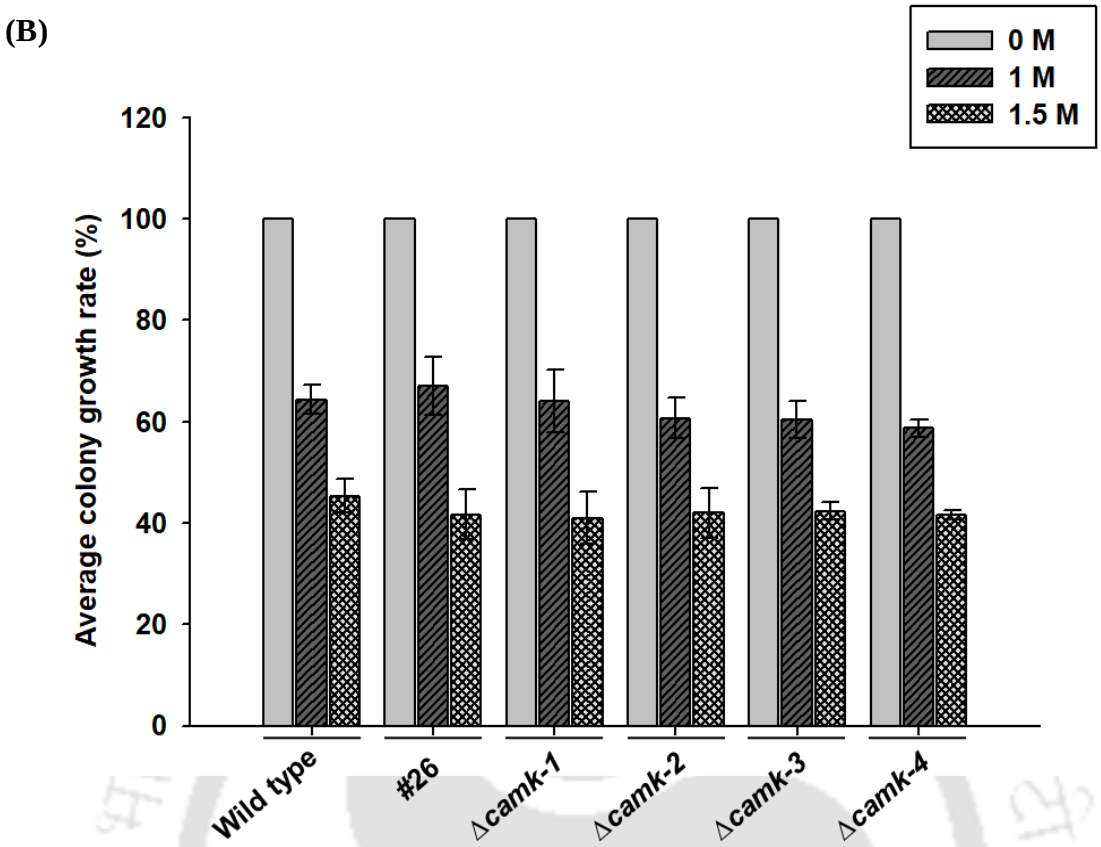

Figure 3.3 Osmotic stress assay. Sensitivity to osmotic stress was evaluated by growing the strains on Vogel's glucose agar medium with and without 0.5 M and 1 M NaCl, and 1M and 1.5 M Sorbitol. Average growth rate (%) in the presence of **(A)** NaCl and **(B)** Sorbitol at the indicated concentrations. Error bars indicate the standard deviations calculated from the data for three independent experiments (n = 3).

3.2.4 The *cmd*^{RIP} (#26), Δ*camk-1*, and Δ*camk-2* knockout mutants showed an increased sensitivity to hydrogen peroxide (H_2O_2) induced oxidative stress

In living organisms, reactive oxygen species (ROS) are continuously generated as side-products of certain metabolic pathways under aerobic living conditions. Simultaneously, ROS is scavenged from the cell to maintain a balance via specific and non-specific mechanisms. The cells come under oxidative stress when the balance between the production and degradation of ROS (redox state) is disturbed, resulting in high concentrations of ROS in the cell (Lushchak 2011). Severe cell damage might occur when ROS reacts with essential biological molecules causing deleterious damages such as peroxidation of lipids, oxidation of proteins, and mutations in DNA which leads to aging and apoptotic cell death (Beckman and Ammes 1998; Curtin et al. 2002; Hamann 2008; Montibus et al. 2015). Changing environmental factors could generate a high amount of intracellular ROS and oxidative stress in fungi; therefore, regulation of cellular ROS concentration is essential for survival and normal physiological development (Belozerskaya and Gessler 2006; Gessler et al. 2006). A cross-talk between Ca^{2+} signaling and ROS production is reported in higher organisms, where the increase in the $[Ca^{2+}]_{in}$ level activates ROS generating enzymes, while on the other hand, ROS also stimulates the increase in $[Ca^{2+}]_{in}$ level (Gordeeva et al. 2003; Görlach et al. 2015). In *Botrytis cinerea*, exposure to calcium chloride ($CaCl_2$), hydrogen peroxide (H_2O_2), and calcofluor white (CFW) directly affected the cellular redox state as a high amount of oxidized glutathione was formed inside the cell (Marshall et al. 2016). Therefore, to determine whether CaM and CaMKs are involved during oxidative stress, I tested the effect of H_2O_2 on the growth and viability of the strains. The conidia of the wild type and the mutant strains were first grown in VGM agar supplemented with or without (control) 10 mM H_2O_2 (Yang and Borkovich 1999; Park et al. 2008), and the percent growth rate was measured as described in chapter 2. H_2O_2 generates the highly reactive ·OH radicals via the Fenton's reaction between H_2O_2 and Fe^{2+} ions, which causes deleterious

modifications to biological molecules (Winterbourn 1999). The percent growth rate for #26, Δ*camk-1*, and Δ*camk-2* mutants were reduced as compared to the wild type at 10 mM H_2O_2 (Figure 3.4 B; Table 3.4 A). To test the survival rate of the strains, I cultured 2 h germlings further for 1 h in VGM liquid with or without 10 mM H_2O_2 and calculated the percent survival as described earlier in chapter 2. The #26, Δ*camk-1*, and Δ*camk-2* mutants showed reduced survival percentage compared to wild type (Figure 3.4 C). However, the Δ*camk-3* and Δ*camk-4* mutants did not show a significant difference in the growth and survival rates at 10 mM H_2O_2 in comparison to the wild type. Therefore, these results indicated that *cmd*, *camk-1*, and *camk-2* genes are required for response to oxidative stress.

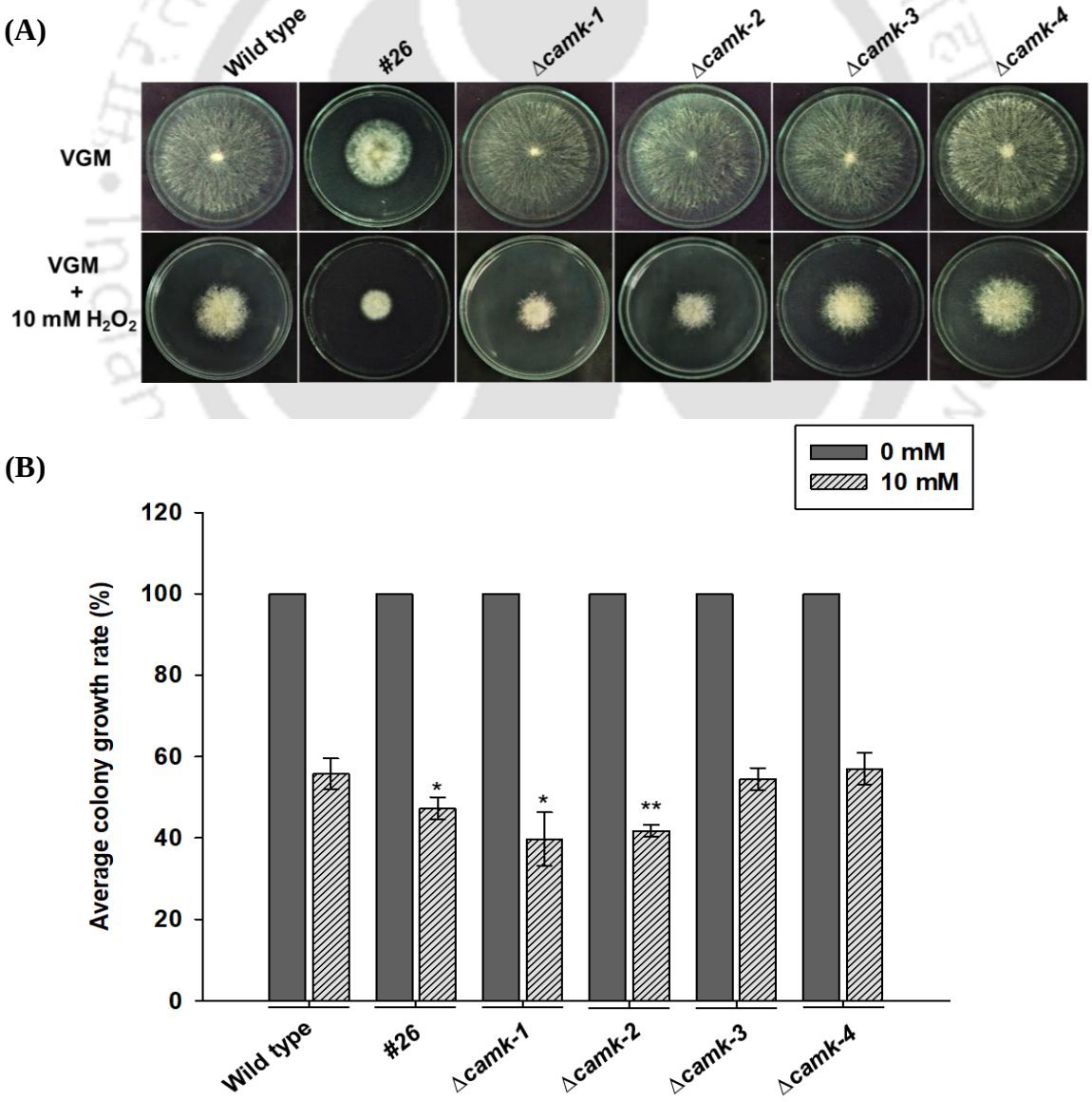

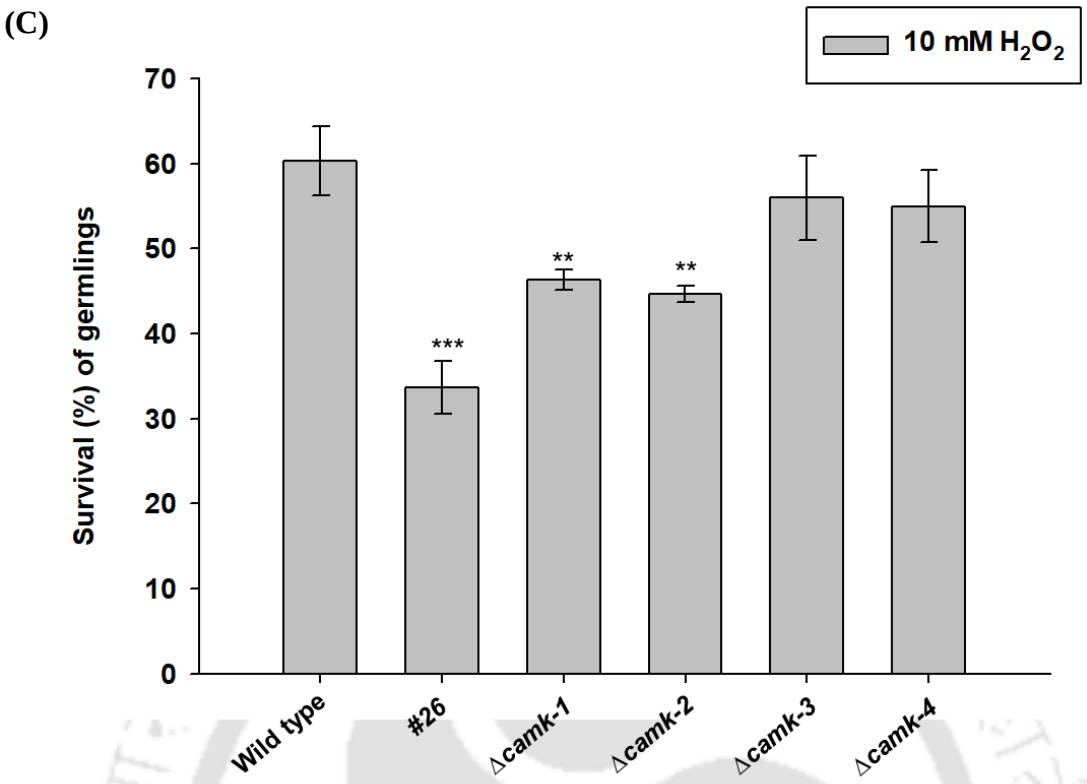

Figure 3.4 Oxidative stress assay. Sensitivity to oxidative stress was evaluated by growing the strains on Vogel's glucose agar medium with and without 10 mM H_2O_2 and incubating in the dark at 30 °C for 24 h. **(A)** Colony growth on Petri-dish, **(B)** Relative colony growth rate (%), (**C**) Survival (%) of 2 h germlings determined after the treatment to 10 mM H_2O_2 for 1 h. Standard deviations are indicated by error bars calculated from three independent experiments (n = 3), and the significance given by *P* values <0.05 (*), <0.01 (**), and <0.001 (***) compared to the wild type strain as measured by one-way ANOVA test.

3.2.5 The *cmd*^{RIP} (#26), Δ*camk-1*, and Δ*camk-2* mutants contributed to ROS production upon exposure to H_2O_2

Under normal physiological conditions, low amounts of ROS are produced due to active aerobic metabolism (Cipak et al. 2008). The #26, Δ*camk-1*, and Δ*camk-2* mutants showed increased sensitivity to H_2O_2-induced oxidative stress suggesting an increased ROS level in these mutants. Therefore, the amount of endogenous ROS produced in the #26, Δ*camk-1*, and Δ*camk-2* mutants was measured using 2',7'- dichlorofluorescein-diacetate (DCFH-DA) dye (Figure 3.5 A). DCFH-DA is a cell-permeable dye, which remains nonfluorescent inside the cell until the acetate group is hydrolyzed by intracellular esterases to 2' 7' dichlorodihydrofluorescein (DCFH), and oxidized by intracellular ROS to the highly fluorescent compound 2'7' dichlorofluorescein (DCF) that can be detected as a measure of intracellular ROS (Figure 3.5 B; Radman et al. 2004; Chen et al. 2010). The ROS levels in the conidia treated with or without H_2O_2 were detected using DCFH-DA. The #26, Δ*camk-1*, and Δ*camk-2* mutants showed an increased number of fluorescent conidia compared to wild type indicating that the #26, Δ*camk-1*, and Δ*camk-2* mutants probably produces more ROS than wild type when treated with 10 mM H_2O_2 (Figure 3.5 C). A more detailed analysis and quantification will be done in the future.

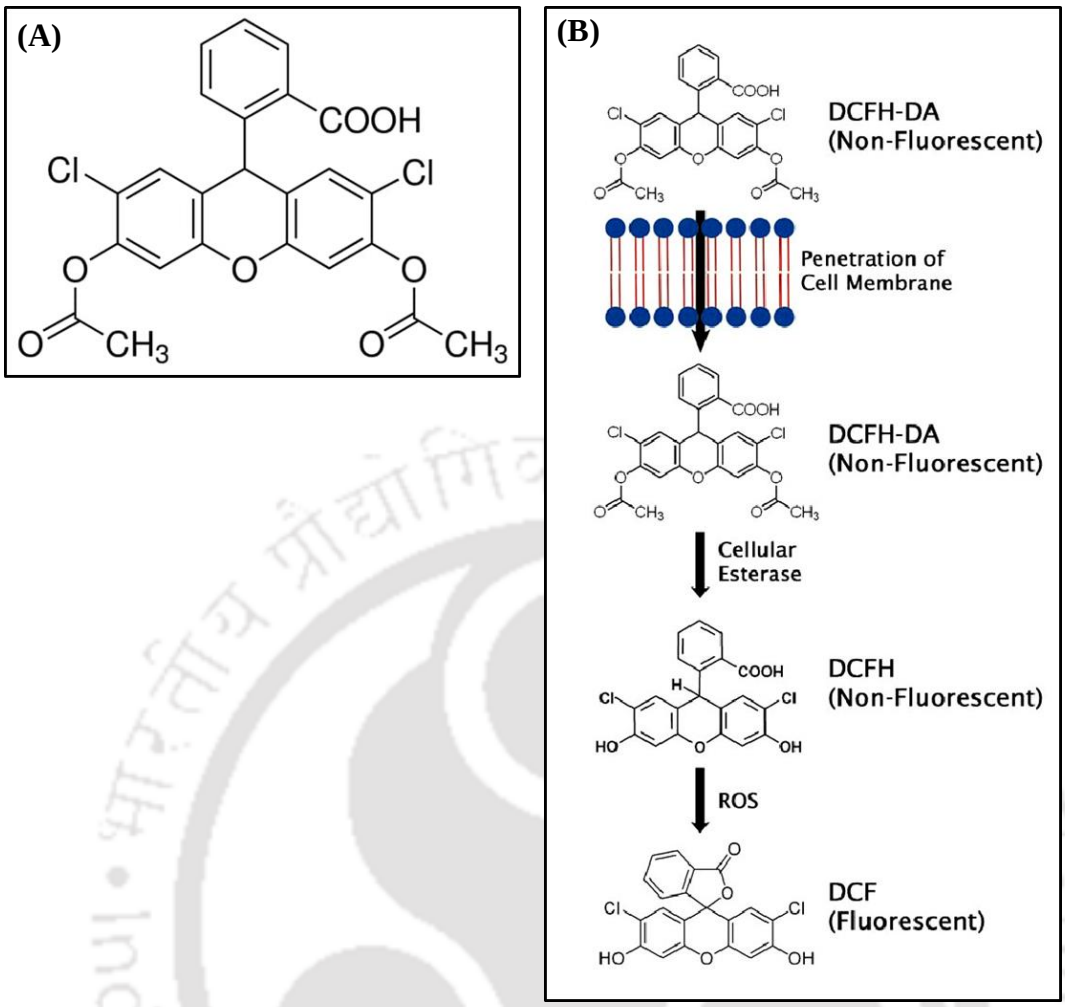

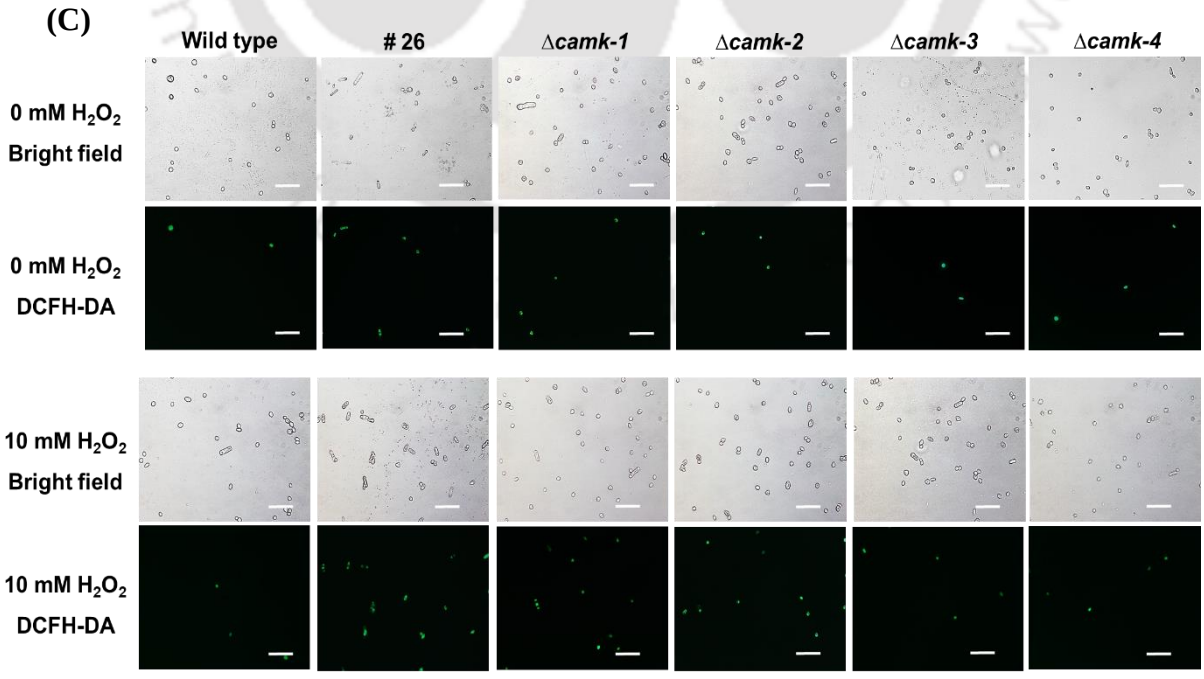

Figure 3.5 Estimation of ROS production of *N. crassa* strains. (A) The chemical structure of 2',7'-dichlorofluorescein-diacetate (DCFH-DA) is available at https://www.sigmaaldrich.com/IN/en/product/sigma/d6883 (DCF; excitation at 488 nm, emission at 515 nm). **(B)** Schematic for the mechanism of action of DCFH-DA as given at https://www.cellbiolabs.com/reactive-oxygen-species-ros-assay#details. **(C)** DCFH-DA assay. To estimate the amount of ROS produced upon exposure to H_2O_2, approximately 1×10^6 conidia of the wild type, #26, Δ*camk-1*, Δ*camk-2*, Δ*camk-3*, and Δ*camk-4* mutant strains were incubated in VG liquid with 10 µM DCFH-DA for 30 min and further treated with 10 mM H_2O_2 for 90 min. An aliquot of conidia was observed under a trinocular inverted microscope (AxioVert A1 FL, Carl Zeiss) with a 450-490 nm excitation filter and a 515 nm emission filter. The cells were analyzed in at least three different aliquots at different times. Scale bar 50 µm.

3.2.6 The *cmd*^{RIP} (#26), Δ*camk-1*, and Δ*camk-2* mutants showed increased sensitivity to dithiothreitol (DTT) induced ER stress

The endoplasmic reticulum (ER) is a multifunctional organelle important for many cellular processes such as (a) synthesis, folding, post-translational modifications, and orderly transport of proteins, (b) biosynthesis of lipids and sterols, and (c) storage of Ca^{2+} within its lumen and their regulated release into the cytoplasm (Berridge 2002; Schröder 2008; Bravo et al. 2013). Perturbations in ER function due to altered redox status and reduction in Ca^{2+} concentration results in the accumulation of misfolded and oxidized proteins, which triggers ER stress (Görlach et al. 2006, 2015; Darling and cook 2014). Therefore, to determine the role of CaM and Ca^{2+}/CaMKs under ER stress, I studied the growth rate of the #26, Δ*camk-1*, Δ*camk-2*, Δ*camk-3*, and Δ*camk-4* mutants in VG liquid media containing different concentrations (0 to 2 mM) of dithiothreitol (DTT). DTT is a potent reducing agent that inhibits disulfide bond formation resulting in the accumulation of unfolded proteins (Zhang et al. 2017; Fiege et al.

2018). The aerial hyphae height was measured after 3 days of incubation in the dark at 30 °C, and the percent growth rate was determined. The #26, Δ*camk-1*, and Δ*camk-2* mutants showed decreased growth at 2 mM DTT, whereas Δ*camk-3* and Δ*camk-4* showed growth similar to the wild type (Figure 3.6). These results suggested that *camk-1*, *camk-2*, and *cmd* genes play a role in tolerance to the ER stress condition.

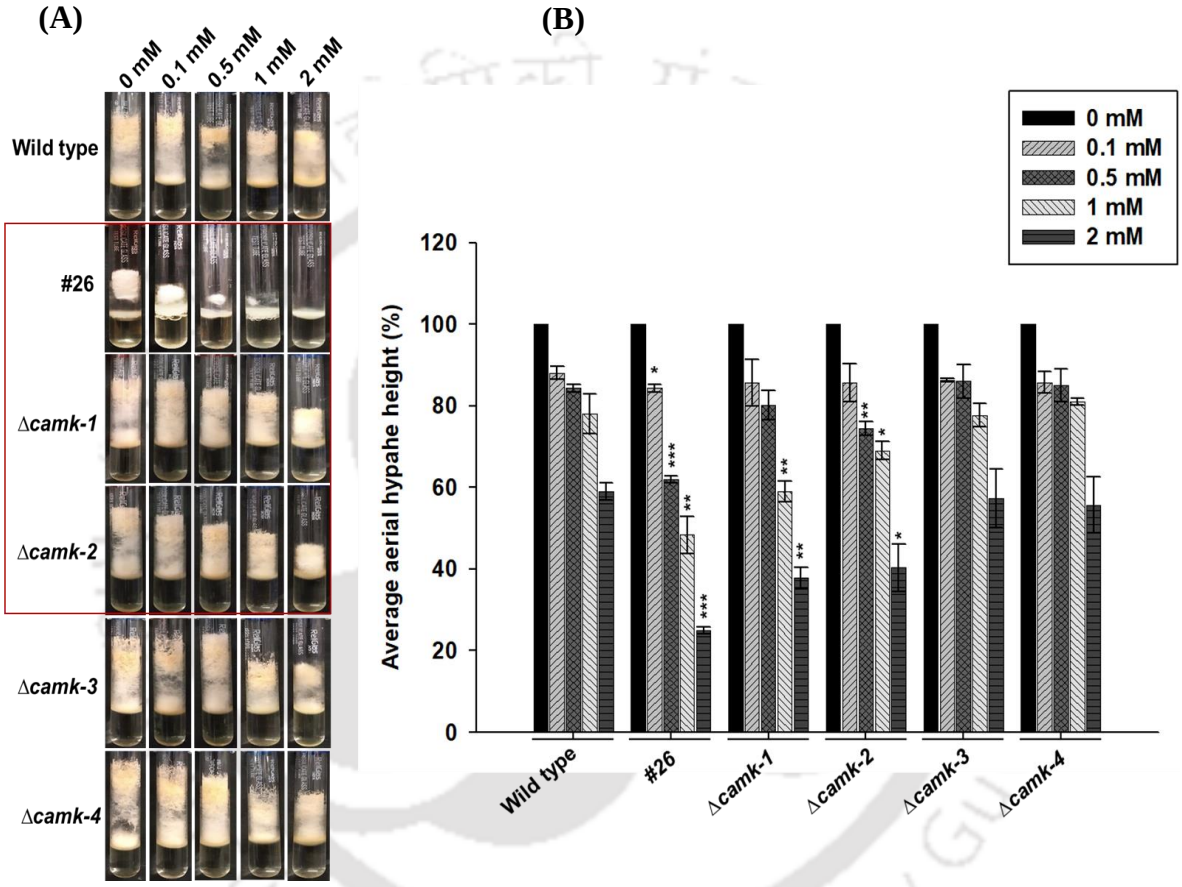

Figure 3.6 Assay for endoplasmic reticulum stress using dithiothreitol. (A) Effect of DTT on aerial hyphae. **(B)** Average aerial hyphae height (%) in response to various amounts of DTT. To evaluate the DTT sensitivity, strains were inoculated in VG liquid medium containing 0.1 mM, 0.5 mM, 1 mM, and 2 mM of DTT, and incubated at 30 °C for 3 days at constant darkness; then the percent growth rate relative to the wild type was determined. Standard deviations are indicated by error bars calculated from three independent experiments (n = 3), and the significance given by *P* values <0.05 (*), <0.01 (**), and <0.001 (***) compared to the wild type strain as measured by one-way ANOVA test.

3.2.7 The *cmd*^{RIP} (#26), Δ*camk-1*, and Δ*camk-2* knockout mutants showed a decrease in thermotolerance

The heat shock response pathway is one of the fundamental features in living organisms that enable adaptation to a sudden rise in temperature. Exposure to a sublethal stress environment enhances the expression of heat shock proteins that imparts stress tolerance and protection to a heat shock temperature (Mager and De Kruijff 1995; Rangel 2011; Liu et al. 2012). In *N. crassa*, cells pre-exposed to a sublethal temperature, which is lower than the lethal temperature value, showed higher survival rates when exposed to lethal temperature than the cell without pre-exposure to sublethal temperature, and this mechanism is known as induced thermotolerance (Kapoor et al. 1990; Yang and Borkovich 1999). The oxidative stress response is also linked to thermotolerance in *N. crassa* (Kapoor 1990). Because the #26, Δ*camk-1*, Δ*camk-2*, Δ*camk-3,* and Δ*camk-4* mutants showed an increased sensitivity to temperature and oxidative stress conditions (Figures 3.1, 3.4); therefore, I also evaluated the thermotolerance of these mutants. The strains were exposed to a lethal temperature of 52 °C with or without pre-exposure to a sublethal temperature of 44 °C. Percent survival was determined from the viable colonies under the different conditions as described in chapter 2. The #26, Δ*camk-1*, Δ*camk-2*, and Δ*camk-4* showed reduced survival rates compared to the wild type under induced thermotolerance, while hardly any survival was seen under the uninduced thermotolerance for all the strains (Figure 3.7). The Δ*camk-3* mutant did not show much difference in survival rate compared to the wild type. These results suggested that *cmd* and *camks* might play a role in the expression of heat shock proteins required for thermotolerance.

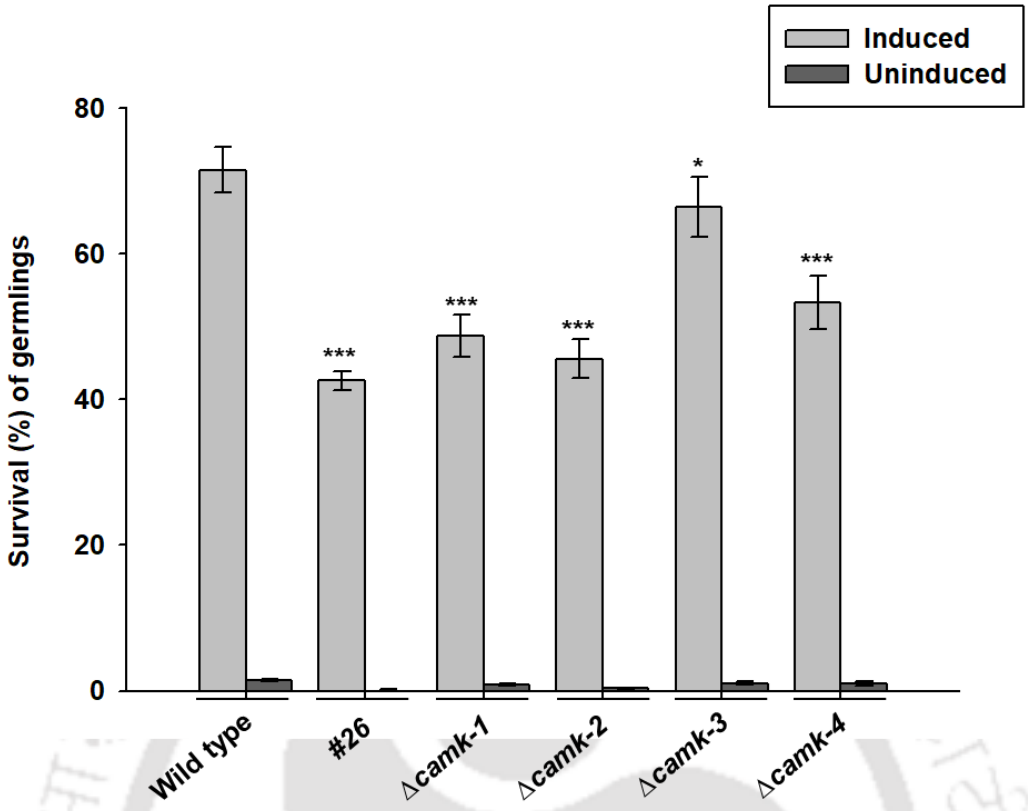

Figure 3.7 Thermotolerance assay. Viability of 2 h old germlings of wild type, #26, Δ*camk-1*, Δ*camk-2*, Δ*camk-3*, and Δ*camk-4* strains after exposure to 52 °C lethal temperature with (induced) or without (uninduced) pre-exposure to a sublethal heat shock temperature of 44 °C. Standard deviations are indicated by error bars calculated from three independent experiments (n = 3), and the significance given by *P* values <0.05 (*), <0.01 (**), and <0.001 (***) compared to the wild type strain as measured by one-way ANOVA test.

3.2.8 Cloning of *camk-1* and *camk-2* genes for complementation analysis

The *camk-1* and *camk-2* genes were cloned to generate *N. crassa* strains for complementation studies. The ORF of *camk-1*(1701 bp) and *camk-2* (1471 bp) genes were PCR amplified from the wild type genomic DNA and ligated to the *Sma*I site of pRS426PVG/*Pnit-6* vector (Figure 3.8 A and B). The ligated products were transformed into the *E. coli* DH5α ultracompetent cells and isolated the pCNM-1($P_{nit\text{-}6}$::*camk-1*::*5xGly*::*V5*::*gfp*) and pCNM-2 ($P_{nit\text{-}6}$::*camk-2*::*5xGly* ::*V5*::*gfp*) clones, which were verified by restriction digestion and PCR analysis (Figure 3.8 C to G).

(A)

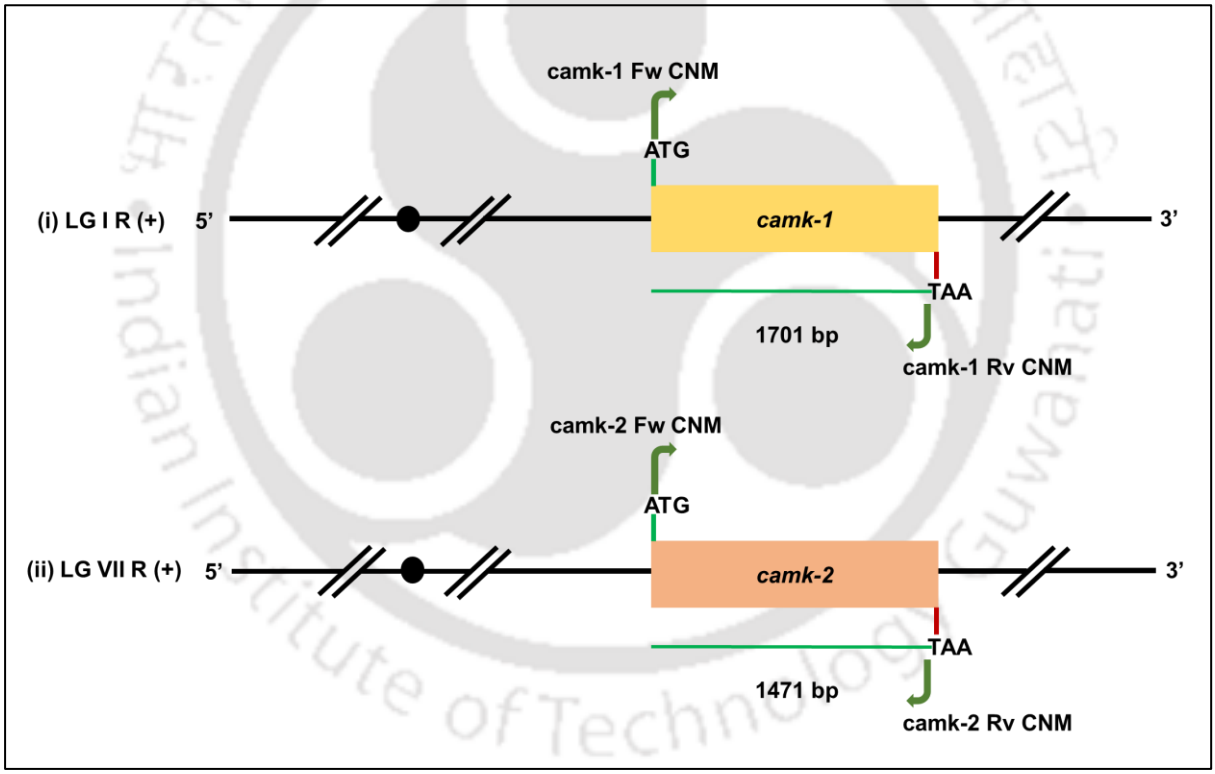

(B)

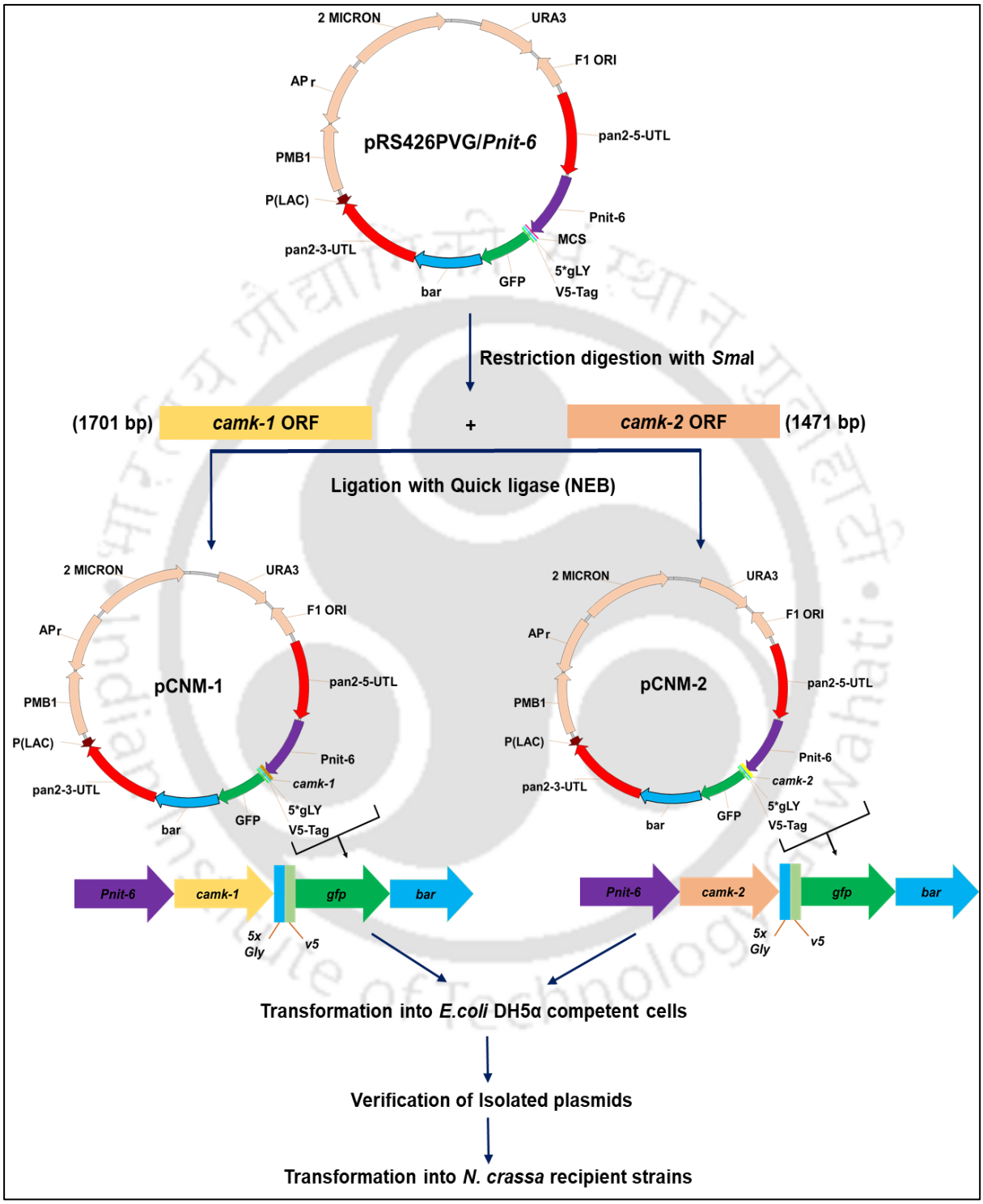

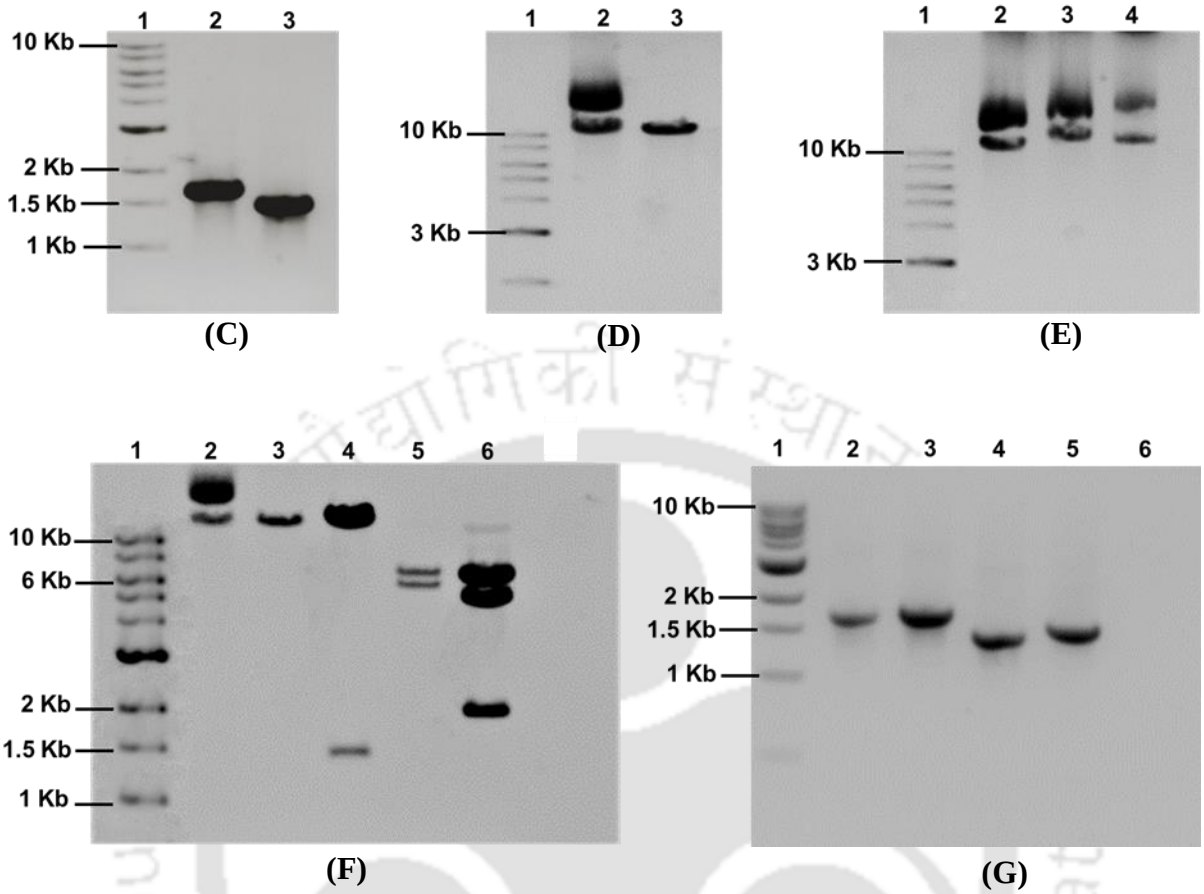

Figure 3.8 Cloning of the *camk-1* and *camk-2* genes for complementation studies. (A) Schematics showing the primers to PCR amplify the *camk-1* and *camk-2* genes using the DNA from wild type. **(B)** Schematics showing the generation of the pCNM-1 and pCNM-2 constructs. Cloning of *camk-1* and *camk-2* ORFs into the *Sma*I site of pRS426PVG/*Pnit-6* plasmid vector (Ouyang et al. 2015). **(C)** Visualization of the PCR amplicon of *camk-1* and *camk-2* genes. The primer pairs, camk-1 CNM Fw and camk-1 CNM Rv (entries 4 and 5; Table 3.1), and camk-2 CNM Fw and camk-2 CNM Rv (entries 6 and 7; Table 3.1) were used to amplify the *camk-1* (1701 bp) and *camk-2* (1471 bp) ORF fragments from the wild type. The PCR products were resolved in 1% agarose gel; lane 1: 1kb DNA ladder (NEB), lane 2: *camk-1* ORF, lane 3: *camk-2* ORF. **(D)** Visualization of the plasmid vector constructs; lane 1: 1kb DNA ladder (NEB), lane 2: undigested pRS426PVG/Pnit-6 plasmid, lane 3: digested

pRS426PVG/*Pnit-6* plasmid (~11.14 kb) with Sma1. **(E)** Visualization of the plasmid constructs. lane 1: 1 kb DNA ladder (NEB), lane 2: pRS426PVG/Pnit-6 vector, lane 3: pRS426PVG/*Pnit-6* vector with *camk-1* insert and designated as pCNM-1 (~12.8 kb); lane 4: pRS426PVG/*Pnit-6* vector with *camk*-2 insert and designated as pCNM-2 (~12.6 kb). **(F)** Restriction digestion to confirm pCNM-1and pCNM-2 plasmid constructs. The pCNM-1 plasmid construct was digested with *Hind*III, while the pCNM-2 plasmid construct was digested with *Apa*I restriction enzyme to confirm the specific gene insertion and correct alignment within the vector; lane 1: 1 kb DNA ladder (NEB), lane 2: pRS426PVG/*Pnit-6* vector (uncut), lane 3: the digestion of pRS426PVG/*Pnit-6* vector with *Hind*III gave a single fragment of size ~11,139 kb while in lane 4: the digestion of pCNM-1 with *Hind*III gave two fragments of size 11,375 bp and 1,465 bp, lane 5: the digestion of pRS426PVG/*Pnit-6* vector with *Apa*I gave two fragments of size 5,926 bp and 5,213 bp while in lane 6: the digestion of pCNM-2 with *Apa*I gave three fragments of size 5,926 bp, 4,731 bp and 1,953 bp. **(G)** PCR amplification of pCNM-1 and pCNM-2 plasmid constructs using primer #8 with #5 and #7, and # 4 and #6 with #9 (Table 3.1). The PCR products were resolved in 1% agarose gel. Lane1: 1 kb DNA ladder (NEB), lane 2: PCR amplified product for verifying *camk-1* insert in the pCNM-1 construct using Pnit-6-Fw and camk-1 CNM Rv (1746 bp); lane 3: another PCR amplified product for verifying *camk-1* insert in the pCNM-1 construct using camk-1 CNM Fw and GFP Rv (1850 bp); lane 4: PCR amplified product for verifying *camk-2* insert in the pCNM-2 construct using Pnit-6 Fw and camk-2 CNM Rv (1516 bp); lane 5: another PCR amplified product for verifying *camk-2* insert in the pCNM-2 construct using camk-2 CNM Fw and GFP Rv (1620 bp), lane 6: pRS426PVG/*Pnit-6* plasmid as negative control (no PCR product as no constructs inserted).

Table 3.1 Primers used for cloning of the *camk-1* and *camk-2* genes and confirmation of homokaryotic strains

Sl. No.	Primer Name	Sequence (5'→3')	Reference
1	6NCU09123F-HI	GCG AAT GGG AGA GCC TTA CA	This study
2	16NCU02283F-HI	AGT ACG AGA TCG ACG GAG GA	Laxmi and Tamuli 2017
3	5HPHR	ATCCACTTAACGTTACTGAAATC	Deka et al. 2011
4	camk-1 Fw CNM	ATGAGCTGTAAGTTCCCTCTAC	This study
5	camk-1 Rv CNM	GCCTTGGAAACTCTTCGC	This study
6	camk-2 Fw CNM	ATGAGTGCCGCCAACGGTCG	This study
7	camk-2 Rv CNM	TCGCTTAACACTAGTCCCAATC	This study
8	Pnit-6 Fw	CTAGTCTTTCTGTCGTCAGC	Gohain and Tamuli 2019
9	GFP-Rv	AACTTGTGGCCGTTTACGTC	Gohain and Tamuli 2019

3.2.9 Transformation of the pCNM-1 and pCNM-2 constructs into the Δ*camk-1*::*hph*; Δ*mus-53*::*hph*; *mat A* and Δ*mus-53*::*hph*; Δ*camk-2*::*hph*; *mat A* recipient strains and generation of homokaryotic strains

The pCNM-1 ($P_{nit\text{-}6}$::*camk-1*::*5xGly*::*V5*::*gfp*) and pCNM-2 ($P_{nit\text{-}6}$::*camk-2*::*5xGly*::*V5*::*gfp*) plasmid constructs were transformed by electroporation (described in chapter 2) into the *N. crassa* recipient strains Δ*camk-1*::*hph*; Δ*mus-53*::*hph*; *mat A* (P- 4) and Δ*mus-53*::*hph*; Δ*camk-2*::*hph*; *mat A* (P-13). The heterokaryotic transformants were selected based on resistance to

basta and then crossed with Δ*camk-1* and Δ*camk-2* strains of the opposite mating type to obtain the homokaryotic progenies (Figure 3.9 A). The *camk-1* and *camk-2* transgenes in the homokaryotic progenies were verified by PCR (Figure 3.9 B and C).

(A)

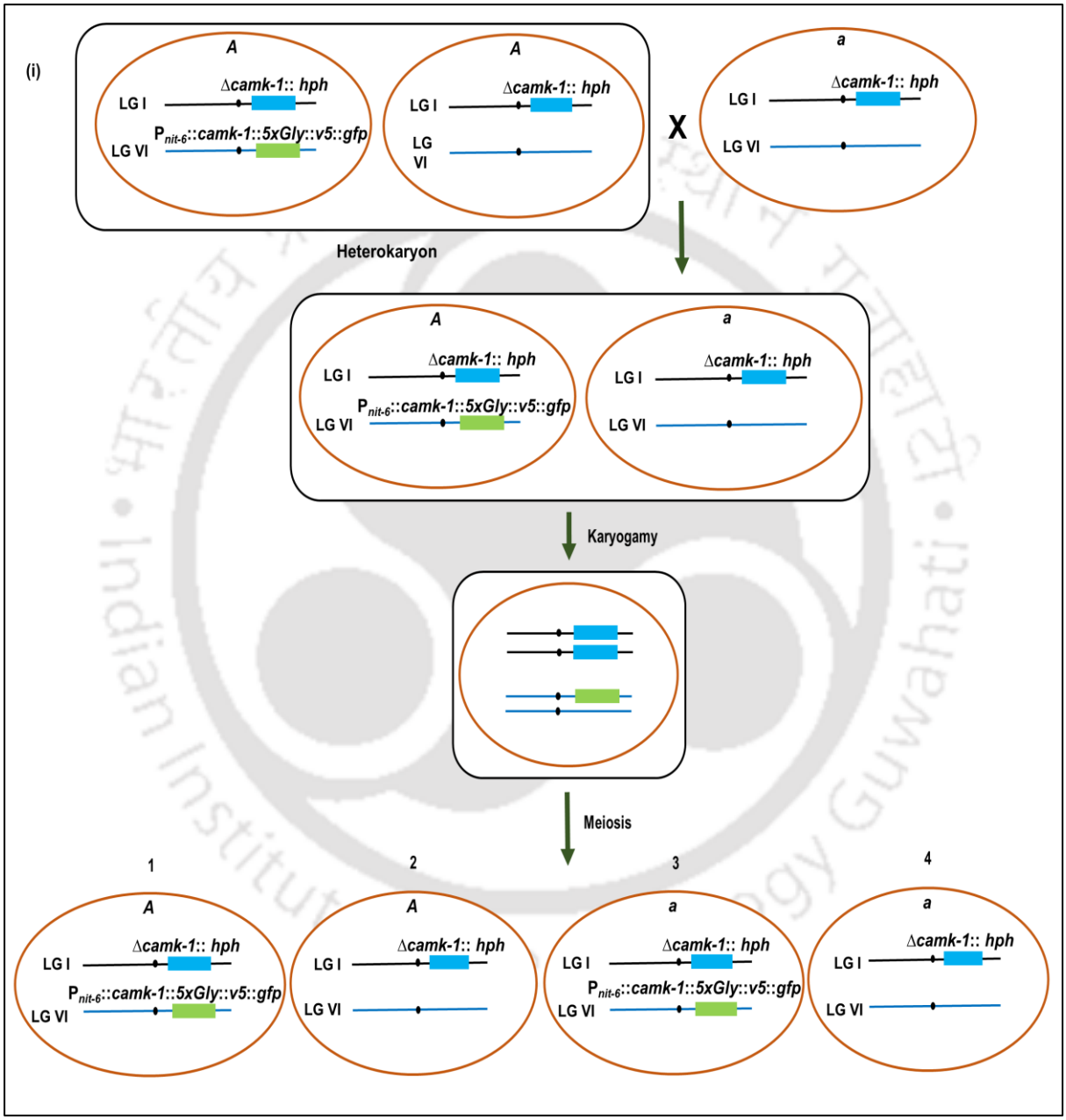

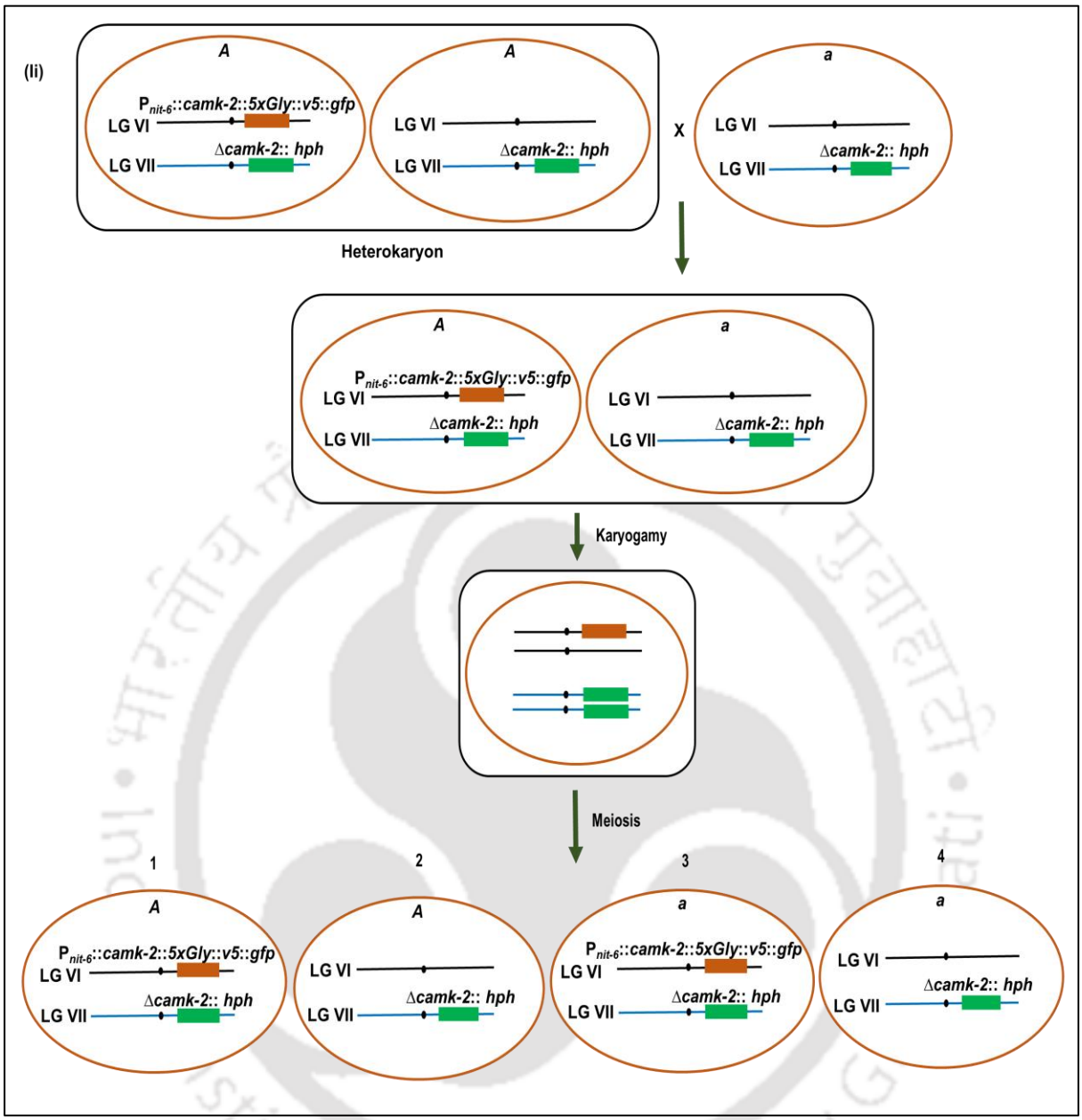

(B)

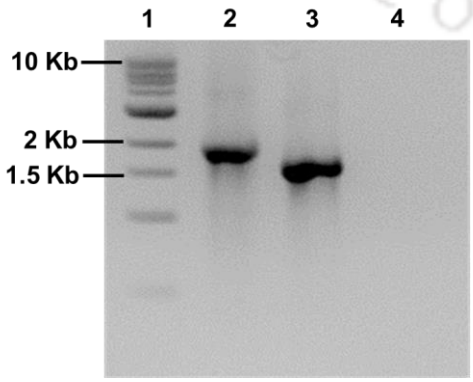

(C)

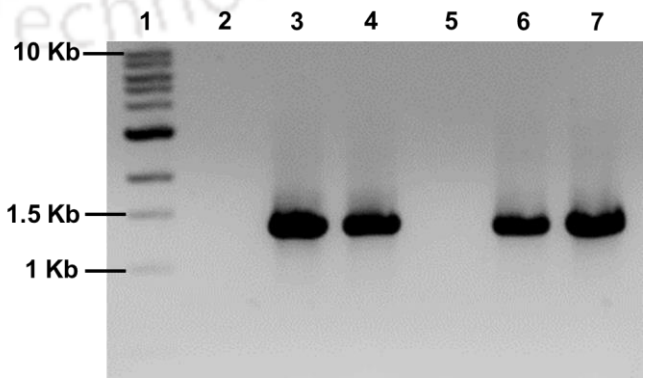

Figure 3.9 Transformation of pCNM-1 and pCNM-2 constructs into *N. crassa* recipient strains and generation of homokaryotic strains. (A) Schematic representation of heterokaryons CNM *camk-1* HT-1 and CNM *camk-2* HT-1 crossed with Δ*camk-1* and Δ*camk-2* mutant strains to generate homokaryotic strains for complementation analysis. Generation of **(i)** Δ*camk-1*::*hph*; Δ*pan-2*::P_{nit-6}::*camk-1*::*V5*::*gfp*; *mat A* (#19), and **(ii)** Δ*camk-2*::*hph;* Δ*pan-2*::P_{nit-6}::*camk-2*::*V5*::*gfp*; *mat A* (#8). **(B)** PCR verification of the homokaryotic strains using the Pnit-6 Fw and GFP-Rv primers (entries 8 and 9; Table 3.1). PCR products were verified using 1% agarose gel; lane 1: 1 kb DNA ladder (NEB), lane 2: PCR amplification verifying the insertion of the construct with *camk-1* allele (1,895 bp), lane 3: PCR amplification verifying the insertion of the construct with *camk-2* allele (1,665 bp), and lane 4: wild type (negative control). **(C)** PCR amplification to verify the presence of the Δ*camk-1* and Δ*camk-2* alleles in the homokaryotic strains using 6NCU09123F-HI and 16NCU02283F-HI forward primers-specific to the upstream of the *camk-1* and *camk-2* ORF, respectively, with the common reverse primer 5HPH Rv (entries 1-3; Table 3.1). PCR products were resolved in 1% agarose gel; lane 1: 1 kb DNA ladder (NEB), lane 2: wild type (negative control for Δ*camk-1* allele, because target sequence for 5HPHR is absent), lane 3: Δ*camk-1* mutant (positive control) that yield a PCR product of size 1,328 bp, lane 4: PCR amplification verifying the Δ*camk-1* allele (1,328 bp) in Δ*camk-1*::*hph;* Δ*pan-2*::P_{nit-6}::*camk-1*::*V5*::*gfp*; *mat A* (#19), lane 5: wild type (negative control; sequence for the 5HPHR is absent in the Δ*camk-2* allele), lane 6: Δ*camk-2* mutant (positive control) yield PCR product of size 1,296 bp, and lane 4: PCR amplification verifying the Δ*camk-2* allele (1,296 bp) in Δ*camk-2*::*hph;* Δ*pan-2*::P_{nit-6}::*camk-2*::*V5*::*gfp*; *mat A* (#8).

3.2.10 Complementation of *cmd*^{RIP}, Δ*camk-1*, and Δ*camk-2* mutants

The *cmd*^{RIP} (#26), Δ*camk-1*, and Δ*camk-2* mutants were defective under various abiotic stress conditions showing decreased growth under the heat-shock, pH, oxidative, and ER stress conditions. In order to confirm that the phenotypic defects were due to the RIP-induced mutations in the *cmd* gene and the knockout mutation of the *camk-1* and *camk-2* genes, I performed complementation studies using the parental strain Δ*pan-2*::*bar*::P_{tcu-1}::*cmd*::*V5*::*gfp*; *mat a* (#850, Laxmi and Tamuli 2017), which was used to generate the Δ*pan-2*::*bar*::P_{tcu-1}::*cmd*^{RIP}::*V5*::*gfp*; *mat A* (#26) mutant. The homokaryotic transformant of Δ*camk-1* carrying the *camk-1* transgenes, Δ*camk-1*::*hph;* Δ*pan-2*::P_{nit-6}::*camk-1*::*V5*::*gfp*; *mat A* (#19) and the homokaryotic transformant of Δ*camk-2* mutant carrying the transgene *camk-2,* Δ*camk-2*::*hph;* Δ*pan-2*::P_{nit-6}::*camk-2*::*V5*::*gfp*; *mat A* (#8) were used for the complementation studies of Δ*camk-1*, and Δ*camk-2* mutant strains. I found that the parental strain #850 and the homokaryotic transformants #19 and #8 complement the colony growth rate at low (20 °C) and elevated (40 °C) temperatures (Figure 3.10.1) and oxidative stress (Figure 3.10.3 B). The aerial hyphae heights of the parental and homokaryotic transformants were similar to that of wild type in pH stress (Figure 3.10.2), and ER stress (Figure 3.10.4), and the survival rate under oxidative stress (Figure 3.10.3 C) and thermotolerance (Figure 3.10.5) were rescued. Therefore, the *cmd*, *camk-1*, and *camk-2* genes are necessary for survival under stress conditions.

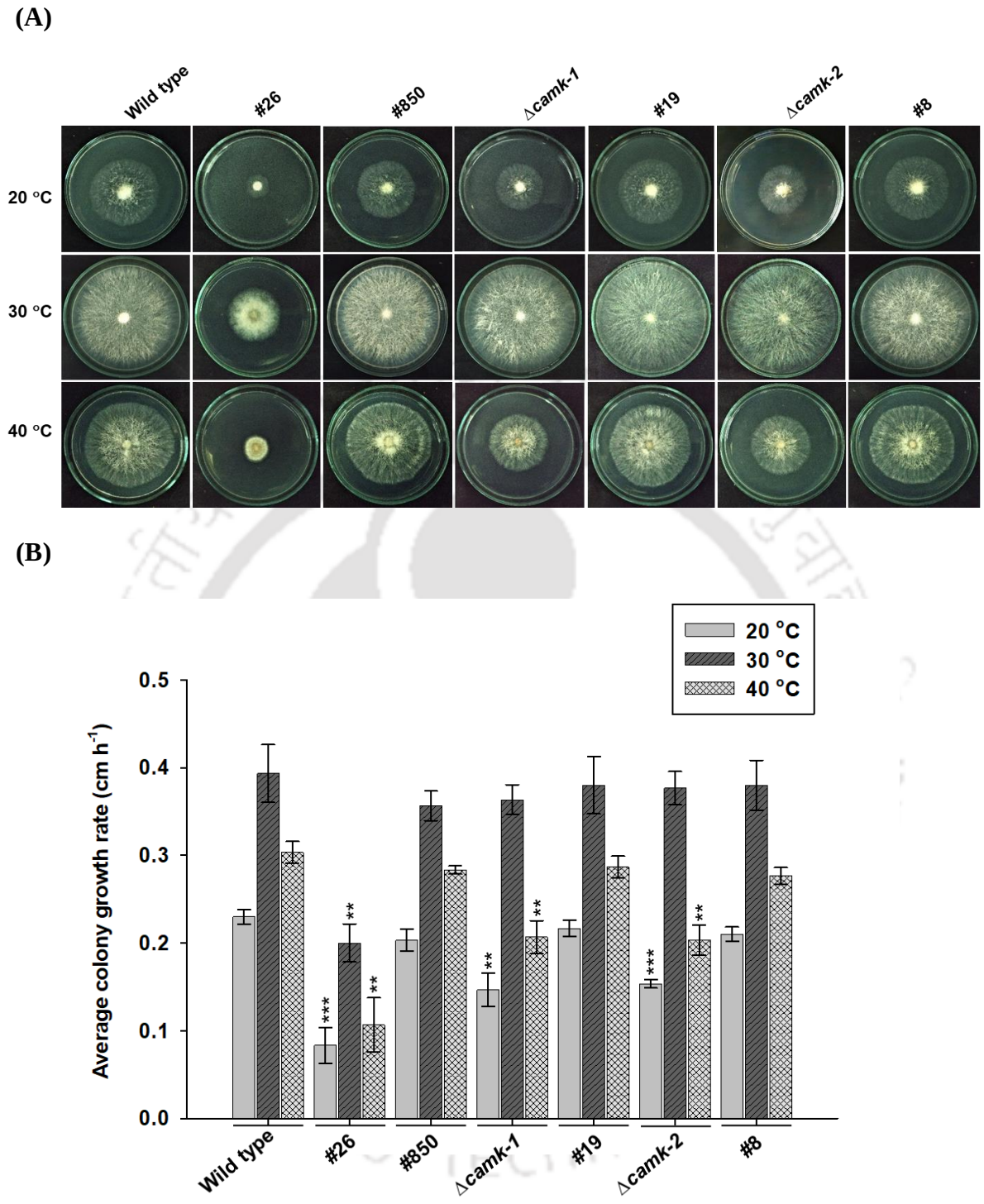

Figure 3.10.1 Complementation studies of *N. crassa* strains for temperature sensitivity. The wild type, #26, #850, Δ*camk-1*, #19, Δ*camk-2*, and #8 strains were grown on Vogel's glucose agar medium and incubated at 20, 30, and 40 °C for 24 h. **(A)** Colony growth on Petri dishes. **(B)** Average colony growth rate (cm h^{-1}). Standard deviations are indicated by error

bars calculated from three independent experiments (n = 3), and the significance given by *P* values <0.05 (*), <0.01 (**), and <0.001 (***) compared to the wild type strain as measured by one-way ANOVA test.

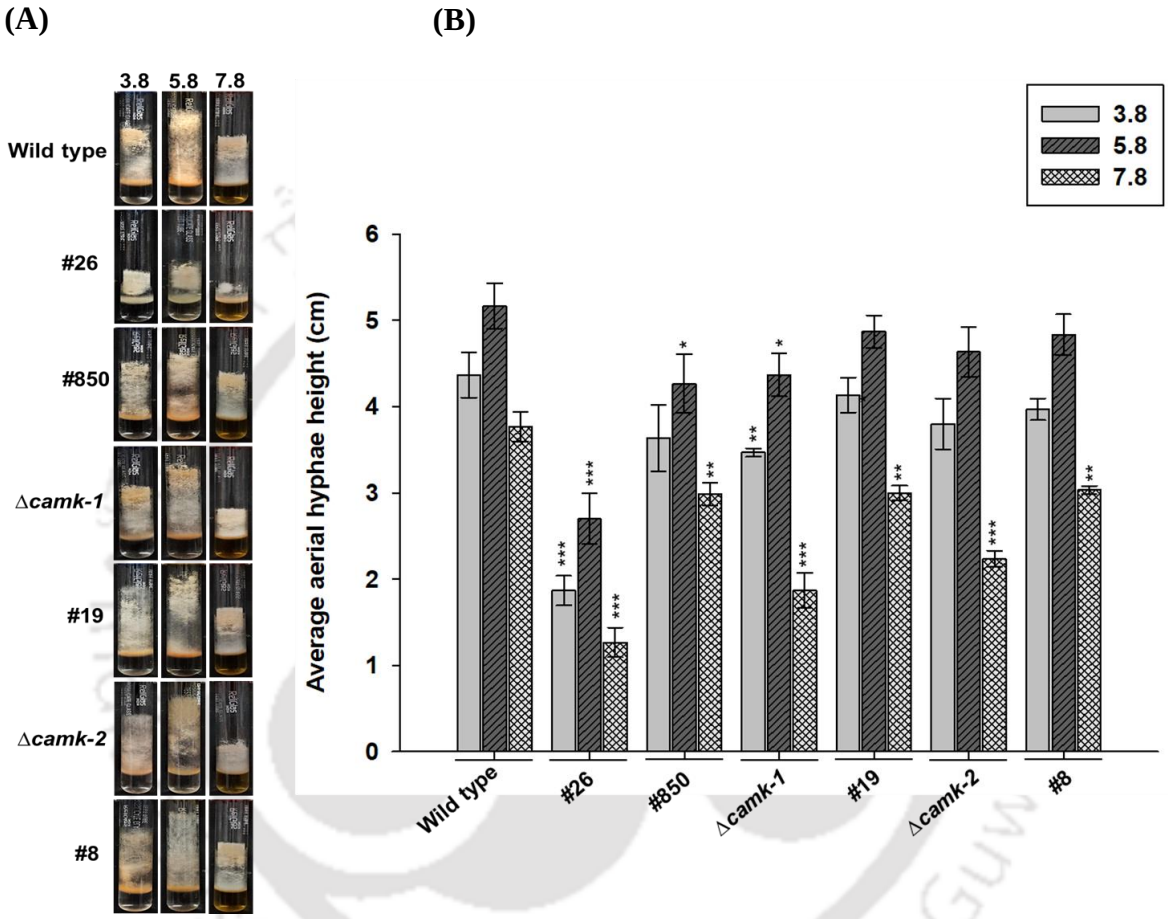

Figure 3.10.2 Complementation studies of *N. crassa* strains for pH stress assay. pH sensitivity of wild type, #26, #850, Δ*camk-1*, #19, Δ*camk-2*, and #8 strains was evaluated by growing them in VG liquid medium adjusted to three pH conditions; acidic (pH 3.8), normal (pH 5.8), and alkaline (pH 7.8) for 3 days at 30 °C. **(A)** Aerial hyphae at different pH conditions **(B)** Average aerial hyphae height (cm). Standard deviations are indicated by error bars calculated from three independent experiments (n = 3), and the significance given by *P* values <0.05 (*), <0.01 (**), and <0.001 (***) compared to the wild type strain as measured by one-way ANOVA test.

(A)

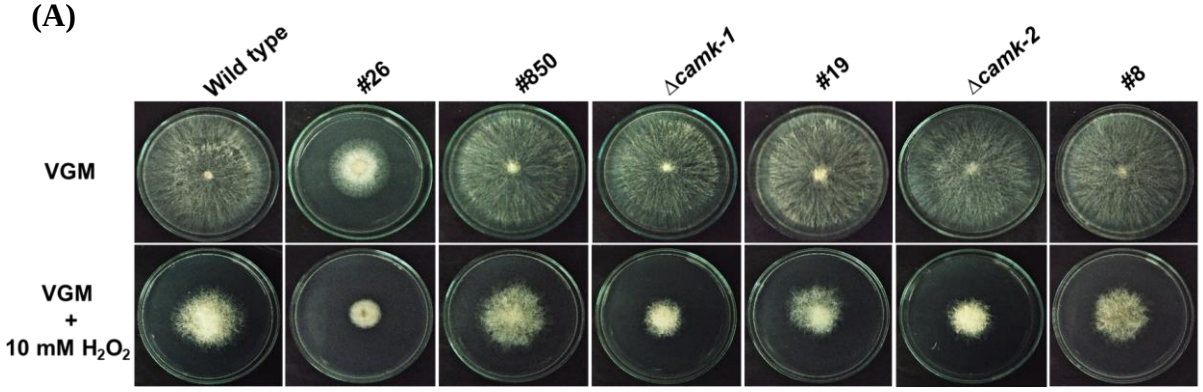

(B)

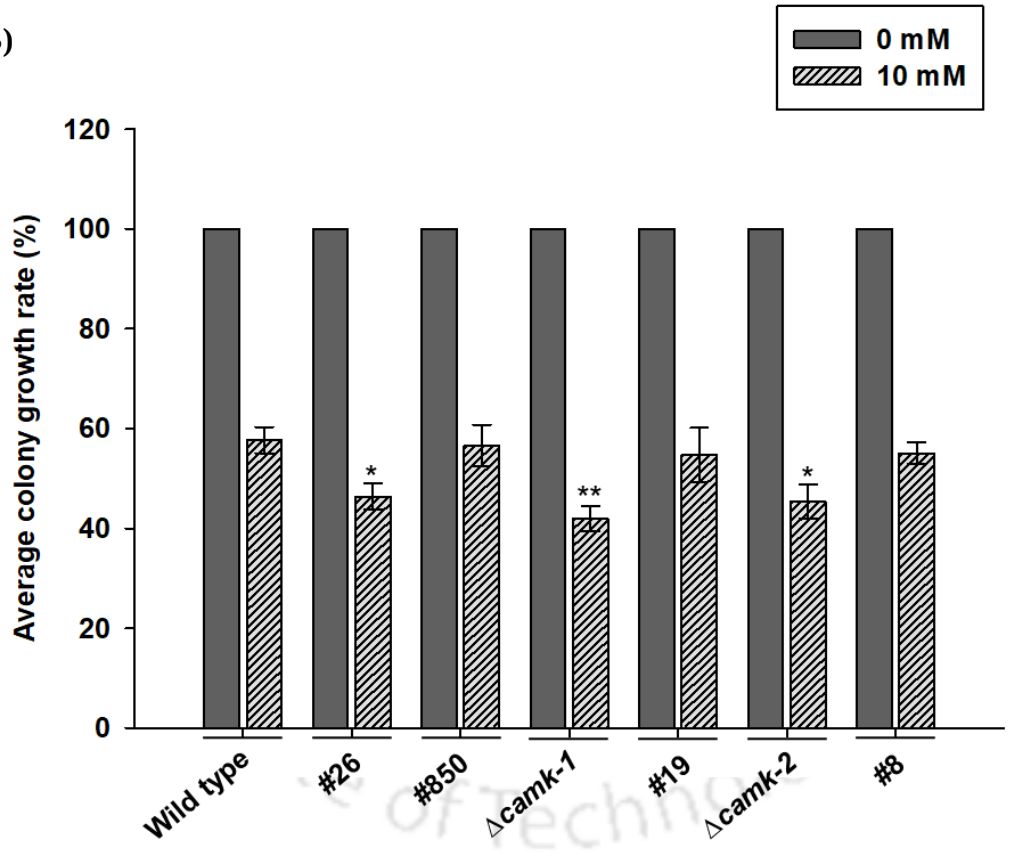

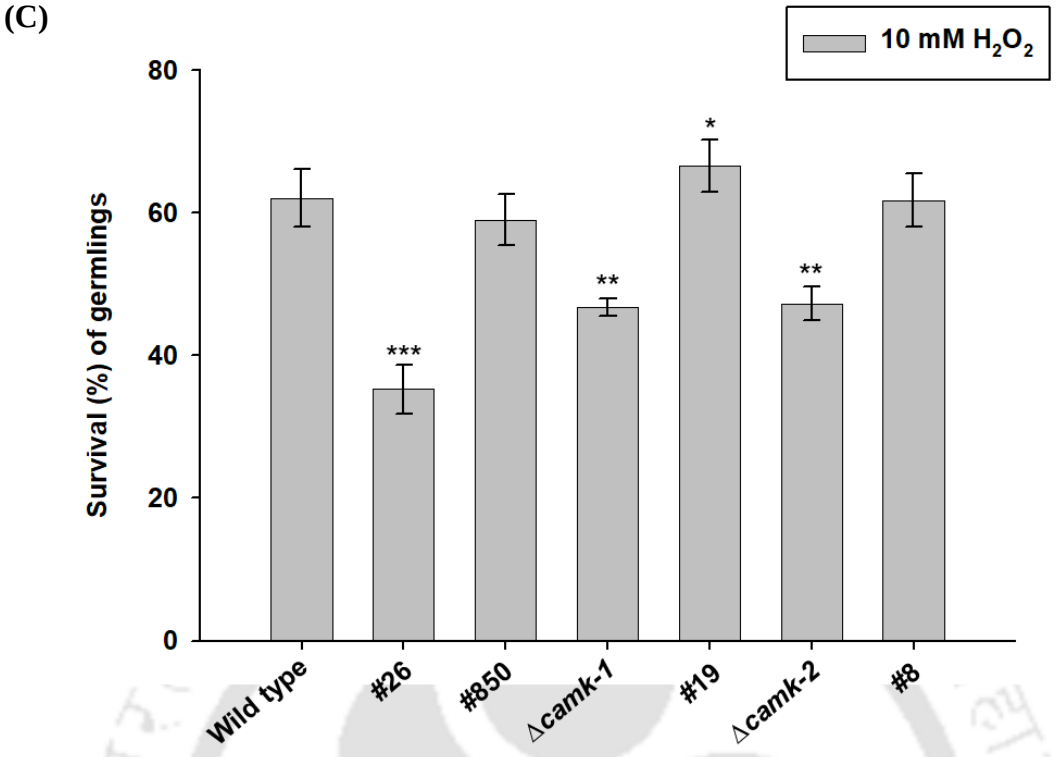

Figure 3.10.3 Complementation studies of *N. crassa* strains to determine sensitivity to oxidative stress. Sensitivity to oxidative stress was evaluated by growing the wild type, #26, #850, Δ*camk-1*, #19, Δ*camk-2*, and #8 strains on Vogel's glucose agar medium with or without 10 mM H_2O_2 and incubating in the dark at 30 °C for 24 h. **(A)** Colony growth in Petri dishes. **(B)** Relative colony growth rate (%). (**C**) Survival (%) of germlings were estimated by treating 2 h germlings to 10 mM H_2O_2 for 1 h and determining the survival percentage in comparison to cells in an untreated condition. Standard deviations are indicated by error bars calculated from three independent experiments (n = 3), and the significance given by *P* values <0.05 (*), <0.01 (**), and <0.001 (***) compared to the wild type strain as measured by one-way ANOVA test.

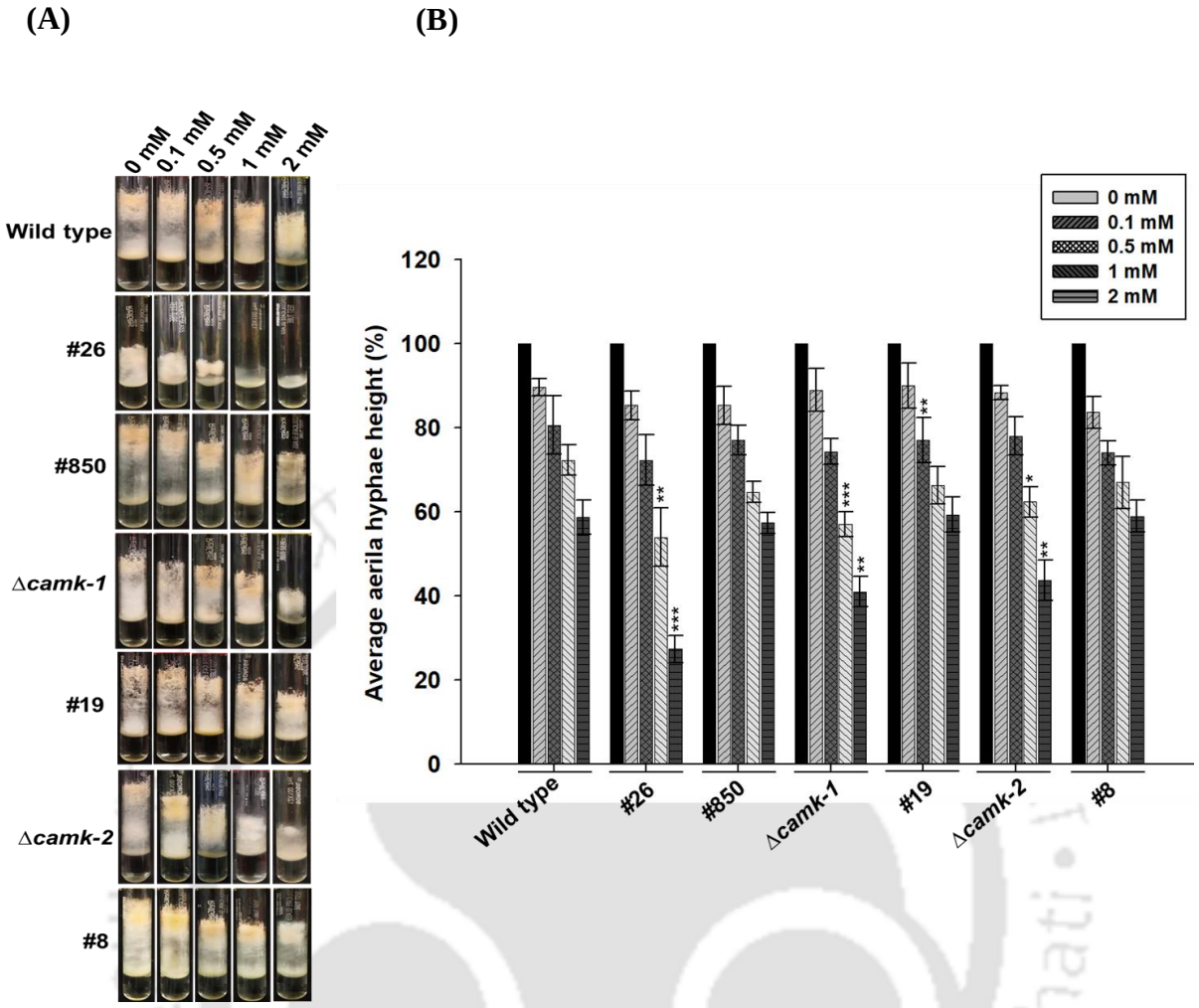

Figure 3.10.4 Complementation studies of *N. crassa* strains for ER stress assay. To evaluate the sensitivity to DTT, the wild type, #26, #850, Δ*camk-1*, #19, Δ*camk-2*, and #8 strains were incubated in VG liquid medium containing 0.1 mM, 0.5 mM, 1 mM, and 2 mM of DTT at 30 °C for 3 days at constant darkness, and percent growth rate determined. **(A)** Effect of DTT on aerial hyphae **(B)** Average aerial hyphae height (%). Standard deviations are indicated by error bars calculated from three independent experiments (n = 3), and the significance given by *P* values <0.05 (*), <0.01 (**), and <0.001 (***) compared to the wild type strain as measured by one-way ANOVA test.

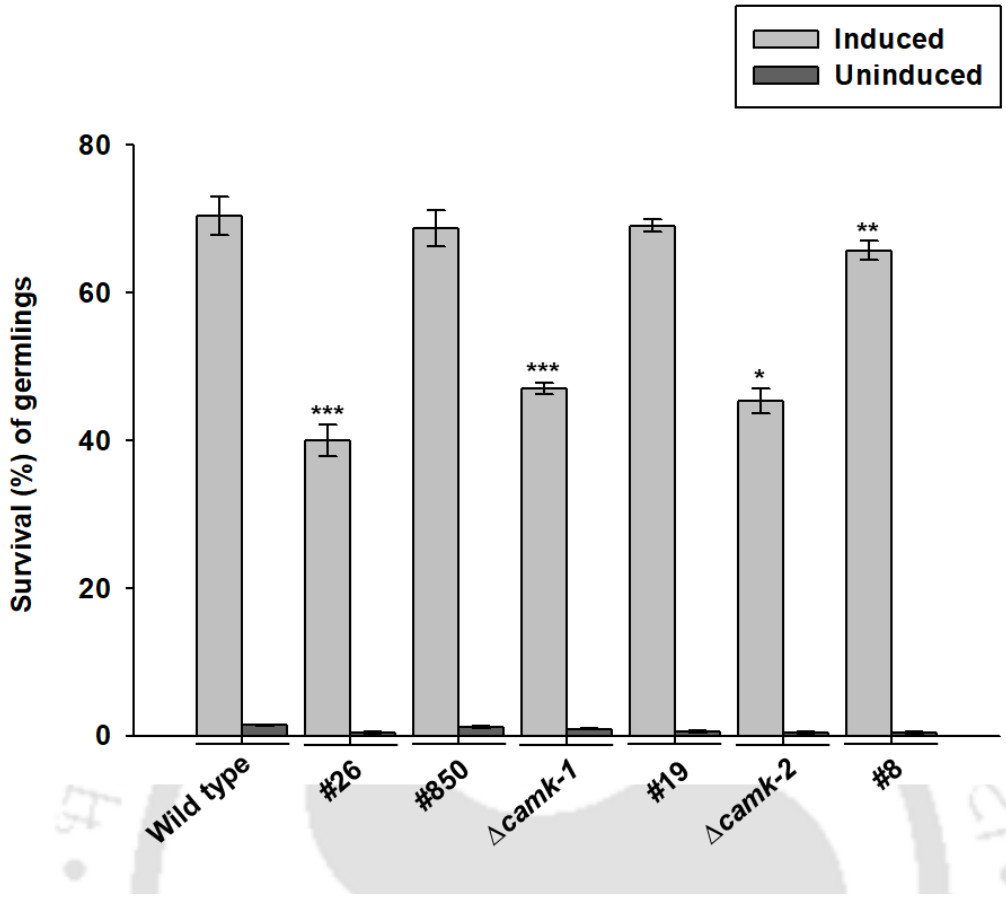

Figure 3.10.5 Complementation studies of the *N. crassa* strains for thermotolerance assay. 2 h old germlings of wild type, #26, #850, Δ*camk-1*, #19, Δ*camk-2*, and #8 strains were exposed to 52 °C lethal temperature with (induced) or without (uninduced) pre-exposure to a sub-lethal heat shock temperature of 44 °C and percent survival calculated. Standard deviations are indicated by error bars calculated from three independent experiments (n = 3), and the significance given by *P* values <0.05 (*), <0.01 (**), and <0.001 (***) compared to the wild type strain as measured by one-way ANOVA test.

3.3 Discussion

In response to various abiotic and biotic stimuli, the cytosolic free Ca^{2+} concentration $[Ca^{2+}]_c$ increases, which activates the Ca^{2+} signaling machinery for appropriate physiological responses (Sanders et al. 2002; Zelter et al. 2004; Tuteja and Mahajan 2007). Calmodulin (CaM), one of the primary Ca^{2+} sensors, plays a prominent role in maintaining the Ca^{2+} homeostasis required for cell survival (Haiech et al. 2019). In *S. cerevisiae*, CaM responds to cellular stress by activating Ca^{2+}/CaM-dependent kinases and Ca^{2+}/CaM-dependent protein phosphatase calcineurin (Moser et al. 1996; Cyert 2003; Kraus and Heitman 2003).

In this chapter, I described the role and mechanism of CaM and its immediate downstream protein CaMKs under different abiotic stress conditions such as temperature, pH, oxidative, and ER stress. I observed that the #26, Δ*camk-1*, and Δ*camk-2* mutants were sensitive to low (20 °C) and elevated (40 °C) temperatures showing reduced growth rates at both temperatures (Figure 3.1). At alkaline pH, the aerial growth of #26, Δ*camk-1*, and Δ*camk-2* was reduced (Figure 3.2), suggesting that *cmd*, *camk-1*, and *camk-2* are required for survival in alkaline pH conditions. Previously, in the promoter regions of *camk-1* and *camk-2* genes, sequences for the yeast pH-responsive regulators were identified (Kumar and Tamuli 2014), indicating that certain transcription factors upon pH change may regulate *camk-1* and *camk-2* genes. However, under osmotic stress caused by high concentrations of NaCl and sorbitol, I did not observe any significant difference in the growth rate between the mutants and the wild type.

The *cmd*^{RIP}, Δ*camk-1*, and Δ*camk-2* mutants showed reduced survival rates under oxidative stress (Figure 3.4), suggesting that *cmd*, *camk-1*, and *camk-2* regulate the redox state of the cell. The *cmd*^{RIP}, Δ*camk-1*, and Δ*camk-2* mutants also produced short aerial hyphae under DTT-induced ER stress conditions (Figure 3.6). In *S. cerevisiae*, CaM and CaM kinase II are required for induced thermotolerance (Iida et al. 1995). The acquisition of induced

thermotolerance is associated with the expression of heat shock proteins that imparts tolerance to other stressors. The #26, Δ*camk-1*, and Δ*camk-2* mutants showed decreased survival rates under induced thermotolerance (Figure 3.7), suggesting their possible role in regulating the heat shock response pathway.

The parental strain #850 of *cmd*^{RIP} (#26) and the complemented strains #19 of Δ*camk-1* and #8 of Δ*camk-2* were able to fully rescue the growth and survival defects in the mutants (Figure 3.10), suggesting that the *cmd*, *camk-1*, and *camk-2* genes are required for temperature, pH, oxidative and ER stress response.

A part of the results from this chapter was presented as posters in (i) National Conference on Fungal Biology: Recent Trends and Future Prospects and 44th Annual meeting of the Mycological Society of India (MSI), University of Jammu, November 2017; (ii) 11th International Conference on Biology of Yeast and Filamentous Fungi, University of Hyderabad, India, November 27-29, 2019.

CHAPTER 4

Role of calmodulin and calcium/calmodulin-dependent kinases in sexual development and circadian clock in *N. crassa*

4.1 Introduction

N. crassa enters the sexual phase of their life cycle when subjected to nitrogen starvation and low temperature. The sexual phase is characterized by the formation of fruiting bodies called perithecium, which produces the sexual spores (Perkins and Barry 1977; Nelson and Metzenberg 1992; Nelson 1996; Coppin et al. 1997). Previously, the inhibition of CaM using CaM antagonist TFP and CPZ caused a sterile phenotype in *N. crassa* (Laxmi and Tamuli 2015). In addition, meiotic silencing of the *cmd* gene also showed a barren phenotype, suggesting that *cmd* is required during meiosis for full fertility (Laxmi and Tamuli 2017). However, the detailed role and mechanism of CaM in fertility are not fully understood.

Circadian clocks are self-sustaining endogenous time-keeping system that controls the behaviour, inner physiological, and molecular rhythms in some prokaryotes and most eukaryotes with an innate periodicity of roughly 1 day. The term comes from the Latin word *circa "*about*"* and *diem* "a day" (Dunlap 1999; Vitaterna et al. 2001; Halberg et al. 2003). The circadian clock organizes the inner physiology of an organism with respect to the external environment to ensure its well-being and survival (Vitaterna et al. 2001; Baker et al. 2012). Clock-controlled genes are associated with cellular processes such as intermediary metabolism, DNA damage repair, stress responses, protein synthesis, and development (Correa et al. 2003; Vitalini et al. 2006). In this chapter, I describe the cellular roles of CaM and CAMKs during sexual development and in the regulation of the circadian clock.

4.2.1 Role of calmodulin during sexual development

4.2.1.1 The *cmd*^{RIP} (#26) mutant is female sterile

The transition from the vegetative to sexual phase is initiated through different morphological changes of the *N. crassa* vegetative mycelium to form the specialized sexual structure "perithecium" (Lichius et al. 2012). The developmental transition of vegetative mycelium to form the specialized tissue depends on various endogenous and exogenous factors, and Ca^{2+} is one of the key factor required for the initiation and the final stages of sexual development (Wilson et al. 2019).

To understand the specific role of CaM during sexual development, I performed the male-female fertility assay. The wild type, #26, and #850 strains were cultured as the female parent on synthetic crossing medium (SCM) and incubated under constant light for seven days at 22 °C, which formed the protoperithecia. Freshly harvested conidia of the opposite mating type of the wild type, #850, and #26 were subsequently inoculated as the male parents to fertilize the protoperithecia. After fourteen days post-fertilization, the plates were observed under the microscope, and the ascospores were harvested. The #26 mutant, when cultured as a male parent, formed mature perithecia and produced abundant ascospores; but, when cultured as a female parent, it showed a complete absence of perithecia and resulted in a sterile phenotype (Figure 4.1; Table 4.1). The wild type and the #850 strains were fully fertile as both male and female parents, producing thousands of ascospores (Figure 4.1; Table 4.1). The #26 mutant was also unable to develop protoperithecia (Figure 4.2), suggesting that CaM is required during the initial stage of female sexual development.

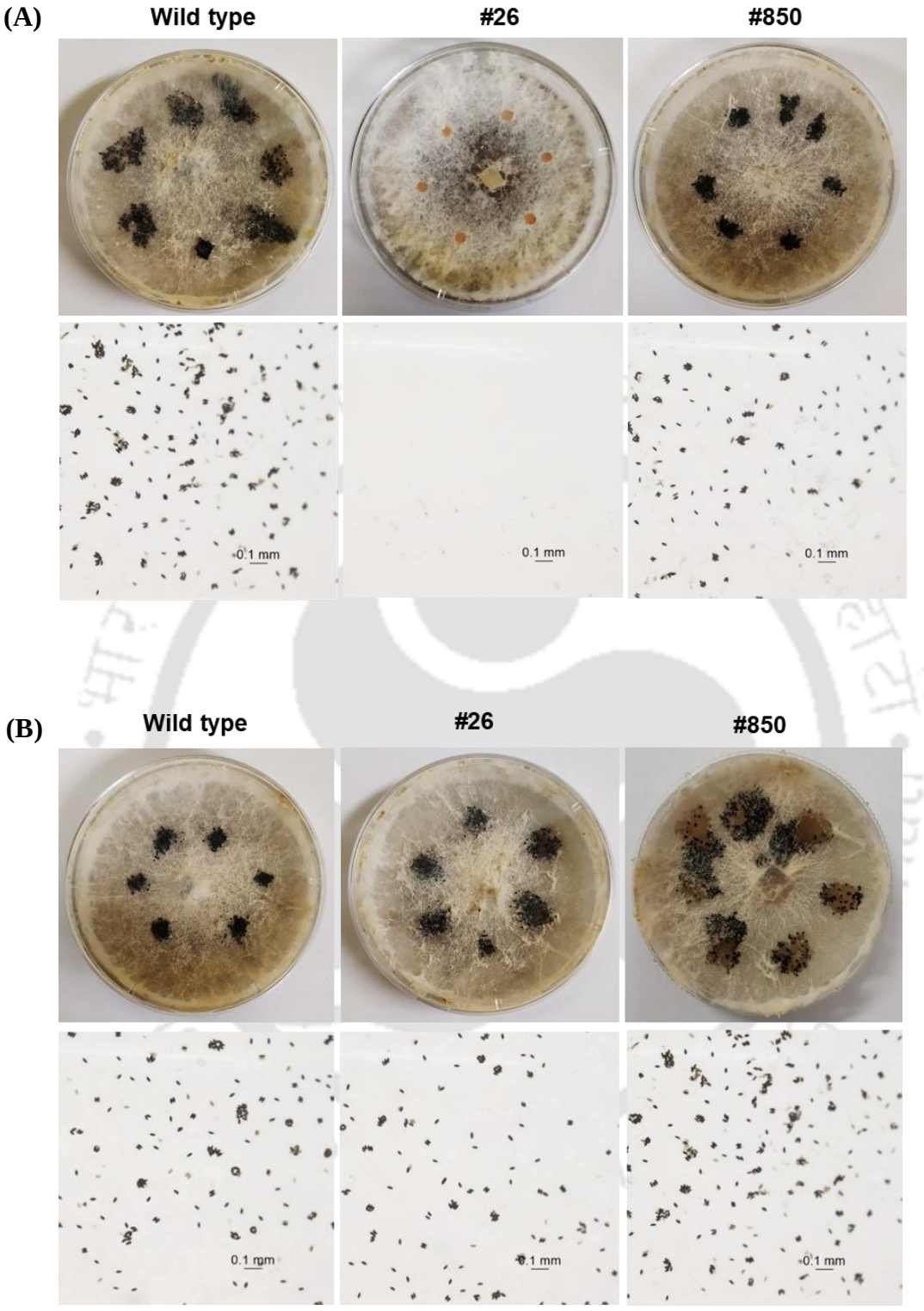

Figure 4.1 Fertility assay of the wild type, #26, and # 850 strain. The *N. crassa* strains were cultured on SCM at 22 °C for seven days. The wild type, #850, and #26 strains were used as **(A)** female parent and **(B)** male parent and subsequently fertilized with wild type, #850, and #26 (*mat A* or *mat a*) conidia as the male parent. Upper panel: visualization of plates after seven

days post fertilization for perithecia formation; Lower panel: ascospores released on the lid after fourteen days post fertilization were observed under a microscope (Leica S9i Stereomiroscope, Leica Microsystems, Wetzlar, Germany).

Table 4.1 Sexual fertility of wild type, #850, and #26 *N. crassa* strains

Female Parent	Male parent	Perithecia formed	Ascospores produced	Phenotype
Wild type; *mat A*	Wild-Type; *mat a*	Yes	Abundant	Fertile
Wild type; *mat a*	Wild-type; *mat A*	Yes	Abundant	Fertile
#850; *mat a*	Wild-type; *mat A*	Yes	Abundant	Fertile
Wild type; *mat A*	#850; *mat a*	Yes	Abundant	Fertile
#26; *mat A*	Wild-type; *mat a*	No	None	Sterile
Wild type; *mat a*	#26; *mat A*	Yes	Abundant	Fertile

Figure 4.2 Protoperithecia formation in the wild type, #26, and #850 strains. To examine the formation of protoperithecia, the strains were grown in SCM agar plates at 22 °C for 7 days under constant light. The plates were then observed under a microscope (Leica S9i Stereomiroscope, Leica Microsystems, Wetzlar, Germany).

4.2.1.2 Perithecia grafting assay

During sexual development, the availability of nutrients is a vital factor for the successful development of fruiting bodies (Debuchy et al. 2010; Wang et al. 2012). Perithecia grating in *Podospora anserina* showed that reactive oxygen species (ROS) signals are generated by NADPH oxidase (Nox) Panox1 in the developing perithecia (Malagnac et al. 2004). The ROS signals are transmitted by three pezizomycotina- specific proteins IDC1, IDC2, and IDC3 to the PaMpk1 MAP kinase cascade located in the underlying mycelium which mobilizes the stored nutrients from the mycelium to feed the developing perithecia (Jamet-Vierny et al. 2007; Lalucque et al. 2017). A competent mycelium is important to provide the required amino acids and other nutrients to support the fruiting body for ripening (Silar 2011; Chinnici et al. 2014). Therefore, I performed perithecia grafting assay to determine the ability of the *cmd*^{RIP} (#26) strain as a host mycelium to support the development of the fertilized protoperithecium graft. The wild type *mat A*/ *mat a* was grown on 0.5 % sucrose SCM agar overlaid with a cellophane sheet for 10 days and further fertilized by the conidia of the opposite mating type for 24 h. The fertilized perithecia were grafted on the mycelium of wild type, #850 and #26 which were also grown for 10 days on 0.5 % sucrose SCM agar. Dissecting the perithecia post-8-days after fertilization showed immature rosette formation in the #26 mutant which ultimately produced few ascospores. While the wild type and the #850 strains formed mature rosettes and produced abundant ascospores (Figure 4.3). The defect in the #26 mutant, suggested that the mycelium was unable to support the developing graft due to nutritional or signaling defect.

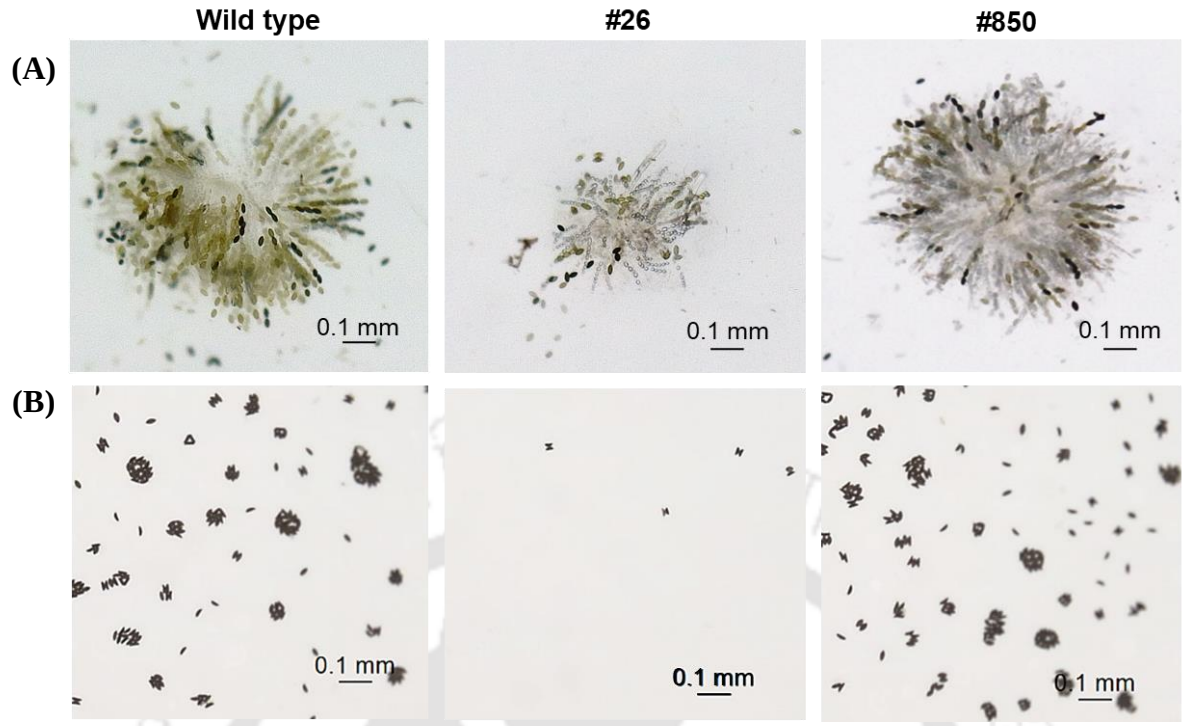

Figure 4.3 Perithecia grafting assay of wild type, # 850, and # 26 mutant. Wild type strain was cultured in 0.5% sucrose SCM media overlaid with cellophane for 10 days and then fertilized with the opposite mating type and incubated for 24 h. Small pieces of the cellophane "graft" were then transferred to the plates of the host strains, grown for 10 days, of the same mating type. **(A)** Post-8-day after fertilization old perithecia were dissected and observed under a microscope (Leica S9i Stereomiroscope, Leica Microsystems, Wetzlar, Germany), **(B)** Post-14-day after fertilization, ascospores were released on the lid.

4.2.1.3 The *cmd*^{RIP} (#26) mutant was defective during cell fusion

The *N. crassa* mycelium is composed of hyphal networks developed by hyphal tip extension, branching, and cell fusion (Fleißner et al. 2008). Cell fusion is associated with the fitness and competitiveness of the mycelial colony (Herzog et al. 2015). The fusion between cells enables the translocation of cellular contents such as water, nutrients, metabolites, organelles, and signaling compounds which promotes growth and reproduction (Fleißner et al. 2008; Herzog et al. 2015). Therefore, I performed cell fusion assay to understand why the vegetative hyphae

of *cmd*^{RIP} (#26) mutant could not support the development of the wild type fertilized protoperithecia. The wild type, #26, and #850 strains were grown in VG liquid media, and cell fusion of the germlings were observed at 3, 5, 7, and 48 h. The wild type and #850 strains showed initial cell fusion at 3 h (Figure 4.4), started to form initial mycelial network at 7 h, and formed mycelial aggregates by 48 h; however, the # 26 mutant did not show any cell fusion at 3 h and formed only clumps even after 48 h (Figure 4.4). Therefore, *cmd*^{RIP} mutant is defective in cell fusion and failed to form a normal mycelial network, which could possibly explain the reason why the vegetative mycelium of the *cmd*^{RIP} mutant was unable to support the wild type perithecia graft and did not develop the female sexual structure protoperithecia.

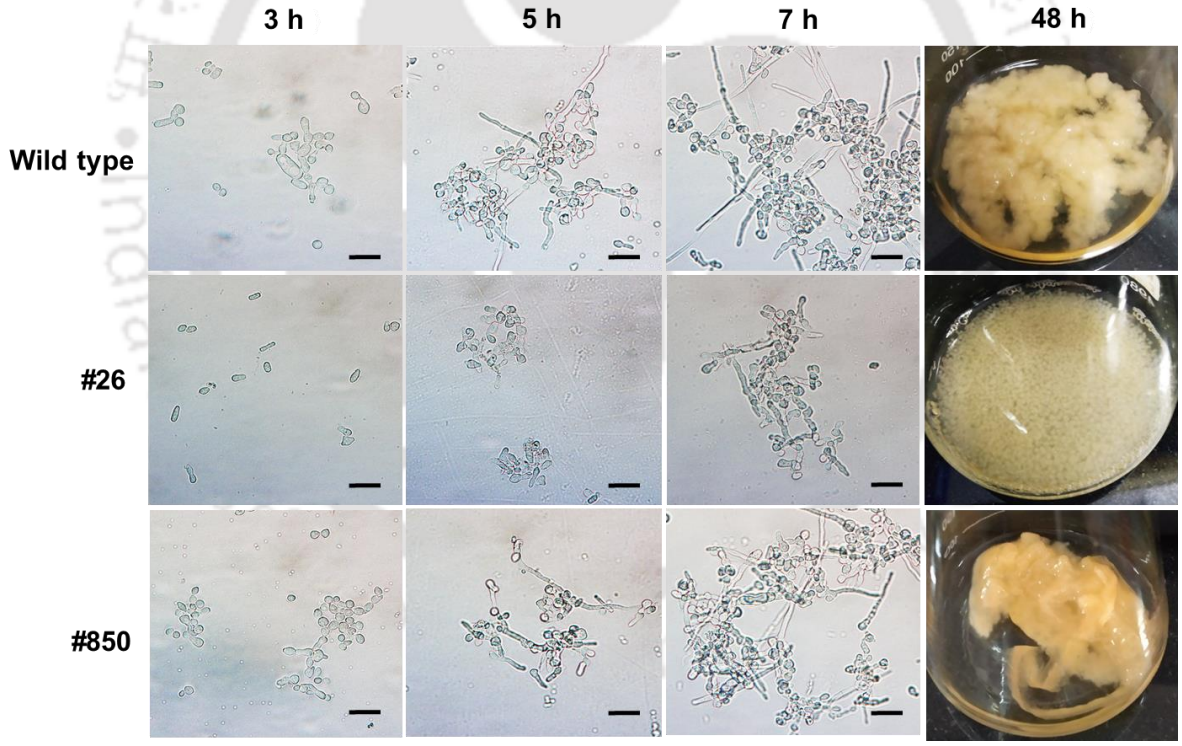

Figure 4.4 Cell fusion assay for wild type, #26, and #850 strains. The fresh conidia at a concentration of 1×10^6 conidia/ml was inoculated in liquid VG medium and incubated in shaking condition at 180 rpm at 30 °C. The cells were observed at the interval of 3 h, 5 h, 7 h, and 48 h under the inverted microscope (AxioVert A1 FL, Carl Zeiss, Göttingen, Germany) at 40X magnification. Scale bar 20 µm.

4.2.2 Chronological aging assay

Chronological aging or chronological life span is the loss of conidial viability over time in a stationary phase (Munkres 1984; Hamann et al. 2008). The aging process is associated with the progressive and irreversible decline in physiological functions such as fertility and resistance to stress (Kirkwood et al. 2000). The *cmd*^{RIP} (#26) mutant is sensitive to various stressors (described in chapter 3) and defective in the formation of female sexual structure. Therefore, I performed chronological aging assay to determine if *cmd* gene is involved during the aging process. The strains were grown in VG agar medium at 30 °C for three days in the dark and then at room temperature for two days under light for proper conidiation. The conidia were harvested on day 5 in 1 ml sterile water and a concentration of ~1 x 10^7 cells/ml was maintained for 30 days at 25 °C (room temperature) to starve them (Case et al. 2014). At each time point (5, 10, 15, 20, 25, and 30 days), approximately 1000 cells (10 µl from 10^{-4} dilution) were plated on the FGS agar medium. To determine the rate of aging, the colonies formed on day 5 were counted and the survival percentage was calculated. The colonies formed on day 5 were taken as 100 % and the survival percentages on the successive days were calculated with respect to day 5. The #26 mutant showed a severe decline in the conidial survival rate, where a 50 % decline in survival was seen after 10 days, and no surviving conidia were observed by 30 days (Figure 4.5; Table 4.2). The survival percentage of wild type and the parental #850 strain were 46% and 48% on day 25, indicating that the estimated median life span was nearly 25 days. This result showed that the *cmd* gene is necessary for normal aging and longevity.

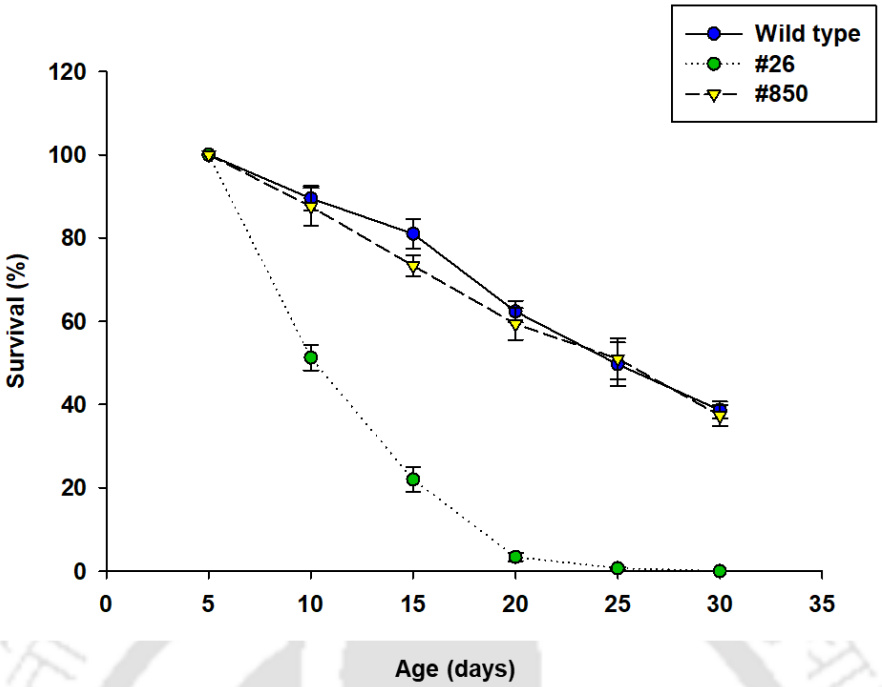

Figure 4.5 Chronological aging of wild type, #26, and # 850 strains over a period of 30 days. The strains were grown on VG agar at 30 °C in dark for 3 days and at room temperature under light for 2 days. The conidia were harvested in sterile water and maintained a concentration of ~1 x10^7/ml conidia, and stored at room temperature. Approximately 1000 cells from each time point (5, 10, 15, 20, 25, and 30 days) were plated in FGS agar medium and grown at 30 °C for 2 days. The colonies were counted to determine the survival percentage with respect to the colonies formed on day 5. The error bars indicate the mean ± standard deviation calculated from three independent experiments (n = 3).

Table 4.2 Percent survival of wild type, # 26, and #850 over a period of 30 days under starved condition

	[+]Percent survival (%)					
Strain	**5 days**	**10 days**	**15 days**	**20 days**	**25 days**	**30 days**
wild type	100 ± 0.00	89.5 ± 2.96	81 ± 3.56	59.7 ± 1.63	46 ± 0.81	38.6 ± 2.05
#26	100 ± 0.00	51.2 ± 3.03 (***)	22 ± 2.94 (***)	3.2 ± 0.91 (***)	0.7 ± 0.28 (***)	0
#850	100 ± 0.00	87.5 ± 4.5	73.3 ± 2.5 (*)	58.7 ± 3.5	48 ± 3	37.33 ± 2.5

[+]Results are shown as mean ± standard deviation for three independent experiments (n = 3) with *P* values < 0.05 (*), < 0.01 (**), and < 0.001 (***) compared with the wild type strain estimated by one-way ANOVA test.

4.2.3 Circadian regulated conidiation assay

The circadian clock regulates multiple cellular processes involved in the asexual and sexual developmental phases of *N. crassa* (Bobrowicz et al. 2002; Dunlap and Lorros 2004; Montenegro-Montero and Larrondo 2013). In *N. crassa band* (*bd*) mutant, the T79I point mutation in the Ras-1 GTPase gene (*ras-1*^{bd}) results in the formation of clear rhythmic conidial bands even in the presence of high CO_2 levels without affecting the circadian mechanism, and therefore used as a control strain in circadian clock studies (Sargent and Kaltenborn 1972; Belden et al. 2007). The circadian rhythm shows three main characteristics (1) a period of approximately a day; (2) sensitivity to light that enables to adjust the phase of the rhythm to the environment; and (3) insensitivity of the period to the growth temperature, a mechanism termed as compensation (Mattern et al. 1982).

To generate the mutants for circadian regulated conidiation assay, the #26, Δ*camk-1*, Δ*camk-2*, Δ*camk-3*, and Δ*camk-4* mutant strains were crossed with *ras-1*^{bd} of opposite mating type and ascospores from these crosses were harvested after 21 days. The progenies from this cross were screened for resistance to hygromycin B (Hyg^{R}), pantothenate auxotrophy, and the banding phenotype. In addition, the presence of the knockout allele was confirmed using the gene specific primers (Figure 4.7; Table 4.4). The double mutants so obtained from each of the crosses are used in this study (Figure 4.6; Table 4.3).

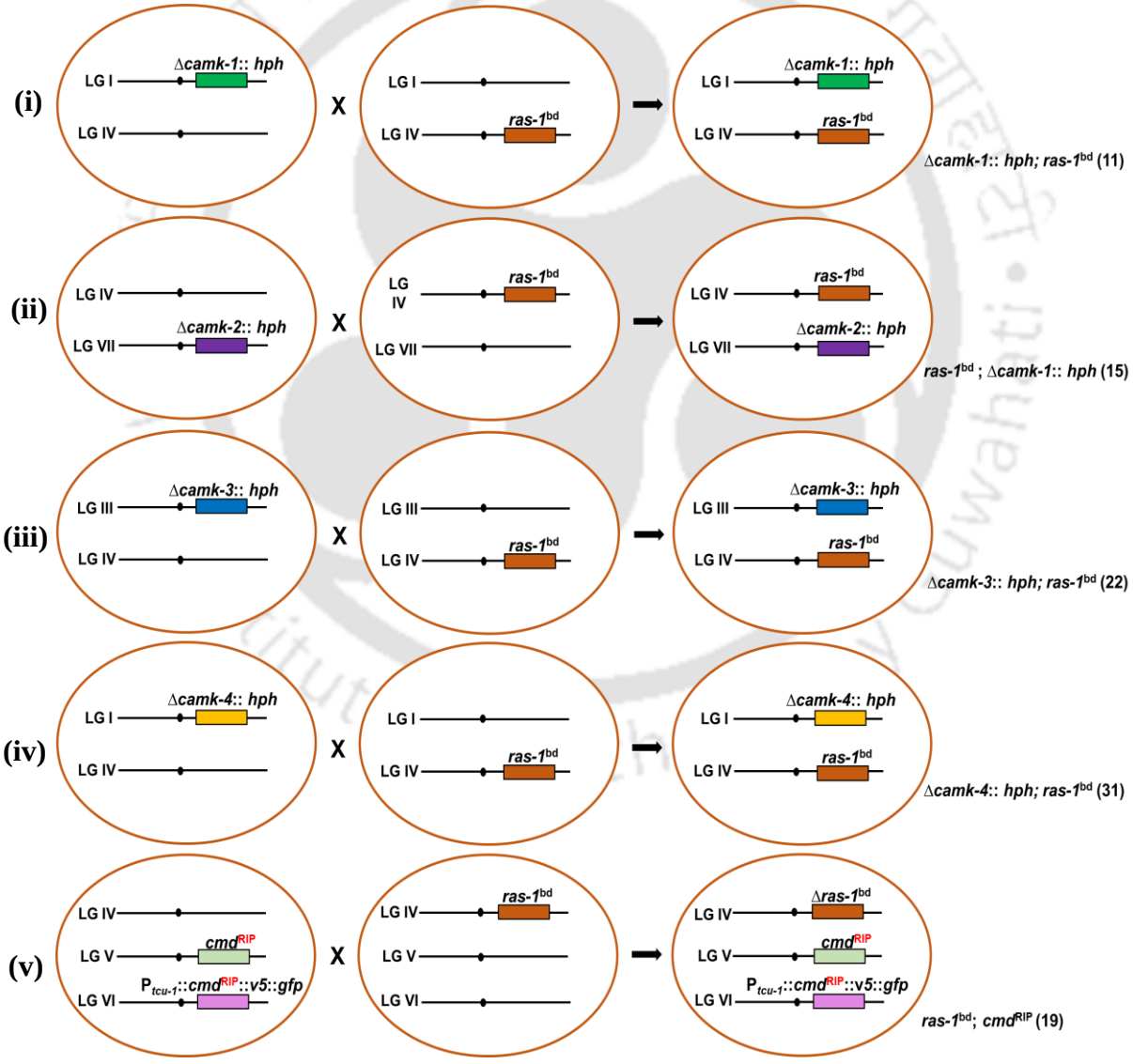

Figure 4.6 Schematic representation for generation of *N. crassa* mutant strains for circadian regulated conidiation assay. The #26, Δ*camk-1*, Δ*camk-2*, Δ*camk-3*, and Δ*camk-4* mutant strains were crossed with *ras-1*^{bd} of opposite mating type strains at 22 °C for 21 days and ascospores were harvested. **(i)** Δ*camk-1* crossed with *ras-1*^{bd} to generate Δ*camk-1; ras-1*^{bd} (11) strain, **(ii)** Δ*camk-2* crossed with *ras-1*^{bd} to generate *ras-1*^{bd}; Δ*camk-2* (15) strain, **(iii)** Δ*camk-3* crossed with *ras-1*^{bd} to generate Δ*camk-3; ras-1*^{bd} (22) strain, **(iv)** Δ*camk-4* crossed with *ras-1*^{bd} to generate Δ*camk-4; ras-1*^{bd} (31) strain, and **(v)** *cmd*^{RIP} (#26) crossed with *ras-1*^{bd} to generate *ras-1*^{bd}; *cmd*^{RIP} (19) strain. The progenies from the crosses were then germinated on FGS agar medium and screened for the resistance to hygromycin B (Hyg^{R}), pantothenate auxotrophy, and the *band* phenotype in race tube.

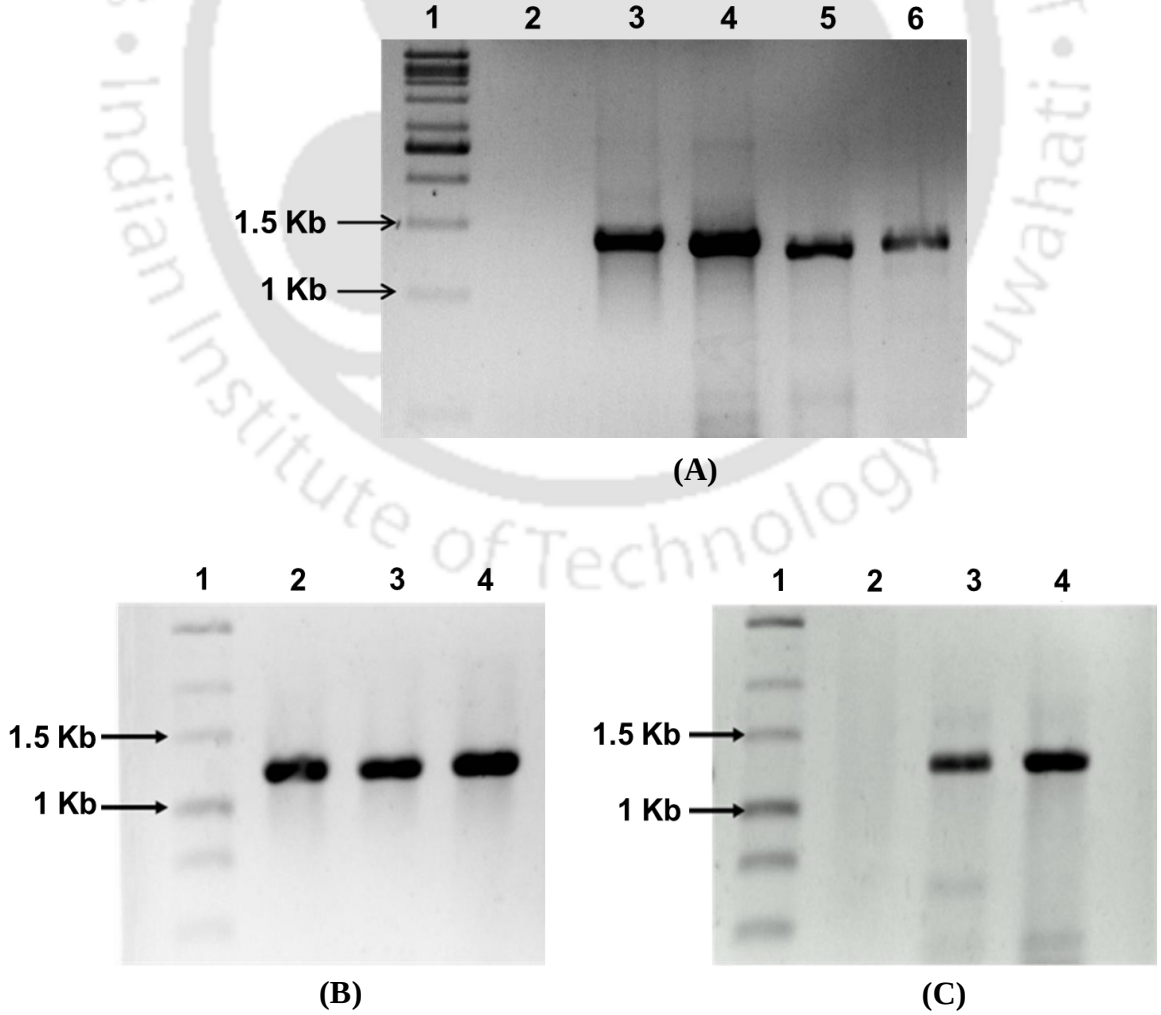

Figure 4.7 PCR confirmation of the mutant strains. (**A)** PCR verification of the *N. crassa* mutant strains for the presence of Δ*camk-1*, Δ*camk-2*, Δ*camk-3*, and Δ*camk-4* alleles using gene specific primers (entries 1 to 5; Table 4.4). The PCR products were resolved using 1% agarose gel, stained with EtBr and visualized using a GelDoc (Bio-PrintST4, Vilber Lourmat, France); lane 1: 1 kb DNA ladder (NEB), lane 2: wild type as negative control (no PCR prduct as target sequence for 5HPHR is absent), lane 3: Δ*camk-1*; *ras-1*^{bd} (11) mutant verification (positive with PCR product of size 1,328 bp), lane 4: Δ*camk-2*; *ras-1*^{bd} (15) mutant verification (positive with PCR product of size 1,296 bp), lane 5: Δ*camk-2*; *ras-1*^{bd} (22) mutant verification (positive with PCR product of size 1,235 bp), and lane 6: Δ*camk-4*; *ras-1*^{bd} (31) mutant verification (positive with PCR product of size 1,280 bp). (**B)** Verification for the presence of endogenous *cmd* allele using specific primers (entries 7 and 8; Table 4.4). The PCR products were resolved using 1% agarose gel, stained with EtBr and visualized using a GelDoc (Bio-PrintST4, Vilber Lourmat, France); lane 1: 1 kb DNA ladder (NEB), lane 2: Wild type (positive control with PCR product of size 1, 241 bp), lane 3: #26 mutant (positive with PCR product of size 1,241 bp), and lane 4: *ras-1*^{bd}; *cmd*^{RIP} (19) mutant (positive with PCR product of size 1, 241 bp). (**C)** Verification for the presence of ectopic *cmd* allele using specific primers (entries 6 and 7; Table 4.4). The PCR products were resolved using 1% agarose gel, stained with EtBr and visualized using a GelDoc (Bio-PrintST4, Vilber Lourmat, France); lane 1: 1 kb DNA ladder (NEB), lane 2: Wild type (negative control no PCR product as the construct is absent), lane 3: #26 mutant (positive with PCR product of size 1,272 bp), and lane 4: *ras-1*^{bd}; *cmd*^{RIP} (19) mutant (positive with PCR product of size 1,272 bp).

Table 4.3 List of *N. crassa* strains used in circadian study

Sl. No.	Strains	Genotype	Source
1	1858	*ras-1*^{bd}; *mat a*	FGSC 1858
2	1859	*ras-1*^{bd}; *mat A*	FGSC 1859
3	Δ*camk-1; ras-1*^{bd} (11)	Δ*camk-1; ras-1*^{bd}; *mat A*	This study
4	*ras-1*^{bd} ; Δ*camk-2* (15)	*ras-1*^{bd} ; Δ*camk-2*; *mat A*	This study
5	Δ*camk-3; ras-1*^{bd} (22)	Δ*camk-3; ras-1*^{bd}; *mat A*	This study
6	Δ*camk-4; ras-1*^{bd} (31)	Δ*camk-4; ras-1*^{bd}; *mat A*	This study
7	*ras-1*^{bd}; *cmd*^{RIP} (19)	*ras-1*^{bd}; *cmd*^{RIP} (19) ; *mat A*	This study

Table 4.4 Primers used for confirmation of *N. crassa* mutant strains

Sl. No.	Primer Name	Sequence	Source
1	5HPHR	ATCCACTTAACGTTACTGAAATC	Deka et al. 2011
2	6NCU09123F-HI	GCG AAT GGG AGA GCC TTA CA	This study
3	16NCU02283F-HI	AGT ACG AGA TCG ACG GAG GA	Laxmi and Tamuli 2017
4	2NCU06177F-HI	ATC ATG CTG TGG TTG TGC CC	This study
5	2NCU09212F-HI	AGC GAG TCT TTC CAT CTC GG	This study
6	GFP Rv	AAC TTG TGG CCG TTT ACG TC	Laxmi and Tamuli 2017
7	CaM-RIP-FP-1	ACC TCC ATA TCT ACC ACT TC	Laxmi and Tamuli 2017
8	CaM-RIP-RP	GAT CCC TTC ACA TCC GAA TG	Laxmi and Tamuli 2017

4.2.3.1 The *camks* genes play a role in regulating the circadian period length

To study the role of *cmd* and *camks* genes in regulating the circadian period length and temperature compensation under different physiological range of temperatures, I determined the period length using the inverted race tube assay at three temperatures 20 °C, 25 °C, and 30 °C for *ras-1*^{bd}, Δ*camk-1*; *ras-1*^{bd} (11), *ras-1*^{bd}; Δ*camk-2* (15), Δ*camk-3*; *ras-1*^{bd} (22), Δ*camk-4*; *ras-1*^{bd} (31), and *ras-1*^{bd}; *cmd*^{RIP} (19) mutant strains (Figure 4.8). The period length for these strains at all three temperatures were measured as discussed in chapter 2.

The Δ*camk-1*; *ras-1*^{bd} (11), *ras-1*^{bd}; Δ*camk-2* (15), Δ*camk-3*; *ras-1*^{bd} (22), and Δ*camk-4*; *ras-1*^{bd} (31) mutant strains showed an increase in period length of ~ 1 h at 25 °C and ~2 h at 30 °C in comparison to the period length of the *ras-1*^{bd} control strain (Figure 4.9; Table 4.5). However, the period length of these mutants did not vary significantly at 20 °C in comparison to the *ras-1*^{bd} strain. The *ras-1*^{bd}; *cmd*^{RIP} (19) mutant showed severe growth retardation (Figure 4.8); therefore, I could not determine the period length in this mutant.

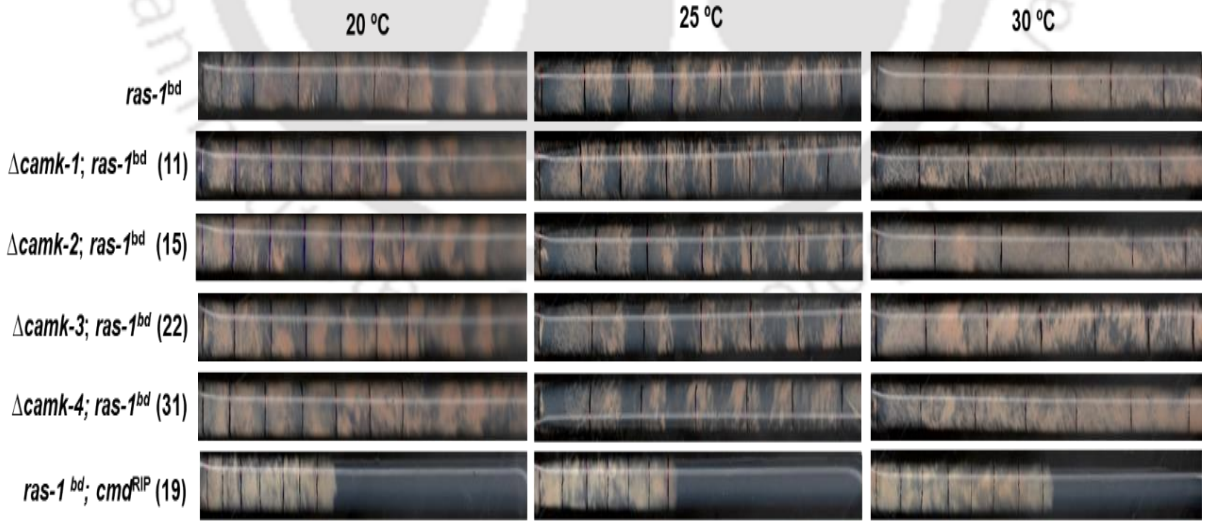

Figure 4.8 Inverted race tube assay for circadian regulated conidiation. The *ras-1*^{bd}, Δ*camk-1*; *ras-1*^{bd} (11), *ras-1*^{bd}; Δ*camk-2* (15), Δ*camk-3*; *ras-1*^{bd} (22), Δ*camk-4*; *ras-1*^{bd} (31), and *ras-1*^{bd}; *cmd*^{RIP} (19) mutant strains were grown in race tube under constant light and at 25

°C for 24 h , then the cultures were transferred to constant darkness and incubated at 25 °C for 7 days. The growth fronts are marked at every 24 h intervals under a safe red light. The experiment was also carried out at 20 and 30 °C.

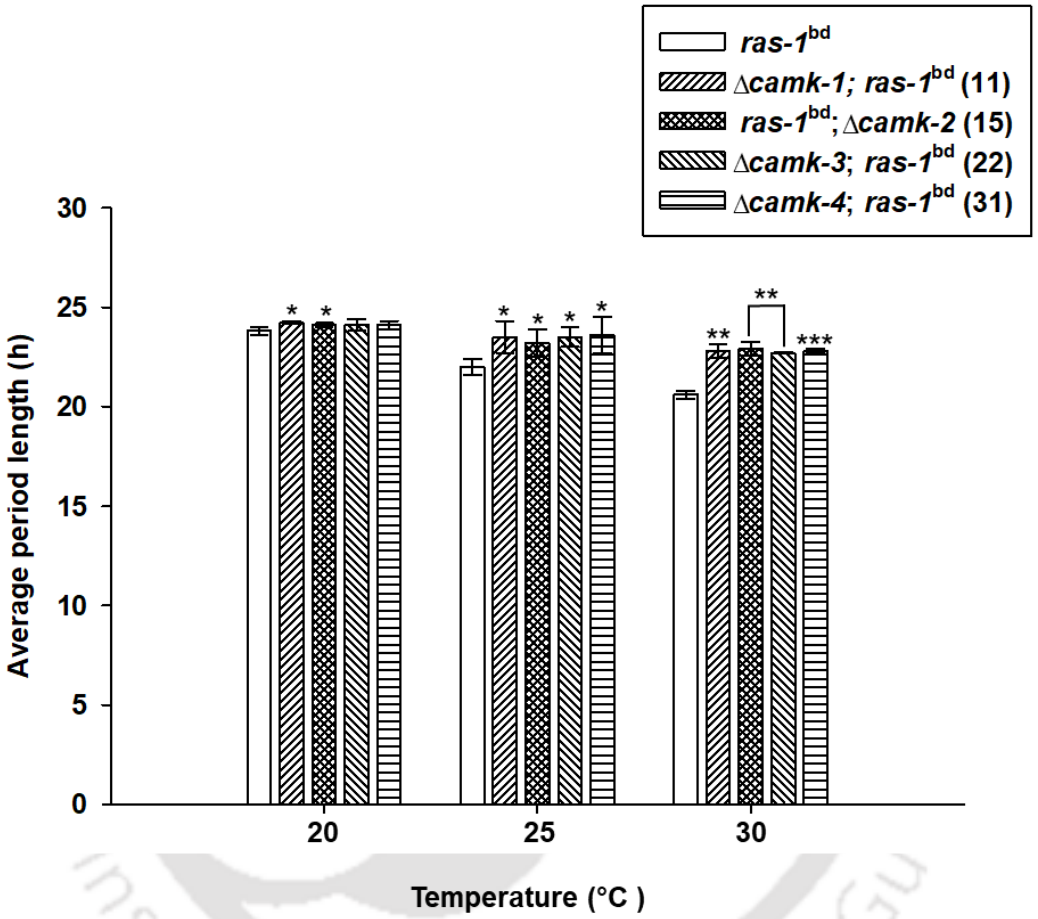

Figure 4.9 Period lengths of *N. crassa* strains at 20, 25, and 30 °C. The *ras-1*^{bd}, Δ*camk-1*; *ras-1*^{bd} (11), *ras-1*^{bd}; Δ*camk-2* (15), Δ*camk-3*; *ras-1*^{bd} (22), Δ*camk-4*; *ras-1*^{bd} (31), and *ras-1*^{bd}; *cmd*^{RIP} (19) mutant strains were inoculated in race tubes and the cultures were incubated at 25 °C under constant light for 24 h, and then incubated at 25 °C under constant darkness for 7 days; growth fronts of the strains were marked at every 24 h under a safe red light. The experiment was also carried out at 20 and 30 °C. Period lengths were calculated by multiplying the distance between conidial bands by the inverse of the slope from the growth rate. Error bars indicate the standard deviations calculated from the data for three independent experiments (n

= 3) and the significance given by *P* values < 0.05 (*), < 0.01 (**), and < 0.001 (***) compared to the *ras-1*^{bd} strain as measured by one-way ANOVA test.

Table 4.5 Period length of the *cmd* and *camks* at different temperatures

Strains	$^{+}$Period lengths ± SD (h)		
	20 °C	**25 °C**	**30 °C**
ras-1^{bd}	23.84 ± 0.19	21.98 ± 0.45	20.65 ± 0.23
Δ*camk-1*; *ras-1*^{bd} (11)	24.25 ± 0.06 (*)	23.50 ± 0.77 (*)	22.8 ± 0.34 (**)
ras-1^{bd}; Δ*camk-2* (15)	24.1± 0.09 (*)	23.18 ± 0.72 (*)	22.94 ± 0.34 (**)
Δ*camk-3*; *ras-1*^{bd} (22)	24.15 ± 0.3	23.48 ± 0.50 (*)	22.76 ± .04 (**)
Δ*camk-4*; *ras-1*^{bd} (31)	24.11 ± 0.25	23.60 ± 0.87 (*)	22.79 ± 0.11 (***)
ras-1^{bd}; *cmd*^{RIP} (19)	Unable to determine	Unable to determine	Unable to determine

$^{+}$Results are shown as mean ± standard deviation for three independent experiments (n = 3) with *P* values < 0.05 (*), < 0.01 (**), and < 0.001 (***) compared with the *ras-1*^{bd} strain estimated by one-way ANOVA test.

4.2.3.2 The *camks* genes do not affect temperature compensation of the circadian clock

One of the important features of circadian clock is that the period length is conserved over a range of temperature, a phenomenon termed as temperature compensation (Gardner and Feldman 1981). This allows the organism to maintain a stable and accurate time over different ambient temperatures and adapt to daily and seasonal variations (Gardner and Feldman 1981; Hunt et al. 2007). Temperature compensation is expressed as the temperature coefficient Q_{10} (the relative rate of enhancement corresponding to 10 °C rise in temperature), which is calculated by using the formula as given below,

$$Q_{10} = \left(\frac{f_1}{f_2}\right)^{\frac{10}{T_2 - T_1}}$$

Where, f_1 and f_2 are the frequencies of the rhythm (24/period) at temperature T_1 and T_2 (where T2 > T1) (Lakin Thomas 1998).

The Q_{10} value for normal circadian rhythms ranges from 0.8 - 1.2 (Mattern et al. 1982). When the Q_{10} value is above the range, the clock is considered to have lost temperature compensation, while the circadian clock is over-compensated when the Q_{10} value is less than the given range (Mattern et al. 1982; Hu et al. 2021). The Q_{10} values for the *camk-1*, *camk-2*, *camk-3*, and *camk-4* mutant strain were in the range of ~1, like the *ras-1*^{bd} strain, suggesting that the circadian clock in these mutants showed temperature compensation (Table 4.6).

Table 4.6 Temperature compensation values for different Ca^{2+} signaling genes

Strains	**Q_{10} Values**		
	T_1 = 20 ºC, T_2 = 25 ºC	**T_1 = 25 ºC, T_2 = 30 ºC**	**T_1 = 20 ºC, T_2 = 30 ºC**
ras-1^{bd}	1.14	1.11	1.15
Δ*camk-1; ras-1*^{bd} (11)	1.08	1.02	1.05
ras-1^{bd}; Δ*camk-2* (15)	1.08	1.02	1.05
Δ*camk-3; ras-1*^{bd} (22)	1.05	1.06	1.06
Δ*camk-4; ras-1*^{bd} (31)	1.04	1.07	1.05
ras-1^{bd}; *cmd*^{RIP} (19)	Not determined	Not determined	Not determined

4.3 Discussion

During the sexual phase in *N. crassa*, the vegetative mycelium differentiates to form the sexual fruiting body called perithecium. The perithecium morphogenesis is primarily divided into ascogonial, protoperithecial, and perithecial stages, during which 14 distinct cell types are formed by various processes such as hyphal aggregation, adhesion, septation, branching, and cell differentiation (Bistis et al. 2003; Lord and Read 2011; Lichius et al. 2012). The ascogonial stage initiates with the vegetative hyphal branch coiling to form a hyphal knot, which transits to the protoperithecial stage when the enveloping hyphae wrap the ascogonium to form a subspherical structure (Bistis et al. 2003; Lord and Read 2011). The transition from protoperithecial to perithecial stage involves the mating of conidium, the 'male' cell, with the trichogyne, a specialized 'female' hypha produced from the protoperithecia (Backus 1939; Bistis 1981). Each ascus undergoes meiosis and post-meiotic mitosis to produce 8 linearly ordered haploid ascospores, where 200 to 400 asci are produced from each perithecium (Raju 1980, 1992, 2008).

To understand the role and mechanism of CaM during sexual development, sexual fertility assay was performed. The *cmd*^{RIP} (#26) mutant was fertile as a male parent but sterile as a female parent (Figure 4.1) because the mutant was unable to form the female sexual structure called 'protoperithecium' (Figure 4.2). The failure to form the protoperithecia is probably due to premature aborting of the sexual phase at the ascogonial stage and failure to proceed to the next stage.

One of the important features required during the development of sexual reproductive structures is cell-cell communication and cell fusion (Fischer and Glass 2019). To determine the competency of the mycelium to communicate and fuse, I performed perithecia grafting assay and cell fusion assay. The #26 mutant was unable to support the development of the wild type perithecia graft as a host (Figure 4.3). Furthermore, during cell fusion assay, the #26

mutant was unable to form normal mycelial aggregates like the parental #850 and wild type strains (Figure 4.4), which could be due to the defect in vegetative hyphal fusion required to form the vegetative mycelial network. Therefore, these results suggested that CaM is necessary to form a competent mycelium network to support the formation of female sexual structures. Similar results were also observed for the mitogen-activated protein kinases *mak-1* and *mak-2* mutants, which were defective in cell fusion and unable to form the protoperithecia (Li et al. 2005; Maerz et al. 2008; Park et al. 2008; Lichius et al. 2012). In mammals, the inhibition of CaM using CaM antagonists resulted in a decreased activity of MAPK signaling pathway (Tebar et al. 2002). In *Arabidopsis*, MAP kinase is activated by Ca^{2+}/CaM through binding and inhibition of a protein phosphatase (DsPTp1) (Kim et al. 2022). The homolog of human striatin-interacting phosphatase and kinase (STRIPAK) complex is involved in sexual development by regulating cell fusion and multicellular differentiation in *N. crassa* and other fungal organisms (Bleomendal et al. 2012). In *N. crassa*, the striatin protein HAM-3, a component of the STRIPAK complex, consists of a CaM binding domain (Simonin et al. 2010). In human brain, the striatin protein (STRN) binds to CaM in a Ca^{2+} dependent manner and acts as an adapter or transducer protein in Ca^{2+}/CaM-dependent events within dendritic spines (Bartoli et al. 1998). Therefore, CaM might be involved in regulating the STRIPAK complex and the MAPK signaling pathway during sexual development in *N. crassa*; however, this needs further investigation.

In the chronological aging assay, a drastic decline in the conidial survivor percentage was observed for the #26 mutant strain compared to the wild type (Figure 4.5). Reactive oxygen species (ROS) have been associated with aging in fungi, plants, and humans (Laun et al. 2001; Kotchoni and Gachomo 2006; Osiewacz and Scheckhuber 2006). NADPH oxidase is the primary source of ROS, which serves as a signal for both defense and differentiation in multicellular organisms (Takemoto et al. 2007; Breitenbach et al. 2015; Schröder 2019). In

Caenorhabditis elegans, overexpression of NADPH oxidase is shown to promote oxidative stress resistance and increased lifespan (Ewald 2018). In *P. anserina*, the deletion of the NADPH oxidase gene *Panox1* drastically reduced the development of sexual fruiting bodies (Malagnac et al. 2004). In addition, the *B. cinerea* strains lacking the NADPH oxidase BcNoxA were unable to undergo cell fusion (Roca et al. 2012). In *N. crassa*, elimination of NOX-1 results in complete female sterility, decreased asexual development, and reduced hyphal growth (Cano-Domínguez et al. 2008). In *Arabidopsis*, CaM1 protein mediates ABA-triggered ROS production and senescence by regulating the expression of NADPH oxidase gene *RbohF* and *senescence-associated gene 12* (*SAG-12*) (Koo et al. 2017; Dai et al. 2018). Moreover, in humans, calmodulin (CaM) regulates NADPH oxidase 5 (NOX5) by binding at the calmodulin-binding domain (CaMBD) in a Ca^{2+} dependent manner and increases the Ca^{2+} sensitivity of the NOX5 response (Tirone and Cox 2007). The *cmd*^{RIP} mutant strain showed phenotypes like the NADPH oxidase mutants. In chapter 3, the *cmd*^{RIP} mutant strain showed growth and survival defects under oxidative stress condition. Moreover, the *cmd*^{RIP} mutant was female sterile (Figure 4.1), formed an incompetent mycelium, unable to support the perithecia graft (Figure 4.3), defective in cell fusion (Figure 4.4), and showed a drastic decline in lifespan (Figure 4.5). These results suggested that CaM might be involved in regulating the ROS-generating enzyme NADPH oxidase in *N. crassa*.

In the mammalian suprachiasmatic nucleus (SCN), calmodulin and Ca^{2+}/calmodulin-dependent protein kinase II (CaMKII) are required for proper circadian responses to light (Golombek and Ralph 1994; Fukushima et al. 1997). Previous reports showed that the inhibition of CaM using CaM antagonists such as trifluoperazine, chlorpromazine, imipramine, alprenolol, W7, and W13 causes phase shifting of the circadian conidiation rhythm in *N. crassa* (Nakashima 1986). In addition, the *camk-1* null mutation affects the period length and light-induced phase shifting of the circadian conidiation rhythm in *N. crassa* (Yang et al. 2001).

Moreover, CaMK-1 is involved in phosphorylating the clock protein FRQ in *N. crassa* (Yang et al. 2001). Temperature compensation is one of the main characteristics of the circadian clock that maintains constancy in the period length at different temperatures for circadian homeostasis (Ruoff et al. 2005). To determine the role of CaM and CaMKs in regulating the circadian clock, the period length of these mutants was determined by performing an inverted race tube assay at three different temperatures (20 °C, 25 °C, and 30 °C). The knockout mutants of *camk-1*, *camk-2*, *camk-3*, and *camk-4* showed longer periods than the *ras-1*^{bd}, particularly at 25 °C and 30 °C (Figure 4.9). At 20 °C, the period length of the mutants did not vary significantly in comparison to the *ras-1*^{bd} strain (Figure 4.9; Table 4.5). In this study, the period length for the *ras-1*^{bd}; *cmd*^{RIP} (19) mutant could not be determined due to the mutant's severe slow growth phenotype (Figure 4.8). The *camk-1*, *camk-2*, *camk-3*, and *camk-4* mutant strains showed temperature compensation as the Q_{10} values were in the range of ~1, without varying much from that of the *ras-1*^{bd} strain (Table 4.6); suggesting that the *camk-1*, *camk-2*, *camk-3*, and *camk-4* genes are required for normal period length, but do not affect the circadian temperature compensation in *N. crassa*.

CHAPTER 5

Molecular analysis of calmodulin, transcriptional regulation of the heat shock and pheromone response pathways in *N. crassa*

5.1 Introduction

Calmodulin (CaM) is a versatile Ca^{2+} sensor that plays a central role in decoding critical Ca^{2+}-dependent signals and controlling various cellular functions (Zhang et al. 2012; Yang and Tsai 2022). CaM is highly conserved in eukaryotes and regulates over 300 intracellular proteins (Halling et al. 2016). The functional versatility of CaM comes from: (i) the ability of CaM to bind in its apo form or in the Ca^{2+}-bound state (holo CaM) to target proteins with different affinities, (ii) the two independently-folded Ca^{2+}-binding lobes interact differentially and to some degree separately with targets proteins, and (iii) the flexibility of its long central linker which enables CaM to adopt multiple orientations that can interchange rapidly (Tidow and Nissen 2013; Villalobo et al. 2018). Thus, due to the high level of conservation, versatility, and the importance for accurate Ca^{2+}-signaling, it was believed that mutations in CaM could not be tolerated. (Halling 2016; Jensen et al. 2018; Chazin and Johnson 2020). In humans, three independent CaM genes (*CALM 1-3*) encode the exact same CaM protein, and the change in the protein sequence or the protein expression level in any one of the three CaM can cause major diseases (Halling et al. 2016). *N. crassa* has only one CaM, which is essential for viability (Tamuli et al. 2013). Previously, the role of CaM in *N. crassa* was studied using CaM inhibitors (Sadakane and Nakashima 1996; Laxmi and Tamuli 2015). In our laboratory, CaM mutant was generated using repeat-induced point mutation (RIP) to study the cell functions of CaM (Laxmi and Tamuli 2017). The *cmd*^{RIP} mutant showed defects in growth, reduced carotenoid accumulation, and sensitivity to UV irradiations (Laxmi and Tamuli 2017). I also found that the *cmd*^{RIP} mutant was defective in both stress responses (chapter 3) and sexual development process (chapter 4). Therefore, in this chapter, I analyzed how the RIP mutations affected the structure of the protein, the Ca^{2+} binding property, and the function of the CaM^{RIP} protein.

Chapter 3 and chapter 4 described the roles of CaM, and CaMKs in stress responses, during sexual development, and in regulating the circadian clock. The Ca^{2+} signaling

machinery coordinates with different signaling pathways to regulate various cellular processes and establishes crosstalk between different signaling pathways (Sanders et al. 2002; Berridge et al. 2003). In *N. crassa*, the synthesis of heat shock proteins belonging to Hsp60, Hsp70, and Hsp90 families are increased at elevated temperatures to impart thermotolerance (Plesofsky-Vig and Brambl 1985; Roychowdhury et al. 1992; Kapoor and Roy 2014). In addition, the pheromone signaling genes, including *pre-1*, *pre-2*, *ccg-4*, *mfa-1*, and *fmf-1* are required for normal sexual development (Bobrowicz et al. 2002; Kim and Borkovich 2004, 2006; Iyer et al. 2009; Kim et al. 2012). Moreover, the core molecular components such as *frequency* (*frq*) and the *white collar* genes (*wc-1* and *wc-2*) have been well characterized for their roles in the *N. crassa* circadian clock (Dunlap and Loros 2004; Baker et al. 2012). Therefore, in order to understand how CaM and CaMKs regulate various cellular processes, I investigated the genetic interactions of CaM and CaMKs for their roles in the heat shock response pathway, pheromone response pathway, and regulations of the *N. crassa* circadian clock.

5.2 Results

5.2.1 Homology modelling and comparison of CaM and CaM^{RIP} protein

Calmodulin (CaM) consists of two globular domains (N- and C- terminal) connected by a flexible linker (Barbato et al. 1992; Chattopadhyaya et al. 1992). Each domain consists of a pair of Ca^{2+} binding motifs known as EF-hands that enables the binding of four Ca^{2+} ions (Lewit-Bentley and Réty 2000). Using a recent method called LITPOMS (ligand titration, fast photochemical oxidation of proteins and mass spectrometry), the Ca^{2+} binding affinity of each EF-hand showed to vary substantially with K_i (Inhibition constant) ranging from 10^4 to 10^6 M^{-1}, and therefore binds to Ca^{2+} in a sequential order where EF-4 binds first followed by EF-3, EF-2, and EF-1 (Liu et al. 2019a and 2019b). Previous work in our laboratory, generated the *cmd*^{RIP} (#26) mutant strain containing mutations in both the endogenous (APB97097.1; D57Y,

Q148H) and ectopic (APB97091.1; M1W, E8K) CaM proteins (Laxmi and Tamuli 2017). Because the crystal structure of *N. crassa* CaM (P61859) is not determined, therefore, I performed homology modelling using SWISSMODEL (SWISS-MODEL Interactive Workspace (expasy.org)), a fully automated protein structure homology modelling server, to understand how the RIP mutations has affected the CaM structure. The 3D modelled structures were further validated using the PROCHECK (Laskowski et al. 1993), ERRAT (Colovos and Yeates 1993), and VERIFY 3D (Bowie et al. 1991) programs available in the Structural Analysis and Verification Server (SAVES, https://saves.mbi.ucla.edu).

For the homology modelling of *N. crassa* CaM, the crystal structure of *Aspergillus niger* CaM (PDB ID: 6XU4; Barykina et al. 2020) with a GMQE (Global Model Quality Estimate) score of 0.76 and 97.99 % sequence identity (E-value *9e-100*) to the CaM from *N. crassa*, was used as a template. The homology model of CaM showed that four Ca^{2+} binds to the wild type CaM and the ectopic CaM^{RIP} (Figure 5.1B), while Ca^{2+} binding was impaired in the EF-Hand 2 of the endogenous CaM^{RIP} (Figure 5.1C), suggesting that the D57Y mutation prevented the binding of Ca^{2+} ion. PROCHECK analysis of the Ramachandran plot revealed that 85.7%, 87.2%, and 86.4% residues of wild type CaM, endogenous CaM^{RIP}, and ectopic CaM^{RIP}, respectively, are within the most favoured regions and no residue is within the disallowed regions (Figure 5.2, Table 5.1). In addition, the "overall quality factor" for non-bonded atomic interactions was determined using ERRAT which showed a good score of 96.38%, 96.38%, and 96.35% for wild type CaM, endogenous CaM^{RIP}, and ectopic CaM^{RIP} (Figure 5.3, Table 5.2). Moreover, the VERIFY 3D analysis predicted that 92.47%, 100%, and 100% of the residues in wild type CaM, endogenous CaM^{RIP}, and ectopic CaM^{RIP} had an average 3D-1D score > 0.2 (Figure 5.4; Table 5.3), thereby verifying the homology modelled structures for the wild type CaM, endogenous CaM^{RIP}, and ectopic CaM^{RIP} proteins. Thus, the homology modelling of *N. crassa* CaM shows that the EF-2 of endogenous CaM^{RIP} is unable

to bind to Ca^{2+} due to the RIP mutation of Asp to Tyr mutation at position one (+X, D57Y), which may be the reason for all the phenotypic defects seen in the strain.

(A)

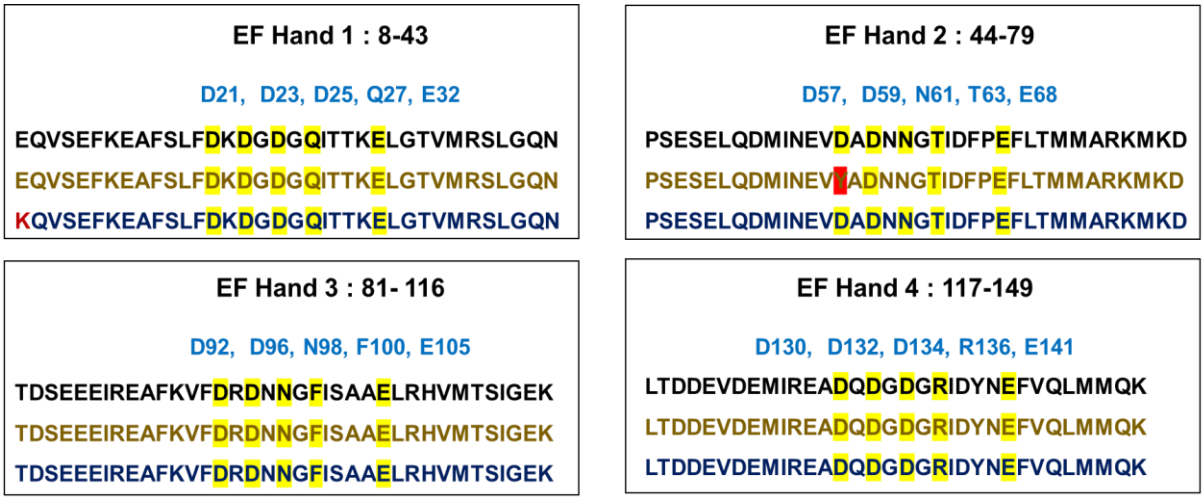

(B)

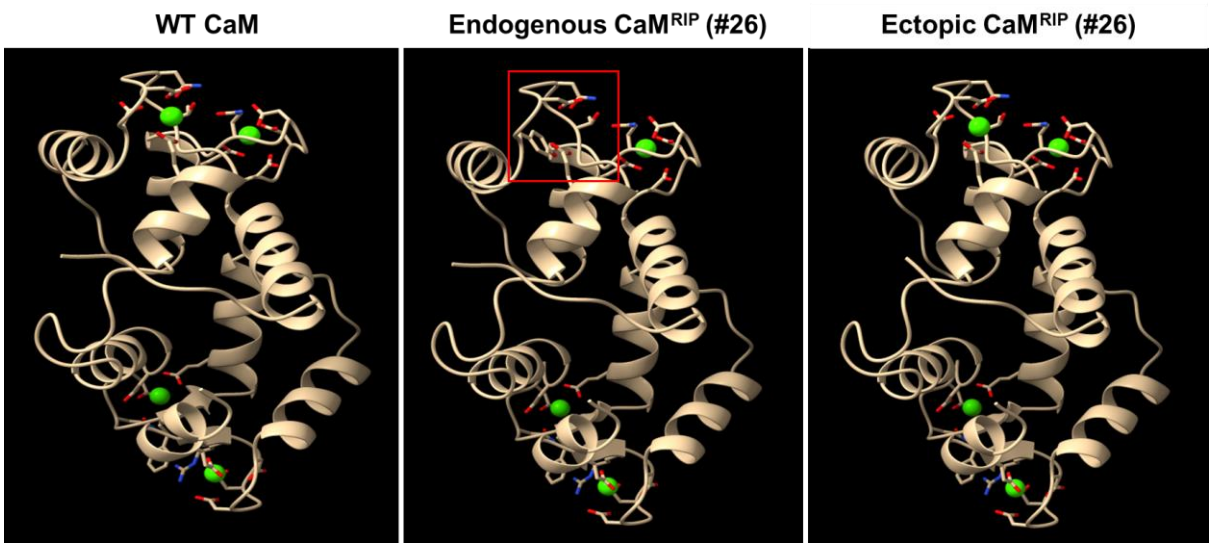

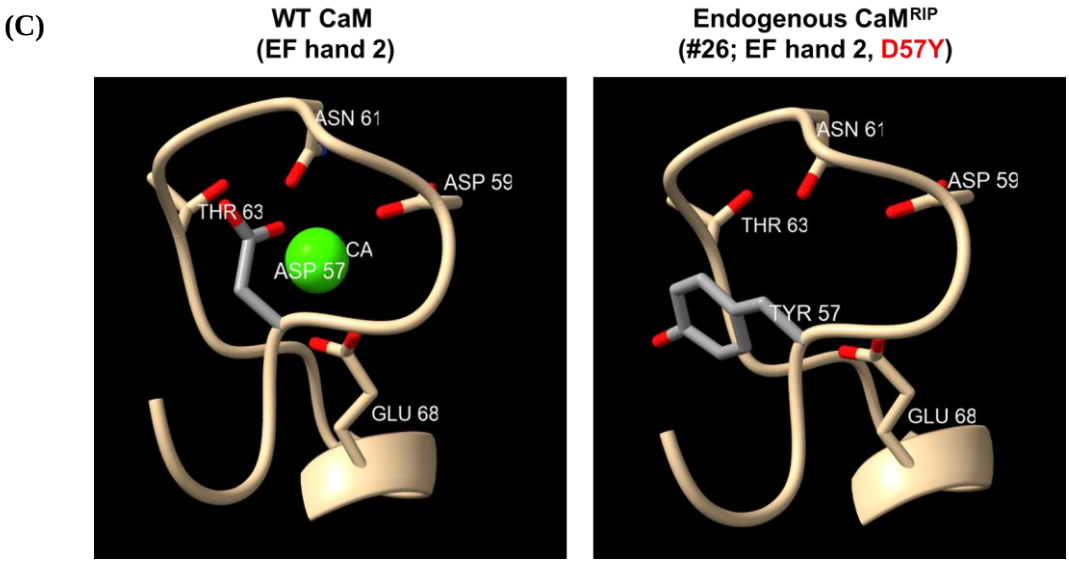

Figure 5.1 Sequence and structure of wild type CaM, endogenous and ectopic copies of CaM in the CaM^{RIP} mutant strain (#26). (A) Comparison of the four EF-hand domain sequences of wild type CaM (black; P61859), endogenous CaM^{RIP} (dark gold; APB97097.1; D57Y, Q148H), and ectopic CaM^{RIP} in the mutant (#26) strain (blue; APB97091.1; M1W, E8K); the residues providing the oxygen ligand are highlighted in yellow. **(B)** Visualization of the 3D structure of wild type CaM, endogenous CaM^{RIP}, and ectopic CaM^{RIP} in the mutant strain (#26) using UCSF Chimera. **(C)** Visualization of 3D structure of EF hand 2 of wild type CaM and endogenous CaM^{RIP} in the mutant (#26) strain using UCSF Chimera.

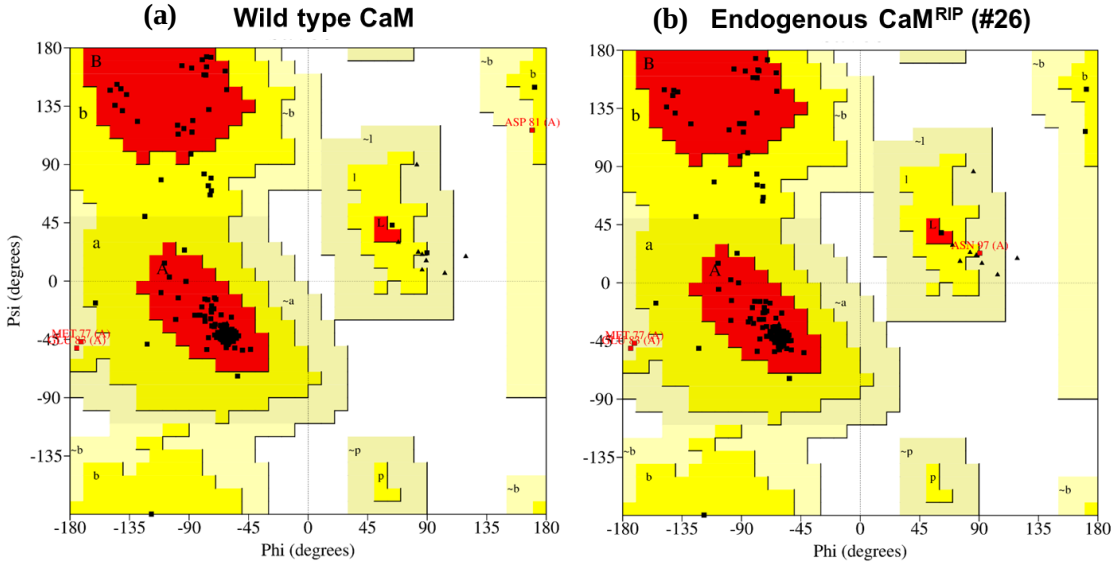

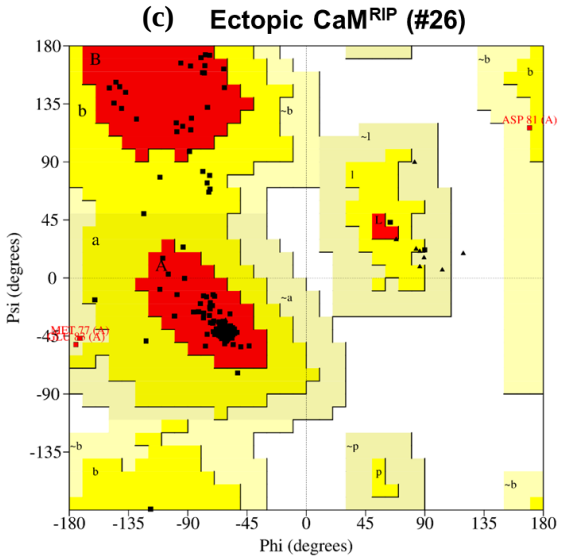

Figure 5.2 PROCHECK analysis to validate the homology modelled structures. Ramachandran plot of **(a)** wild type CaM, **(b)** endogenous CaM^{RIP}, and **(c)** ectopic CaM^{RIP} in the mutant (#26) strain. The different color-coded regions represent the most favoured regions (red), allowed regions (yellow), generously allowed areas (pale yellow), and disallowed regions (white).

Table 5.1 Percentage of residues in different Ramachandran plot regions

Plot statistics	**Percentage (%)**		
Residues	**Wild type CaM**	**Endogenous CaM^{RIP} (#26)**	**Ectopic CaM^{RIP} (#26)**
Residues in most favoured regions [A, B, L]	85.7	87.2	86.4
Residues in additional allowed regions [a, b, l, p]	12	10.5	11.4
Residues in generously allowed regions [~a, ~b, ~l, ~p]	2.3	2.3	2.3
Residues in disallowed regions	0	0	0

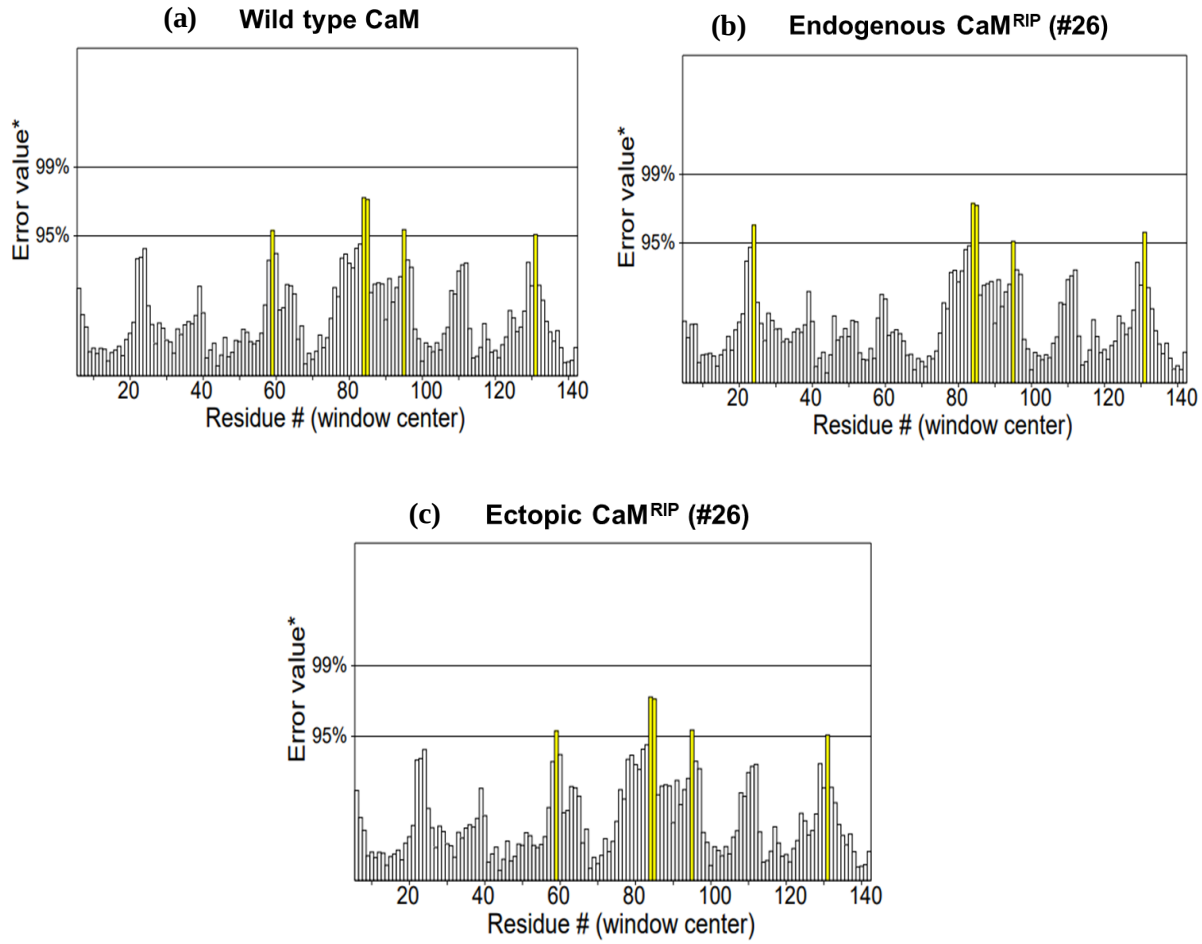

Figure 5.3 The "overall quality factor" for non-bonded atomic interactions scored using ERRAT analysis. ERRAT plots of **(a)** wild type CaM, **(b)** endogenous CaM^{RIP} (#26), and **(c)** ectopic CaM^{RIP} (#26). The two lines indicate the confidence level, and the regions to be rejected on crossing the error values. The "y" axis presents the error value and "x" axis presents the amino acid sequences. An error value exceeding 99% confidence level indicates poorly modelled regions.

Table 5.2 Percentage of overall quality factor

	Percentage (%)		
Overall quality factor	**WT CaM**	**Endogenous CaM^{RIP} (#26)**	**Ectopic CaM^{RIP} (#26)**
	96.38	96.38	96.35

(a) **Wild type CaM**

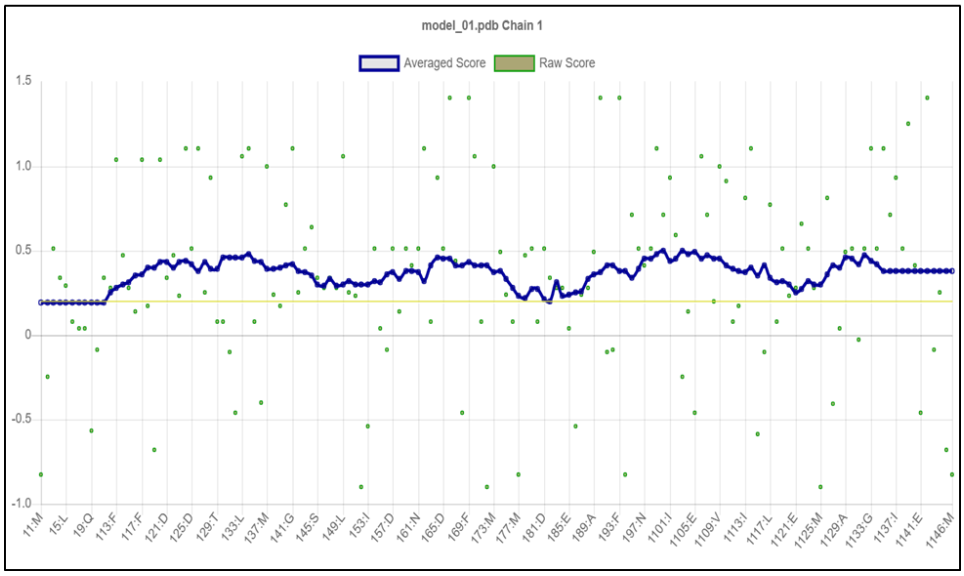

(b) **Endogenous CaM^{RIP} (#26)**

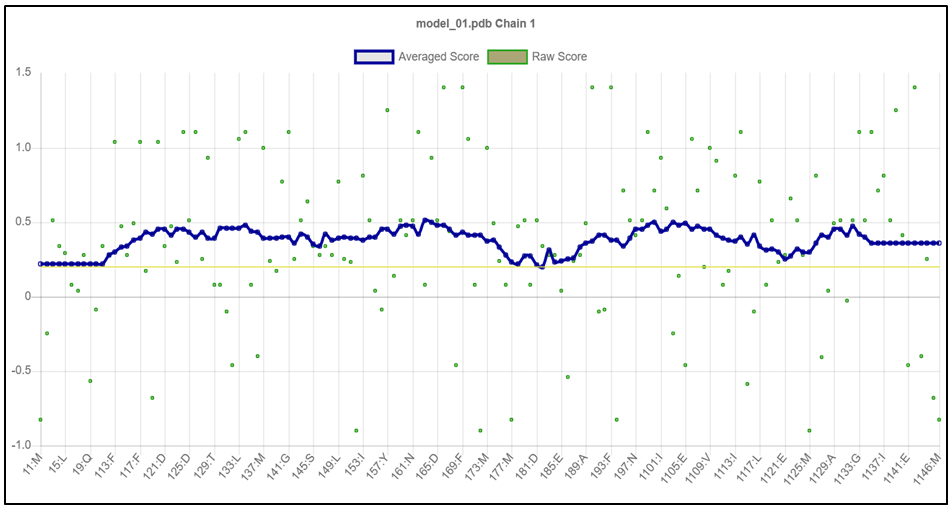

(c) **Ectopic CaM^{RIP} (#26)**

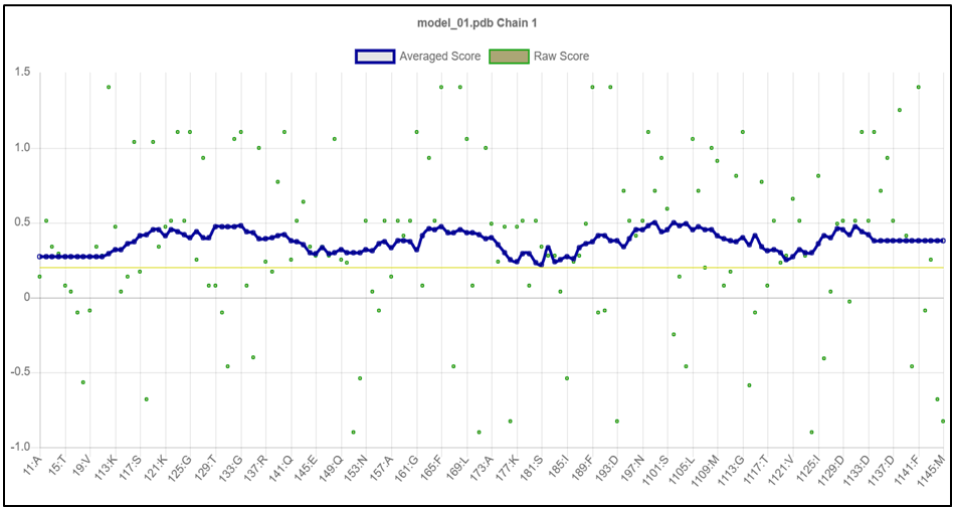

Figure 5.4 VERIFY 3D profile-window plots. (a) wild type CaM, **(b)** endogenous CaM^{RIP} (#26), and **(c)** ectopic CaM^{RIP} (#26). The compatibility of an atomic model (3D) with its own amino acid sequence (1D) is assessed by its environment profile. The vertical axis gives the average 3D-1D score for residues within a 21-residue sliding window.

Table 5.3 Percentage of residues with a preferred 3D-1D score

Average 3D-1D score>=0.2	Percentage (%)		
	WT CaM	Endogenous CaM^{RIP} (#26)	Ectopic CaM^{RIP} (#26)
	92.47	100	100

5.2.2 Visualization of intracellular Ca^{2+} distribution in the *cmd*^{RIP} (#26) mutant

In *N. crassa*, the maintenance of a tip-high gradient of cytoplasmic Ca^{2+} is important for hyphal growth (Schmid and Harold 1988; Torralba et al. 2001). The Ca^{2+} gradient is generated and maintained internally by the IP_3-activated Ca^{2+} channels and the Ca^{2+}-ATPase-mediated sequestration of Ca^{2+} into the endoplasmic reticulum and vesicles (Torralba et al. 2001; Silverman-Gavrila and Lew 2001, 2002, 2003). The Ca^{2+} gradient modulates the actin-based components of cytoskeleton, which controls the extensibility and synthesis of the hyphal apex (Jackson and Heath 1993; Torralba and Heath 2001). The disruption of *vma-1*, a vacuolar H^+-ATPase in *N. crassa*, resulted in abnormal vacuolar morphology, depleted Ca^{2+} vacuolar stores and showed defects in female fertility, colony growth, and morphology (Bowman et al. 2000). The *cmd*^{RIP} mutant showed defects in female fertility (as described in chapter 4), colony growth and morphology (Laxmi and Tamuli 2017). I further visualized the intracellular stored Ca^{2+} vesicles in wild type and the *cmd*^{RIP} mutant strains using chlortetracycline (CTC, Sigma), a cell-permeable fluorescent probe which binds to the sequestered Ca^{2+} within the intracellular

stores and forms a highly fluorescent complex (Engelmann et al. 1990). Microscopic analysis using CTC showed severely depleted Ca^{2+} storage vesicles in the *cmd*^{RIP} mutant strain as compared to the enhanced and multiple Ca^{2+} storage vesicles seen in the wild type strain (Figure 5.5C). Because CTC fluorescence is also affected by Mg^{2+} ions and intracellular distribution of membranes (Caswell 1979; Blinks et al. 1982), therefore, the hyphae were also visualized in the presence of 1-N-Phenylnapthylamine (NPN), a fluorescent probe that binds to cell membranes. No enhanced fluorescence vesicles were observed in both strains indicating that fluorescence was from Ca^{2+} ions and not from membrane density or Mg^{2+} ions (Figure 5.5 C). This result suggested that the RIP mutation in CaM caused disruptions in Ca^{2+} homeostasis that might be causing various phenotypic defects in the *cmd*^{RIP} mutant strain.

(A)

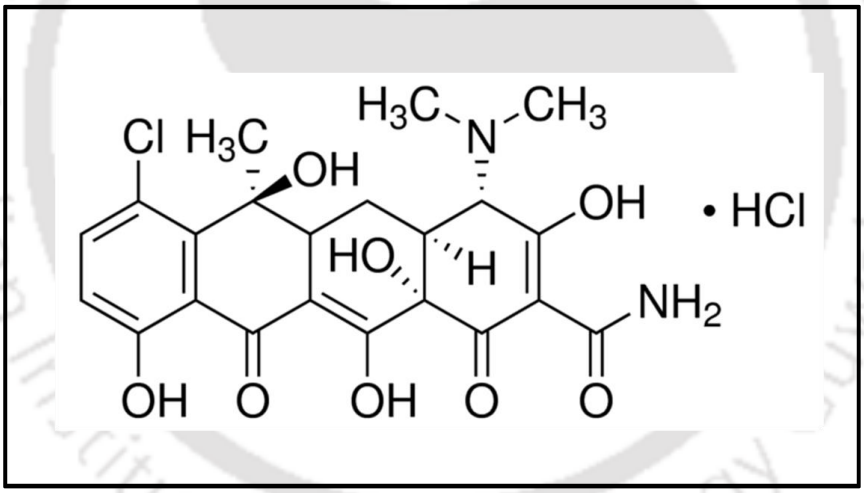

(B)

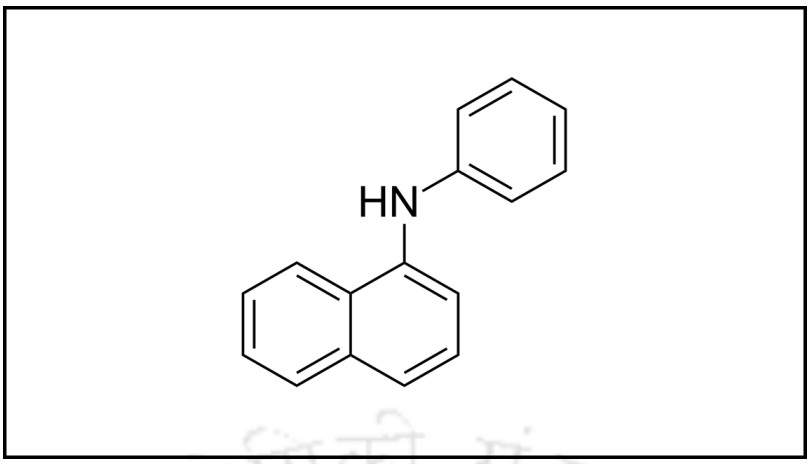

(C)

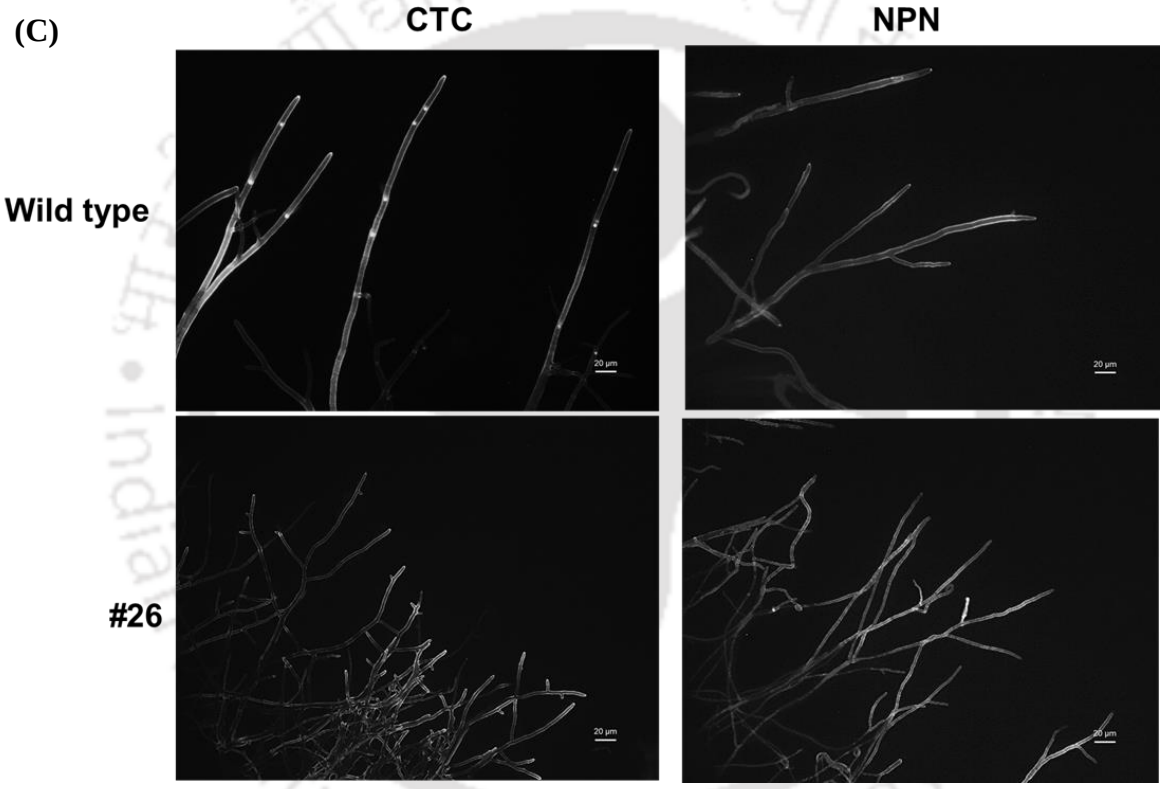

Figure 5.5 Assay for visualization of intracellular distribution of Ca^{2+}. (A) The chemical structure of chlortetracycline hydrochloride (CTC, Sigma, Cat. No. 26430) **(B)** The chemical structure of N-Pheny-1-lnapthylamine (NPN, Sigma, Cat no. 104043), **(C)** The hyphae of wild type and mutant (#26) strains were grown in VG agar medium supplemented with 200 µM CTC and 20 µM NPN dissolved in 0.1% dimethyl sulphoxide (DMSO). CTC and NPN fluorescence were observed under a Trinocular inverted fluorescence microscope (AxioVert A1 FL, Carl Zeiss) under DAPI filters with exposure time of 300-400 ms. Scale bar 20 µm.

5.2.3 Visualization of the internal septation in wild type and *cmd*^{RIP} (#26) mutant

In *N. crassa*, the growth of the mycelium is properly balanced since the elongation or length of the hyphae, number of branches, number of septa in the hyphal network are well coordinated with the distribution of nuclei, mitochondria, amount of DNA, RNA, proteins and cell wall polymers (Trinci et al. 1994; Potapova et al. 2016). The hyphal cells are compartmentalized by cross walls called "septa", which retain a central pore and allow nuclei and organelles to travel between cells freely to maintain cytoplasmic continuity in a colony (Hunsley and Gooday 1974; Degado-Alvarez 2014). The small monomeric Rho-type GTPases are involved in regulating septation in *N. crassa* and other fungi (Nakano et al. 2003; Santos et al. 2003; Rasmussen and Glass 2005; Kwon et al.2011; Zhang et al. 2013; An et al 2015; Perez et al. 2016). In *Xenopus*, Rho GTPases act downstream of Ca^{2+} signals to trigger spinal cord growth cone turning (Jin et al. 2005). The *cmd*^{RIP} mutant (#26) showed abnormal vegetative growth with reduced aerial hyphae (Laxmi 2016; Laxmi and Tamuli 2017); a similar phenotype of suppressed vegetative growth and conidiation was seen in Rho3-GTPase mutant in *Botrytis cinerea* (An et al. 2015). Therefore, I examined the internal septation in the wild type and *cmd*^{RIP} mutant (#26) using calcofluor white (CFW). CFW is a fluorescent probe that binds to cellulose and chitin present in the fungal cell wall (Galbraith 1981; Boyce et al. 2012). The *cmd*^{RIP} mutant (#26) strain showed hyper hyphal branching, increased septation, and decreased hyphal width in comparison to the wild type (Figure 5.6, Table 5.4). Therefore, a normal and functional CaM is required for proper septation and hyphal growth and development in *N. crassa*.

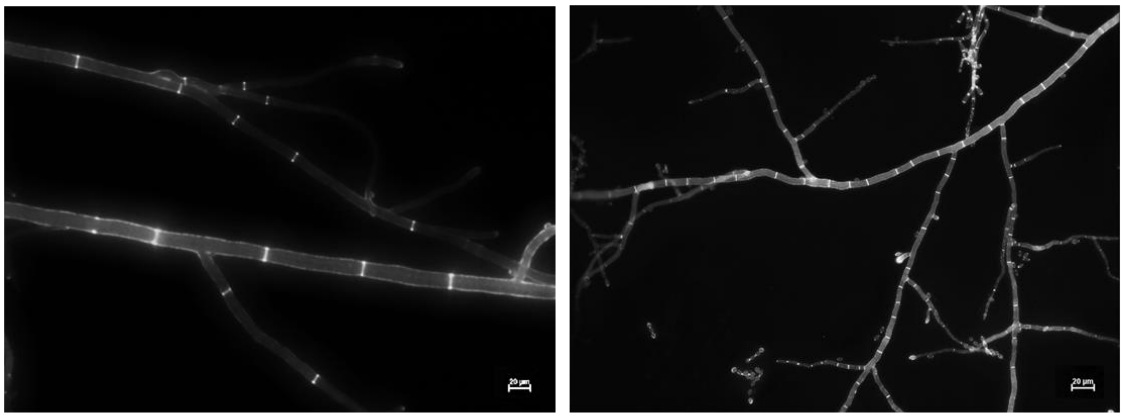

Figure 5.6 Assay for visualization of internal septation in wild type and *cmd*^{RIP} (#26) mutant hyphae. Strains were grown in VG agar medium overlaid on a glass slide at 30 °C for 12 h. The hyphae were then stained with CFW (0.1% in 0.05 M PBS) and observed under a Trinocular inverted fluorescence microscope (AxioVert A1 FL, Carl Zeiss) under DAPI filters with an exposure time of 300-400 ms.

Table 5.4 Average hyphal width and septation length of wild type and *cmd*^{RIP} (#26) strains

Strain	Average length (µm)		Septation length (µm)	
	$^{+}$Hyphal width (n = 30)	$^{+}$Septation length (n = 30)	Maximum	Minimum
wild type	10.2 ± 0.6	82.3 ± 19.75	139	48
***cmd*^{RIP}(#26)**	4 ± 0.3 (***)	23.5 ± 8.3 (***)	44	6

$^{+}$Results are shown as mean ± standard deviation for three independent experiments (n = 3). In each experiment, the hyphal width and septation length were measured for 30 sets (n = 30), with *P* values < 0.05 (*), < 0.01 (**), and < 0.001 (***) compared with the wild type strain as estimated by one-way ANOVA test.

5.2.4 Expression analysis of *cmd* and *camks* under heat stress

To understand the role of CaM and CaMKs in survival on exposure to heat stress condition, I analysed the expression level of *cmd*, *camk-1*, *camk-2*, *camk-3*, and *camk-4* genes in the wild type strain using qRT-PCR. The wild type strain was grown for 14 h at normal (28 °C) and treated with heat stress (heat shock at 48 °C for 1 h), RNA was then isolated and qRT-PCR was performed using the gene specific primers (Entries 1, 2, 15 to 24; Table 5.5). The transcript levels of *cmd*, *camk-1*, and *camk-2* were increased (Figure 5.7), indicating that the *cmd*, *camk-1*, and *camk-2* genes are upregulated under the heat stress condition.

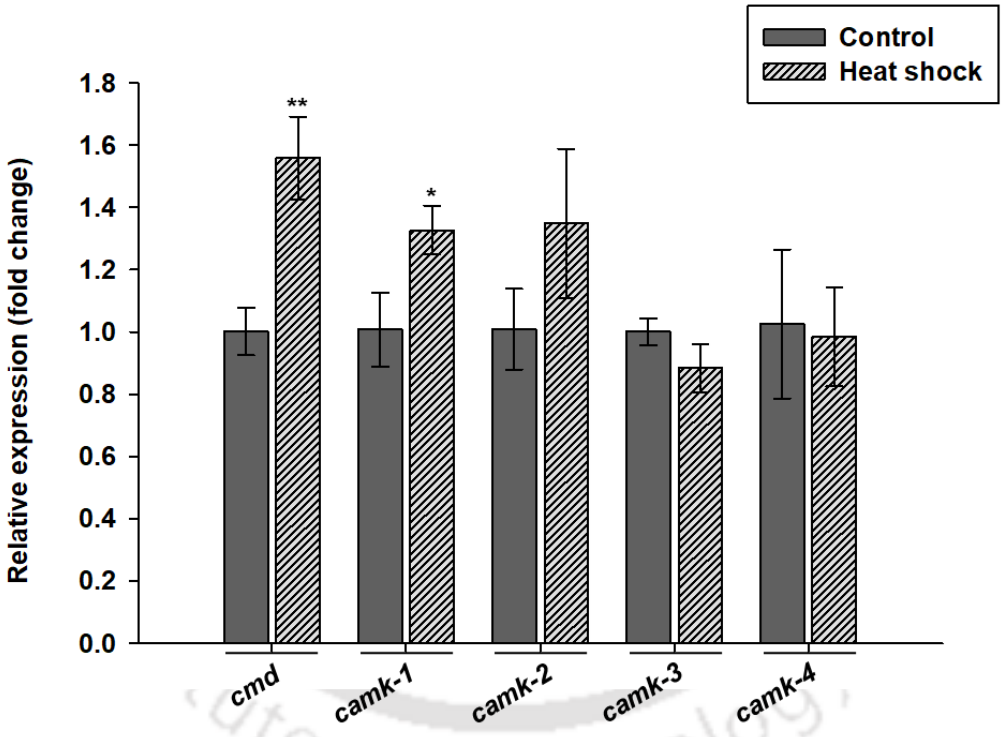

Figure 5.7 Expression analysis of *cmd, camk-1, camk-2, camk-3* and *camk-4* genes under heat shock condition. RNA was isolated from the wild type strain grown in liquid VG medium at 28 °C in dark for 14 h (control) and further given heat shock at 48 °C for 1 h. The expression of each gene was studied using qRT-PCR and normalized to the expression of *β-tubulin* gene. Standard deviations are indicated by error bars calculated from three independent experiments

(n = 3), and the significance given by *P* values <0.05 (*), <0.01 (**), and <0.001 (***) as measured by one-way ANOVA test.

Table 5.5 Primers used for qRT-PCR analysis

Sl. No.	Primer Name	Sequence (5'→3')	Reference
1	q-B-tub-Fw	CCCAAGAACATGATGGCTGC	Barman and Tamuli 2017
2	q-B-tub-Rv	TTGTTCTGAACGTTGCGCATC	Barman and Tamuli 2017
3	Qccg-4-Fw	CAGCCTCCAAGAGAAGTTCG	Barman and Tamuli 2017
4	Qccg-4-Rv	CACGCTTCTTCCAGCACGAT	Barman and Tamuli 2017
5	Qfmf-1-Fw	CGGACAAGACAGCAGTTCT	Barman and Tamuli 2017
6	Qfmf-1-Rv	TTTCGGTGGTTGCTGTTCATC	Barman and Tamuli 2017
7	Qmfa-1-Fw	ATGCCTTCCACCGCTGCTTC	Barman and Tamuli 2017
8	Qmfa-1-Rv	CATAACAACGCAGTAGCCGT	Barman and Tamuli 2017
9	HSP 60 ARrt Fw	GTCCTCATCGAGTCCAGCTT	Roy and Tamuli 2021
10	HSP 60 ARrt Rv	CCGAGGTTCTCGAACTTGTC	Roy and Tamuli 2021
11	HSP 80 RT-Fw	CGAACAAGACCCTCACCATC	Roy and Tamuli 2021

12	HSP 80 RT-Rv	GAGCGGGCAATAGTACCAAG	Roy and Tamuli 2021
13	RT-NCU09602 Fw	CTTGGGTGGTGAGGATTTCG	This study
14	RT-NCU09602 Rv	CGATCTCAATGGAGGTCTGG	This study
15	RT-NCU04120 F	GTGAGGCCTTCAAGGTGTTC	This study
16	RT-NCU04120 R	CGTCATCAGTGAGCTTCTCG	This study
17	qRT-NCU09123 F	CGCCAACATGCTTAATCGCC	This study
18	RT-NCU09123 R	GAACCATCTGTTCGTTGCCC	This study
19	qRT-NCU02283 F	GCAGCCGTGTCGATACAAAG	This study
20	RT-NCU02283 R	ACCTTCTTGAGCACGGCGAT	This study
21	RT-NCU06177 F	CTTTGCCCGAGGAACAATGC	This study
22	RT-NCU06177 R	GGAGACTCCAAAGTCGACGA	This study
23	RT-NCU09212 F	TAGTGAGGATCTCTCCAGGC	This study
24	RT- NCU09212 R	ATCACCTGGCTGCTTGGGTT	This study
25	RT-NCU00138 Fw	CAAGTTCGCAATCGTGGTGG	This study
26	RT-NCU00138 Rv	CGTAGTTTGTGCAGGGTTTAG	This study
27	RT-NCU05758 Fw	CGACATGCAAATCAGCGTGG	This study
28	RT-NCU05758 Rv	GCCTGGAAAATGCAGTTGGC	This study

5.2.5 Expression analysis of *hsp60, hsp70,* and *hsp80* under heat stress in the wild type, *cmd*^{RIP} (#26) and Δ*camks* mutants

The folding of native proteins is affected under heat and other stress conditions, which may cause protein misfolding and aggregation, resulting in loss of protein function and toxicity in the cell (Sharma et al. 2009; Nakajima and Suzuki 2013; Weids et al. 2016). Heat shock proteins (Hsps), are molecular chaperones that are constitutively expressed and up-regulated

in response to various stress conditions (Tiwari et al. 2015). Hsps function to reduce the aggregation of proteins damaged by heat or other proteotoxic stress, and assist in the refolding or degradation of stress-damaged proteins (Feder and Hoffman 1999; Wallace et al. 2015; Chen et al. 2018). Under heat stress, Hsps belonging to the Hsp60, Hsp70, and Hsp90 families are rapidly produced (Roychowdhury et al. 1992). In *N. crassa*, Hsp80, the homolog of mammalian Hsp90, is the most abundant heat shock protein that is strongly induced by hyperthermia, low levels of sodium arsenite, ethanol, and carbon source depletion (Roychowdhury 1992). Hsp80 was also found to physically interact with Hsp70, another major heat-inducible protein in *N. crassa* (Freitag et al. 1997). In *Aspergillus fumigatus* and *A. terreus*, increased expression of *hsp60* mRNA was observed at 40 °C as compared to the samples at 25 °C and suggested that fungal Hsp60 may act as immunogenic triggers under temperature-related stress conditions (Raggam et al. 2011). In this study, I found that the *cmd*^{RIP} (#26), Δ*camk-1*, and Δ*camk-2* mutants are defective in the acquisition of thermotolerance (chapter 3). Because thermotolerance is associated with the production of Hsps, therefore, I studied the expression of genes encoding the heat shock proteins Hsp60, Hsp70, and Hsp80 in the wild type and mutant strains under heat stress condition. The expressions of *hsp70* and *hsp80* in the *cmd*^{RIP} (#26), Δ*camk-1*, and Δ*camk-2* mutants were reduced, and the expression of *hsp60* was slightly reduced in all the *camk* mutants in comparison to the wild type (Figure 5.8). This results suggested that CaM, CaMK-1 and CaMK-2 are involved in the heat shock response pathway in *N. crassa*.

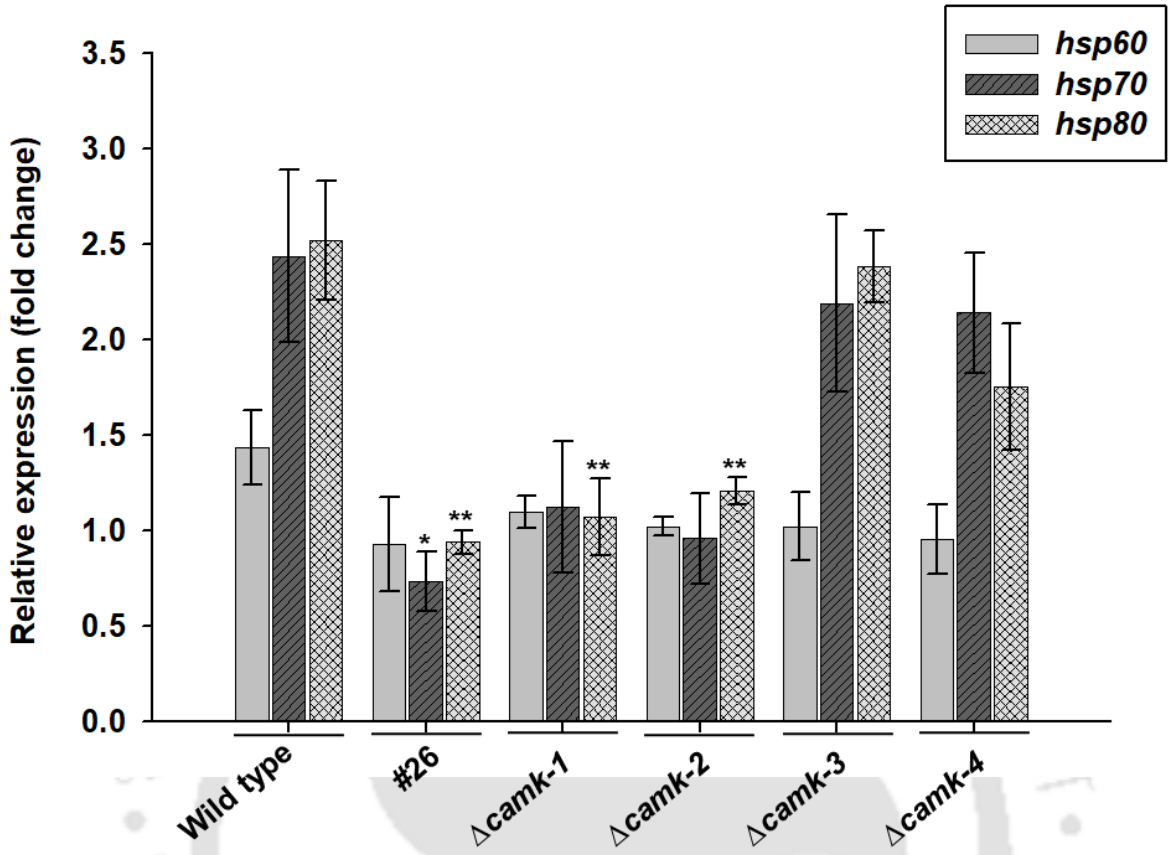

Figure 5.8 Expression of heat shock response genes *hsp60*, *hsp70*, and *hsp80* in wild type, *cmd*^{RIP} (#26), and Δ*camks* mutants. RNA was isolated from the *N. crassa* wild type and mutant strains grown for 14 h at 30 °C with shaking at 180 rpm which were then given heat shock for 1 h at 48 °C. The expression of the heat shock response genes *hsp60*, *hsp70*, and *hsp80* were studied using the qRT-PCR and normalized to the expression of *β-tubulin* gene. Standard deviations are indicated by error bars calculated from three independent experiments (n = 3), and the significance given by *P* values <0.05 (*), <0.01 (**), and <0.001 (***) as measured by one-way ANOVA test.

5.2.6 Expression analysis of *cmd* and *camks* under nitrogen starved condition

The *cmd*^{RIP} mutant is female sterile and defective during cell fusion (described in chapter 4). In addition, the crosses homozygous for Δ*camk-1* and Δ*camk-2* display an intermediate and barren phenotype, respectively (Kumar and Tamuli 2014). To understand the role of CaM and CaMKs in sexual development, I analyzed expression levels of *cmd*, *camk-1*, *camk-2*, *camk-3*, and *camk-4* genes in the wild type strain grown under nitrogen starved condition. RNA was isolated form wild type strain grown at low temperature (22 °C) for 18 h, and qRT-PCR was performed using the gene specific primers (Entries 1, 2, 15 to 24; Table 5.5). Increased transcript levels of *cmd*, *camk-1*, and *camk-2* were observed (Figure 5.9), suggesting that the *cmd*, *camk-1*, and *camk-2* genes are upregulated under sexual development.

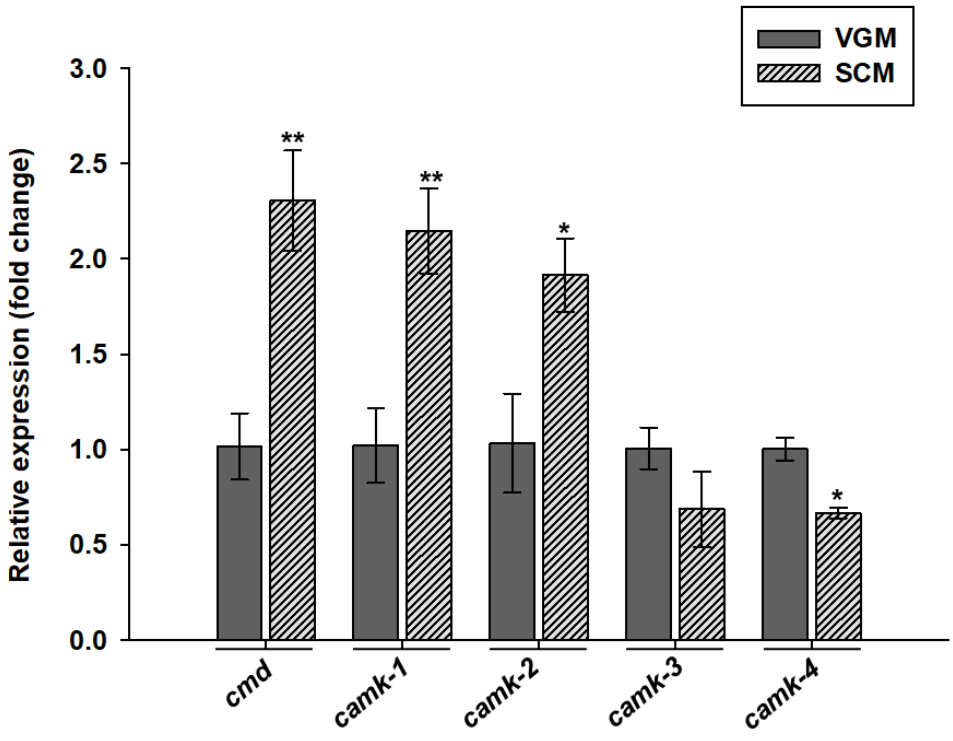

Figure 5.9 Expression analysis of *cmd, camk-1, camk-2, camk-3* and *camk-4* genes in wild type strain under nitrogen starved condition. RNA from the wild type was extracted from liquid VGM and SCM cultures grown at 22 °C for 18 h under constant darkness. The relative

expression of each gene was studied by qRT-PCR and normalized to the expression of *β-tubulin* gene. Standard deviations are indicated by error bars calculated from three independent experiments (n = 3), and the significance given by *P* values <0.05 (*), <0.01 (**), and <0.001 (***) as measured by one-way ANOVA test.

5.2.7 Expression analysis of pheromone receptor genes *pre-1* and *pre-2* and pheromone precursor genes *ccg-4*, *mfa-1*, and *fmf-1* in wild type and mutants under nitrogen starved conditions

During sexual phase, haploid cells of opposite mating types secrete different peptide pheromones that are recognized by their cognate transmembrane G protein-coupled receptors and result in the activation of the pheromone response MAPK pathway for proper sexual development (Fleißner et al. 2008; Kim et al. 2012). In *N. crassa*, the *mat A* cells express the pheromone receptor gene *pre-1* and the pheromone precursor gene *clock control gene-4* (*ccg-4*), while the *mat a* cells express the pheromone receptor gene *pre-2* and the pheromone precursor gene *mating factor a-1* (*mfa-1*) (Bobrowicz et al. 2002). MFA-1 and CCG-4 bind to their respective receptors, PRE-1 and PRE-2, and regulate cell fusion, perithecial development, and ascospore production (Kim and Borkovich 2004, 2006; Kim et al. 2012). In addition, another gene known as *female male fertility -1* (*fmf-1*), which is the homolog of *Saccharomyces pombe* gene *ste11*, is also required for mating pheromone signaling in both the male and female parents in *N. crassa* (Johnson 1979; Iyer et al. 2009). Therefore, to examine whether the pheromone signaling pathway is affected in the *cmd*^{RIP} (#26), Δ*camk-1*, and Δ*camk-2* mutants, I determined the expression profiles of the pheromone-related genes *pre-1*, *pre-2*, *ccg-4*, *mfa-1*, and *fmf-1* under nitrogen-starved condition. In consistency with the observed phenotypes, reduced expression of the *pre-1*, *pre-2*, *ccg-4*, *mfa-1*, and *fmf-1* genes were observed in the *cmd*^{RIP} (#26), Δ*camk-1*, and Δ*camk-2* mutants in comparison to the wild type (Figure 5.10).

This result suggested that pheromone signaling might be affected in these mutant strains, and CaM and Ca^{2+}/CaMKs play a role in regulating the pheromone response pathway during sexual development.

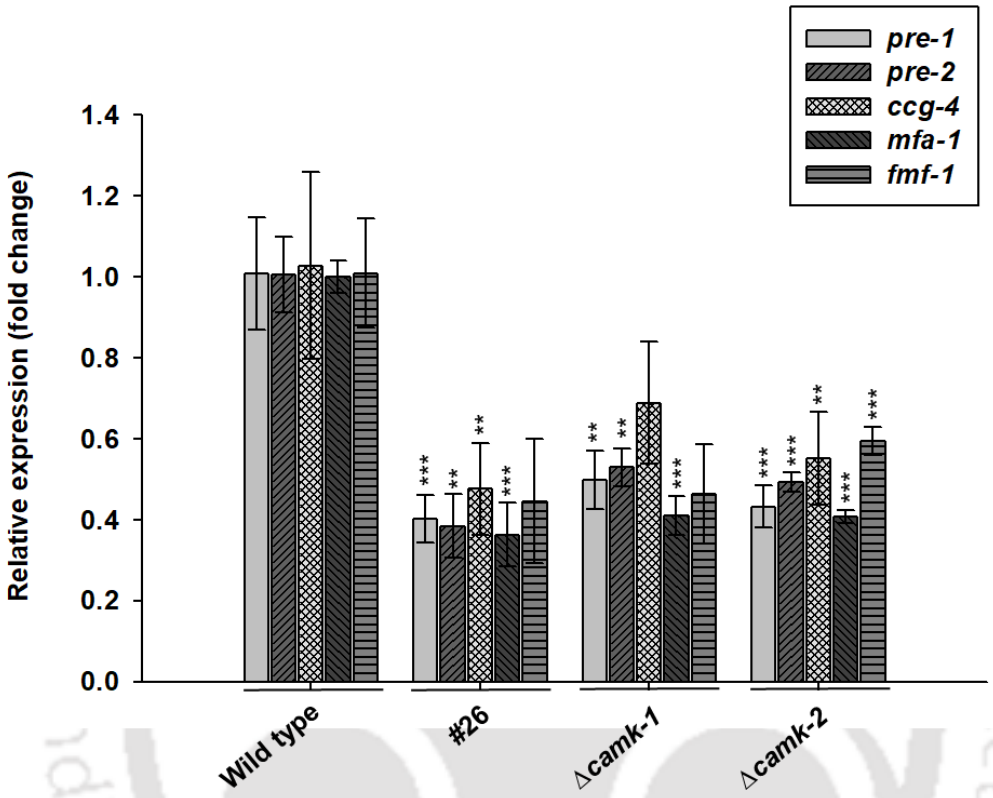

Figure 5.10 Expression analysis of the pheromone signaling genes *pre-1, pre-3, ccg-4, mfa-1,* and *fmf-1* in the wild type, *cmd*^{RIP} (#26), Δ*camk-1* and Δ*camk-2* mutant strains. RNA was isolated from the *N. crassa* strains cultured in liquid SCM, and the expression of pheromone signaling genes *pre-1*, *pre-2*, *ccg-4*, *mfa-1*, and *fmf-1* were studied by qRT-PCR and normalized to the expression of *β-tubulin* gene. Standard deviations are indicated by error bars calculated from three independent experiments (n = 3), and the significance given by *P* values <0.05 (*), <0.01 (**), and <0.001 (***) as measured by one-way ANOVA test.

5.2.8 Expression analysis of *frq* and *wc-1* at 20 and 25 ℃

The circadian system in *N. crassa* is based on a transcriptional/translational feedback loop run by a core clock complex that consists of the core oscillator protein frequency (FRQ), FRQ-interacting RNA helicase (FRH), and the White Collar Complex (WCC) that is a heterodimeric complex formed by the two GATA-family transcription factors White Collar-1 (WC-1) and White Collar-2 (WC-2) (Crosthwaite et al. 1997; Guo and Liu 2010; Hurley et al. 2015). The WCC binds to the *frq* promoter and promotes the rhythmic expression of *frq* (Schaifmeier et al. 2008). FRQ regulates its own expression in a negative feedback loop through FRQ-dependent inhibition of WCC complex activity (Dunlap 1999; Baker et al. 2012). The proteins in the circadian system are regulated through numerous distinct post-translational modifications (PTMs) (Baker et al. 2009; Mehra et al. 2009). The FRQ protein is progressively phosphorylated and becomes extensively phosphorylated before its degradation (Tang et al. 2009). The Δ*camk-1*, Δ*camk-2*, Δ*camk-3*, and Δ*camk*-4 mutants showed increased period length (discussed in chapter 4) with increase in temperature above 20 ℃ (Figure 4.9; Table 4.5). To understand if, *camks* are involved in regulating the core circadian clock proteins, I studied the expression of *frq* and *wc-1* in the *ras-1*^{bd} and Δ*camk-1*, Δ*camk-2*, Δ*camk-3*, and Δ*camk*-4 mutants at 20 ℃ and 25 ℃. The *ras-1*^{bd} strain has a T79I point mutation in the Ras-1 GTPase gene that enables clear visualization of circadian-regulated spore formation by enhancing the clock output signals without affecting the circadian clock (Belden et al. 2007). There was no significant change in the expression level of *frq* (Figure 5.11A) and *wc-1* (Figure 5.11B) in the mutants in comparison to the *ras-1*^{bd}, indicating that CaMKs are not essential for regulating the core clock proteins.

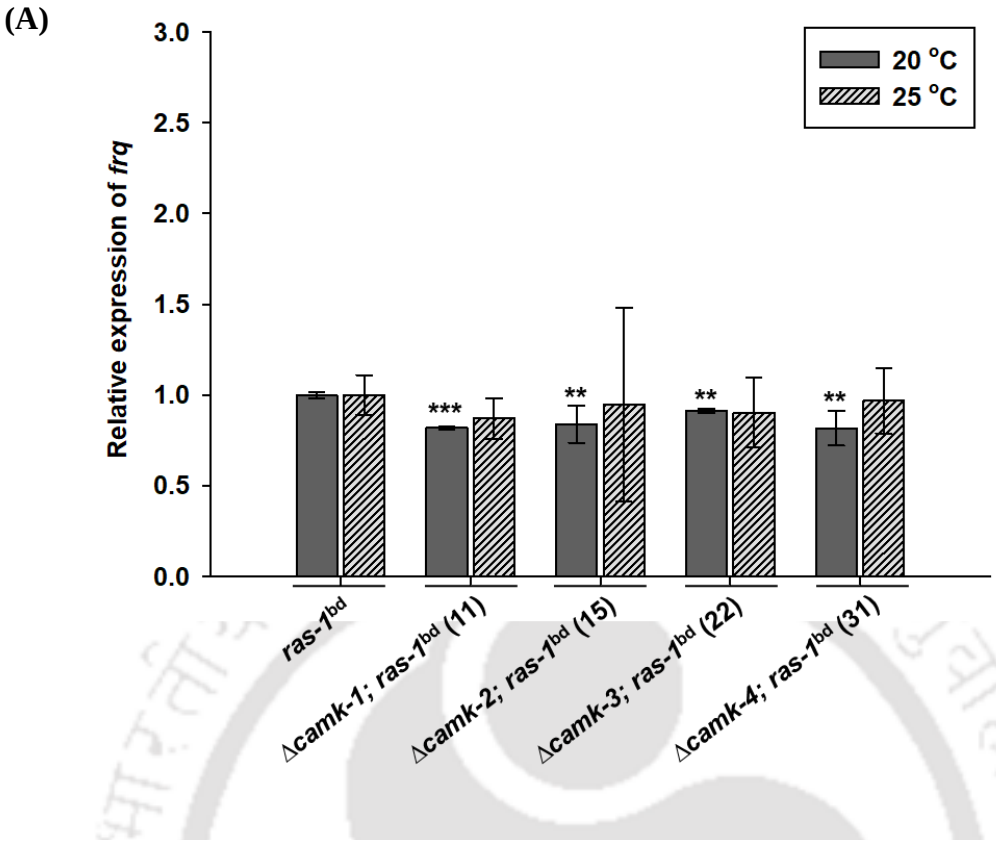

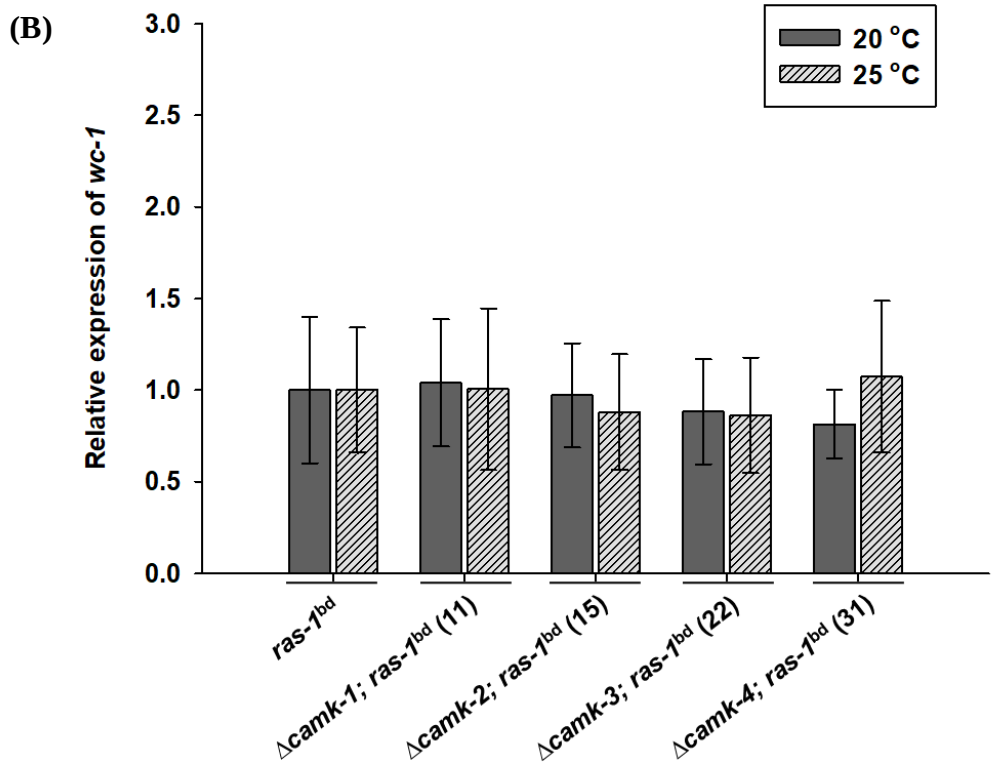

Figure 5.11 Expression analysis of *frequency* (*frq*) and *white collar-1* (*wc-1*) during circadian-regulated conidiation at 20 °C and 25 °C. RNA was isolated from the *N. crassa* strains cultured under circadian-regulated conidiation conditions at 20 ℃ or 25 ℃ and the expression of the *frequency* (*frq*) and *white collar-1* (*wc-1*) genes were determined using qRT-PCR. The relative expression of **(A)** *frq* and **(B)** *wc-1* was normalized to the expression of *β-tubulin* gene and expression values were compared with that of *ras-1*^{bd}. Error bars indicate standard deviations calculated from the data for three independent experiments (n = 3) with significance given by *P* values <0.05 (*), <0.01 (**), and <0.001 (***) compared with the *ras-1*^{bd} strain as measured by one-way ANOVA test.

5.2.9 Identification of PP-1 transcription factor regulatory sequence in the *cmd* promoter region by promoter analysis

To understand the transcriptional regulation of *cmd* during various cellular processes, I analyzed the *cmd* promoter region to identify putative binding sites for transcriptional regulators. Approximately 2 kb upstream of the 5' flanking region of the *cmd* gene was analyzed using MatInspector (Quandt *et al.* 1995). Among the putative sequences identified for several transcription factors, the yeast pheromone response element STE12 binding site was further investigated. In *N. crassa*, Protoperithecium-1(PP-1), is a C2H2-Zn^{2+} transcription factor homologous to the *S. cerevisiae* Ste12p that is involved in pheromone response pathway (Li et al. 2005; Leeder et al. 2013).

Table 5.6 Promoter analysis of the *cmd* gene

Sl. No.	Elements	Binding Sequence (5'→3')
1	Yeast stress response elements (MSN2)	gttctgaGGGcata
2	**Pheromone response elements (STE12)**	**aactgtAACAcac**
3	*Aspergillus*/*Neurospora* activator of genes induced by nitrogen (NIT2)	TATCtcg
4	Yeast mating factors (MATA1)	tacctaTGTAata
5	Fungal basic leucine zipper family (YAP1)	ttgctgttaTTACataggtag
6	Skn7 response regulator of Saccharomyces cerevisiae(SKN7)	TGGCgggcccc
7	Core promoter initiator elements (HMTE)	tcTCATtttag

5.2.10. Generation of the Δ*pp-1* mutant strain

I generated the Δ*pp-1* mutant strains to examine the role of PP-1 as the transcriptional regulator of *cmd* gene during sexual development. The *pp-1*^{KO} heterokaryotic strain (FGSC 21335) was a kind gift of Prof. Qun He (State Key Laboratory of Agrobiotechnology, College of Biological Sciences, China Agricultural University, Beijing, China). To generate the Δ*pp-1* homokaryotic mutants, the *pp-1*^{KO} heterokaryon strain was crossed with opposite mating type of wild type. The progenies obtained from this cross were screened for resistance to hygromycin B (Hyg^{R}), and further confirmed for the presence of *Δpp-1::hph* knockout allele using specific primers

(entries 1and 2; Table 5.7; Figure 5.12A), and for the absence of the *pp-1* ORF using ORF specific primers (entries 3 and 4; Table 5.7; Figure 5.12 B).

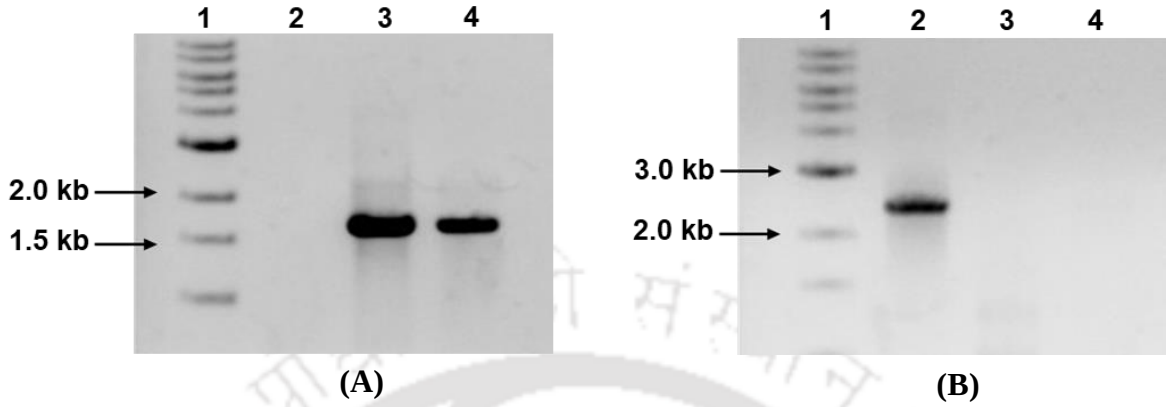

Figure 5.12 PCR confirmation of the Δ*pp-1* mutant strains. (**A)** PCR verification of the *N. crassa* mutant strains for the presence of Δ*pp-1* allele using gene specific primers (entries 1 and 2; Table 5.7). The PCR products were resolved using an 1% agarose gel, stained with EtBr (0.5 mg/ml) and visualized using a GelDoc (Bio-PrintST4, Vilber Lourmat, France); lane 1, 1 kb DNA ladder (NEB); lane 2, wild type (negative control; no PCR product, because target sequence for 5HPHR is absent); lane 3, Δ*pp-1*; *mat A* (3) mutant; lane 4, Δ*pp-1*; *mat a* (11) mutant. The PCR product of size 1,743 bp (lanes 3 and 4) in the Δ*pp-1*; *mat A* (3) and Δ*pp-1*; *mat a* (11) mutants confirmed the presence of the Δ*pp-1::hph* allele. **(B)** PCR verification for the absence of *pp-1* ORF using gene specific primers (entries 3 to 4; Table 5.7). The PCR products were resolved using an 1% agarose gel, stained with EtBr and visualized using a GelDoc (Bio-PrintST4, Vilber Lourmat, France); lane 1, 1 kb DNA ladder (NEB); lane 2, wild type (positive control with PCR product of size 2,411 bp); lane 3, Δ*pp-1*; *mat A* (3) mutant (no PCR product), lane 4, Δ*pp-1*; *mat a* (11) mutant (no PCR product).

Table 5.7 Primers used for conformation of the Δ*pp-1* mutant strains

S. No.	Primer	Sequence (5'→3')	Reference
1	NCU00340-HI Fw	CCAAGACACTCACTCTTTCG	This study
2	5HPHR	ATCCACTTAACGTTACTGAAATC	Deka et al. 2011
3	PP-1 Fw	ATGTATTCTTCGCAGCATGCC	This study
4	PP-1 Rv	AAACTCTAGCTCGTTTCGCAT	This study

5.2.11 The Δ*pp-1* mutant showed morphology similar to the *cmd*^{RIP} (#26) mutant

To determine if PP-1 is the transcription regulator of *cmd*, I compared phenotypes of the wild type, Δ*pp-1*, and *cmd*^{RIP} (#26) mutant strains. The Δ*pp-1* strain showed matty-like growth (Figure 5.13), stunted aerial hyphae (Figure 5.14; Table 5.8), and female sterility (Figure 5.15) phenotypes like the *cmd*^{RIP} (#26) mutant. These results suggested that PP-1 is necessary for normal asexual and sexual developments in *N. crassa*.

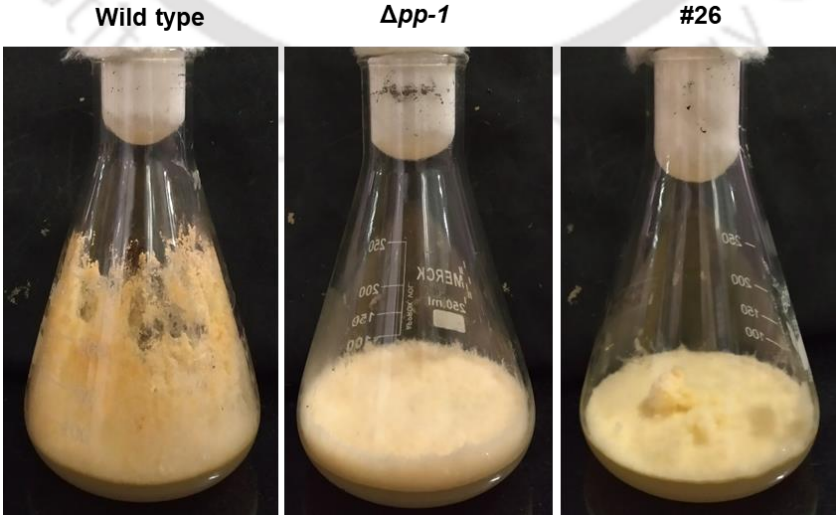

Figure 5.13 Flask morphology of the wild type, Δ*pp-1*, and *cmd*^{RIP} (#26) strains. Strains were grown in 250 ml flask containing VG agar medium and incubated at 30 °C for three days in dark followed by four days at room temperature under constant light and photographed.

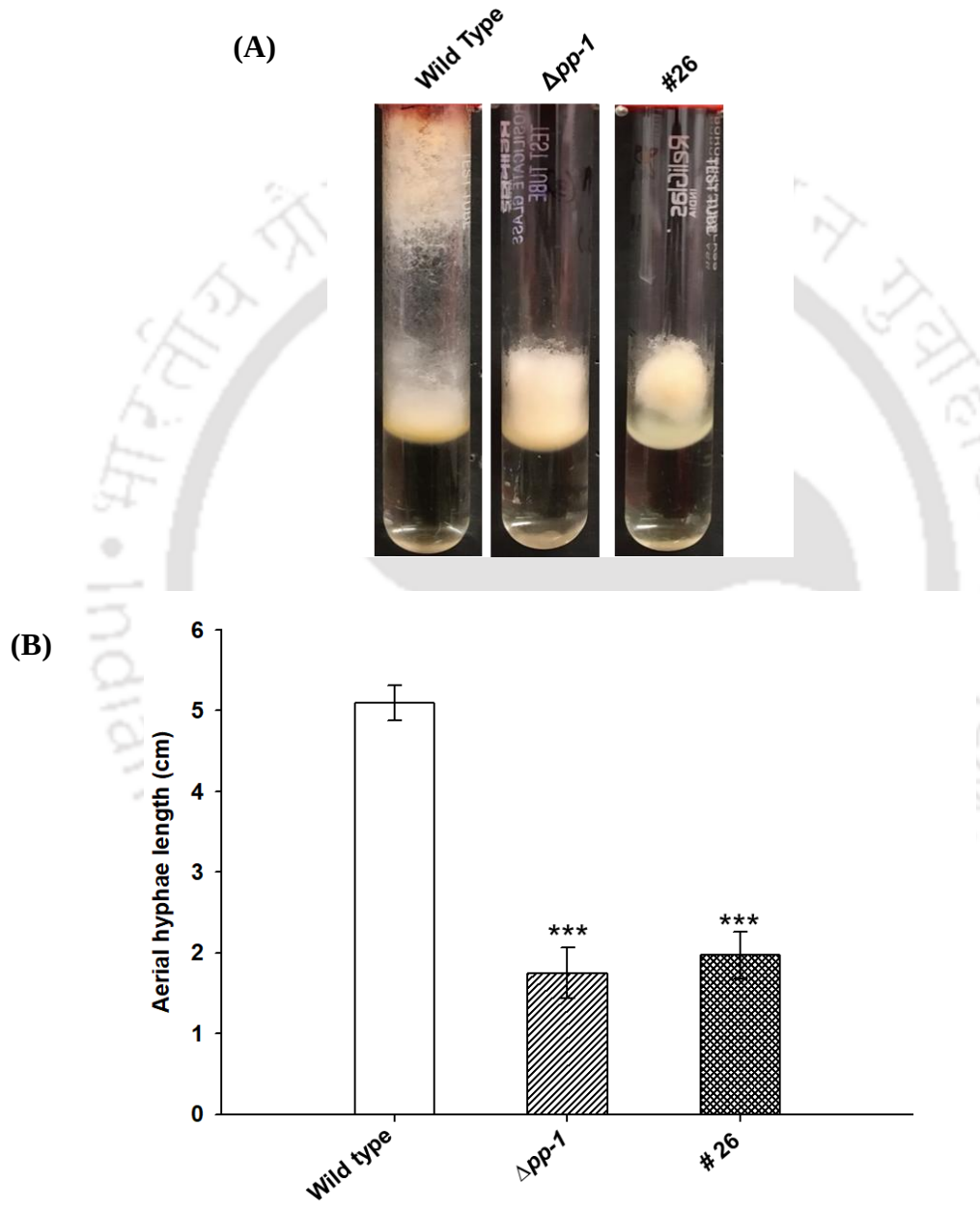

Figure 5.14 Aerial hyphae of the wild type, Δ*pp-1*, and *cmd*^{RIP} (#26) strains. Conidial suspensions of the *N. crassa* strains were inoculated in VG liquid medium, incubated at 30 °C for 3 days under dark condition. The aerial hyphae tip from the surface of the medium was

measured and photographed. **(A)** Aerial hyphae growth in tube, **(B)** Average aerial hyphae height (cm). Error bars indicate the standard deviations calculated from the data for three independent experiments (n = 3) with significance given by *P* values <0.05 (*), <0.01 (**), and <0.001 (***) compared to wild type as measured by one-way ANOVA test.

Table 5.8 Average aerial hyphae height of the wild type, Δ*pp-1*, and *cmd*^{RIP} (#26) strains

S. No.	Strain	[+]Height (cm)
1	wild type	5.1 ± 0.216
2	Δ*pp-1*	1.747 ± 0.316 (***)
3	# 26	1.97 ± 0.286 (***)

[+]Results are shown as mean ± standard deviation for three independent experiments (n = 3) with *P* values < 0.05 (*), < 0.01 (**), and < 0.001 (***) compared with the wild type strain as measured by one-way ANOVA test.

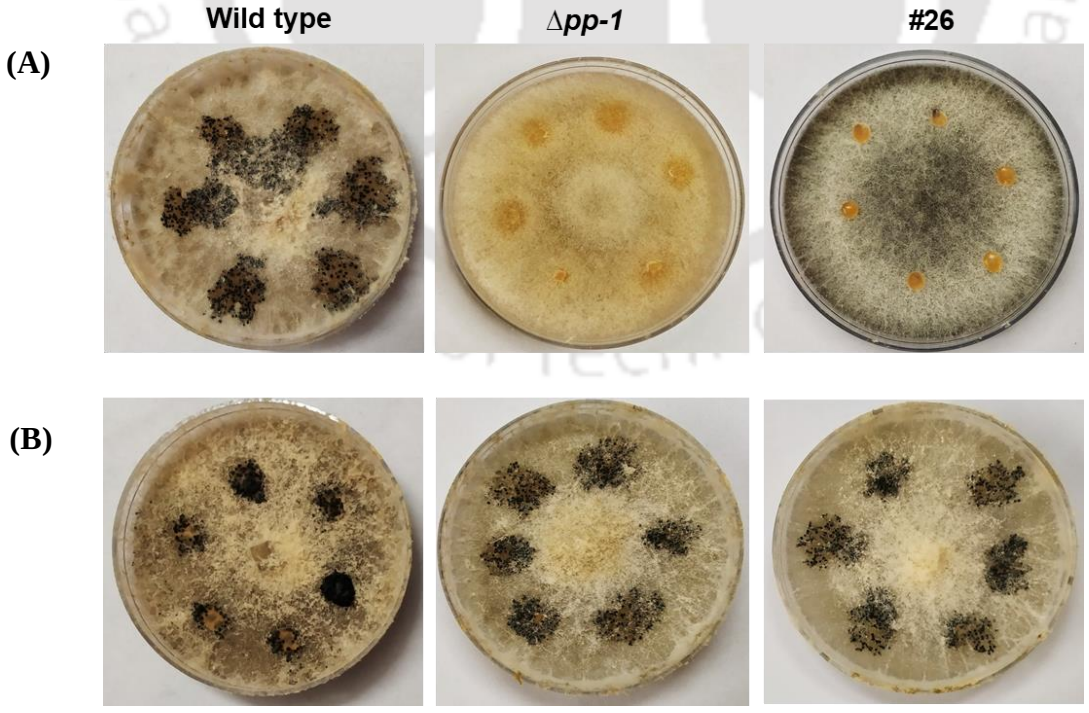

Figure 5.15 Fertility assay of the wild type, *cmd*^{RIP} (#26), and Δ*pp-1* mutant strains. Strains were cultured on SCM at 22 °C with constant light for seven days and subsequently fertilized with conidia from the wild type strain of opposite mating types (*mat A* or *mat a*). The *N. crassa* strains were used as a **(A)** female parent, and **(B)** male parent.

5.2.12 Expression analysis of *cmd* in the wild type and Δ*pp-1* mutant strains under nitrogen starved condition

To confirm the role of PP-1 as the transcriptional regulator of the *cmd* gene, I studied the expression of *cmd* in the wild type and Δ*pp-1* mutant strains. The expression of *cmd* in the Δ*pp-1* mutant was significantly decreased in comparison to the wild type (Figure 5.16), suggesting that PP-1 regulates *cmd* during sexual development. Therefore, Ca^{2+} and pheromone signaling pathways are inter-linked and required for normal sexual development in *N. crassa*.

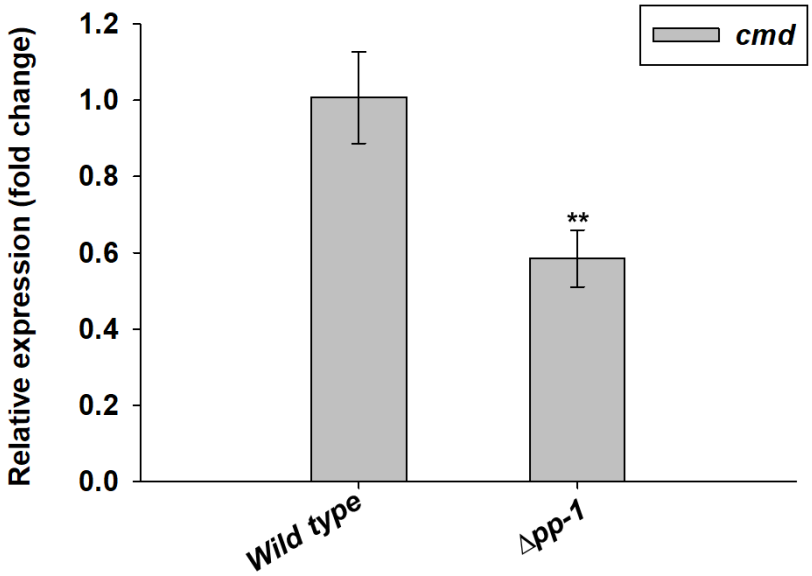

Figure 5.16 Expression analysis of the *cmd* gene in wild type and Δ*pp-1* mutant. RNA from the wild type was extracted from SCM liquid cultures grown at 22 °C for 18 h under constant darkness. The relative expression of each gene was studied by qRT-PCR and normalized to the expression of *β-tubulin* gene. Error bars indicate the standard deviations calculated from the data for three independent experiments (n = 3) and the significance values $P<0.05$ (*), $P<0.01$ (**), and $P<0.001$ (***) between the strains were measured by one-way ANOVA test.

5.3 Discussions

Proteins containing the 'EF-hand' Ca^{2+} binding motifs constitute a large and functionally diverse family, and these proteins play an essential role in eukaryotic cell signaling (Gifford et al. 2007). The EF-hand motif of calmodulin is composed of a helix-loop-helix structural unit where the Ca^{2+} binding loop consists of 12 residues, with the 1(+X), 3(+Y), 5(+Z), 7(−Y), 9(−X), 12(−Z) residues providing six to seven ligands to chelate the Ca^{2+} ion in a pentagonal bipyramid geometry (Babu et al. 1988; Gifford et al. 2007). The binding of Ca^{2+} to the EF-hand loops of CaM results in the conformational change from a closed to open configuration which exposes significant hydrophobic surfaces for interaction with target proteins (Bhattacharya et al. 2004; Zhang et al. 2012). Calmodulin has 2 EF-hand lobes, EF-1 and EF-2 belong to N-lobe, EF-3 and EF-4 belong to C-lobe, and a central linker that connects the two lobes between EF-2 and EF-3 (Villarroel et al. 2014). Each lobe is reported to influence the Ca^{2+} binding property of the other, where the four EF-hands work cooperatively in Ca^{2+} binding (Sorensen and Shea 1998; Liu et al. 2019a). To study the role of CaM in *N. crassa*, cmd^{RIP} (#26) mutant was generated in a previous study, which showed defects in colony morphology, growth, carotenoid accumulation, and UV survival (Laxmi and Tamuli 2017). The cmd^{RIP} (#26) mutant was also defective in stress tolerance (described in chapter 3) and during sexual development (described in chapter 4). In order to understand the effect of RIP mutation on the

structure and function of CaM, homology modelling of *N. crassa* wild type CaM and CaM^{RIP} protein was performed using the *A. niger* CaM protein as a template, and the modelled structures were validated using PROCHECK, ERRAT, and VERIFY 3D. The homology modelling revealed that due to the Asp to Tyr mutation at position one (+X, D57Y) of EF-2 loop, the endogenous CaM^{RIP} was unable to bind to Ca^{2+}. In a previous study using the CaM from human, the mutations of Asp to Ala at position one of the loop of each EF-hand resulted in CaM mutant proteins that were unable to bind Ca^{2+} in either the N-lobe EF hands (CaM_{12}), C-lobe EF hands (CaM_{34}) or all four EF Hands (CaM_{1234}) causing potential structural changes (Piazza et al. 2017). These structural changes caused human CaM to adopt a non-native apoCaM structure which disallowed the interactions with its target proteins (Piazza et al. 2017). In addition, small conductance calcium-activated potassium (SK) channels are regulated by CaM in response to cellular Ca^{2+}, where the N-lobe binds Ca^{2+} to activate the SK channel and maintains a stable SK-CaM interaction, while the C-lobe and the linker regulate the constitutive binding to SK channels independent of Ca^{2+} (Li et al. 2009; Halling et al. 2022). Therefore, taking together, the RIP mutation (D57Y) in *N. crassa* endogenous CaM probably disrupts the binding of CaM to its target protein and its ability to activate target ion channels.

The CTC staining of *cmd*^{RIP} (#26) mutant showed severely depleted Ca^{2+} stores across the hyphae (Figure 5.5), indicating that the Ca^{2+} homeostasis was disrupted in the mutant. In addition, the *cmd*^{RIP} (#26) mutant also showed abnormally increased septation with decrease in the hyphal width (Figure 5.6, Table 5.4). The RHO-1 specific GTPase–activating protein LRG-1 was shown to be important for apical tip extension and hyphal compartment size in *N. crassa* (Vogt and Seiler 2008). In humans, Rac1 and Cdc42, members of the Rho family of small GTPases, interact with CaM in a Ca^{2+}-dependent manner to regulate cellular activities such as spine morphology and development, spinogenesis, synaptic plasticity, proliferation, and migration (Elsaraj and Bhuller 2008; Tebar et al. 2020). Extrapolation from these reports,

it is possible to interpret that CaM might interact with the RHO-GTPases in a Ca^{2+}-dependent fashion to regulate the apical tip extension, hyphal septation, and width which is essential for the normal growth and development of *N. crassa*.

The promoter regions of *cmd*, *camk-1*, and *camk-2* genes contain sequences for yeast stress response elements (Kumar and Tamuli 2014). The expressions of the *cmd*, *camk-1*, and *camk-2* genes were increased in response to heat shock in the wild type (Figure 5.7). The expression level of *hsp70* and *hsp80* was reduced in the cmd^{RIP} (#26), Δ*camk-1*, and Δ*camk-2* mutants, while the expression of *hsp60* in the mutants was comparable to that in the wild type (Figure 5.8). Therefore, CaM, CaMK-1, and CaMK-2 are involved in regulating the production of heat shock proteins Hsp70 and Hsp80 under heat stress for the acquisition of thermotolerance in *N. crassa*. In mammals, the CaMK II-δB (isoform of CaMKII) is involved in phosphorylating and activating the HSF1, which subsequently induces the expression of HSP70 family proteins that protect the heart from multiple death-inducing stimuli (Peng et al. 2010). In *Beauveria bassiana*, BbHsp70 was identified as one of the direct targets of CaM using co-immunoprecipitation (CoIP) and MALDI-TOF/TOF method (Kim et al. 2018). In *Sporothrix schenkii*, the interaction of SSCMK1 with HSP90 was shown using a yeast two-hybrid assay (Rodriguez-Caban et al. 2011). In maize, Ca^{2+} and CaM are involved in the HSP gene expression by regulating the activity of heat shock transcription factor (HSF) under heat shock condition (Li et al. 2004). Therefore, it is possible that CaM, CaMK-1, and CaMK-2 might regulate the expression of heat shock proteins either by activating the HSF-1 transcription factor or through direct interaction with heat shock proteins in *N. crassa* (Figure 5.17).

Under the nitrogen starved condition, which induces sexual development, increased expression of *cmd*, *camk-1*, and *camk-2* genes were observed in the wild type (Figure 5.9), suggesting that these genes are upregulated during the sexual development phase. In *N. crassa*,

sexual development is regulated by the pheromone response pathway, which includes pheromone receptors PRE-1 and PRE-2, the homologs of *S. cerevisiae* Ste3p and STe2p, and the pheromone precursors MFA-1 and CCG-4, the homologs of *S. cerevisiae* a- and α-mating factors, respectively (Pöggeler and Kück 2001; Borkovich et al. 2004; Kim et al. 2002; Kim and Borkovich, 2006). In addition, FMF-1, the homolog of *S. pombe* transcription factor Ste11p, is also required for pheromone signaling in *N. crassa* (Iyer et al. 2009). In *S. cerevisiae*, the calmodulin mutant *cmd1-6* (consisting of three mutations that block Ca^{2+} binding to calmodulin) and the knockout mutants of *CMK1* and *CMK2* genes are unable to survive after pheromone-induced cell cycle arrest (Moser et al. 1996). In addition, inhibition of CaM using W-7 and trifluoperazine suppressed the production of the sex pheromone bombykol, while CaMKII was also shown to be important for phosphorylating the lipid storage droplet-1(BmLsd1), which is essential for TAG lipolysis to release stored pheromone precursors for final modifications in *Bombyx mori* (Matsumoto et al. 1995a,1995b; Ohnishi et al. 2011; Hull and Fonagy 2020). In *N. crassa*, the presence of pheromone response elements in the upstream of the promoter regions of *cmd*, *camk-1*, and *camk*-2 gene was reported previously (Kumar and Tamuli 2014; Laxmi 2016). In this study, I observed significant reductions in the expression of genes *pre-1*, *pre-2*, *ccg-4*, *mfa*-1, and *fmf-1*, involved in the pheromone response pathway, in the cmd^{RIP} (#26), *Δcamk-1*, and *Δcamk-2* mutants in comparison to the wild type (Figure 5.10). Therefore, these results suggested that the *cmd*, *camk-1*, and *camk*-2 genetically interact with the pheromone signaling pathway during sexual development in *N. crassa*.

In *N. crassa*, the molecular components, *frequency* (*frq*) and the white-collar (*wc-1* and *wc-2*) genes, involved in the circadian clock are well characterized (Brunner et al. 2008). The Δ*camk-1*, Δ*camk-2*, Δ*camk-3*, and Δ*camk*-4 mutants showed increased period length with increase in temperature above 20 ℃ (described in chapter 4), therefore, I performed expression analysis of *frq* and *wc-1* genes in the Δ*camk-1*, Δ*camk-2*, Δ*camk-3*, and Δ*camk*-4 mutants to

test if *camks* interact with the clock regulators. There was no significant change in the transcript levels of *frq* and *wc-1* in the mutants both at 20 ℃ and 25 ℃ (Figure 5.11). Earlier, CaMK-1 was reported to phosphorylate FRQ at multiple sites *in vitro* (Yang et al. 2001). In a recent study, genetic analysis showed that mutations in certain *frq* phospho-sites and Δ*camk*-2 were epistatic to Δ*nca-2* in regulating the pace of the clock oscillator, suggesting that *nca-2* and *camk-2* function in the same pathway to regulate the circadian period (Wang et al. 2021). The FRQ protein is progressively phosphorylated upto 113 sites before degradation, and casein kinase 1a (CK1a) is reported to phosphorylates FRQ upto 46 nonconsensus sites (Querfurth et al. 2011). Moreover, the FRQ-CK1 interaction and CK1-mediated FRQ phosphorylations were proposed as the main mechanisms for circadian period determination and temperature compensations in *N. crassa* (Hu et al. 2021). Thus, despite the increased period length caused by the mutations in the *camks* (chapter 4), the transcript level of *frq* and *wc-1* in the *camk* mutants were not altered, suggesting that the Ca^{2+}/CaMKs may be involved in phosphorylating some distinct sites (which are yet to be found) as they increase the period length but are not involved in regulating the expression of the clock regulators *frq* and *wc-1* in *N. crassa* circadian clock.

In order to determine how *cmd* is regulated under different cellular conditions, I analysed the promoter region of *cmd* gene using MatInspector (Quandt et al. 1995). The promoter analysis revealed binding sites for several important transcription factors, including the yeast transcription factor STE12 (Table 5.6), which is involved in pheromone response pathway (Bardwell 2005). The *N. crassa* homolog of *ste12* was identified as *protoperithecium-1* (*pp-1*) gene (Li et al. 2005). The Δ*pp-1* mutant showed defects in flask morphology (Figure 5.13), reduced aerial hyphae growth (Figure 5.14), and sterile phenotype as a female parent (Figure 5.15) like the cmd^{RIP} (#26) mutant. Previous studies showed that PP-1 is important for normal, growth, protoperithecia development, cell-cell communication, and cell fusion (Li et

al. 2005; Leeder et al. 2013; Fischer et al. 2018). In addition, I also observed a decreased expression of *cmd* in the Δ*pp-1* mutant under nitrogen-starved condition (Figure 5.16), suggesting that PP-1 regulates the *cmd* gene during sexual development in *N. crassa*.

In *N. crassa*, PP-1 is the downstream target of MAK-2 MAP kinase signaling pathway (Li et al. 2005; Herzog et al. 2015). The Δ*pp-1* mutant phenocopies the Δ*mak-2* mutant, with reduced growth rate, short aerial hyphae, and failure in protoperithecia development (Li et al. 2005). In addition, the misexpression of *pp-1* in the Δ*mak-2* mutant fails to induce transcription of downstream target proteins such as *adv-1* (NCU07392; a $Zn(II)_2Cys_6$ transcription factor), which suggested that MAK-2 directly activates or de-represses PP-1(Fischer et al. 2018, 2019). Furthermore, the MAK-2 pathway of *N. crassa* shows homology to the pheromone response pathway in *S. cerevisiae* (Fischer et al. 2018). In this study, I showed that CaM is involved in regulating the pheromone response pathway (Figure 5.10), and PP-1 regulates the transcription of the *cmd* gene during sexual development (Figure 5.16). Taken together, these results suggested a crosstalk between the Ca^{2+} signaling and the pheromone signaling pathway (Figure 5.17) to regulate the sexual development in *N. crassa*.

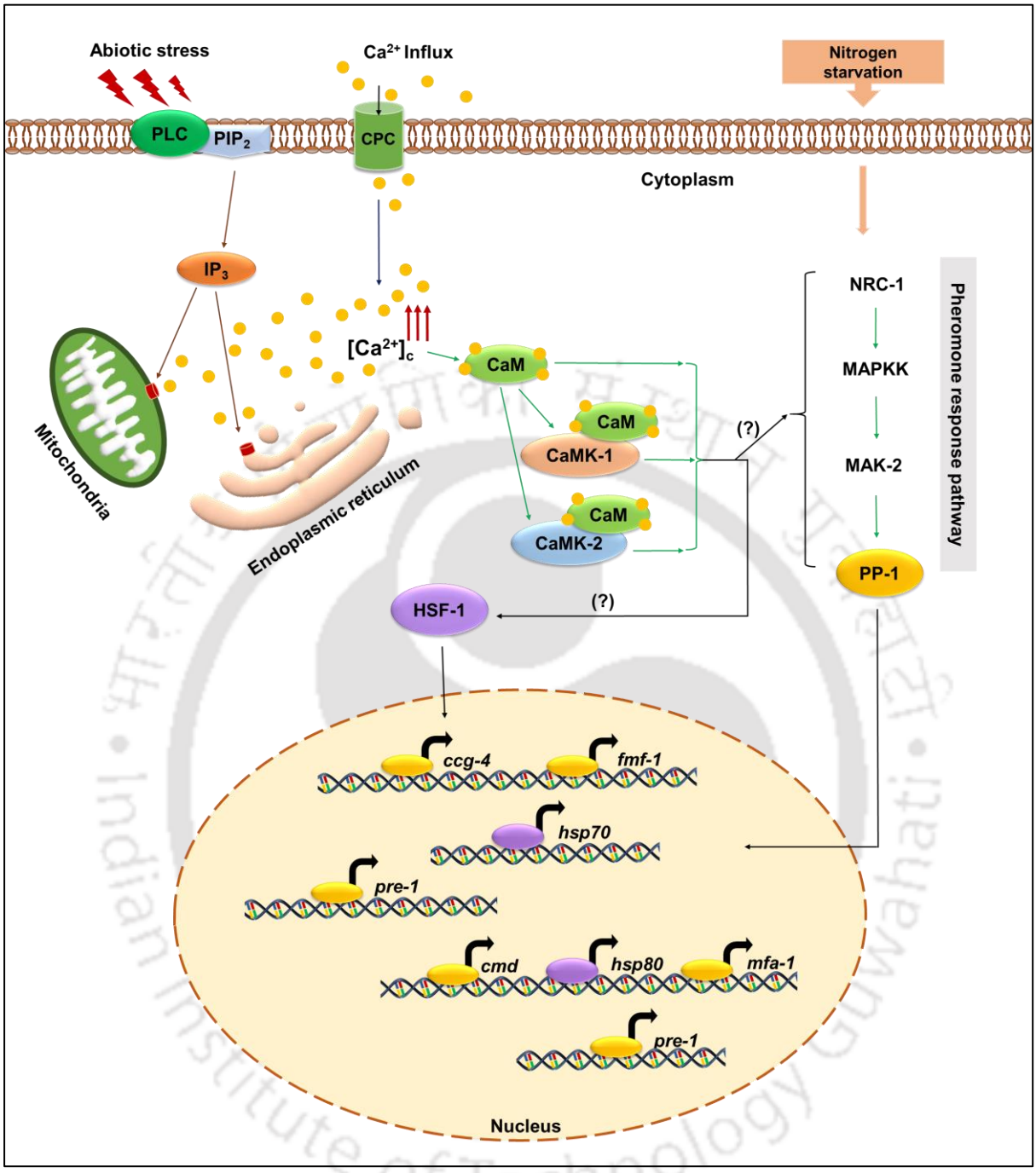

Figure 5.17 A proposed model depicting the mechanism of CaM and Ca^{2+}/CaMKs in regulating heat shock response and pheromone response pathway in *N. crassa*. Stress condition results in Ca^{2+} influx into the cell through Ca^{2+} permeable channels. Ca^{2+} is also released from intracellular stores such as mitochondria and endoplasmic reticulum. The transient increase in the cytosolic calcium level $[Ca^{2+}]_c$ activates calmodulin (CaM), the primary Ca^{2+} sensor which further binds and activates its downstream target proteins such as

CaMK-1 and CaMK-2. CaM, CaMK-1 and CaMK-2 regulate the expression of *hsp70* (LG II) and *hsp80* (LG V) in response to heat stress probably by activating the heat shock transcription factor HSF-1 like in maize and in mammalian heart (Li et al. 2004; Peng et al. 2010). In *N. crassa*, the MAK-2 kinase pathway is homologous to the pheromone response pathway in *S. cerevisiae* consisting of the NRC-1 (MAPKKK), MEK-2 (MAPKK), MAK-2 (MAPK), and the downstream target PP-1, a C2H2 zinc finger transcription factor (Li et al. 2005; Fischer et al. 2018). Under nitrogen-starved condition, CaM, CaMK-1, and CaMK-2 activates the pheromone response pathway and increases the expression of pheromone receptors *pre-1* (LG III) and *pre-2* (LG VII) as well as the pheromone precursor genes *ccg-4* (LG I), *fmf-1* (LG I), and *mfa-1* (LG V). PP-1 also increases the expression of *cmd* gene (LG V) under nitrogen starvation suggesting a crosstalk between the calcium signaling and the MAK-2 MAP kinase signaling pathway during sexual development. How HSF-1 and the pheromone response pathway is activated by CaM and Ca^{2+}/CaMKs is not known yet in *N. crassa* (indicated with a question mark in the parentheses).

Conclusions and Future perspectives

6.1 Major conclusions of this study

In this work, I have studied the cellular roles and mechanism of CaM and Ca^{2+}/CaMKs in stress responses, sexual development, and in the regulation of the circadian clock in *N. crassa*. The *cmd*^{RIP} (#26), Δ*camk-1*, and Δ*camk-2* mutants were sensitive to changes in temperature and pH, hydrogen peroxide (H_2O_2) induced oxidative stress, and dithiothreitol (DTT) induced ER stress conditions. The complementation studies using the parental strain Δ*pan-2*::*bar*::P_{tcu-1}::*cmd*::*V5*::*gfp*; *mat a* (#850) of *cmd*^{RIP} (#26), the homokaryotic transformants Δ*camk-1*::*hph*; Δ*pan-2*::P_{nit-6}::*camk-1*::*V5*::*gfp*; *mat A* (#19) and Δ*camk-2*::*hph*; Δ*pan-2*::P_{nit-6}::*camk-2*::*V5*::*gfp*; *mat A* (#8) carrying the *camk-1* and *camk-2* transgenes showed complete rescued phenotypes of the mutants strains. Therefore, CaM, CaMK-1, and CaMK-2 are required for adaptation to various stress conditions mediated by temperature, pH, oxidative, and ER targeting compounds.

To understand the role of CaM during sexual development, I performed sexual fertility assay, which showed that the *cmd*^{RIP} (#26) mutant was fertile as a male parent but sterile as a female parent. I also found that CaM is required for the formation of the female sexual structure called protoperithecium. In addition, the *cmd*^{RIP} (#26) mutant formed incompetent mycelium that showed defectives in cell fusion and aging process, necessary for normal sexual development. Therefore, CaM plays an important role at different stages during sexual development.

From the inverted race tube assay, I found that Δ*camk-1*; *ras-1*^{bd} (11), *ras-1*^{bd}; Δ*camk-2* (15), Δ*camk-3*; *ras-1*^{bd} (22), and Δ*camk-4*; *ras-1*^{bd} (31) mutants exhibited increased period lengths at 20, 25, and 30 °C in comparison to the *ras-1*^{bd} control strain. However, the mutants did not show any role in temperature compensation because the Q_{10} values for the mutants were in the range of ~1 like the *ras-1*^{bd} strain.

Homology model of the *N. crassa* wild type CaM, endogenous CaM^{RIP}, and ectopic CaM^{RIP} of the mutant (#26) strain using *A. niger* CaM as a template was generated to analyze the effect of RIP mutations on the structure and function of the CaM^{RIP} protein. I found that due to the RIP mutation of Asp to Tyr mutation at position one (+X, D57Y), the EF-2 of endogenous CaM^{RIP} was unable to bind to Ca^{2+}. Moreover, the cmd^{RIP} (#26) mutant showed severely depleted Ca^{2+} stores across the hyphae and abnormally increased septation number with decreased hyphal width. Thus, the RIP-induced D57Y mutation in endogenous CaM resulted in the disruption of Ca^{2+} homeostasis and defects in hyphal septation and width, which affected the normal growth and development in *N. crassa*.

In addition, I found that the expression level of *cmd*, *camk-1*, and *camk-2* genes were increased under heat stress and nitrogen-starved conditions in the wild type. Moreover, the expression level of heat shock protein-encoding genes *hsp70* and *hsp80*, and pheromone response pathway genes *pre-1*, *pre-2*, *ccg-4*, *mfa-1*, and *fmf-1* were reduced in the cmd^{RIP}, Δ*camk-1*, and Δ*camk-2* mutant strains compared to the wild type, revealing that CaM and CaMKs are involved in regulating the heat stress tolerance and pheromone response pathways. Finally, the *cmd* gene was found to be regulated by PP-1, a transcription factor involved in the pheromone response pathway, hence establishing a crosstalk between the MAK-2 MAP kinase and Ca^{2+} signaling pathways in *N. crassa*.

6.2 Future perspectives of this research work

Future directions of this research work will be:

(i) to investigate the interaction of the transcriptional factor PP-1 in the promoter region of the *cmd* gene using chromatin immunoprecipitation (ChIP), followed by

electrophoretic mobility shift assay (EMSA) to determine the specific binding sequence of PP-1 in the promoter of *cmd* gene,

(ii) to determine how CaM and CaMKs interact with the MAPK signaling pathway,

(iii) to investigate the mechanism of CaM and CaMKs in activating the heat shock transcription factor (HSF-1), and

(iv) to understand the role and mechanism of CaM and CaMKs in the regulation of reactive oxygen species (ROS) homeostasis.

References

Ahmad, R. Z., Khalid, R., Aqeel, M., Ameen, F., & Li, C. J. (2020). Fungal endophytes trigger *Achnatherum inebrians* germination ability against environmental stresses. *South African Journal of Botany*, *134*, 230-236

Alexander, W. G., Raju, N. B., Xiao, H., Hammond, T. M., Perdue, T. D., Metzenberg, R. L., ... & Shiu, P. K. (2008). DCL-1 colocalizes with other components of the MSUD machinery and is required for silencing. *Fungal Genetics and Biology*, *45*(5), 719-727.

Altschul, S. F., Gish, W., Miller, W., Myers, E. W., & Lipman, D. J. (1990). Basic local alignment search tool. *Journal of molecular biology*, *215*(3), 403-410.

Altschul, S. F., Madden, T. L., Schäffer, A. A., Zhang, J., Zhang, Z., Miller, W., & Lipman, D. J. (1997). Gapped BLAST and PSI-BLAST: a new generation of protein database search programs. *Nucleic acids research*, *25*(17), 3389-3402.

Altschul, S. F., Wootton, J. C., Gertz, E. M., Agarwala, R., Morgulis, A., Schäffer, A. A., & Yu, Y. K. (2005). Protein database searches using compositionally adjusted substitution matrices. *The FEBS journal*, *272*(20), 5101-5109.

An, B., Li, B., Qin, G., & Tian, S. (2015). Function of small GTPase Rho3 in regulating growth, conidiation and virulence of *Botrytis cinerea*. *Fungal Genetics and Biology*, *75*, 46-55.

Anraku, Y., Ohya, Y., & Iida, H. (1991). Cell cycle control by calcium and calmodulin in *Saccharomyces cerevisiae*. *Biochimica et Biophysica Acta (BBA)-Molecular Cell Research*, *1093*(2-3), 169-177.

Aramayo, R., & Selker, E. U. (2013). *Neurospora crassa*, a model system for epigenetics research. *Cold Spring Harbor Perspectives in Biology*, *5*(10), a017921.

Ardiel, E. L., McDiarmid, T. A., Timbers, T. A., Lee, K. C., Safaei, J., Pelech, S. L., & Rankin, C. H. (2018). Insights into the roles of CMK-1 and OGT-1 in interstimulus interval-

dependent habituation in *Caenorhabditis elegans*. *Proceedings of the Royal Society B*, *285*(1891), 20182084.

Aronson, B. D., Johnson, K. A., Loros, J. J., & Dunlap, J. C. (1994). Negative feedback defining a circadian clock: autoregulation of the clock gene frequency. *Science*, *263*(5153), 1578-1584.

Babu, Y. S., Bugg, C. E., & Cook, W. J. (1988). Structure of calmodulin refined at 2.2 Å resolution. *Journal of molecular biology*, *204*(1), 191-204.

Backus, M. P. (1939). The mechanics of conidial fertilization in *Neurospora sitophila*. *Bulletin of the Torrey Botanical Club*, 63-76.

Bakar, N. A., Karsani, S. A., & Alias, S. A. (2020). Fungal survival under temperature stress: a proteomic perspective. *PeerJ*, *8*, e10423.

Baker, C. L., Kettenbach, A. N., Loros, J. J., Gerber, S. A., & Dunlap, J. C. (2009). Quantitative proteomics reveals a dynamic interactome and phase-specific phosphorylation in the *Neurospora* circadian clock. *Molecular cell*, *34*(3), 354-363.

Baker, C. L., Loros, J. J., & Dunlap, J. C. (2012). The circadian clock of *Neurospora crassa*. *FEMS microbiology reviews*, *36*(1), 95-110.

Bartoli, M., Monneron, A., & Ladant, D. (1998). Interaction of calmodulin with striatin, a WD-repeat protein present in neuronal dendritic spines. *Journal of Biological Chemistry*, *273*(35), 22248-22253.

Barbato, G., Ikura, M., Kay, L. E., Pastor, R. W., & Bax, A. (1992). Backbone dynamics of calmodulin studied by nitrogen-15 relaxation using inverse detected two-dimensional NMR spectroscopy: the central helix is flexible. *Biochemistry*, *31*(23), 5269-5278.

Bardwell, L. (2005). A walk-through of the yeast mating pheromone response pathway. *Peptides*, *26*(2), 339-350.

Barman, A., & Tamuli, R. (2017). The pleiotropic vegetative and sexual development phenotypes of *Neurospora crassa* arise from double mutants of the calcium signaling genes plc-1, splA2, and cpe-1. *Current Genetics*, *63*(5), 861-875.

Barykina, N. V., Sotskov, V. P., Gruzdeva, A. M., Wu, Y. K., Portugues, R., Subach, O. M., ... & Subach, F. V. (2020). FGCaMP7, an improved version of fungi-based ratiometric calcium indicator for in vivo visualization of neuronal activity. *International journal of molecular sciences*, *21*(8), 3012.

Basit, A., Yadav, A. K., & Bandyopadhyay, P. (2022). Calcium Ion Binding to the Mutants of Calmodulin: A Structure-Based Computational Predictive Model of Binding Affinity Using a Charge Scaling Approach in Molecular Dynamics Simulation. *Journal of chemical information and modeling*, *62*(11), 2821–2834.

Beadle, G. W., & Tatum, E. L. (1941). Genetic control of biochemical reactions in *Neurospora*. *Proceedings of the National Academy of Sciences*, *27*(11), 499-506.

Beckman, K. B., & Ames, B. N. (1998). The free radical theory of aging matures. *Physiological reviews*.

Belden, W. J., Larrondo, L. F., Froehlich, A. C., Shi, M., Chen, C. H., Loros, J. J., & Dunlap, J. C. (2007). The band mutation in *Neurospora crassa* is a dominant allele of *ras-1* implicating RAS signaling in circadian output. *Genes & development*, *21*(12), 1494-1505.

Belozerskaya, T. A., & Gessler, N. N. (2006). Oxidative stress and differentiation in *Neurospora crassa*. *Microbiology*, *75*(4), 427-431.

Berchtold, M. W., & Villalobo, A. (2014). The many faces of calmodulin in cell proliferation, programmed cell death, autophagy, and cancer. *Biochimica et Biophysica Acta (BBA)-Molecular Cell Research*, *1843*(2), 398-435.

Berridge, M. J., Lipp, P., & Bootman, M. D. (2000). The versatility and universality of calcium signalling. *Nature reviews Molecular cell biology*, *1*(1), 11-21.

Berridge, M. J., Bootman, M. D., & Roderick, H. L. (2003). Calcium signalling: dynamics, homeostasis and remodelling. *Nature reviews Molecular cell biology*, *4*(7), 517-529.

Bhat, A., Tamuli, R., & Kasbekar, D. P. (2004). Genetic transformation of *Neurospora tetrasperma*, demonstration of repeat-induced point mutation (RIP) in self-crosses and a screen for recessive RIP-defective mutants. *Genetics*, *167*(3), 1155-1164.

Bhattacharya, S., Bunick, C. G., & Chazin, W. J. (2004). Target selectivity in EF-hand calcium binding proteins. *Biochimica et Biophysica Acta (BBA)-Molecular Cell Research*, *1742*(1-3), 69-79.

Bistis, G. N. (1981). Chemotropic interactions between trichogynes and conidia of opposite mating-type in *Neurospora crassa*. *Mycologia*, *73*(5), 959-975.

Bistis, G. N., Perkins, D. D., & Read, N. D. (2003). Different cell types in *Neurospora crassa*. *Fungal Genetics Newsletter*, 17-19.

Blinks, J. R., Wier, W. G., Hess, P., & Prendergast, F. G. (1982). Measurement of Ca^{2+} concentrations in living cells. *Progress in biophysics and molecular biology*, *40*, 1-114.

Bloemendal, S., Bernhards, Y., Bartho, K., Dettmann, A., Voigt, O., Teichert, I., ... & Kück, U. (2012). A homologue of the human STRIPAK complex controls sexual development in fungi. *Molecular microbiology*, *84*(2), 310-323.

Bobrowicz, P., Pawlak, R., Correa, A., Bell-Pedersen, D., & Ebbole, D. J. (2002). The *Neurospora crassa* pheromone precursor genes are regulated by the mating type locus and the circadian clock. *Molecular microbiology*, *45*(3), 795-804.

Bootman, M. D., Collins, T. J., Peppiatt, C. M., Prothero, L. S., MacKenzie, L., De Smet, P., ... & Lipp, P. (2001, February). Calcium signalling—an overview. In *Seminars in cell & developmental biology* (Vol. 12, No. 1, pp. 3-10). Academic Press.

Borkovich, K. A., Alex, L. A., Yarden, O., Freitag, M., Turner, G. E., Read, N. D., ... & Pratt, R. (2004). Lessons from the genome sequence of *Neurospora crassa*: tracing the path from genomic blueprint to multicellular organism. *Microbiology and molecular biology reviews*, *68*(1), 1-108.

Bowie, J. U., Lüthy, R., & Eisenberg, D. (1991). A method to identify protein sequences that fold into a known three-dimensional structure. *Science*, *253*(5016), 164-170.

Bowman, E. J., Kendle, R., & Bowman, B. J. (2000). Disruption of *vma-1*, the gene encoding the catalytic subunit of the vacuolar H^+-ATPase, causes severe morphological changes in *Neurospora crassa*. *Journal of biological chemistry*, *275*(1), 167-176.

Bowman, B. J., Abreu, S., Margolles-Clark, E., Draskovic, M., & Bowman, E. J. (2011). Role of four calcium transport proteins, encoded by *nca-1*, *nca-2*, *nca-3*, and *cax*, in maintaining intracellular calcium levels in *Neurospora crassa*. *Eukaryotic Cell*, *10*(5), 654-661.

Boyce, K. J., Bugeja, H. E., Weerasinghe, H., Payne, M. J., Schreider, L., Park, C., ... & Andrianopoulos, A. (2012). Strategies for the molecular genetic manipulation and visualization of the human fungal pathogen *Penicillium marneffei*. *Fungal Genet Rep*, *59*(1), 1-12.

Braun, A. P., & Schulman, H. (1995). The multifunctional calcium/calmodulin-dependent protein kinase: from form to function. *Annual review of physiology*, *57*(1), 417-445.

Bravo, R., Parra, V., Gatica, D., Rodriguez, A. E., Torrealba, N., Paredes, F., ... & Lavandero, S. (2013). Endoplasmic reticulum and the unfolded protein response: dynamics and metabolic integration. *International review of cell and molecular biology*, *301*, 215-290

Bredow, M., & Monaghan, J. (2022). Cross-kingdom regulation of calcium-and/or calmodulin-dependent protein kinases by phospho-switches that relieve autoinhibition. *Current Opinion in Plant Biology*, *68*, 102251.

Breitenbach, M., Weber, M., Rinnerthaler, M., Karl, T., & Breitenbach-Koller, L. (2015). Oxidative stress in fungi: its function in signal transduction, interaction with plant hosts, and lignocellulose degradation. *Biomolecules*, *5*(2), 318-342.

Brown, E. M., Gamba, G., Riccardi, D., Lombardi, M., Butters, R., Kifor, O., ... & Hebert, S. C. (1993). Cloning and characterization of an extracellular Ca^{2+}-sensing receptor from bovine parathyroid. *Nature*, *366*(6455), 575-580.

Brown, S. M., Campbell, L. T., & Lodge, J. K. (2007). *Cryptococcus neoformans*, a fungus under stress. *Current opinion in microbiology*, *10*(4), 320-325.

Brunner, M., & Diernfellner, A. (2006). How temperature affects the circadian clock of *Neurospora crassa*. *Chronobiology international*, *23*(1-2), 81-90.

Cambareri, E. B., Jensen, B. C., Schabtach, E., & Selker, E. U. (1989). Repeat-induced GC to AT mutations in *Neurospora*. *Science*, *244*(4912), 1571-1575.

Cambareri, E. B., Singer, M. J., & Selker, E. (1991). Recurrence of repeat-induced point mutation (RIP) in *Neurospora crassa*. *Genetics*, *127*(4), 699-710.

Cano-Domínguez, N., Álvarez-Delfín, K., Hansberg, W., & Aguirre, J. (2008). NADPH oxidases NOX-1 and NOX-2 require the regulatory subunit NOR-1 to control cell differentiation and growth in *Neurospora crassa*. *Eukaryotic cell*, *7*(8), 1352-1361.

Capelli, N., Van Tuinen, D., Perez, R. O., Arrighi, J. F., & Turian, G. (1993). Molecular cloning of a cDNA encoding calmodulin from *Neurospora crassa*. *FEBS letters*, *321*(1), 63-68.

Capelli, N., Barja, F., Van Tuinen, D., Monnat, J., Turian, G., & Ortega Perez, R. (1997). Purification of a 47-kDa calmodulin-binding polypeptide as an actin-binding protein from *Neurospora crassa*. *FEMS microbiology letters*, *147*(2), 215-220.

Carafoli, E. (2005). Calcium-a universal carrier of biological signals. (vol 272, pg 1073, 2005). *The FEBS Journal*, *272*, 1815-1815.

Carlier, F., Nguyen, T. S., Mazur, A. K., & Gladyshev, E. (2021). Regulation of DIM-2-dependent repeat-induced point mutation (RIP) by the recombination-independent homologous DNA pairing in *Neurospora crassa*. *bioRxiv*.

Case, M. E., Griffith, J., Dong, W., Tigner, I. L., Gaines, K., Jiang, J. C., ... & Georgia Centenarian Study. (2014). The aging biological clock in *Neurospora crassa*. *Ecology and evolution*, *4*(17), 3494-3507.

Castanera, R., Lopez-Varas, L., Borgognone, A., LaButti, K., Lapidus, A., Schmutz, J., ... & Ramirez, L. (2016). Transposable elements versus the fungal genome: impact on whole-genome architecture and transcriptional profiles. *PLoS genetics*, *12*(6), e1006108.

Caswell, A. H. (1979). Methods of measuring intracellular calcium. *International review of cytology*, *56*, 145-181.

Catalanotto, C., Azzalin, G., Macino, G., & Cogoni, C. (2000). Gene silencing in worms and fungi. *Nature*, *404*(6775), 245-245.

Catalanotto, C., Azzalin, G., Macino, G., & Cogoni, C. (2002). Involvement of small RNAs and role of the *qde* genes in the gene silencing pathway in *Neurospora*. *Genes & development*, *16*(7), 790-795.

Catalanotto, C., Pallotta, M., ReFalo, P., Sachs, M. S., Vayssie, L., Macino, G., & Cogoni, C. (2004). Redundancy of the two dicer genes in transgene-induced posttranscriptional gene silencing in *Neurospora crassa*. *Molecular and cellular biology*, *24*(6), 2536-2545.

Catalanotto, C., Nolan, T., & Cogoni, C. (2006). Homology effects in *Neurospora crassa*. *FEMS microbiology letters*, *254*(2), 182-189.

Chattopadhyaya, R., Meador, W. E., Means, A. R., & Quiocho, F. A. (1992). Calmodulin structure refined at 1.7 Å resolution. *Journal of molecular biology*, *228*(4), 1177-1192.

Chazin, W. J., & Johnson, C. N. (2020). Calmodulin mutations associated with heart arrhythmia: a status report. *International Journal of Molecular Sciences*, *21*(4), 1418.

Chen, S., Song, Y., Cao, J., Wang, G., Wei, H., Xu, X., & Lu, L. (2010). Localization and function of calmodulin in live-cells of *Aspergillus nidulans*. *Fungal Genetics and Biology*, *47*(3), 268-278.

Chen, B., Feder, M. E., & Kang, L. (2018). Evolution of heat-shock protein expression underlying adaptive responses to environmental stress. *Molecular ecology*, *27*(15), 3040-3054.

Cheung, W. Y. (1970). Cyclic 3′, 5′-nucleotide phosphodiesterase: demonstration of an activator. *Biochemical and biophysical research communications*, *38*(3), 533-538.

Chin, D., & Means, A. R. (2000). Calmodulin: a prototypical calcium sensor. *Trends in cell biology*, *10*(8), 322-328.

Chinnici, J. L., Fu, C., Caccamise, L. M., Arnold, J. W., & Free, S. J. (2014). *Neurospora crassa* female development requires the PACC and other signal transduction pathways, transcription factors, chromatin remodeling, cell-to-cell fusion, and autophagy. *PLoS One*, *9*(10), e110603.

Cipak, A., Jaganjac, M., Tehlivets, O., Kohlwein, S. D., & Zarkovic, N. (2008). Adaptation to oxidative stress induced by polyunsaturated fatty acids in yeast. *Biochimica et Biophysica Acta (BBA)-Molecular and Cell Biology of Lipids*, *1781*(6-7), 283-287.

Clapham, D. E. (2007). Calcium signaling. *Cell*, *131*(6), 1047-1058.

Cogoni, C., & Macino, G. (1997). Isolation of quelling-defective (*qde*) mutants impaired in posttranscriptional transgene-induced gene silencing in *Neurospora crassa*. *Proceedings of the National Academy of Sciences*, *94*(19), 10233-10238.

Cogoni, C., & Macino, G. (1999). Gene silencing in *Neurospora crassa* requires a protein homologous to RNA-dependent RNA polymerase. *Nature*, *399*(6732), 166-169.

Cogoni, C., & Macino, G. (1999). Posttranscriptional gene silencing in *Neurospora* by a RecQ DNA helicase. *Science*, *286*(5448), 2342-2344.

Coleman, C. E., Landin, C., Neuer, A., Sayegh, F. M., & Marshall, P. A. (2022). Calmodulin kinase 2 genetically interacts with Rch1p to negatively regulate calcium import into *Saccharomyces cerevisiae* after extracellular calcium pulse. *Archives of Microbiology*, *204*(8), 1-15

Collopy, P. D., Colot, H. V., Park, G., Ringelberg, C., Crew, C. M., Borkovich, K. A., & Dunlap, J. C. (2010). High-throughput construction of gene deletion cassettes for generation of *Neurospora crassa* knockout strains. In *Molecular and cell biology methods for fungi* (pp. 33-40). Humana Press.

Colot, H. V., Park, G., Turner, G. E., Ringelberg, C., Crew, C. M., Litvinkova, L., ... & Dunlap, J. C. (2006). A high-throughput gene knockout procedure for *Neurospora* reveals functions for multiple transcription factors. *Proceedings of the National Academy of Sciences*, *103*(27), 10352-10357.

Colovos, C., & Yeates, T. O. (1993). Verification of protein structures: patterns of nonbonded atomic interactions. *Protein science*, *2*(9), 1511-1519.

Coppin, E., Debuchy, R., Arnaise, S., & Picard, M. (1997). Mating types and sexual development in filamentous ascomycetes. *Microbiology and Molecular Biology Reviews*, *61*(4), 411-428.

Correa, A., Lewis, Z. A., Greene, A. V., March, I. J., Gomer, R. H., & Bell-Pedersen, D. (2003). Multiple oscillators regulate circadian gene expression in *Neurospora*. *Proceedings of the National Academy of Sciences*, *100*(23), 13597-13602.

Cox, J. A., Ferraz, C., Demaille, J. G., Perez, R. O., van Tuinen, D., & Marme, D. (1982). Calmodulin from *Neurospora crassa*. General properties and conformational changes. *Journal of Biological Chemistry*, *257*(18), 10694-10700.

Crosthwaite, S. K., Dunlap, J. C., & Loros, J. J. (1997). *Neurospora wc-1* and *wc-2*: transcription, photoresponses, and the origins of circadian rhythmicity. *Science*, *276*(5313), 763-769.

Curtin, J. F., Donovan, M., & Cotter, T. G. (2002). Regulation and measurement of oxidative stress in apoptosis. *Journal of immunological methods*, *265*(1-2), 49-72.

Cusick, K. D., Fitzgerald, L. A., Pirlo, R. K., Cockrell, A. L., Petersen, E. R., & Biffinger, J. C. (2014). Selection and evaluation of reference genes for expression studies with quantitative PCR in the model fungus *Neurospora crassa* under different environmental conditions in continuous culture. *PloS one*, *9*(12), e112706.

Cyert, M. S. (2001). Genetic analysis of calmodulin and its targets in *Saccharomyces cerevisiae*. *Annual review of genetics*, *35*, 647.

Cyert, M. S. (2003). Calcineurin signaling in *Saccharomyces cerevisiae*: how yeast go crazy in response to stress. *Biochemical and biophysical research communications*, *311*(4), 1143-1150.

Dai, C., Lee, Y., Lee, I. C., Nam, H. G., & Kwak, J. M. (2018). Calmodulin 1 regulates senescence and ABA response in *Arabidopsis*. *Frontiers in Plant Science*, *9*, 803.

Darling, N. J., & Cook, S. J. (2014). The role of MAPK signalling pathways in the response to endoplasmic reticulum stress. *Biochimica et Biophysica Acta (BBA)-Molecular Cell Research*, *1843*(10), 2150-2163.

Davis, R. H., & De Serres, F. J. (1970). Genetic and microbiological research techniques for *Neurospora crassa*. In *Methods in enzymology* (Vol. 17, pp. 79-143). Academic press.

Davis, R.H. (2000) *Neurospora*: contributions of a model organism. Oxford University Press.

Davis, R. H., & Perkins, D. D. (2002). *Neurospora*: a model of model microbes. *Nature Reviews Genetics*, *3*(5), 397-403.

Davis, T. R., Zucchi, P. C., & Kumamoto, C. A. (2013). Calmodulin binding to Dfi1p promotes invasiveness of *Candida albicans*. *PLoS One*, *8*(10), e76239.

Dayton, J. S., & Means, A. R. (1996). Ca^{2+}/Calmodulin-dependent kinase is essential for both growth and nuclear division in *Aspergillus nidulans*. *Molecular biology of the cell*, *7*(10), 1511–1519.

Debuchy, R., Berteaux-Lecellier, V., & Silar, P. (2010). Mating systems and sexual morphogenesis in ascomycetes. *Cellular and molecular biology of filamentous fungi*, 499-535.

Decker, L. M., Boone, E. C., Xiao, H., Shanker, B. S., Boone, S. F., Kingston, S. L., ... & Shiu, P. K. (2015). Complex formation of RNA silencing proteins in the perinuclear region of *Neurospora crassa*. *Genetics*, *199*(4), 1017-1021.

Deka, R., Kumar, R., & Tamuli, R. (2011). *Neurospora crassa* homologue of Neuronal Calcium Sensor-1 has a role in growth, calcium stress tolerance, and ultraviolet survival. *Genetica*, *139*(7), 885-894.

Delgado-Álvarez, D. L., Bartnicki-García, S., Seiler, S., & Mouriño-Pérez, R. R. (2014). Septum development in *Neurospora crassa*: the septal actomyosin tangle. *PloS one*, *9*(5), e96744.

Dhillon, N. K., Sharma, S., & Khuller, G. K. (2003). Influence of W-7, a calmodulin antagonist on phospholipid biosynthesis in *Candida albicans*. *Letters in applied microbiology*, *36*(6), 382-386.

Dodge, B. O. (1939). Some problems in the genetics of the fungi. *Science*, *90*(2339), 379-385.

Dominguez, D. C. (2004). Calcium signalling in bacteria. *Molecular microbiology*, *54*(2), 291-297.

Dudgeon, D. D., Zhang, N., Ositelu, O. O., Kim, H., & Cunningham, K. W. (2008). Nonapoptotic death of *Saccharomyces cerevisiae* cells that is stimulated by Hsp90 and inhibited by calcineurin and Cmk2 in response to endoplasmic reticulum stresses. *Eukaryotic cell*, *7*(12), 2037-2051.

Dunlap, J. C. (1999). Molecular bases for circadian clocks. *Cell*, *96*(2), 271-290.

Dunlap, J. C., & Loros, J. J. (2004). The *Neurospora* circadian system. *Journal of biological rhythms*, *19*(5), 414-424.

Edlind, T., Smith, L., Henry, K., Katiyar, S., & Nickels, J. (2002). Antifungal activity in *Saccharomyces cerevisiae* is modulated by calcium signalling. *Molecular microbiology*, *46*(1), 257-268.

Elsaraj, S. M., & Bhullar, R. P. (2008). Regulation of platelet Rac1 and Cdc42 activation through interaction with calmodulin. *Biochimica et Biophysica Acta (BBA)-Molecular Cell Research*, *1783*(5), 770-778.

Engelmann, B., Schumacher, U., & Duhm, J. (1990). Use of chlortetracycline fluorescence for the detection of Ca storing intracellular vesicles in normal human erythrocytes. *Journal of cellular physiology*, *143*(2), 357-363.

Ewald, C. Y. (2018). Redox signaling of NADPH oxidases regulates oxidative stress responses, immunity and aging. *Antioxidants*, *7*(10), 130.

Exley, G. E., Colandene, J. D., & Garrett, R. H. (1993). Molecular cloning, characterization, and nucleotide sequence of *nit-6*, the structural gene for nitrite reductase in *Neurospora crassa*. *Journal of bacteriology*, *175*(8), 2379-2392.

Feder, M. E., & Hofmann, G. E. (1999). Heat-shock proteins, molecular chaperones, and the stress response: evolutionary and ecological physiology. *Annual review of physiology*, *61*(1), 243-282.

Fedrizzi, L., Lim, D., & Carafoli, E. (2008). Calcium and signal transduction. *Biochemistry and Molecular Biology Education*, *36*(3), 175-180.

Feige, M.J., Braakman, I., Hendershot, L.M. (2018). CHAPTER 1.1 Disulfide Bonds in Protein Folding and Stability. In *Oxidative Folding of Proteins: Basic Principles, Cellular Regulation and Engineering*; The Royal Society of Chemistry: London, UK, 1–33.

Fischer, T. H., Herting, J., Tirilomis, T., Renner, A., Neef, S., Toischer, K., ... & Sossalla, S. (2013). Ca^{2+}/calmodulin-dependent protein kinase II and protein kinase A differentially regulate sarcoplasmic reticulum Ca^{2+} leak in human cardiac pathology. *Circulation*, *128*(9), 970-981.

Fischer, M. S., Wu, V. W., Lee, J. E., O'Malley, R. C., & Glass, N. L. (2018). Regulation of cell-to-cell communication and cell wall integrity by a network of MAP kinase pathways and transcription factors in *Neurospora crassa*. *Genetics*, *209*(2), 489-506.

Fischer, M. S., & Glass, N. L. (2019). Communicate and fuse: how filamentous fungi establish and maintain an interconnected mycelial network. *Frontiers in microbiology*, *10*, 619.

Fleißner, A., Simonin, A. R., & Glass, N. L. (2008). Cell fusion in the filamentous fungus, *Neurospora crassa*. *Cell Fusion*, 21-38.

Freitag, D. G., Ouimet, P. M., Girvitz, T. L., & Kapoor, M. (1997). Heat shock protein 80 of *Neurospora crassa*, a cytosolic molecular chaperone of the eukaryotic stress 90 family, interacts directly with heat shock protein 70. *Biochemistry*, *36*(33), 10221-10229.

Freitag, M., Williams, R. L., Kothe, G. O., & Selker, E. U. (2002). A cytosine methyltransferase homologue is essential for repeat-induced point mutation in *Neurospora crassa*. *Proceedings of the National Academy of Sciences*, *99*(13), 8802-8807.

Freitas, F. Z., Virgilio, S., Cupertino, F. B., Kowbel, D. J., Fioramonte, M., Gozzo, F. C., ... & Bertolini, M. C. (2016). The SEB-1 transcription factor binds to the STRE motif in *Neurospora crassa* and regulates a variety of cellular processes including the stress response and reserve carbohydrate metabolism. *G3: Genes, Genomes, Genetics*, *6*(5), 1327-1343.

Flory, M. R., Morphew, M., Joseph, J. D., Means, A. R., & Davis, T. N. (2002). Pcp1p, an Spc110p-related calmodulin target at the centrosome of the fission yeast

Schizosaccharomyces pombe. *Cell growth & differentiation: the molecular biology journal of the American Association for Cancer Research*, *13*(2), 47–58.

Fu, C., Iyer, P., Herkal, A., Abdullah, J., Stout, A., & Free, S. J. (2011). Identification and characterization of genes required for cell-to-cell fusion in *Neurospora crassa*. *Eukaryotic cell*, *10*(8), 1100-1109.

Fuchs, B. B., & Mylonakis, E. (2009). Our paths might cross: the role of the fungal cell wall integrity pathway in stress response and cross talk with other stress response pathways. *Eukaryotic cell*, *8*(11), 1616-1625.

Fukushima, T., Shimazoe, T., Shibata, S., Watanabe, A., Ono, M., Hamada, T., & Watanabe, S. (1997). The involvement of calmodulin and Ca2+/calmodulin-dependent protein kinase II in the circadian rhythms controlled by the suprachiasmatic nucleus. *Neuroscience letters*, *227*(1), 45-48.

Fulci, V., & Macino, G. (2007). Quelling: post-transcriptional gene silencing guided by small RNAs in *Neurospora crassa*. *Current opinion in microbiology*, *10*(2), 199-203.

Galagan, J. E., Calvo, S. E., Borkovich, K. A., Selker, E. U., Read, N. D., Jaffe, D., ... & Birren, B. (2003). The genome sequence of the filamentous fungus *Neurospora crassa*. *Nature*, *422*(6934), 859-868.

Galagan, J. E., & Selker, E. U. (2004). RIP: the evolutionary cost of genome defense. *TRENDS in Genetics*, *20*(9), 417-423.

Galbraith, D. W. (1981). Microfluorimetric quantitation of cellulose biosynthesis by plant protoplasts using Calcofluor White. *Physiologia Plantarum*, *53*(2), 111-116.

Gardner, G. F., & Feldman, J. F. (1981). Temperature compensation of circadian period length in clock mutants of *Neurospora crassa*. *Plant Physiology*, *68*(6), 1244-1248.

Geiser, J. R., Sundberg, H. A., Chang, B. H., Muller, E. G., & Davis, T. N. (1993). The essential mitotic target of calmodulin is the 110-kilodalton component of the spindle pole body in *Saccharomyces cerevisiae*. *Molecular and cellular biology*, *13*(12), 7913-7924.

Gessler, N. N., Leonovich, O. A., Rabinovich, Y. M., Rudchenko, M. N., & Belozerskaya, T. A. (2006). A comparative study of the components of the antioxidant defense system during growth of the mycelium of a wild-type *Neurospora crassa* strain and mutants, *white collar-1* and *white collar-2*. *Applied Biochemistry and Microbiology*, *42*(3), 293-297.

Gifford, J. L., Walsh, M. P., & Vogel, H. J. (2007). Structures and metal-ion-binding properties of the Ca^{2+}-binding helix–loop–helix EF-hand motifs. *Biochemical Journal*, *405*(2), 199-221.

Gladieux, P., Bellis, F. D., Hann-Soden, C., Svedberg, J., Johannesson, H., & Taylor, J. W. (2020). *Neurospora* from natural populations: population genomics insights into the life history of a model microbial eukaryote. *Statistical population genomics*, 313-336.

Gladyshev, E. (2017). Repeat-induced point mutation (RIP) and other genome defense mechanisms in fungi. *Microbiol Spectr 5: 10.1128/microbiolspec*. FUNK-0042-2017. doi: 10.1128/microbiolspec. FUNK-0042-2017.

Glass, N. L., Grotelueschen, J., & Metzenberg, R. L. (1990). *Neurospora crassa A* mating-type region. *Proceedings of the National Academy of Sciences*, *87*(13), 4912-4916.

Golombek, D. A., & Ralph, M. R. (1994). KN-62, an inhibitor of Ca^{2+}/calmodulin kinase II, attenuates circadian responses to light. *Neuroreport: An International Journal for the Rapid Communication of Research in Neuroscience*.

Golovkin, M., & Reddy, A. S. (2003). A calmodulin-binding protein from *Arabidopsis* has an essential role in pollen germination. *Proceedings of the National Academy of Sciences*, *100*(18), 10558-10563.

Gonçalves, A. P., & Videira, A. (2014). Programmed cell death in *Neurospora crassa*. *New Journal of Science*, *2014*.

Gordeeva, A. V., Zvyagilskaya, R. A., & Labas, Y. A. (2003). Cross-talk between reactive oxygen species and calcium in living cells. *Biochemistry (Moscow)*, *68*(10), 1077-1080.

Görlach, A., Klappa, P., & Kietzmann, D. T. (2006). The endoplasmic reticulum: folding, calcium homeostasis, signaling, and redox control. *Antioxidants & redox signaling*, *8*(9-10), 1391-1418.

Görlach, A., Bertram, K., Hudecova, S., & Krizanova, O. (2015). Calcium and ROS: A mutual interplay. *Redox biology*, *6*, 260-271.

Grayburn, W. S., & Selker, E. U. (1989). A natural case of RIP: degeneration of the DNA sequence in an ancestral tandem duplication. *Molecular and cellular biology*, *9*(10), 4416-4421.

Griffith, L. C. (2004). Calcium/calmodulin-dependent protein kinase II: an unforgettable kinase. *Journal of Neuroscience*, *24*(39), 8391-8393.

Guo, J., & Liu, Y. (2010). Molecular mechanism of the *Neurospora* circadian oscillator. *Protein & cell*, *1*(4), 331-341.

Haiech, J., Moreau, M., Leclerc, C., & Kilhoffer, M. C. (2019). Facts and conjectures on calmodulin and its cousin proteins, parvalbumin and troponin C. *Biochimica et Biophysica Acta (BBA)-Molecular Cell Research*, *1866*(7), 1046-1053.

Halberg, F., Cornélissen, G., Katinas, G., Syutkina, E. V., Sothern, R. B., Zaslavskaya, R., ... & Siggelova, J. (2003). Transdisciplinary unifying implications of circadian findings in the 1950s. *Journal of circadian rhythms*, *1*(1), 1-61.

Halling, D. B., Liebeskind, B. J., Hall, A. W., & Aldrich, R. W. (2016). Conserved properties of individual Ca^{2+}-binding sites in calmodulin. *Proceedings of the National Academy of Sciences*, *113*(9), E1216-E1225.

Halling, D. B., Philpo, A. E., & Aldrich, R. W. (2022). Calcium dependence of both lobes of calmodulin is involved in SK channel gating. *bioRxiv*.

Hamann, A., Brust, D., & Osiewacz, H. D. (2008). Apoptosis pathways in fungal growth, development and ageing. *Trends in microbiology*, *16*(6), 276-283.

Hammond, T. M., Xiao, H., Boone, E. C., Perdue, T. D., Pukkila, P. J., & Shiu, P. K. (2011). SAD-3, a putative helicase required for meiotic silencing by unpaired DNA, interacts with other components of the silencing machinery. *G3: Genes| Genomes| Genetics*, *1*(5), 369-376.

Hammond, T. M., Xiao, H., Boone, E. C., Decker, L. M., Lee, S. A., Perdue, T. D., ... & Shiu, P. K. (2013). Novel proteins required for meiotic silencing by unpaired DNA and siRNA generation in *Neurospora crassa*. *Genetics*, *194*(1), 91-100.

Harding, R. W. (1974). The effect of temperature on photo-induced carotenoid biosynthesis in *Neurospora crassa*. *Plant physiology*, *54*(2), 142-147.

Harris, J. L., Howe Jr, H. B., & Roth, I. L. (1975). Scanning electron microscopy of surface and internal features of developing perithecia of *Neurospora crassa*. *Journal of bacteriology*, *122*(3), 1239-1246.

Herker, E., Jungwirth, H., Lehmann, K. A., Maldener, C., Fröhlich, K. U., Wissing, S., ... & Madeo, F. (2004). Chronological aging leads to apoptosis in yeast. *The Journal of cell biology*, *164*(4), 501-507.

Herzog, S., Schumann, M. R., & Fleißner, A. (2015). Cell fusion in *Neurospora crassa*. *Current opinion in microbiology*, *28*, 53-59.

Higuchi, S., Tamura, J., Giri, P. R., Polli, J. W., & Kincaid, R. L. (1991). Calmodulin-dependent protein phosphatase from *Neurospora crassa*. Molecular cloning and expression of recombinant catalytic subunit. *Journal of Biological Chemistry*, *266*(27), 18104-18112.

Hoeflich, K. P., & Ikura, M. (2002). Calmodulin in action: diversity in target recognition and activation mechanisms. *Cell*, *108*(6), 739-742.

Holyoak, C. D., Thompson, S., Ortiz Calderon, C., Hatzixanthis, K., Bauer, B., Kuchler, K., ... & Coote, P. J. (2000). Loss of Cmk1 Ca^{2+}–calmodulin-dependent protein kinase in yeast results in constitutive weak organic acid resistance, associated with a post-transcriptional activation of the Pdr12 ATP-binding cassette transporter. *Molecular microbiology*, *37*(3), 595-605.

Hook, S. S., & Means, A. R. (2001). Ca^{2+}/CaM-dependent kinases: from activation to function. *Annual review of pharmacology and toxicology*, *41*, 471.

Hu, Y., Liu, X., Lu, Q., Yang, Y., He, Q., Liu, Y., & Liu, X. (2021). FRQ-CK1 Interaction Underlies Temperature Compensation of the *Neurospora* Circadian Clock. *Mbio*, *12*(3), e01425-21.

Hudmon, A., & Schulman, H. (2002). Neuronal Ca^{2+}/calmodulin-dependent protein kinase II: The role of structure and autoregulation in cellular function. *Annual review of biochemistry*, *71*, 473.

Hull, J. J., & Fónagy, A. (2020). A Sexy Moth Model–The Molecular Basis of Sex Pheromone Biosynthesis in the Silkmoth *Bombyx mori*. In *Insect Sex Pheromone Research and Beyond* (pp. 111-150). Springer, Singapore.

Hunsley, D., & Gooday, G. W. (1974). The structure and development of septa in *Neurospora crassa*. *Protoplasma*, *82*(1), 125-146.

Hunt, S. M., Elvin, M., Crosthwaite, S. K., & Heintzen, C. (2007). The PAS/LOV protein VIVID controls temperature compensation of circadian clock phase and development in *Neurospora crassa*. *Genes & development*, *21*(15), 1964-1974.

Hurley, J., Loros, J. J., & Dunlap, J. C. (2015). Dissecting the mechanisms of the clock in Neurospora. *Methods in enzymology*, *551*, 29-52.

Iida, H., Ohya, Y., & Anraku, Y. (1995). Calmodulin-dependent protein kinase II and calmodulin are required for induced thermotolerance in *Saccharomyces cerevisiae*. *Current genetics*, *27*(2), 190-193.

Inoue, H., Nojima, H., & Okayama, H. (1990). High efficiency transformation of Escherichia coli with plasmids. *Gene*, *96*(1), 23-28.

Irelan, J. T., Hagemann, A. T., & Selker, E. U. (1994). High frequency repeat-induced point mutation (RIP) is not associated with efficient recombination in *Neurospora*. *Genetics*, *138*(4), 1093-1103.

Itadani, A., Nakamura, T., Hirata, A., & Shimoda, C. (2010). *Schizosaccharomyces pombe* calmodulin, Cam1, plays a crucial role in sporulation by recruiting and stabilizing the spindle pole body components responsible for assembly of the Forespore membrane. *Eukaryotic cell*, *9*(12), 1925-1935.

Iyer, S. V., Ramakrishnan, M., & Kasbekar, D. P. (2009). *Neurospora crassa fmf-1* encodes the homologue of the *Schizosaccharomyces pombe* Ste11p regulator of sexual development. *Journal of genetics*, *88*(1), 33-39.

Jackson, S. L., & Heath, I. B. (1993). Roles of calcium ions in hyphal tip growth. *Microbiological Reviews*, *57*(2), 367-382.

Jaiswal, J. K. (2001). Calcium—how and why?. *Journal of biosciences*, *26*(3), 357-363.

James, P., Vorherr, T., & Carafoli, E. (1995). Calmodulin-binding domains: just two faced or multi-faceted?. *Trends in biochemical sciences*, *20*(1), 38-42.

Jamet-Vierny, C., Debuchy, R., Prigent, M., & Silar, P. (2007). IDC1, a pezizomycotina-specific gene that belongs to the PaMpk1 MAP kinase transduction cascade of the filamentous fungus *Podospora anserina*. *Fungal Genetics and Biology*, *44*(12), 1219-1230.

Jensen, B. C., Schabtach, E., & Selker, E. U. (1989). Repeat-induced GC to AT mutations in Neurospora. *Science*, *244*(4912), 1571-1575.

Jensen, H. H., Brohus, M., Nyegaard, M., & Overgaard, M. T. (2018). Human calmodulin mutations. *Frontiers in Molecular Neuroscience*, *11*, 396.

Jin, M., Guan, C. B., Jiang, Y. A., Chen, G., Zhao, C. T., Cui, K., ... & Yuan, X. B. (2005). Ca^{2+}-dependent regulation of rho GTPases triggers turning of nerve growth cones. *Journal of Neuroscience*, *25*(9), 2338-2347.

Joseph, J. D., & Means, A. R. (2000). Identification and characterization of two Ca^{2+}/CaM-dependent protein kinases required for normal nuclear division in *Aspergillus nidulans*. *Journal of Biological Chemistry*, *275*(49), 38230-38238.

Jurado, L. A., Chockalingam, P. S., & Jarrett, H. W. (1999). Apocalmodulin. *Physiological reviews*, *79*(3), 661-682.

Justa-Schuch, D., Heilig, Y., Richthammer, C., & Seiler, S. (2010). Septum formation is regulated by the RHO4-specific exchange factors BUD3 and RGF3 and by the landmark protein BUD4 in *Neurospora crassa*. *Molecular microbiology*, *76*(1), 220-235.

Kader, M. A., & Lindberg, S. (2010). Cytosolic calcium and pH signaling in plants under salinity stress. *Plant signaling & behavior*, *5*(3), 233-238.

Kakiuchi, S., & Yamazaki, R. (1970). Calcium dependent phosphodiesterase activity and its activating factor (PAF) from brain: studies on cyclic 3′, 5′-nucleotide phosphodiesterase (III). *Biochemical and biophysical research communications*, *41*(5), 1104-1110.

Kahl, C. R., & Means, A. R. (2003). Regulation of cell cycle progression by calcium/calmodulin-dependent pathways. *Endocrine reviews*, *24*(6), 719-736.

Kapoor, M., & Lewis, J. (1987). Heat shock induces peroxidase activity in *Neurospora crassa* and confers tolerance toward oxidative stress. *Biochemical and biophysical research communications*, *147*(3), 904-910.

Kapoor, M., Sreenivasan, G. M., Goel, N., & Lewis, J. (1990). Development of thermotolerance in *Neurospora crassa* by heat shock and other stresses eliciting peroxidase induction. *Journal of bacteriology*, *172*(5), 2798-2801.

Kapoor, M., & Roy, S. S. (2014). A BIRD'S EYE-VIEW OF MOLECULAR CHAPERONES AND SOME FACETS OF THE HEAT SHOCK RESPONSE OF *NEUROSPORA CRASSA*. *Annual Review of Plant Pathology (Vol. 6)*, *6*, 1.

Karabinos, A., Büssing, I., Schulze, E., Wang, J., Weber, K., & Schnabel, R. (2003). Functional analysis of the single calmodulin gene in the nematode *Caenorhabditis elegans* by RNA interference and 4-D microscopy. *European journal of cell biology*, *82*(11), 557-563.

Kikuchi, Y., Iwano, I., & Kato, K. (1984). Effects of calmodulin antagonists on human ovarian cancer cell proliferation in vitro. *Biochemical and biophysical research communications*, *123*(1), 385-392.

Kim, Y. K., Li, D., & Kolattukudy, P. E. (1998). Induction of Ca^{2+}-calmodulin signaling by hard-surface contact primes *Colletotrichum gloeosporioides* conidia to germinate and form appressoria. *Journal of Bacteriology*, *180*(19), 5144-5150.

Kim, H., & Borkovich, K. A. (2004). A pheromone receptor gene, *pre-1*, is essential for mating type-specific directional growth and fusion of trichogynes and female fertility in *Neurospora crassa*. *Molecular microbiology*, *52*(6), 1781-1798.

Kim, H., & Borkovich, K. A. (2006). Pheromones are essential for male fertility and sufficient to direct chemotropic polarized growth of trichogynes during mating in *Neurospora crassa*. *Eukaryotic cell*, *5*(3), 544-554.

Kim, H., Wright, S. J., Park, G., Ouyang, S., Krystofova, S., & Borkovich, K. A. (2012). Roles for receptors, pheromones, G proteins, and mating type genes during sexual reproduction in *Neurospora crassa*. *Genetics*, *190*(4), 1389-1404.

Kim, Y. E., Hipp, M. S., Bracher, A., Hayer-Hartl, M., & Ulrich Hartl, F. (2013). Molecular chaperone functions in protein folding and proteostasis. *Annual review of biochemistry*, *82*, 323-355.

Kim, J., Park, H., Han, J. G., Oh, J., Choi, H. K., Kim, S. H., & Sung, G. H. (2015). Regulation of a phenylalanine ammonia lyase (BbPAL) by calmodulin in response to environmental changes in the entomopathogenic fungus *Beauveria bassiana*. *Environmental microbiology*, *17*(11), 4484-4494.

Kim, J., Oh, J., & Sung, G. H. (2016). Regulation of MAP kinase Hog1 by calmodulin during hyperosmotic stress. *Biochimica et Biophysica Acta (BBA)-Molecular Cell Research*, *1863*(11), 2551-2559.

Kim, J., Yoon, D. H., Oh, J., Hyun, M. W., Han, J. G., & Sung, G. H. (2016). Calmodulin-mediated suppression of 2-ketoisovalerate reductase in *Beauveria bassiana* beauvericin biosynthetic pathway. *Environmental Microbiology*, *18*(11), 4136-4143.

Kim, J., Oh, J., Yoon, D. H., & Sung, G. H. (2017). Suppression of a methionine synthase by calmodulin under environmental stress in the entomopathogenic fungus *Beauveria bassiana*. *Environmental microbiology reports*, *9*(5), 612-617.

Kim, J., Oh, J., Yoon, D. H., & Sung, G. H. (2018). Identification of calmodulin binding proteins in the entomopathogenic fungus *Beauveria bassiana*. *Folia microbiologica*, *63*(1), 13-16.

Kim, M. H., Choi, Y. J., Kwon, B., Choo, Y. M., Yu, K. Y., & Kim, J. (2019). Regulation of secondary metabolism by calmodulin signaling in filamentous fungi. *Revista Iberoamericana de Micología*, *36*(3), 167-168.

Kim, K. E., Nguyen, N. T., Kim, S. H., Bahk, S., Cheong, M. S., Park, H. C., ... & Chung, W. S. (2022). Ca^{2+}/Calmodulin Activates an MAP Kinase Through the Inhibition of a Protein Phosphatase (DsPTP1) in *Arabidopsis*. *Journal of Plant Biology*, *65*(1), 65-74.

Kirchhefer, U., Schmitz, W., Scholz, H., & Neumann, J. (1999). Activity of cAMP-dependent protein kinase and Ca^{2+}/calmodulin-dependent protein kinase in failing and nonfailing human hearts. *Cardiovascular research*, *42*(1), 254-261.

Kirkwood, T. B., & Austad, S. N. (2000). Why do we age?. *Nature*, *408*(6809), 233-238.

Koga, T., & Kawakami, A. (2018). The role of CaMK4 in immune responses. *Modern rheumatology*, *28*(2), 211-214.

Koo, J. C., Lee, I. C., Dai, C., Lee, Y., Cho, H. K., Kim, Y., ... & Kwak, J. M. (2017). The protein trio RPK1–CaM4–RbohF mediates transient superoxide production to trigger age-dependent cell death in *Arabidopsis*. *Cell reports*, *21*(12), 3373-3380.

Kotchoni, S. O., & Gachomo, E. W. (2006). The reactive oxygen species network pathways: an essential prerequisite for perception of pathogen attack and the acquired disease resistance in plants. *Journal of biosciences*, *31*(3), 389-404.

Kouzminova, E., & Selker, E. U. (2001). *dim-2* encodes a DNA methyltransferase responsible for all known cytosine methylation in *Neurospora*. *The EMBO journal*, *20*(15), 4309-4323.

Kozubowski, L., Lee, S. C., & Heitman, J. (2009). Signalling pathways in the pathogenesis of *Cryptococcus*. *Cellular microbiology*, *11*(3), 370-380.

Krajewska-Kułak, E., & Niczyporuk, W. (1993). Effects of the combination of ketoconazole and calmodulin inhibitors against *Candida albicans* in vitro. Short communication. *Arzneimittel-forschung*, *43*(9), 1018-1019.

Kraus, P. R., & Heitman, J. (2003). Coping with stress: calmodulin and calcineurin in model and pathogenic fungi. *Biochemical and biophysical research communications*, *311*(4), 1151-1157.

Kraus, P. R., Nichols, C. B., & Heitman, J. (2005). Calcium-and calcineurin-independent roles for calmodulin in *Cryptococcus neoformans* morphogenesis and high-temperature growth. *Eukaryotic cell*, *4*(6), 1079-1087.

Kronholm, I., Johannesson, H., & Ketola, T. (2016). Epigenetic control of phenotypic plasticity in the filamentous fungus *Neurospora crassa*. *G3: Genes, Genomes, Genetics, 6*(12), 4009-4022.

Kronholm, I., & Ketola, T. (2018). Effects of acclimation time and epigenetic mechanisms on growth of *Neurospora* in fluctuating environments. *Heredity*, *121*(4), 327-341.

Kumar, R., & Tamuli, R. (2014). Calcium/calmodulin-dependent kinases are involved in growth, thermotolerance, oxidative stress survival, and fertility in *Neurospora crassa*. *Archives of microbiology*, *196*(4), 295-305.

Kurian, S. M., Lichius, A., & Read, N. D. (2022). Ca^{2+} Signalling Differentially Regulates Germ-Tube Formation and Cell Fusion in *Fusarium oxysporum*. *Journal of Fungi*, *8*(1), 90.

Kwon, M. J., Arentshorst, M., Roos, E. D., van den Hondel, C. A., Meyer, V., & Ram, A. F. (2011). Functional characterization of Rho GTPases in *Aspergillus niger* uncovers conserved and diverged roles of Rho proteins within filamentous fungi. *Molecular microbiology*, *79*(5), 1151-1167.

Lakin-Thomas, P. L. (1998). Choline depletion, *frq* mutations, and temperature compensation of the circadian rhythm in *Neurospora crassa*. *Journal of biological rhythms*, *13*(4), 268-277.

Lalucque, H., Malagnac, F., Green, K., Gautier, V., Grognet, P., Tong, L. C. H., ... & Silar, P. (2017). IDC2 and IDC3, two genes involved in cell non-autonomous signaling of fruiting body development in the model fungus *Podospora anserina*. *Developmental biology*, *421*(2), 126-138.

Laskowski, R. A., MacArthur, M. W., Moss, D. S., & Thornton, J. M. (1993). PROCHECK: a program to check the stereochemical quality of protein structures. *Journal of applied crystallography*, *26*(2), 283-291.

Laun, P., Pichova, A., Madeo, F., Fuchs, J., Ellinger, A., Kohlwein, S., ... & Breitenbach, M. (2001). Aged mother cells of *Saccharomyces cerevisiae* show markers of oxidative stress and apoptosis. *Molecular microbiology*, *39*(5), 1166-1173.

Laxmi, V., & Tamuli, R. (2015). The *Neurospora crassa cmd*, *trm-9*, and *nca-2* Genes Play a Role in Growth, Development, and Survival in Stress conditions. *Genomics and Applied Biology*, *6*.

Laxmi, V. (2016). Understanding of calcium signaling pathway mediated by calmodulin and related proteins in *Neurospora crassa* (Doctoral dissertation).

Laxmi, V., & Tamuli, R. (2017). The calmodulin gene in *Neurospora crassa* is required for normal vegetative growth, ultraviolet survival, and sexual development. *Archives of microbiology*, *199*(4), 531-542.

Lange, M., & Peiter, E. (2020). Calcium transport proteins in fungi: the phylogenetic diversity of their relevance for growth, virulence, and stress resistance. *Frontiers in microbiology*, *10*, 3100.

Lee, S. C., & Lee, Y. H. (1998). Calcium/calmodulin-dependent signaling for appressorium formation in the plant pathogenic fungus *Magnaporthe grisea*. *Molecules & Cells (Springer Science & Business Media BV)*, *8*(6).

Lee, D. W., Pratt, R. J., McLaughlin, M., & Aramayo, R. (2003). An argonaute-like protein is required for meiotic silencing. *Genetics*, *164*(2), 821.

Lee, D. W., Millimaki, R., & Aramayo, R. (2010). QIP, a component of the vegetative RNA silencing pathway, is essential for meiosis and suppresses meiotic silencing in *Neurospora crassa*. *Genetics*, *186*(1), 127-133.

Leeder, A. C., Jonkers, W., Li, J., & Glass, N. L. (2013). Early colony establishment in *Neurospora crassa* requires a MAP kinase regulatory network. *Genetics*, *195*(3), 883-898.

Lewit-Bentley, A., & Réty, S. (2000). EF-hand calcium-binding proteins. *Current opinion in structural biology*, *10*(6), 637-643.

Li, B., Liu, H. T., Sun, D. Y., & Zhou, R. G. (2004). Ca^{2+} and calmodulin modulate DNA-binding activity of maize heat shock transcription factor in vitro. *Plant and Cell Physiology*, *45*(5), 627-634.

Li, D., Bobrowicz, P., Wilkinson, H. H., & Ebbole, D. J. (2005). A mitogen-activated protein kinase pathway essential for mating and contributing to vegetative growth in *Neurospora crassa*. *Genetics*, *170*(3), 1091-1104.

Li, W., Halling, D. B., Hall, A. W., & Aldrich, R. W. (2009). EF hands at the N-lobe of calmodulin are required for both SK channel gating and stable SK–calmodulin interaction. *Journal of General Physiology*, *134*(4), 281-293.

Li, G., Liu, S., Wu, L., Wang, X., Cuan, R., Zheng, Y., ... & Yuan, Y. (2022). Characterization and Functional Analysis of a New Calcium/Calmodulin-Dependent Protein Kinase (CaMK1) in the Citrus Pathogenic Fungus *Penicillium italicum*. *Journal of Fungi*, *8*(7), 667.

Lichius, A., Lord, K. M., Jeffree, C. E., Oborny, R., Boonyarungsrit, P., & Read, N. D. (2012). Importance of MAP kinases during protoperithecial morphogenesis in *Neurospora crassa*. *PloS one*, *7*(8), e42565.

Linse, S., Helmersson, A., & Forsen, S. (1991). Calcium binding to calmodulin and its globular domains. *Journal of Biological Chemistry*, *266*(13), 8050-8054.

Liu, Z. M., & Kolattukudy, P. E. (1999). Early expression of the calmodulin gene, which precedes appressorium formation in *Magnaporthe grisea*, is inhibited by self-inhibitors and requires surface attachment. *Journal of Bacteriology*, *181*(11), 3571-3577.

Liu, Q., Chen, B., Ge, Q., & Wang, Z. W. (2007). Presynaptic Ca^{2+}/calmodulin-dependent protein kinase II modulates neurotransmitter release by activating BK channels at *Caenorhabditis elegans* neuromuscular junction. *Journal of Neuroscience*, *27*(39), 10404-10413.

Liu, J., Wisniewski, M., Droby, S., Norelli, J., Hershkovitz, V., Tian, S., & Farrell, R. (2012). Increase in antioxidant gene transcripts, stress tolerance and biocontrol efficacy of *Candida oleophila* following sublethal oxidative stress exposure. *FEMS microbiology ecology*, *80*(3), 578-590.

Liu, W., Xie, Y., Ma, J., Luo, X., Nie, P., Zuo, Z., ... & Ren, J. (2015). IBS: an illustrator for the presentation and visualization of biological sequences. *Bioinformatics*, *31*(20), 3359-3361.

Liu, X. R., Zhang, M. M., Rempel, D. L., & Gross, M. L. (2019). A single approach reveals the composite conformational changes, order of binding, and affinities for calcium binding to calmodulin. *Analytical chemistry*, *91*(9), 5508-5512.

Liu, X. R., Rempel, D. L., & Gross, M. L. (2019). Composite conformational changes of signaling proteins upon ligand binding revealed by a single approach: Calcium-calmodulin study. *Analytical chemistry*, *91*(19), 12560-12567.

Liu, L., Xiang, Y., Yan, J., Di, P., Li, J., Sun, X., ... & Zhang, A. (2021). BRASSINOSTEROID-SIGNALING KINASE 1 phosphorylating

CALCIUM/CALMODULIN-DEPENDENT PROTEIN KINASE functions in drought tolerance in maize. *New Phytologist*, *231*(2), 695-712.

Livak, K. J., & Schmittgen, T. D. (2001). Analysis of relative gene expression data using real-time quantitative PCR and the $2^{-\Delta\Delta C_T}$ method. *methods*, *25*(4), 402-408.

Lord, K. M., & Read, N. D. (2011). Perithecium morphogenesis in *Sordaria macrospora*. *Fungal Genetics and Biology*, *48*(4), 388-399.

Lu, K. P., Rasmussen, C. D., May, G. S., & Means, A. R. (1992). Cooperative regulation of cell proliferation by calcium and calmodulin in *Aspergillus nidulans*. *Molecular Endocrinology*, *6*(3), 365-374.

Lu, K. P., Nanthakumar, N. N., Dayton, J. S., & Means, A. R. (1995). Calcium and calmodulin regulation of the nuclear division cycle of *Aspergillus nidulans*. In *Advances in Molecular and Cell Biology* (Vol. 13, pp. 89-136). Elsevier.

Lu, Y. T., Hidaka, H., & Feldman, L. J. (1996). Characterization of a calcium/calmodulin-dependent protein kinase homolog from maize roots showing light-regulated gravitropism. *Planta*, *199*(1), 18-24.

Lushchak, V. I. (2011). Adaptive response to oxidative stress: Bacteria, fungi, plants and animals. *Comparative Biochemistry and Physiology Part C: Toxicology & Pharmacology*, *153*(2), 175-190.

Ma, Z. B., Zhao, J. X., Wang, L. A., & Zheng, X. B. (2009). Cloning, prokaryotic expression, and bioactivity of the calmodulin gene of *Magnaporthe grisea*. *FEMS microbiology letters*, *300*(1), 107-114.

Maerz, S., Ziv, C., Vogt, N., Helmstaedt, K., Cohen, N., Gorovits, R., ... & Seiler, S. (2008). The nuclear Dbf2-related kinase COT1 and the mitogen-activated protein kinases MAK1

and MAK2 genetically interact to regulate filamentous growth, hyphal fusion and sexual development in *Neurospora crassa*. *Genetics*, *179*(3), 1313-1325.

Mager, W. H., & De Kruijff, A. J. (1995). Stress-induced transcriptional activation. *Microbiological reviews*, *59*(3), 506-531.

Magnan, F., Ranty, B., Charpenteau, M., Sotta, B., Galaud, J. P., & Aldon, D. (2008). Mutations in AtCML9, a calmodulin-like protein from *Arabidopsis thaliana*, alter plant responses to abiotic stress and abscisic acid. *The Plant Journal*, *56*(4), 575-589.

Maier, L. S., & Bers, D. M. (2007). Role of Ca^{2+}/calmodulin-dependent protein kinase (CaMK) in excitation–contraction coupling in the heart. *Cardiovascular research*, *73*(4), 631-640.

Malagnac, F., Lalucque, H., Lepère, G., & Silar, P. (2004). Two NADPH oxidase isoforms are required for sexual reproduction and ascospore germination in the filamentous fungus *Podospora anserina*. *Fungal Genetics and Biology*, *41*(11), 982-997.

Marchler-Bauer, A., Anderson, J. B., Chitsaz, F., Derbyshire, M. K., DeWeese-Scott, C., Fong, J. H., ... & Bryant, S. H. (2009). CDD: specific functional annotation with the Conserved Domain Database. *Nucleic acids research*, *37*(suppl_1), D205-D210.

Margolin, B. S., Freitag, M., & Selker, E. U. (1997). Improved plasmids for gene targeting at the *his-3* locus of *Neurospora crassa* by electroporation. *Fungal Genetics Newsletter*, 34-36.

Marín-Briggiler, C. I., Jha, K. N., Chertihin, O., Buffone, M. G., Hgerr, J. C., Vazquez-Levin, M. H., & Visconti, P. E. (2005). Evidence of the presence of calcium/calmodulin-dependent protein kinase IV in human sperm and its involvement in motility regulation. *Journal of Cell Science*, *118*(9), 2013-2022.

Marschall, R., Schumacher, J., Siegmund, U., & Tudzynski, P. (2016). Chasing stress signals–exposure to extracellular stimuli differentially affects the redox state of cell compartments in the wild type and signaling mutants of *Botrytis cinerea*. *Fungal Genetics and Biology*, *90*, 12-22.

Martins, M. P., Martinez-Rossi, N. M., Sanches, P. R., & Rossi, A. (2020). The PAC-3 transcription factor critically regulates phenotype-associated genes in *Neurospora crassa*. *Genetics and molecular biology*, *43*.

Matsumoto, S., Ozawa, R., Nagamine, T., Kim, G. H., Uchiumi, K., Shono, T., & Mitsui, T. (1995). Intracellular transduction in the regulation of pheromone biosynthesis of the silkworm, *Bombyx mori*: suggested involvement of calmodulin and phosphoprotein phosphatase. *Bioscience, biotechnology, and biochemistry*, *59*(3), 560-562.

Matsumoto, S., Ozawa, R., Uchiumi, K., Kurihara, M., & Mitsui, T. (1995). Intracellular signal transduction of PBAN action in the common cutworm, *Spodoptera litura*: effects of pharmacological agents on sex pheromone production in vitro. *Insect biochemistry and molecular biology*, *25*(9), 1055-1059.

Mattern, D. L., Forman, L. R., & Brody, S. (1982). Circadian rhythms in *Neurospora crassa*: a mutation affecting temperature compensation. *Proceedings of the National Academy of Sciences*, *79*(3), 825-829.

McCluskey, K. (2003). The fungal genetics stock center. *from molds to molecules*, *52*, 245-262.

MCNELLY-INGLE, C. A., & Frost, L. C. (1965). The effect of temperature on the production of perithecia by *Neurospora crassa*. *Microbiology*, *39*(1), 33-42.

Meador, W. E., Means, A. R., & Quiocho, F. A. (1992). Target enzyme recognition by calmodulin: 2.4 Å structure of a calmodulin-peptide complex. *Science*, *257*(5074), 1251-1255.

Meador, W. E., Means, A. R., & Quiocho, F. A. (1993). Modulation of calmodulin plasticity in molecular recognition on the basis of x-ray structures. *Science*, *262*(5140), 1718-1721.

Means, A. R., & Dedman, J. R. (1980). Calmodulin—an intracellular calcium receptor. *Nature*, *285*(5760), 73-77.

Mehra, A., Baker, C. L., Loros, J. J., & Dunlap, J. C. (2009). Post-translational modifications in circadian rhythms. *Trends in biochemical sciences*, *34*(10), 483-490.

Melnick, M. B., Melnick, C., Lee, M., & Woodward, D. O. (1993). Structure and sequence of the calmodulin gene from *Neurospora crassa*. *Biochimica et Biophysica Acta (BBA)-Gene Structure and Expression*, *1171*(3), 334-336.

Minhas, F. U. A. A., & Ben-Hur, A. (2012). Multiple instance learning of Calmodulin binding sites. *Bioinformatics*, *28*(18), i416-i422.

Meng, E. C., Pettersen, E. F., Couch, G. S., Huang, C. C., & Ferrin, T. E. (2006). Tools for integrated sequence-structure analysis with UCSF Chimera. *BMC bioinformatics*, *7*(1), 1-10.

Montagne, C. (1843). Quatrieme centurie plantes cellulaires exotiques nouvelles. Decades VIII, IX, X. *Ann. Sci. Nat. Bot., Ser. 2*, *20*, 352-39.

Montenegro-Montero, A., & Larrondo, L. F. (2013). The *Neurospora* circadian system: From genes to proteins and back in less than 24 hours. *Neurospora. Genomics and Molecular Biology*.

Montibus, M., Pinson-Gadais, L., Richard-Forget, F., Barreau, C., & Ponts, N. (2015). Coupling of transcriptional response to oxidative stress and secondary metabolism regulation in filamentous fungi. *Critical Reviews in Microbiology*, *41*(3), 295-308.

Moser, M. J., Geiser, J. R., & Davis, T. N. (1996). Ca^{2+}-calmodulin promotes survival of pheromone-induced growth arrest by activation of calcineurin and Ca^{2+}-calmodulin-dependent protein kinase. *Molecular and Cellular Biology*, *16*(9), 4824-4831.

Moser, M. J., Flory, M. R., & Davis, T. N. (1997). Calmodulin localizes to the spindle pole body of *Schizosaccharomyces pombe* and performs an essential function in chromosome segregation. *Journal of cell science*, *110*(15), 1805-1812.

Munkres, K. D., & Furtek, C. A. (1984). [31] Assay of rate of aging of conidia of *Neurospora crassa*. In *Methods in enzymology* (Vol. 105, pp. 263-270). Academic Press.

Muthukumar, G., & Nickerson, K. W. (1984). Ca (II)-calmodulin regulation of fungal dimorphism in *Ceratocystis ulmi*. *Journal of bacteriology*, *159*(1), 390-392.

Muthukumar, G., & Nickerson, K. W. (1985). Ca (II)—calmodulin regulation of morphological commitment in *Ceratocystis ulmi*. *FEMS Microbiology letters*, *27*(2), 199-202.

Muthukumar, G., Luby, M. T., & Nickerson, K. W. (1986). Calmodulin activity in yeast and mycelial phases of *Ceratocystis ulmi*. *FEMS microbiology letters*, *37*(3), 313-316**.**

Nakajima, Y., & Suzuki, S. (2013). Environmental stresses induce misfolded protein aggregation in plant cells in a microtubule-dependent manner. *International journal of molecular sciences*, *14*(4), 7771-7783.

Nakano, K., Mutoh, T., Arai, R., & Mabuchi, I. (2003). The small GTPase Rho4 is involved in controlling cell morphology and septation in fission yeast. *Genes to Cells*, *8*(4), 357-370.

Nakashima, H. (1986). Phase shifting of the circadian conidiation rhythm in *Neurospora crassa* by calmodulin antagonists. *Journal of Biological Rhythms, 1*(2), 163-169.

Nakayama, S., & Kretsinger, R. H. (1994). Evolution of the EF-hand family of proteins. *Annual review of biophysics and biomolecular structure*, *23*(1), 473-507.

Naz, H., Tarique, M., Ahamad, S., Alajmi, M. F., Hussain, A., Rehman, M. T., ... & Hassan, M. I. (2019). Hesperidin-CAMKIV interaction and its impact on cell proliferation and apoptosis in the human hepatic carcinoma and neuroblastoma cells. *Journal of Cellular Biochemistry*, *120*(9), 15119-15130.

Nelson, M. A., & Metzenberg, R. L. (1992). Sexual development genes of *Neurospora crassa*. *Genetics*, *132*(1), 149-162.

Nicholas, K. B. (1997). GeneDoc: analysis and visualization of genetic variation. *Embnew. news*, *4*, 14.

Ochiai, E. I. (1991). Why calcium? Principles and applications in bioorganic chemistry-IV. *Journal of Chemical Education*, *68*(1), 10.

Ohnishi, A., Hull, J. J., Kaji, M., Hashimoto, K., Lee, J. M., Tsuneizumi, K., ... & Matsumoto, S. (2011). Hormone signaling linked to silkmoth sex pheromone biosynthesis involves Ca^{2+}/calmodulin-dependent protein kinase II-mediated phosphorylation of the insect PAT family protein *Bombyx mori* lipid storage droplet protein-1 (BmLsd1). *Journal of Biological Chemistry*, *286*(27), 24101-24112.

Osiewacz, H. D., & Scheckhuber, C. Q. (2006). Impact of ROS on ageing of two fungal model systems: Saccharomyces cerevisiae and *Podospora anserina*. *Free radical research*, *40*(12), 1350-1358.

Ouimet, P. M., & Kapoor, M. (1998). Analysis of complex formation between Hsp80 and Hsp70, cytosolic molecular chaperones of *Neurospora crassa*, by enzyme-linked immunosorbent assays (ELISA). *Biochemistry and cell biology*, *76*(1), 97-106.

Ouyang, S., Beecher, C. N., Wang, K., Larive, C. K., & Borkovich, K. A. (2015). Metabolic impacts of using nitrogen and copper-regulated promoters to regulate gene expression in *Neurospora crassa*. *G3: Genes, Genomes, Genetics*, *5*(9), 1899-1908.

Pall, M. L. (1993). The use of Ignite (Basta; glufosinate; phosphinothricin) to select transformants of bar-containing plasmids in *Neurospora crassa*. *Fungal Genet Newsl*, *40*(1), 58.

Pan, G., Vickers, S. M., Pickens, A., Phillips, J. O., Ying, W., Thompson, J. A., ... & McDonald, J. M. (1999). Apoptosis and tumorigenesis in human cholangiocarcinoma cells: involvement of Fas/APO-1 (CD95) and calmodulin. *The American journal of pathology*, *155*(1), 193-203.

Pang, Z. P., Cao, P., Xu, W., & Südhof, T. C. (2010). Calmodulin controls synaptic strength via presynaptic activation of calmodulin kinase II. *Journal of Neuroscience*, *30*(11), 4132-4142.

Park, G., Pan, S., & Borkovich, K. A. (2008). Mitogen-activated protein kinase cascade required for regulation of development and secondary metabolism in *Neurospora crassa*. *Eukaryotic cell*, *7*(12), 2113-2122.

Park, G., Colot, H. V., Collopy, P. D., Krystofova, S., Crew, C., Ringelberg, C., ... & Borkovich, K. A. (2011). High-throughput production of gene replacement mutants in *Neurospora crassa*. In *Fungal Genomics* (pp. 179-189). Humana Press.

Park, H. S., Lee, S. C., Cardenas, M. E., & Heitman, J. (2019). Calcium-calmodulin-calcineurin signaling: a globally conserved virulence cascade in eukaryotic microbial pathogens. *Cell host & microbe*, *26*(4), 453-462.

Pausch, M. H., Kaim, D., Kunisawa, R., Admon, A., & Thorner, J. (1991). Multiple Ca^{2+}/calmodulin-dependent protein kinase genes in a unicellular eukaryote. *The EMBO journal*, *10*(6), 1511-1522.

Payen, A. D. (1843). Extrait d'un rapport adresse a M. Le Marechal Duc de Dalmatie, Ministre de la Guerre, President du Conseil, sur une alteration extraordinaire du pain de munition. *Ann. Chim. Phys. 3rd Ser*, *9*, 5-21.

Peng, W., Zhang, Y., Zheng, M., Cheng, H., Zhu, W., Cao, C. M., & Xiao, R. P. (2010). Cardioprotection by CaMKII-δB is mediated by phosphorylation of heat shock factor 1 and subsequent expression of inducible heat shock protein 70. *Circulation research*, *106*(1), 102-110.

Perez, R. O., Van Tuinen, D., Marmé, D., Cox, J. A., & Turian, G. (1981). Purification and identification of calmodulin from *Neurospora crassa*. *FEBS letters*, *133*(2), 205-208.

Pérez, P., Cortés, J. C., Martín-García, R., & Ribas, J. C. (2016). Overview of fission yeast septation. *Cellular microbiology*, *18*(9), 1201-1207.

Perkins, D. D., Radford, A., Newmeyer, D., & Björkman, M. (1982). Chromosomal loci of *Neurospora crassa*. *Microbiological reviews*, *46*(4), 426-570.

Perkins, D. D. (1992). *Neurospora*: the organism behind the molecular revolution. *Genetics*, *130*(4), 687.

Perkins, D. D., & Barry, E. G. (1977). The cytogenetics of *Neurospora*. *Advances in genetics*, *19*, 133-285.

Permyakov, E. A., & Kretsinger, R. H. (2009). Cell signaling, beyond cytosolic calcium in eukaryotes. *Journal of inorganic biochemistry*, *103*(1), 77-86.

Petersen, O. H., Michalak, M., & Verkhratsky, A. (2005). Calcium signalling: past, present and future. *Cell calcium*, *38*(3-4), 161-169.

Piazza, M., Taiakina, V., Dieckmann, T., & Guillemette, J. G. (2017). Structural consequences of calmodulin EF hand mutations. *Biochemistry*, *56*(7), 944-956.

Plesofsky-Vig, N., & Brambl, R. (1985). Heat shock response of *Neurospora crassa*: protein synthesis and induced thermotolerance. *Journal of bacteriology*, *162*(3), 1083–1091.

Pöggeler, S., & Kück, U. (2001). Identification of transcriptionally expressed pheromone receptor genes in filamentous ascomycetes. *Gene*, *280*(1-2), 9-17.

Potapova, T. V., Boitsova, L. Y., Golyshev, S. A., & Dunina-Barkovskaya, A. Y. (2016). Tip growth of *Neurospora crassa* upon resource shortage: Disturbances of the coordination of elongation, branching, and septation. *Cell and Tissue Biology*, *10*(6), 486-499.

Pratt, R. J., Lee, D. W., & Aramayo, R. (2004). DNA methylation affects meiotic trans-sensing, not meiotic silencing, in *Neurospora*. *Genetics*, *168*(4), 1925-1935.

Quandt, K., Frech, K., Karas, H., Wingender, E., & Werner, T. (1995). Matlnd and Matlnspector: new fast and versatile tools for detection of consensus matches in nucleotide sequence data. *Nucleic acids research*, *23*(23), 4878-4884.

Querfurth, C., Diernfellner, A. C., Gin, E., Malzahn, E., Höfer, T., & Brunner, M. (2011). Circadian conformational change of the *Neurospora* clock protein FREQUENCY triggered by clustered hyperphosphorylation of a basic domain. *Molecular cell*, *43*(5), 713-722.

Radman, R., Bucke, C., & Keshavarz, T. (2004). Elicitor effects on reactive oxygen species in liquid cultures of *Penicillium chrysogenum*. *Biotechnology letters*, *26*(2), 147-152.

Raggam, R. B., Salzer, H. J., Marth, E., Heiling, B., Paulitsch, A. H., & Buzina, W. (2011). Molecular detection and characterisation of fungal heat shock protein 60. *Mycoses*, *54*(5), e394-e399.

Raju, N. B. (1980). Meiosis and ascospore genesis in *Neurospora*. *European journal of cell biology*, *23*(1), 208-223.

Raju, N. B. (1992). Genetic control of the sexual cycle in *Neurospora*. *Mycological research*, *96*(4), 241-262.

Raju, N. B. (2008). Six decades of *Neurospora* ascus biology at Stanford. *Fungal Biology Reviews*, *22*(1), 26-35.

Raju, N. B. (2009). *Neurospora* as a model fungus for studies in cytogenetics and sexual biology at Stanford. *Journal of biosciences*, *34*(1), 139-159.

Rangel, D. E. (2011). Stress induced cross-protection against environmental challenges on prokaryotic and eukaryotic microbes. *World Journal of Microbiology and Biotechnology*, *27*(6), 1281-1296.

Rasmussen, C. D., Means, R. L., Lu, K. P., May, G. S., & Means, A. R. (1990). Characterization and expression of the unique calmodulin gene of *Aspergillus nidulans*. *Journal of Biological Chemistry*, *265*(23), 13767-13775.

Rasmussen, C. D., Lu, K. P., Means, R. L., & Means, A. R. (1992). Calmodulin and cell cycle control. *Journal of Physiology-Paris*, *86*(1-3), 83-88.

Rasmussen, C., & Rasmussen, G. (1994). Inhibition of G2/M progression in *Schizosaccharomyces pombe* by a mutant calmodulin kinase II with constitutive activity. *Molecular biology of the cell*, *5*(7), 785-795.

Rasmussen, C. D. (2000). Cloning of a Calmodulin Kinase I Homologue from *Schizosaccharomyces pombe*. *Journal of Biological Chemistry*, *275*(1), 685-690.

Rasmussen, C. G., & Glass, N. L. (2005). A Rho-type GTPase, *rho-4*, is required for septation in *Neurospora crassa*. *Eukaryotic cell*, *4*(11), 1913-1925.

Reig, J. A., Téllez-Iñón, M. T., Flawiá, M. M., & Torres, H. N. (1984). Activation of *Neurospora crassa* soluble adenylate cyclase by calmodulin. *Biochemical Journal*, *221*(2), 541.

Reiner, D. J., Newton, E. M., Tian, H., & Thomas, J. H. (1999). Diverse behavioural defects caused by mutations in *Caenorhabditis elegans* unc-43 CaM kinase II. *Nature*, *402*(6758), 199-203.

Rensing, L., Monnerjahn, C., & Meyer, U. (1998). Differential stress gene expression during the development of *Neurospora crassa* and other fungi. *FEMS microbiology letters*, *168*(2), 159-166.

Ringer, S. (1883). A further contribution regarding the influence of the different constituents of the blood on the contraction of the heart. *The Journal of physiology*, *4*(1), 29.

Robatzek, M., & Thomas, J. H. (2000). Calcium/calmodulin-dependent protein kinase II regulates *Caenorhabditis elegans* locomotion in concert with a G_o/G_q signaling network. *Genetics*, *156*(3), 1069-1082.

Roca, M. G., Weichert, M., Siegmund, U., Tudzynski, P., & Fleißner, A. (2012). Germling fusion via conidial anastomosis tubes in the grey mould *Botrytis cinerea* requires NADPH oxidase activity. *Fungal Biology*, *116*(3), 379-387.

Roche, C. M., Loros, J. J., McCluskey, K., & Glass, N. L. (2014). *Neurospora crassa*: looking back and looking forward at a model microbe. *American journal of botany*, *101*(12), 2022-2035.

Rodriguez-Caban, J., Gonzalez-Velazquez, W., Perez-Sanchez, L., Gonzalez-Mendez, R., & Valle, N. R. D. (2011). Calcium/calmodulin kinase1 and its relation to thermotolerance and HSP90 in *Sporothrix schenckii*: an RNAi and yeast two-hybrid study. *BMC microbiology*, *11*(1), 1-16**.**

Romano, N., & Macino, G. (1992). Quelling: transient inactivation of gene expression in *Neurospora crassa* by transformation with homologous sequences. *Molecular microbiology*, *6*(22), 3343-3353.

Rose, A. J., Kiens, B., & Richter, E. A. (2006). Ca^{2+}–calmodulin-dependent protein kinase expression and signalling in skeletal muscle during exercise. *The Journal of physiology*, *574*(3), 889-903.

Roy, B. G., & Datta, A. (1987). A calmodulin inhibitor blocks morphogenesis in *Candida albicans*. *FEMS Microbiology letters*, *41*(3), 327-329.

Roychowdhury, H. S., MacAlister, T. J., Costerton, J. W., & Kapoor, M. (1992). Induction and intracellular localization of the 80-kilodalton heat-shock protein of *Neurospora crassa*. *Biochemistry and Cell Biology*, *70*(12), 1347-1355.

Ruoff, P., Loros, J. J., & Dunlap, J. C. (2005). The relationship between FRQ-protein stability and temperature compensation in the *Neurospora* circadian clock. *Proceedings of the National Academy of Sciences*, *102*(49), 17681-17686.

Sabie, F. T., & Gadd, G. M. (1989). Involvement of a Ca^{2+}-calmodulin interaction in the yeast-mycelial (YM) transition of *Candida albicans*. *Mycopathologia*, *108*(1), 47-54.

Sadakane, Y., & Nakashima, H. (1996). Light-induced phase shifting of the circadian conidiation rhythm is inhibited by calmodulin antagonists in *Neurospora crassa*. *Journal of biological rhythms*, *11*(3), 234-240.

Sambrook, J., & Russell, D. W. (2001). edition 3. Molecular cloning: a laboratory manual. New York.

Sanders, D., Pelloux, J., Brownlee, C., & Harper, J. F. (2002). Calcium at the crossroads of signaling. *The Plant Cell*, *14*(suppl_1), S401-S417.

Santos, B., Gutiérrez, J., Calonge, T. M., & Pérez, P. (2003). Novel Rho GTPase involved in cytokinesis and cell wall integrity in the fission yeast *Schizosaccharomyces pombe*. *Eukaryotic cell*, *2*(3), 521-533.

Sargent, M. L., & Kaltenborn, S. H. (1972). Effects of medium composition and carbon dioxide on circadian conidiation in *Neurospora*. *Plant physiology*, *50*(1), 171-175.

Sato, T., Ueno, Y., Watanabe, T., Mikami, T., & Matsumoto, T. (2004). Role of Ca^{2+}/calmodulin signaling pathway on morphological development of *Candida albicans*. *Biological and Pharmaceutical Bulletin*, *27*(8), 1281-1284.

Schafmeier, T., Diernfellner, A., Schäfer, A., Dintsis, O., Neiss, A., & Brunner, M. (2008). Circadian activity and abundance rhythms of the *Neurospora* clock transcription factor WCC associated with rapid nucleo–cytoplasmic shuttling. *Genes & development*, *22*(24), 3397-3402.

Schindelin, J., Arganda-Carreras, I., Frise, E., Kaynig, V., Longair, M., Pietzsch, T., ... & Cardona, A. (2012). Fiji: an open-source platform for biological-image analysis. *Nature methods*, *9*(7), 676-682.

Schmid, Jan, and Franklin M. Harold (1988). "Dual roles for calcium ions in apical growth of *Neurospora crassa*." *Microbiology* 134.9, 2623-2631.

Schmit, J. C., & Brody, S. T. U. A. R. T. (1976). Biochemical genetics of *Neurospora crassa* conidial germination. *Bacteriological Reviews*, *40*(1), 1-41.

Schröder, M. (2008). Endoplasmic reticulum stress responses. *Cellular and molecular life sciences*, *65*(6), 862-894.

Schröder, K. (2019). NADPH oxidase-derived reactive oxygen species: Dosis facit venenum. *Experimental physiology*, *104*(4), 447-452.

Schumann, U., Ayliffe, M., Kazan, K., & Wang, M. B. (2010). RNA silencing in fungi. *Frontiers in Biology*, *5*(6), 478-494.

Schwede, T., Kopp, J., Guex, N., & Peitsch, M. C. (2003). SWISS-MODEL: an automated protein homology-modeling server. *Nucleic acids research*, *31*(13), 3381-3385.

Seale, T. (1973). Life cycle of *Neurospora crassa* viewed by scanning electron microscopy. *Journal of bacteriology*, *113*(2), 1015-1025.

Seibert, T., Thieme, N., & Benz, J. P. (2016). The renaissance of *Neurospora crassa*: how a classical model system is used for applied research. *Gene expression systems in fungi: advancements and applications*, 59-96.

Seifikalhor, M., Aliniaeifard, S., Shomali, A., Azad, N., Hassani, B., Lastochkina, O., & Li, T. (2019). Calcium signaling and salt tolerance are diversely entwined in plants. *Plant Signaling & Behavior*, *14*(11), 1665455.

Selker, E. U. (1990). Premeiotic instability of repeated sequences in *Neurospora crassa*. *Annual review of genetics*, *24*(1), 579-613.

Sharma, S., Kaur, H., & Khuller, G. K. (2001). Cell cycle effects of the phenothiazines: trifluoperazine and chlorpromazine in *Candida albicans*. *FEMS microbiology letters*, *199*(2), 185-190.

Sharma, S. K., Christen, P., & Goloubinoff, P. (2009). Disaggregating chaperones: an unfolding story. *Current Protein and Peptide Science*, *10*(5), 432-446.

Shear, C. L., & Dodge, B. O. (1927). Life histories and heterothallism of the red bread-mold fungi of the *Monilia sitophila* group (pp. 1019-1042). Washington, DC: US Government Printing Office.

Shiber, A., & Ravid, T. (2014). Chaperoning proteins for destruction: diverse roles of Hsp70 chaperones and their co-chaperones in targeting misfolded proteins to the proteasome. *Biomolecules*, *4*(3), 704-724.

Shiu, P. K., Raju, N. B., Zickler, D., & Metzenberg, R. L. (2001). Meiotic silencing by unpaired DNA. *Cell*, *107*(7), 905-916.

Shiu, P. K., & Metzenberg, R. L. (2002). Meiotic silencing by unpaired DNA: properties, regulation and suppression. *Genetics*, *161*(4), 1483-1495.

Shiu, P. K., Zickler, D., Raju, N. B., Ruprich-Robert, G., & Metzenberg, R. L. (2006). SAD-2 is required for meiotic silencing by unpaired DNA and perinuclear localization of SAD-1 RNA-directed RNA polymerase. *Proceedings of the National Academy of Sciences*, *103*(7), 2243-2248.

Silar, P. (2011). Grafting as a method for studying development in the filamentous fungus *Podospora anserina*. *Fungal biology*, *115*(8), 793-802.

Silverman-Gavrila, L. B., & Lew, R. R. (2001). Regulation of the tip-high [Ca^{2+}] gradient in growing hyphae of the fungus *Neurospora crassa*. *European journal of cell biology*, *80*(6), 379-390

Silverman-Gavrila, L. B., & Lew, R. R. (2002). An IP3-activated Ca^{2+} channel regulates fungal tip growth. *Journal of cell science*, *115*(24), 5013-5025.

Silverman-Gavrila, L. B., & Lew, R. R. (2003). Calcium gradient dependence of *Neurospora crassa* hyphal growth. *Microbiology*, *149*(9), 2475-2485.

Simonin, A. R., Rasmussen, C. G., Yang, M., & Glass, N. L. (2010). Genes encoding a striatin-like protein (*ham-3*) and a forkhead associated protein (*ham-4*) are required for hyphal fusion in *Neurospora crassa*. *Fungal Genetics and Biology*, *47*(10), 855-868.

Sinclair, W., Oliver, I., Maher, P., & Trewavas, A. (1996). The role of calmodulin in the gravitropic response of the *Arabidopsis thaliana agr-3* mutant. *Planta*, *199*(3), 343-351.

Soderling, T. R., & Stull, J. T. (2001). Structure and regulation of calcium/calmodulin-dependent protein kinases. *Chemical reviews*, *101*(8), 2341-2352.

Sokolovsky, V., Kaldenhoff, R., Ricci, M., & Russo, V. E. A. (1990). Fast and reliable mini-prep RNA extraction from *Neurospora crassa*. *Fungal Genetics Newsletters*, *37*, 39-40.

Sorensen, B. R., & Shea, M. A. (1998). Interactions between domains of apo calmodulin alter calcium binding and stability. *Biochemistry*, *37*(12), 4244-4253.

Sorensen, A. B., Søndergaard, M. T., & Overgaard, M. T. (2013). Calmodulin in a heartbeat. *The FEBS journal*, *280*(21), 5511-5532.

Springer, M. L., & Yanofsky, C. (1989). A morphological and genetic analysis of conidiophore development in *Neurospora crassa*. *Genes & development*, *3*(4), 559-571.

Springer, M. L. (1993). Genetic control of fungal differentiation: the three sporulation pathways of *Neurospora crassa*. *Bioessays*, *15*(6), 365-374.

Staben, C., & Yanofsky, C. (1990). *Neurospora crassa a* mating-type region. *Proceedings of the National Academy of Sciences*, *87*(13), 4917-4921.

Stevens, F. C. (1983). Calmodulin: an introduction. *Canadian journal of biochemistry and cell biology*, *61*(8), 906-910.

Stigler, J., & Rief, M. (2012). Calcium-dependent folding of single calmodulin molecules. *Proceedings of the National Academy of Sciences*, *109*(44), 17814-17819.

Stirling, D. A., Welch, K. A., & Stark, M. J. (1994). Interaction with calmodulin is required for the function of Spc110p, an essential component of the yeast spindle pole body. *The EMBO Journal*, *13*(18), 4329-4342.

Strynadka, N. C., & James, M. N. (1989). Crystal structures of the helix-loop-helix calcium-binding proteins. *Annual review of biochemistry*, *58*(1), 951-999.

Sun, G. H., Hirata, A., Ohya, Y., & Anraku, Y. (1992). Mutations in yeast calmodulin cause defects in spindle pole body functions and nuclear integrity. *The Journal of cell biology*, *119*(6), 1625-1639. Takeda, T., & Yamamoto, M. (1987). Analysis and in vivo disruption of the gene coding for calmodulin in *Schizosaccharomyces pombe*. *Proceedings of the National Academy of Sciences*, *84*(11), 3580-3584.

Suresh, K., & Subramanyam, C. (1997). A putative role for calmodulin in the activation of *Neurospora crassa* chitin synthase. *FEMS microbiology letters*, *150*(1), 95-100.

Suzuki, S., Katagiri, S., & Nakashima, H. (1996). Mutants with altered sensitivity to a calmodulin antagonist affect the circadian clock in *Neurospora crassa*. *Genetics*, *143*(3), 1175-1180.

Swulius, M. T., & Waxham, M. N. (2008). Ca^{2+}/calmodulin-dependent protein kinases. *Cellular and Molecular Life Sciences*, *65*(17), 2637-2657.

Takahashi, F., Mizoguchi, T., Yoshida, R., Ichimura, K., & Shinozaki, K. (2011). Calmodulin-dependent activation of MAP kinase for ROS homeostasis in *Arabidopsis*. *Molecular cell*, *41*(6), 649-660.

Takeda, T., & Yamamoto, M. (1987). Analysis and in vivo disruption of the gene coding for calmodulin in *Schizosaccharomyces pombe*. *Proceedings of the National Academy of Sciences*, *84*(11), 3580-3584.

Takeda, T., Imai, Y., & Yamamoto, M. (1989). Substitution at position 116 of *Schizosaccharomyces pombe* calmodulin decreases its stability under nitrogen starvation and results in a sporulation-deficient phenotype. *Proceedings of the National Academy of Sciences*, *86*(24), 9737-9741.

Takemoto, D., Tanaka, A., & Scott, B. (2007). NADPH oxidases in fungi: diverse roles of reactive oxygen species in fungal cellular differentiation. *Fungal Genetics and Biology*, *44*(11), 1065-1076.

Tamuli, R., Kumar, R., & Deka, R. (2011). Cellular roles of neuronal calcium sensor-1 and calcium/calmodulin-dependent kinases in fungi. *Journal of basic microbiology*, *51*(2), 120-128.

Tamuli, R. (2013). Genome Defense Mechanisms in *Neurospora* and Associated Specialized Proteins. *Journal of Proteins & Proteomics*, *1*(1).

Tamuli, R., Kumar, R., Srivastava, D.A., and Deka, R. (2013) Calcium signaling. In: D.P. Kasbekar, and McCluskey, K. (eds.), *Neurospora Genomics and Molecular Biology* (pp 35–57). Norfolk: Caister Academic Press.

Tang, C. T., Li, S., Long, C., Cha, J., Huang, G., Li, L., ... & Liu, Y. (2009). Setting the pace of the *Neurospora* circadian clock by multiple independent FRQ phosphorylation events. *Proceedings of the National Academy of Sciences*, *106*(26), 10722-10727.

Tebar, F., Villalonga, P., Sorkina, T., Agell, N., Sorkin, A., & Enrich, C. (2002). Calmodulin regulates intracellular trafficking of epidermal growth factor receptor and the MAPK signaling pathway. *Molecular biology of the cell*, *13*(6), 2057-2068.

Tebar, F., Chavero, A., Agell, N., Lu, A., Rentero, C., Enrich, C., & Grewal, T. (2020). Pleiotropic roles of calmodulin in the regulation of KRas and Rac1 GTPases: functional diversity in health and disease. *International Journal of Molecular Sciences*, *21*(10), 3680.

Tellez-Inon, M. T., Ulloa, R. M., Glikin, G. C., & Torres, H. N. (1985). Characterization of *Neurospora crassa* cyclic AMP phosphodiesterase activated by calmodulin. *Biochemical journal*, *232*(2), 425-430.

Tereshina, V. M. (2005). Thermotolerance in fungi: the role of heat shock proteins and trehalose. *Microbiology*, *74*(3), 247-257.

Thompson, J. D., Gibson, T. J., Plewniak, F., Jeanmougin, F., & Higgins, D. G. (1997). The CLUSTAL_X windows interface: flexible strategies for multiple sequence alignment aided by quality analysis tools. *Nucleic acids research*, *25*(24), 4876-4882.

Tidow, H., & Nissen, P. (2013). Structural diversity of calmodulin binding to its target sites. *The FEBS journal*, *280*(21), 5551-5565.

Timmins, J. M., Ozcan, L., Seimon, T. A., Li, G., Malagelada, C., Backs, J., ... & Tabas, I. (2009). Calcium/calmodulin-dependent protein kinase II links ER stress with Fas and mitochondrial apoptosis pathways. *The Journal of clinical investigation*, *119*(10), 2925-2941.

Tirone, F., & Cox, J. A. (2007). NADPH oxidase 5 (NOX5) interacts with and is regulated by calmodulin. *FEBS letters*, *581*(6), 1202-1208.

Tiwari, S., Thakur, R., & Shankar, J. (2015). Role of Heat-Shock Proteins in Cellular Function and in the Biology of Fungi. *Biotechnology research international*, *2015*, 132635.

Tokumitsu, H., Enslen, H., & Soderling, T. R. (1995). Characterization of a Ca^{2+}/Calmodulin-dependent Protein Kinase Cascade: MOLECULAR CLONING AND EXPRESSION OF CALCIUM/CALMODULIN-DEPENDENT PROTEIN KINASE KINASE (∗). *Journal of Biological Chemistry*, *270*(33), 19320-19324.

Torralba, S., Heath, I. B., & Ottensmeyer, F. P. (2001). Ca^{2+} shuttling in vesicles during tip growth in *Neurospora crassa*. *Fungal Genetics and Biology*, *33*(3), 181-193.

Torralba, S., & Heath, I. B. (2001). Cytoskeletal and Ca^{2+} regulation of hyphal tip growth and initiation. *Current topics in developmental biology*, *51*, 135-187.

Trinci, A. P. J., Wiebe, M. G., & Robson, G. D. (1994). The mycelium as an integrated entity. In *Growth, differentiation and sexuality* (pp. 175-193). Springer, Berlin, Heidelberg.

Turner, B. C., Perkins, D. D., & Fairfield, A. (2001). *Neurospora* from natural populations: a global study. *Fungal Genetics and Biology*, *32*(2), 67-92.

Tuteja, N., & Mahajan, S. (2007). Calcium signaling network in plants: an overview. *Plant signaling & behavior*, *2*(2), 79-85.

Valle-Aviles, L., Valentin-Berrios, S., Gonzalez-Mendez, R. R., & Rodriguez-del Valle, N. (2007). Functional, genetic and bioinformatic characterization of a calcium/calmodulin kinase gene in *Sporothrix schenckii*. *BMC microbiology*, *7*(1), 1-12.

Van Tuinen, D., Marmé, D., & Turian, G. (1983). Calmodulin-stimulated cyclic nucleotide phosphodiesterase from *Neurospora crassa*. *Biochimica et Biophysica Acta*, *758*(1), 84-87.

Villalobo, A., Ishida, H., Vogel, H. J., & Berchtold, M. W. (2018). Calmodulin as a protein linker and a regulator of adaptor/scaffold proteins. *Biochimica Et Biophysica Acta (BBA)-Molecular Cell Research*, *1865*(3), 507-521.

Villarroel, A., Taglialatela, M., Bernardo-Seisdedos, G., Alaimo, A., Agirre, J., Alberdi, A., ... & Areso, P. (2014). The ever changing moods of calmodulin: how structural plasticity entails transductional adaptability. *Journal of molecular biology*, *426*(15), 2717-2735.

Vitalini, M. W., de Paula, R. M., Park, W. D., & Bell-Pedersen, D. (2006). The rhythms of life: circadian output pathways in *Neurospora*. *Journal of Biological Rhythms*, *21*(6), 432-444.

Vitaterna, M. H., Takahashi, J. S., & Turek, F. W. (2001). Overview of circadian rhythms. *Alcohol Research & Health*, *25*(2), 85.

Vogel, H. J. A convenient growth medium for *Neurospora crassa* (N medium). *Microb Genet*, *677*, 42-3.

Vogel, H. J. (1964). Distribution of lysine pathways among fungi: evolutionary implications. *The American Naturalist*, *98*(903), 435-446.

Vogt, N., & Seiler, S. (2008). The RHO1-specific GTPase-activating protein LRG1 regulates polar tip growth in parallel to Ndr kinase signaling in *Neurospora*. *Molecular biology of the cell*, *19*(11), 4554-4569.

Vyas, M., & Kasbekar, D. P. (2005). Collateral damage: Spread of repeat-induced point mutation from a duplicated DNA sequence into an adjoining single-copy gene in *Neurospora crassa*. *Journal of Biosciences*, *30*(1), 15-20.

Wallace, E. W., Kear-Scott, J. L., Pilipenko, E. V., Schwartz, M. H., Laskowski, P. R., Rojek, A. E., ... & Drummond, D. A. (2015). Reversible, specific, active aggregates of endogenous proteins assemble upon heat stress. *Cell*, *162*(6), 1286-1298.

Walsh, M. P. (1983). Review Article Calmodulin and its roles in skeletal muscle function. *Canadian Anaesthetists' Society Journal*, *30*(4), 390-398.

Wang, L., Liang, S., & Lu, Y. T. (2001). Characterization, physical location and expression of the genes encoding calcium/calmodulin-dependent protein kinases in maize (*Zea mays* L.). *Planta*, *213*(4), 556-564.

Wang, G., Lu, L., Zhang, C. Y., Singapuri, A., & Yuan, S. (2006). Calmodulin concentrates at the apex of growing hyphae and localizes to the Spitzenkörper in *Aspergillus nidulans*. *Protoplasma*, *228*(4), 159-166.

Wang, Z., Lehr, N., Trail, F., & Townsend, J. P. (2012). Differential impact of nutrition on developmental and metabolic gene expression during fruiting body development in *Neurospora crassa*. *Fungal Genetics and Biology*, *49*(5), 405-413.

Wang, B., Zhou, X., Gerber, S. A., Loros, J. J., & Dunlap, J. C. (2021). Cellular calcium levels influenced by NCA-2 impact circadian period determination in *Neurospora*. *Mbio*, *12*(3), e01493-21.

Warwar, V., & Dickman, M. B. (1996). Effects of calcium and calmodulin on spore germination and appressorium development in *Colletotrichum trifolii*. *Applied and Environmental Microbiology*, *62*(1), 74-79.

Watters, M. K., Randall, T. A., Margolin, B. S., Selker, E. U., & Stadler, D. R. (1999). Action of repeat-induced point mutation on both strands of a duplex and on tandem duplications of various sizes in *Neurospora*. *Genetics*, *153*(2), 705-714.

Weids, A. J., Ibstedt, S., Tamás, M. J., & Grant, C. M. (2016). Distinct stress conditions result in aggregation of proteins with similar properties. *Scientific reports*, *6*(1), 1-12.

Westergaard, M., & Mitchell, H. K. (1947). *Neurospora* V. A synthetic medium favoring sexual reproduction. *American Journal of Botany*, 573-577.

Wiest, A., Baker, S.E. & McCluskey, K. (2013). *Neurospora* Gene and Genome Analysis: Past Through Future. In: D.P. Kasbekar, and McCluskey, K. (eds.), *Neurospora* Genomics and Molecular Biology (pp 35– 57). Norfolk: Caister Academic Press.

Wilson, A. M., Wilken, P. M., van der Nest, M. A., Wingfield, M. J., & Wingfield, B. D. (2019). It's all in the genes: the regulatory pathways of sexual reproduction in filamentous ascomycetes. *Genes*, *10*(5), 330.

Winterbourn, C. C. (1995). Toxicity of iron and hydrogen peroxide: the Fenton reaction. *Toxicology letters*, *82*, 969-974.

Wu, X., Ahn, E. Y., McKenna, M. A., Yeo, H., & McDonald, J. M. (2005). Fas binding to calmodulin regulates apoptosis in osteoclasts. *Journal of Biological Chemistry*, *280*(33), 29964-29970.

Xiao, H., Alexander, W. G., Hammond, T. M., Boone, E. C., Perdue, T. D., Pukkila, P. J., & Shiu, P. K. (2010). QIP, a protein that converts duplex siRNA into single strands, is required for meiotic silencing by unpaired DNA. *Genetics*, *186*(1), 119-126.

Xu, X. M. (1996). On estimating non-linear response of fungal development under fluctuating temperatures. *Plant Pathology*, *45*(2), 163-171.

Yang, Q., & Borkovich, K. A. (1999). Mutational activation of a Gαi causes uncontrolled proliferation of aerial hyphae and increased sensitivity to heat and oxidative stress in *Neurospora crassa*. *Genetics*, *151*(1), 107-117.

Yang, Y., Cheng, P., Zhi, G., & Liu, Y. (2001). Identification of a calcium/calmodulin-dependent protein kinase that phosphorylates the *Neurospora* circadian clock protein FREQUENCY. *Journal of Biological Chemistry*, *276*(44), 41064-41072.

Yang, C. F., & Tsai, W. C. (2022). Calmodulin: The switch button of calcium signaling. *Tzu-Chi Medical Journal*, *34*(1), 15.

Yap, K. L., Kim, J., Truong, K., Sherman, M., Yuan, T., & Ikura, M. (2000). Calmodulin target database. *Journal of structural and functional genomics*, *1*(1), 8-14.

Zamore, P. D., Tuschl, T., Sharp, P. A., & Bartel, D. P. (2000). RNAi: double-stranded RNA directs the ATP-dependent cleavage of mRNA at 21 to 23 nucleotide intervals. *cell*, *101*(1), 25-33.

Zelter, A., Bencina, M., Bowman, B. J., Yarden, O., & Read, N. D. (2004). A comparative genomic analysis of the calcium signaling machinery in *Neurospora crassa*, *Magnaporthe grisea*, and *Saccharomyces cerevisiae*. *Fungal Genetics and Biology*, *41*(9), 827-841.

Zhang, M., Abrams, C., Wang, L., Gizzi, A., He, L., Lin, R., ... & Zhang, J. F. (2012). Structural basis for calmodulin as a dynamic calcium sensor. *Structure*, *20*(5), 911-923.

Zhang, C., Wang, Y., Wang, J., Zhai, Z., Zhang, L., Zheng, W., ... & Wang, Z. (2013). Functional characterization of Rho family small GTPases in *Fusarium graminearum*. *Fungal Genetics and Biology*, *61*, 90-99.

Zhang, S., Zheng, H., Chen, Q., Chen, Y., Wang, S., Lu, L., & Zhang, S. (2017). The lectin chaperone calnexin is involved in the endoplasmic reticulum stress response by regulating Ca^{2+} homeostasis in *Aspergillus nidulans*. *Applied and environmental microbiology*, *83*(15), e00673-17.

Zhen, Z., Zhang, G., Yang, L., Ma, N., Li, Q., Ma, Y., ... & Yang, J. (2019). Characterization and functional analysis of calcium/calmodulin-dependent protein kinases (CaMKs) in the nematode-trapping fungus *Arthrobotrys oligospora*. *Applied microbiology and biotechnology*, *103*(2), 819-832.

Zhou, Y., David, M. A., Chen, X., Wan, L. Q., Duncan, R. L., Wang, L., & Lu, X. L. (2016). Effects of osmolarity on the spontaneous calcium signaling of in situ juvenile and adult articular chondrocytes. *Annals of biomedical engineering*, *44*(4), 1138-1147.

Zhu, Y., Yan, J., Liu, W., Liu, L., Sheng, Y., Sun, Y., ... & Zhang, A. (2016). Phosphorylation of a NAC transcription factor by a calcium/calmodulin-dependent protein kinase regulates abscisic acid-induced antioxidant defense in maize. *Plant physiology*, *171*(3), 1651-1664.

Publications, Conferences, and Workshop

Publications

1. **Marak CN and Tamuli R**. Calmodulin, calcium/calmodulin-dependent kinases-1 and 2 have a role in the expressions of heat shock protein 80 in response to heat shock and pheromone signaling genes during sexual development in *Neurospora crassa*. (Under revision)
2. Baruah D, **Marak CN**, Roy A, Gohain D, Kumar A, Das P, Borkovich K, and Tamuli R. Multiple calcium signaling genes play a role in the circadian period of *Neurospora crassa*. FEMS Microbiology Letters (In press)

Conference presentations

1. **Marak K CN and Tamuli R (2017)** Understanding the molecular mechanism of calmodulin and calcium/calmodulin-dependent kinases in *Neurospora crassa*. Research Conclave, IIT Guwahati 17-20 March
2. **Marak K CN and Tamuli R (2017)** Calcium/calmodulin-dependent kinases play a role in the regulation of normal period length in *Neurospora crassa* circadian clock. National Conference on Fungal Biology: Recent Trends and Future Prospects and 44th Annual meeting of the Mycological Society of India (MSI), University of Jammu, Jammu, India, November 16-18
3. **Marak K CN and Tamuli R (2018)** Calmodulin and calcium/calmodulin-dependent kinases are important for normal growth and development in *Neurospora crassa*. Research Conclave, IIT Guwahati, India, March 8-11. (Best Poster Presentation Award)
4. **Marak K CN and Tamuli R (2019)** Insight on the mechanism of calmodulin and calcium/calmodulin-dependent kinases in regulating stress tolerance and sexual

development in *Neurospora crassa*. XI International conference on Biology of Yeast and Filamentous Fungi. 27-29 November 2019, Hyderabad, India.

Workshop

1. **Marak K CN (2019)** Workshop on "Skill Development in molecular Strategies for Understanding Biodiversity and Human Diseases". Bioinformatic Centre, Northeastern hill University, Shillong, Febuary 28- March 2, 2019